The Pennsylvania State University

The Graduate School

DENDRITIC MICROTUBULE POLARITY IS MAINTAINED BY KINESIN-2 STEERING AND POSITIONING OF NUCLEATION SITES BY ENDOSOMAL WNT SIGNALING PROTEINS

A Dissertation in

Molecular, Cellular and Integrative Biosciences

by

Alexis Thomas Weiner

Submitted in Partial Fulfillment
of the Requirements
for the Degree of

Doctor of Philosophy

May 2020

The dissertation of Alexis Thomas Weiner was reviewed and approved* by the following:

Melissa Rolls
Paul Berg Professor of Biochemistry and Molecular Biology
Chair of the Molecular, Cellular and Integrative Biosciences Graduate Program
Dissertation Advisor
Chair of Committee

Timothy Jegla
Associate Professor of Biology

Lorraine Santy
Associate Professor of Biochemistry and Molecular Biology

William Hancock
Professor of Bioengineering
Chair of the Intercollege Graduate Program in Bioengineering

ABSTRACT

Cells rely heavily on an intact and tightly organized microtubule cytoskeleton to facilitate vital functions including cell division, structural support and transport of cargoes. These cargoes include mRNAs, proteins, and organelles. Unfortunately, inefficient transport of cargoes due to a disorganized cytoskeletal network can lead to various diseases and pathologies. This reason alone emphasizes the importance of an organized cytoskeletal network to cellular health over an organism's lifetime.

Due to their size and shape neurons experience challenges in organizing their microtubule network. Neurons rely on acentrosomal microtubule organization and how this network is supported remains poorly understood. It is known that within the dendritic compartment microtubule polarity is maintained by a few mechanisms. Previously, our lab discovered a microtubule polarity maintenance mechanism controlled by Kinesin-2. The proposed mechanism involves a complex that includes two members of the Adenomatous polyposis coli (Apc) protein family of tumor suppressors, Apc and Apc2. Apc2 recruits Apc to dendrite branch points where Apc is proposed to function as a linker between growing microtubule plus-ends via End binding protein 1 (Eb1) and Kinesin-2. Protein-protein interactions strengthened the proposal that these complex members work together and it was found that neuronal specific loss of complex members resulted in mixed microtubule polarity in dendrites. However, it was left unclear whether this mechanism functioned specifically at dendrite branch points. We came up with two hypotheses that could explain the steering phenomena. Microtubules could be pre-bundled to stable microtubule tracks before entering branch points or they could be steered at branch points only after encountering a stable microtubule track there. Therefore, we tested both models by examining precise moments when microtubules encountered branch points. By reducing Kinesin-2 subunits we determined that Kinesin-2 mediates

microtubule steering not by bundling microtubules but by resolving microtubule collisions within branch points at pre-existing stable microtubule tracks.

Due to the ability of Apc2 to target Apc to branch points we sought to investigate upstream regulators of Apc2 positioning to further understand requirements of the steering complex components. We determined through a targeted screen that mitochondrial energy, branched actin, submembrane cytoskeletal elements such as Ankyrin, and members of Wnt signaling contribute to the localization of Apc2 at dendrite branch points. We also visualized that many of the proteins involved in Apc2 targeting were themselves localized to branch points. To follow up on this we determined which molecular players were involved in their own targeting to branch points. This pinpointed the branch point as a region of microtubule control. Intriguingly, it has also been suggested that local microtubule nucleation occurs at dendritic branch points and contributes to dendritic polarity. Because γTub seems to act specifically at branch points we asked how γTub was targeted to branch points to better understand how local nucleation sites are positioned in dendrites. To determine how γTub enriches at its specific site of action we adopted the same candidate proteins screened for Apc2 since both proteins localize to the same region.

We discovered that γTub shares some of the machinery required to localize Apc2. The candidates that overlapped between the two microtubule regulators involved members of the canonical Wnt signaling pathway. These proteins include G-protein coupled receptors frizzled and frizzled2, heterotrimeric G-protein alpha subunit, casein kinase 1γ, and scaffolding proteins disheveled and Axin. Ultimately, the pathway converges on Axin and we were able to show that Axin was sufficient to recruit γTub to ectopic cellular sites confirming Axin as a major regulator of nucleation machinery. To test the functional significance of loss of γTub enrichment due to targeted depletion of Wnt signaling proteins we used two established assays in the lab. One measures the overall polarity of the dendrite by using Eb1 as a proxy for overall microtubule

directionality. By severely reducing γTub levels we have observed mixed microtubule polarity in the dendrite. The second functional assay specifically tests the ability of γTub to nucleate microtubules. By injuring the axon with a UV pulse laser, we have shown that there is an upregulation of microtubules which relies on γTub nucleation. Both of these assays have been previously tested by reducing γTub levels. Therefore, we hypothesized that by reducing Wnt signaling proteins required for γTub enrichment at branch points we would phenocopy the loss of γTub. In fact, depletion of Wnt proteins required for γTub localization resulted in disrupted microtubule polarity and blocked the neuronal ability to upregulate dendritic microtubules in response to axon injury.

To examine at which subcellular location this pathway organizes nucleation sites, we investigated membrane bound organelles due to fact that the receptors in the pathway are embedded in membranes at either the cell surface or on internal vesicles. Previously it has been reported that the small Golgi fragments function to organize nucleation sites but we have shown Golgi are dispensable for γTub organization in dendrites. We looked to endosomes which have previously been implicated in regulating Wnt signaling and identified a sub population of early endosomes that house the Wnt signaling proteins necessary to localize γTub to branch points. From these endosomes we witnessed microtubule polymerization events providing evidence that early endosomes housing Wnt Signaling proteins function as the microtubule organizing centers at dendrite branch points.

These investigations solidify how two mechanisms work at dendritic branch points. Steering utilizes a complex of precisely targeted proteins to guide microtubules along pre-existing microtubule tracks. Additionally, microtubule nucleation occurs off endosomes that house Wnt signaling proteins to target nucleation machinery at branch points. Both of these pathways describe mechanisms that contribute to an overall understanding of microtubule polarity.

TABLE OF CONTENTS

LIST OF FIGURES

ACKNOWLEDGEMENTS

I would like to give my most sincere appreciation to my advisor Dr. Melissa Rolls for the many years of mentorship and friendship through both the most rewarding and trying times. Her dedication toward making me the scientist I am today began when I was an undergraduate without me having any knowledge of how a research lab works. She has encouraged me to be the best mentor I can be with regard to the undergraduates and graduate students I educate. Without her this thesis would not be possible. In addition to Melissa, I would like to thank the graduate and undergraduate members of the Rolls Lab both past and present. I have shared so many experiences with you over the years and it is hard to not appreciate all that I have learned and continue to learn from you all. Thank you to the rest of my committee members, Tim Jegla, Will Hancock and Lorraine Santy for their guidance.

I would also like to thank my siblings, their spouses, and their wonderful children who bring me so much happiness. Their support has helped me to persevere. Thank you to my in laws Dan and Marie Boyle. You both accepted this misfit into your family without question and helped Elizabeth and I to have so many of our cross-country trips during the duration of my studies. We have had so many fun times and there are many more to come!

To my friends before college as well as the ones I have made over the last 11 years at Penn State, thank you. Table tennis practices and various shenanigans have all led to this point.

I owe so much to my parents Tom and Michele for fostering the most supportive environment a son could ever ask for. From a young age they never once impeded my desire to ask questions and instead with an unwavering talent, encouraged me to seek out knowledge. It began with dinosaurs and then came the rest of the living world. Now I am a cellular neurobiologist who looks at these little “rooms” with a unique perspective because of you. Thank

you, mom and dad I love you. Mom you were always my inspiration and I know you are proud. I wish I could have beaten you just once at Jeopardy. For you I will give the world all I can.

Lastly, I would like to thank my wife Elizabeth. When we both graduated from Penn State, we never would have thought that we would spend 6 years apart. I am not sure how to put into words how monumental you have been to my success. You have never doubted, said you can't, or put up any barrier of any kind. Because of your constant support I have survived. WE have survived. I love you with all of my heart and cannot wait to write more than just thesis chapters with you. To you this thesis is dedicated.

Chapter 1

Introduction

The Microtubule Cytoskeleton

Microtubules have been studied for decades for their role in providing cells with structural stability, aiding in chromosomal segregation during cell division, assisting in cell migration and offering a platform for motor protein-based transport of cargoes (Bodakuntla, Jijumon, Villablanca, Gonzalez-Billault, & Janke, 2019). One attribute of the microtubule cytoskeleton is known as dynamic instability and underlies many of its various functions. (Mitchison & Kirschner, 1984). Dynamic instability refers to the constant switch between growth and shrinkage of microtubules. The purpose of dynamic instability is exemplified during cell division. By constantly growing and shrinking microtubules search through the cell, exploring regions seemingly at random (Holy & Leibler, 1994; Kirschner & Mitchison, 1986). However, during cell division once microtubules encounter a complex of proteins known as the kinetochore, microtubules become stabilized and attached to the chromosomes (Hayden, Bowser, & Rieder, 1990). This phenomenon has been referred to as search and capture and intriguingly microtubules remain bound and resistant to disassembly once captured (Kirschner & Mitchison, 1986). Newer studies have shown this principle to hold true in cells where kinetochore attachment to individual microtubules starts at the lattice, gradually resolves to plus-end on attachment, and remains on the order of minutes (Heald & Khodjakov, 2015; Kalinina et al., 2013; Magidson et al., 2011; Rieder & Alexander, 1990; Tanaka et al., 2005)

In order to further understand dynamic instability, it is important to understand microtubule structure. Microtubules are typically made of 13 protofilaments that come together

into a long hollow cylindrical structure (Chaaban & Brouhard, 2017). On a smaller scale, a single microtubule protofilament is formed by obligate heterodimers of alpha and beta tubulin (αTub and βTub) bound in an alternate fashion (Figure 1). The base of the microtubule to which the

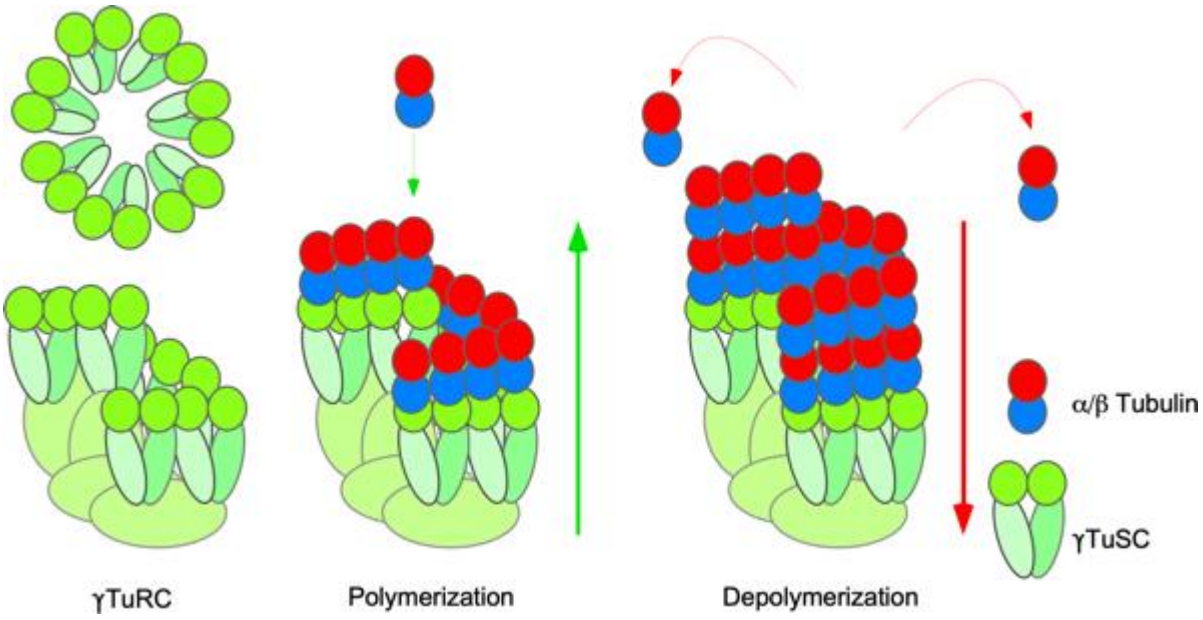

Figure 1-1. Microtubule growth and shrinkage: Depicted is the basic microtubule structure starting with the gamma tubulin ring complex (γTuRC) minus-end capping complex on the left. The complex is made of 6-7 gamma tubulin small complexes (γTuSCs) which are each in turn made of 2 γTub monomers (circles) held together by 2 gamma tubulin ring proteins (Grips) (Grip84 in light green and Grip91 in darker green). The γTuSCs are then brought together by an additional 4 grip proteins shown as large ovals. These help to arrange the γTuSCs into a cone shaped arrangement. A top view is provided to give a different perspective on the ring complex. The middle and right images show the process of microtubule polymerization and depolymerization. The addition of α/β heterodimers (α is blue and β is red) to the 13 protofilaments and their dynamic removal underlies this process. αTub is the end of the dimer that binds to exposed γTub. This leaves βTub exposed at the freely growing end.

first alpha and beta tubulin dimer binds is called the minus-end and is comprised of a specialized complex called the gamma tubulin ring complex (γTuRC). The γTuRC is comprised of 6-7 gamma tubulin small complexes (γTuSC) that are held together by gamma tubulin ring complex proteins (Grips). Each γTuSC in turn is made up of 2 γTub monomers and held together by the proteins Grip84 and Grip91. γTub is the core microtubule nucleation protein as its only known

function is in forming microtubules (Moritz, Braunfeld, Sedat, Alberts, & Agard, 1995). Due to the single-turn helical organization a final 13 protofilament arrangement results (Kollman et. al. 2011). The 4 remaining Grips, which include 71, 75, 128 and 163, help to laterally bind the γTuSCs forming an "ice cream cone" shape (Tovey & Conduit, 2018). αTub is the end of the dimer that binds to an exposed γTub and this binding event helps to create the intrinsic polarity of the microtubule. As soon as this binding event occurs the end that is created is called the minus-end and the opposite end that has a βTub exposed is known as the plus-end. The presence of the γTuRC at the minus-end effectively caps the microtubule and limits growth at this end. However, at the dynamically unstable plus-end after an α/βTub dimer binds to the microtubule, βTub is quickly hydrolyzed from being GTP to GDP bound (Desai & Mitchison, 1997). This change causes the βTub to have weaker lateral interactions within the microtubule lattice and subsequently the process of depolymerization occurs naturally. However, a growing microtubule population exists that is capped by a protective GTP cap that effectively blocks depolymerization due to the slower off rate of GTP bound tubulin subunits (Mitchison & Kirschner, 1984; Roostalu et al., 2020). Only when this cap is removed is the microtubule subject to the natural depolymerization. In addition to natural polymerization and depolymerization, proteins have been discovered that directly regulate microtubule stability. Some members can also facilitate communication between the microtubule cytoskeleton and other proteins. These proteins are known as microtubule associated proteins (MAPs).

Microtubule Regulation by MAPs

MAPS were originally discovered when tubulin was purified from chick brains. During these *in vitro* assembly and disassembly assays two components were found to be integral parts of

microtubule assembly (Sloboda, Rudolph, Rosenbaum, & Greengard, 1975). The two proteins to emerge from this study, MAP 1 and 2 were followed up with the identification of another MAP named Tau. Tau was identified via a similar procedure using pig brain extracts and *in vitro* microtubule assembly was shown to depend on it (Weingarten, Lockwood, Hwo, & Kirschner, 1975). Tau, is highly expressed in neuronal tissues and acts as a microtubule stabilizing protein primarily in axons (Cleveland, Hwo, & Kirschner, 1977; Weingarten et al., 1975). Tau primarily stabilizes microtubules by helping to strengthen the binding site between tubulins within the lattice thus protecting against depolymerization (Kadavath et al., 2015). Tau emphasizes the importance of MAPs for neuronal health because various neurodegenerative diseases manifest when it is phosphorylated. In Alzheimer's disease self-assembling hyperphosphorylated tau clusters form tangles of filaments which induce progressive degeneration (Alonso, Zaidi, Novak, Grundke-Iqbal, & Iqbal, 2001). The dendritic counterpart to tau is MAP2 which helps to stabilize microtubules in dendrites (Dehmelt & Halpain, 2005). Due to the integral nature of these proteins in promoting microtubule assembly and stabilization they are known as structural MAPs. Over the years more MAPs have been discovered that help with connecting microtubules to membranes, regulating motor motility, and even crosslink microtubules to other cytoskeletal elements such as actin (Bodakuntla et al., 2019). For instance, it has been shown that MAP1B helps to regulate the proteasomal degradation of Rab35 in neurons showing a relationship between MAPs and membranes (Villarroel-Campos et al., 2016).

In addition to understanding classical structural MAPs, it is important to understand other MAPs have been identified with functions specific to location on the microtubule. Understanding these MAPs is essential for understanding the assays and logic used throughout this thesis. One family of MAPs that has been critical in understanding microtubule regulation is known as end-binding proteins (EB proteins). Due to their function as tip-binding proteins, fusion constructs of EB proteins with fluorescent protein tags have been made to help visualize the polymerizing state

of microtubules at both ends of the microtubule (Mimori-Kiyosue, Shiina, & Tsukita, 2000b). The development of EB proteins fused to fluorescent tags is integral to the study conducted here. They are the primary way in which microtubules are visualized in the *in vivo* microtubule assays conducted throughout this thesis. EB proteins have an affinity for GTP bound βTub and help recruit additional heterodimers and many other tip associated proteins (Mustyatsa, Boyakhchyan, Ataullakhanov, & Gudimchuk, 2017). For instance, EB interacting proteins such as the CLASP proteins containing the highly conserved SxIP domain are targeted to plus-ends of microtubules to tether microtubule plus-ends to the cell cortex of HeLa cells (Jiang et al., 2012; Lansbergen et al., 2006). More pertinent to this current work is the interaction between EB1 and Apc that is proposed to facilitate the link between a growing microtubule and Kinesin-2 (Mattie et al., 2010). In the current study we evaluate microtubule behavior using Eb1-GFP and test this proposed mechanism.

Another set of proteins that act at the plus-end are known as polymerases and depolymerases. Polymerases such as mini spindles (XMAP215) help recruit α/βTub dimers which allows the microtubule to grow more efficiently (Brouhard et al., 2008). On the other hand, other proteins such as Klp59C, a member of the Kinesin-13 family of motors, acts as a microtubule depolymerase and peels the plus-end of the microtubule like a banana causing it to shrink (Ems-McClung & Walczak, 2010). The way in which Kinesin-13 proteins function as depolymerases is by taking advantage of the bent protofilament conformation of GDP bound tubulin (Peng, Hsu, Bonomi, Agard, & Jacobson, 2014). These motors then bend tubulin even more via their neck domain to pop tubulin heterodimers off the microtubule tip (Moores & Milligan, 2006). Therefore, it is important to keep polymerases and depolymerases in mind when evaluating any mechanism that may be controlling microtubule growth or abundance such as studies done assessing nucleation events performed in chapter 4.

Regulation is not limited to the dynamic plus-end of microtubules. Microtubule severing proteins can split microtubules. These MAPs create breaks in the microtubule by dislodging tubulin via a pulling mechanism at the c-terminal tail of both α and β tubulin (Roll-Mecak & Vale, 2008). The break effectively creates two microtubules where one has a new plus-end and the other an uncapped minus-end that can be targeted by minus-end regulators. Ironically, it has been shown recently that severing enzymes such as Spastin and Katanin can help create more stable microtubules. After they dislodge tubulin, soluble GTP bound tubulin can be reincorporated into the microtubule lattice (Vemu et al., 2018). This makes the microtubule resistant to subsequent depolymerization. In mammalian neurons it has been shown that generation of new microtubules helps to create small microtubule fragments easily transported from the cell body into dendrites (Baas & Yu, 1996). These fragments help to populate the newly developing dendrite with microtubules. However, this mechanism has not been shown in *Drosophila*. In *Drosophila*, microtubule severing activity of fidgetin has been shown to promote dendrite degeneration (Tao, Feng, & Rolls, 2016). In addition, *Drosophila* dendritic pruning requires the severing protein Katanin 60-like (Lee, Jan, & Jan, 2009). Since severing enzymes are one way to produce more microtubules an increase in dynamic microtubule number could be a result of severing enzyme activity. When axons are injured an increase an upregulation of microtubules results globally throughout the cell dependent on the regulator nicotinamide mononucleotide adenylyltransferase (Nmnat) (L. Chen et al., 2016). But what causes the increase in microtubule number? Severing enzymes or newly generated microtubules via nucleation could explain the increase in microtubule number. Indeed it was shown that this increase in microtubule dynamics is γTub nucleation dependent and not via severing proteins (L. Chen, Stone, Tao, & Rolls, 2012). This emphasizes the importance of how microtubule nucleation sites are regulated in neurons.

At the minus end, other than γTuRCs, minus-end regulators such as the calmodulin-regulated spectrin-associated protein (CAMSAP)/Nezha/Patronin family of proteins have been characterized (Akhmanova & Steinmetz, 2019). The sole *Drosophila member* of this family, patronin, was first identified in an S2 cell screen for spindle defects (Goshima et al., 2007). Three homologues of patronin exist in mammals and are thought to stabilize the lattice or side of the microtubule and provide a seed by which microtubule plus-end growth can initiate (Hendershott & Vale, 2014; Jiang et al., 2014). In fact, growing minus-ends have been observed in both fish and fly neurons helping to populate regions of the neuron with microtubules (Feng et al., 2019). Therefore, regulation of minus-end growth and location in addition to the plus-end is important to microtubule organization.

Microtubule Organizing Centers

In most cells, microtubules are organized at regions that hold the minus-end in place. By tethering the minus-end this frees the plus-end to explore regions of the cell. The structure that helps tether microtubule minus-ends is known as a microtubule organizing center (MTOC). The classic MTOC is the centrosome composed of mother and daughter centrioles contained in a pericentriolar matrix (PCM) (Woodruff, Wueseke, & Hyman, 2014). In animal cells the centrosome functions in most mitotic cell types to help segregate chromosomes during cell division. However, in post mitotic cells centrosomal function routinely follows a pattern of taking the backseat to other microtubule organizers (Moritz et al., 1995; Sanchez & Feldman, 2017; Wu & Akhmanova, 2017). For instance, in both neurons and cardiomyocytes, mitosis is terminated after a short round of cell divisions. In the case of cardiomyocytes, PCM1 and pericentrin are relocalized to the nuclear envelope resulting in loss of paired centriolar arrangement (Zebrowski et al., 2015). In the case of neurons, the site for microtubule organization has been controversial

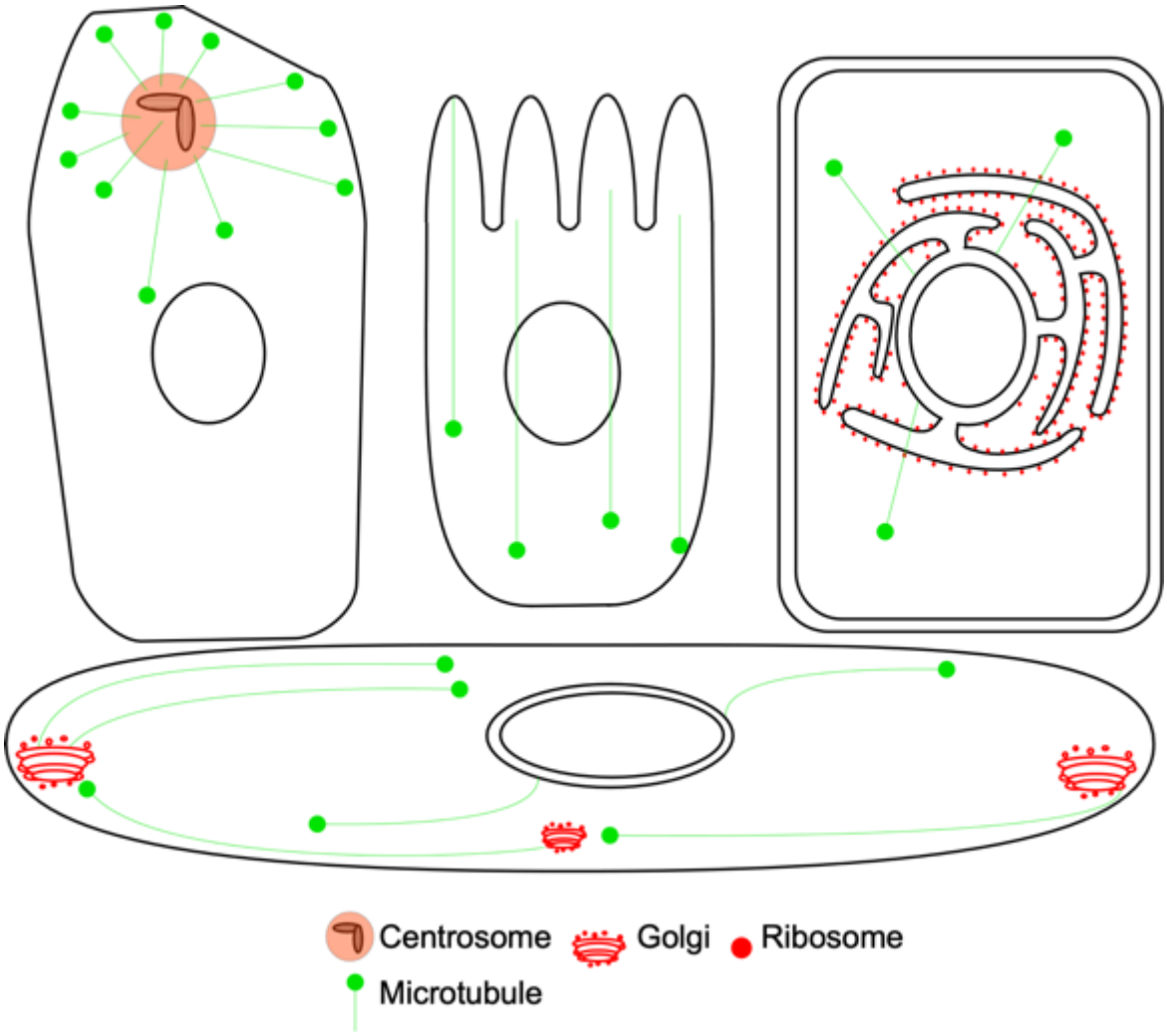

Figure 1-2. Microtubule organizing centers of various cell types: MTOCs of class epithelial cells, intestinal cells, plant cells, and muscle cells are shown. The microtubules are shown in green with their growing plus-end marked with a circle to represent what EB proteins look like when fused to a green fluorescent protein (GFP. The examples include the centrosome, plasma membrane of the apical surface of the intestinal cell, nuclear envelope and Golgi apparatus. The centrosome helps facilitate critical steps of mitosis such as a chromatid segregation. The apically docked microtubules of the intestinal cell help to separate which proteins are transported to the apical or basal side of the cell. Since the intestinal cell is specialized for nutrient absorption on the apical side with villi, it is critical that the right structural components make it to the correct regions of the cell. In addition, tight junctions would be localized to the apical side of the cell because they are most critical to the cellular function as a barrier within the intestine. In many plants, nuclear envelope derived microtubules help carry out mitotic spindle formation in the absence of a centrosome. In different types of muscle cells microtubules may be derived from the nuclear envelope or Golgi apparatus.

and will be discussed later. Instances of other non-standard MTOCs have been described in numerous cells of animals, plants, and yeast (Figure 2) (Sanchez & Feldman, 2017). The nuclear envelope and Golgi apparatus of developing myotube and striated muscle cells have been shown to tether minus-ends (Oddoux et al., 2013; Starr, 2017). At the Golgi minus-ends are anchored by AKAP450, which like pericentrin interacts with CDK5RAP2 and normally helps to position nucleation sites at the centrosome (Rios, 2014). In the intestinal lumen, microtubule minus-ends have been shown to dock on the apical side and helps establish the apical/basal polarity (Waschke & Drenckhahn, 2000). In these specialized epithelial cells it has been demonstrated that a complex between the spectraplakin family protein shortstop and minus-end capping protein patronin help tether apical minus-ends (Khanal, Elbediwy, Diaz de la Loza, Fletcher, & Thompson, 2017). Multiciliated cells of the lungs utilize basal body centrioles that function as a MTOC at the base of each sensory cilium (Vladar & Stearns, 2007). In this scenario one of the centrioles known as the mother centriole migrates to be positioned under the membrane to function as the MTOC of the cilium (Pearson, 2014). In addition, the cortex and nuclear envelope of plant cells have been shown to function in microtubule anchoring and transport (Elliott & Shaw, 2018). At the membrane of these cells the augmin complex has been shown to organize cortical microtubule nucleation off of existing microtubule bundles held in place by and CLASP1 (Ambrose & Wasteneys, 2008). In addition to plant cells, microtubule lattice-based nucleation by the augmin complex has been shown to function in animal cells (Cao et al., 2013; Goshima, Mayer, Zhang, Stuurman, & Vale, 2008; Petry, Groen, Ishihara, Mitchison, & Vale, 2013). In yeast the spindle pole body replaces the function of the centrosome during division (Segal & Bloom, 2001). Major regulators of spindle pole body microtubule organization are not conserved and thus represent a functionally divergent organelle for microtubule organization (Kilmartin, 2014). Thus, based on the myriad of other non-classical MTOCs it has been revealed that the

centrosome is not the only MTOC and this is critically important in the context of how microtubules are organized in neurons.

Neurons have not been shown to not use any of these sites of microtubule organization. In vertebrate systems such as primary rat hippocampal and cortical neuron cell culture it has been shown γTub is reduced at the centrosome after mitotic developmental stages are terminated (Leask, Obrietan, & Stearns, 1997; Stiess et al., 2010). This was validated in *Drosophila* studies that found centrosomal γTub is reduced in mature peripheral neurons and redistributes to axons and dendritic branch points (Nguyen, Stone, & Rolls, 2011). Furthermore, it has not been shown whether this redistribution into dendrites occurs in vertebrate neurons. In mouse hippocampal neurons local nucleation has been shown to be regulated by the 8-subunit HAUS/Augmin complex (Cunha-Ferreira et al., 2018; Sanchez-Huertas et al., 2016). Intriguingly, in C. *elegans* it has been suggested that a MTOC functions at the tip of ciliated neurons and the URX neuron for microtubule organization and correct cargo transport (Harterink et al., 2018). In this study, nucleation machinery was shown to concentrate at this proposed MTOC. However, the identity of this MTOC has not been revealed. Based on these studies there may be diverse sites of microtubule nucleation in different neuronal populations. In *Drosophila* dendrites, the branch point of peripheral sensory neurons has been pinpointed as a local source of microtubule nucleation (Nguyen et al., 2014; Nguyen et al., 2011). Golgi outposts have been suggested to function throughout the dendrite including at branch points as sites of microtubule nucleation (Ori-McKenney, Jan, & Jan, 2012; Yalgin et al., 2015). However, this premise was called into question (Nguyen et al., 2014) and this topic will be discussed in more detail in the next section. Ultimately, the investigations into control of local nucleation sites in vertebrate and invertebrate neurons have provided a strong motivation to explore which MTOCs may regulate nucleation in axons and dendrites.

The Golgi as a Proposed Neuronal MTOC

The Golgi is one contender that has been proposed to organize microtubule nucleation sites in *Drosophila* dendrites (Ori-McKenney et al., 2012). This organelle was a prime candidate as it is known that Golgi nucleate microtubules in a variety of cell types (Sanders & Kaverina, 2015). For example, Golgi have been suggested to organize microtubules in neuroglia such as

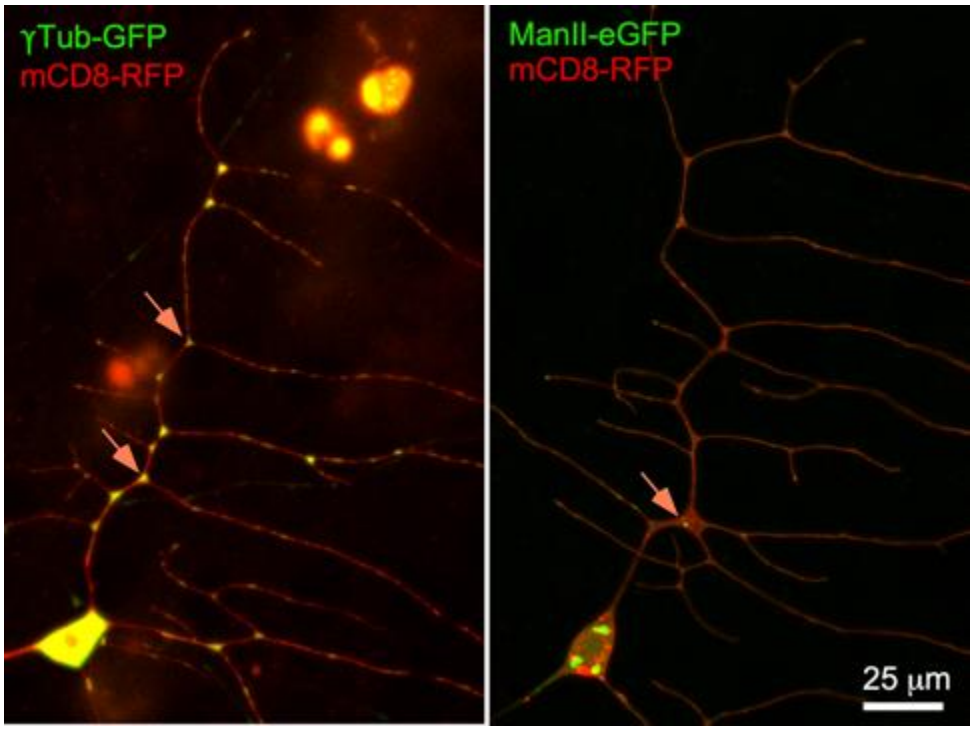

Figure 1-3 γTub and Golgi outpost localization patterns differ: Two images are shown of Class I ddaE sensory neurons. Each image was generated while imaging a live mounted Drosophila third instar larva. In both instances genetic constructs are driven with 221 Gal4 and UAS-mCD8-RFP marks the membranes. In the picture on the left UAS-γTub-GFP shows the γTub localization pattern and in the picture on the right UAS-ManII-eGFP shows ManII Golgi localization. Orange arrows mark examples of branch points with either γTub or ManII localization. ManII localizes to only one proximal branch point while γTub localizes to every branch point of the arbor.

oligodendrocytes via tubulin polymerizing promoting protein (TPPP) (Fu et al., 2019). The Golgi generates microtubules via γTub nucleation, has proteins that help tether the minus-end to it and facilitates microtubule growth from it via Clip-associated proteins (CLASPS). One study in 2012

implicated small Golgi fragments known as outposts to be the source of local γTub nucleation in dendrites (Ori-McKenney et al., 2012). However, the marker used to label Golgi is characteristically leaky and its distribution is concerning because it localizes to axons, which should be devoid of Golgi (Nguyen et al., 2014). It was also noted that when our lab visualized this same marker, Golgi fragments were only seen rarely in the first branch point of Drosophila sensory neuron dendrites (Figure 3) (Nguyen et al., 2014; Weiner et al., 2020). Only with very high laser intensity were we able to see small Golgi puncta at other branch points. This localization did not coincide with the distribution of γTub which localizes to every branch point of the dendrite (Figure 3) (Nguyen et al., 2014; Weiner et al., 2020). In addition, a follow-up study demonstrated that when Golgi outposts are mislocalized via a kinesin-Golgi fusion construct, γTub localization is unaffected (Nguyen et al., 2014). It appeared to us that the Golgi does not perform a MTOC role in dendrites and most likely functions as it does in many other cell types; as a primary sorting network in the cell body and nucleating microtubules for short distance transport between cis and trans stacks for its own use locally (Zhu & Kaverina, 2013). If Golgi outposts are not the site of dendritic microtubule regulation then what could be the dendritic MTOC? So far, no alternatives have been given. Using *Drosophila* da neurons as a model system we have investigated the mechanisms controlling dendritic microtubule polarity. Before new evidence can be added to an ever-growing model of neuronal microtubule organization it is important to understand why microtubule maintenance is important in neurons.

Neuronal Microtubule Polarity

Neurons act as the body's primary method of communication between systems within the body and with the outside world. In the context of a large animal a single neuron may extend processes up to a meter in length. These long processes known as axons are needed to relay information to other neurons and cell types which is received by the commonly post synaptic and

often highly branched portion of the neuron known as the dendrite. However, to grow and maintain these long processes a neuron cannot merely rely on the diffusion of proteins to reach their action site. This process would take on the order of weeks to happen randomly (Milo & Phillips, 2016). The efficient transport of proteins and mRNAs from the point of generation in the cell body down processes up to a meter long requires microtubule-based transport. To segregate proteins specifically to axons and dendrites, the microtubule network in neurons has been specialized for each compartment and organization varies across animal lineages.

Substantial research has been done on neuronal microtubule polarity in vertebrate neurons. Some of the first experiments were done on cat sciatic nerves and utilized a technique called hooking which determines microtubule orientation by the clockwise or counterclockwise pattern visualized via electron microscopy. (Baas & Lin, 2011; Heidemann, Landers, & Hamborg, 1981). It was determined from these studies that microtubule polarity in vertebrate axons is nearly 100% plus-end out. These studies were validated in both chick dorsal root ganglion and rat hippocampal neurons (Baas, Deitch, Black, & Banker, 1988; Baas, White, & Heidemann, 1987). Interestingly, in the studies done on rat neurons it was shown dendrites contain a non-uniform microtubule polarity. This raised the idea that microtubule polarity may underly neuronal polarity and compartment identity. More recent work with more advanced techniques has validated reported vertebrate axonal and dendritic microtubule polarity both *in vitro* and *in vivo* (Stepanova et al., 2003). Importantly the introduction of EB protein fusion constructs made visualizing and analyzing microtubule dynamics and polarity much easier (Stepanova et al., 2003). These studies substantiated EB proteins as a reliable tool by validating previous reports of mixed microtubule polarity using cultured mouse hippocampal neurons. Additional studies have included visualizing dendritic microtubule polarity of cortical neurons in live mice through a cranial window (Kleele et al., 2014). Furthermore, a method of mapping microtubule orientation via super resolution microscopy and tracking motor proteins bound to

chemically fixed microtubules has given even more insight into the composition of plus-end or minus-end out microtubules in dendrites (Tas et al., 2017). Even after the advent of these newer techniques and further investigation it was concluded from vertebrate studies that microtubules in axons are plus-end out and dendrites are mixed with both plus and minus-end out microtubules.

Studies done in *Drosophila* and C. *elegans* have shaken up the understanding of microtubule organization in neurons. This is especially true for dendrites where visualizing microtubules *in vivo* has revealed these microtubules to be almost completely minus-end out (Maniar et al., 2011; Stone, Roegiers, & Rolls, 2008). In the case of axons, invertebrate neurons align with how microtubules are arranged in vertebrate axons (Stone et al., 2008). The difference between invertebrate and vertebrate dendritic microtubule polarity is intriguing but does not necessarily mean the dendrites are different. Therefore, dendritic identity may rely on the presence of substantial amounts of minus-end out microtubules. This is in stark contrast to the axons of all phyla which have almost zero minus-end out microtubules and rely on a uniform plus-end out arrangement. Since these two arrangements of microtubules exist are different cargoes trafficked into axons and dendrites?

It is thought by orienting microtubules in different arrays within neuronal compartments, cargoes such as organelles, mRNAs and proteins can be trafficked differentially. For instance, the minus-end directed motor dynein, which primarily traffics cargo toward the minus-end is responsible for the transport of cargoes such as endosomes, mitochondria, and AMPA receptors into dendrites (Kapitein et al., 2010; Satoh et al., 2008; Yu et al., 2000). Different adaptor proteins such as miro help to correctly link cargoes like mitochondria to dynein for transport into dendrites (Babic et al., 2015). On the other hand, the plus-end directed motor kinesin-1 facilitates a subset of cargo trafficked into axons (Lim, Rechtsteiner, & Saxton, 2017). Other kinesins can also be plus-end directed such as kinesin-3 which traffics synaptic vesicles intended for the axonal boutons (Pack-Chung, Kurshan, Dickman, & Schwarz, 2007). However, it is not as simple

as dynein transports cargoes to the minus-end and kinesins transport cargoes to the plus-end. This is especially important in the case of vertebrate dendrites that house both plus and minus-end out microtubules. In the case of kinesins there exist specific microtubule populations that different kinesins bind to preferentially. Kinesin-1 has been found to prefer acetylated microtubules while kinesin-3 more readily associates with tyrosinated microtubules (Tas et al., 2017). Since dendrites house a concentration of tyrosinated microtubules this could explain one mechanism how the compartments receive specific cargo. Even so it is intriguing to consider how microtubule polarity is developed in axons and dendrites to first enable these specific transportation events.

In order to establish these distinct microtubule arrangements in axons and dendrites mechanisms must be in place to establish and maintain microtubule polarity. The microtubule orientation in these compartments rules out centrosome-housed minus-ends, especially in the case of dendritic microtubule polarity. In fact, it has been demonstrated in both vertebrate and invertebrate systems that once neurons are finished with their last round of cell divisions the centrosome loses its γTub and thus its nucleation capabilities (Leask et al., 1997; Nguyen et al., 2011). In addition, laser ablation of the centrosome does not impair neurite differentiation or extension (Stiess et al., 2010). Thus, these results indicate the centrosome is not important for axonal or dendritic microtubule organization.

In studies done using cultured mammalian neurons efforts have been made to uncover mechanisms that both establish and maintain microtubule polarity in axons and dendrites. In axons, the 8-subunit complex known as the HAUS/augmin complex is necessary for proper microtubule polarity and when subunits were reduced in primary mouse hippocampal cell culture the total number of microtubules also decreased (Figure 4) (Cunha-Ferreira et al., 2018; Sanchez-Huertas et al., 2016). Augmin works by helping to recruit nucleation machinery to the side of a microtubule and similar to the way Arp2/3 facilitates the polymerization of actin off an existing actin filament, helps to nucleate a new microtubule off the side of an existing microtubule. The

branch angle is flexible and enables parallel microtubule arrays to be generated which would be needed for complete plus-end out polarity in axons (Petry et al., 2013). While studies on Augmin are limited it is plausible that a group of plus-end out microtubules that nucleate in the cell body

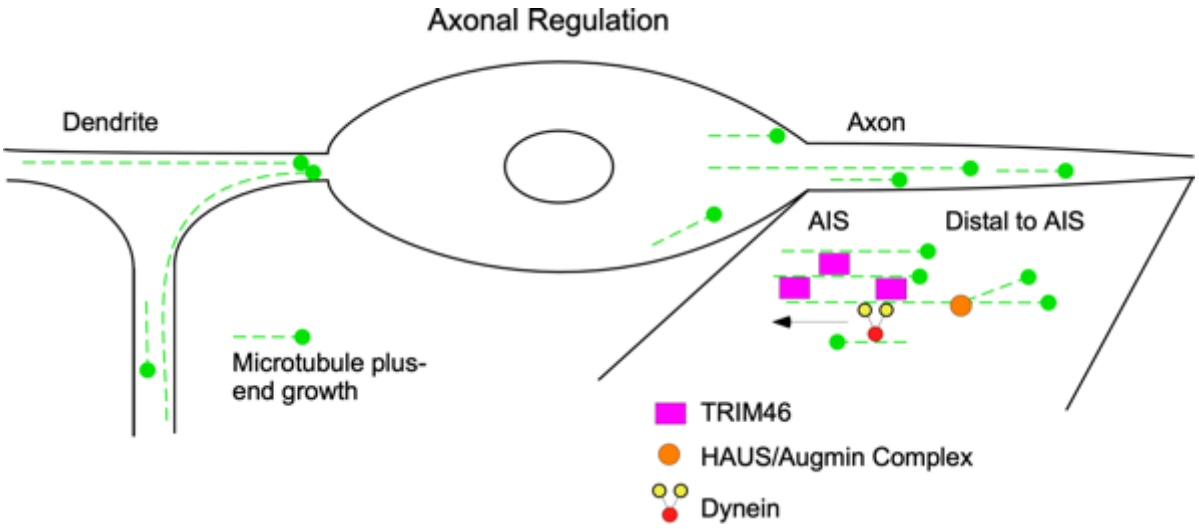

Figure 1-4. Microtubule polarity and Regulation in Axons: Axons are completely plus-end out. Three mechanisms of maintaining plus-end out microtubule polarity are shown in the diagram. TRIM46 shown as a magenta box has been shown to bundle proximal microtubules in the AIS and helps contribute to overall microtubule polarity. The motor Dynein has been shown to be important for transporting minus-end out microtubules out of the axon to help maintain plus-end out arrays. Distal to the AIS, the HAUS/Augmin complex (orange circle) helps to nucleate parallel microtubules off of existing microtubules and strengthens plus-end out polarity. The microtubules are shown in green with their growing plus-end marked with a circle to represent what EB proteins look like when fused to a green fluorescent protein (GFP).

early help to populate the axon. Then Augmin may proceed to nucleate microtubules from the pioneer group. However, that is speculative. In addition to augmin, positive reinforcers of parallel microtubule orientation help to strengthen the polarity within axons.

For example it has been shown in the same mouse neurons the tripartite motif containing (TRIM) protein, TRIM46 enables parallel microtubule arrays in the axon to reinforce plus-end out polarity (Figure 4) (Curcio & Bradke, 2015; van Beuningen et al., 2015). First, TRIM46 localizes to the proximal portion of the Axon through a ring finger domain and then associates

with axonal microtubules via a coiled-coiled COS box domain. Analysis of microtubule dynamics showed that with depleted Trim46 axonal microtubules exhibited mixed microtubule polarity. Further studies revealed that TRIM46 associates with axon initial segment (AIS) microtubules to contribute to microtubule fasciculation by sustaining microtubule cross-bridging helping to regularly space microtubules at the AIS (Harterink et al., 2019). In addition to nucleation sites recruited by augmin and microtubule bundling by TRIM46 other regulators of axonal microtubule polarity have been identified. Intriguingly, analysis of axonal microtubule polarity in *Drosophila* dynein mutants has showcased a role for dynein in maintaining axonal microtubule polarity (Figure 4) (Zheng et al., 2008). This role for dynein in maintaining microtubule polarity indicates that motors have intimate links to control of microtubule organization in neurons.

In fact, in dendrites one of the strongest claims for establishing polarity is that microtubule fragments are slid into dendrites via a motor-based mechanism and this helps populate dendrites with minus-end out microtubules (Baas & Yu, 1996). These studies done on cultured rat sympathetic neurons showcase a role for the motor CHO1/MKLP1 and demonstrate it is a motor needed for microtubule transport into dendrites (Figure 6) (Sharp et al., 1997). There have been follow up studies that validate the importance of a similar mechanism in establishing axonal polarity through dynein sorting of microtubules (Rao et al., 2017). This is in agreement with studies done *in vitro* on *Drosophila* neurons in which dynein helps slide minus-end out microtubules from the axon to establish uniform polarity (del Castillo, Winding, Lu, & Gelfand, 2015). Therefore, it seems that there is evidence that motor mediated sliding can influence polarity early in both vertebrate and invertebrate neurons. But these mechanisms are not the only ones to be revealed.

Drosophila dendrites are initially mixed during development and then resolve to almost

complete minus-end out microtubule polarity (Figure 5) (Hill et al., 2012). Recently, it was shown in developing *Drosophila* neurons that microtubule minus-end growth mediated by the

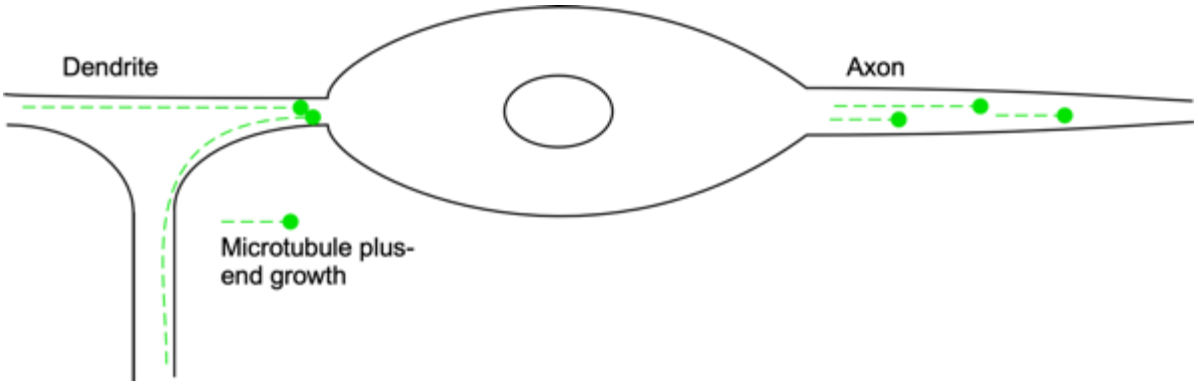

Figure 1-5. Microtubule polarity in Drosophila neurons: The microtubule polarity in axons and dendrites is opposite in Drosophila sensory neurons. Axons are completely plus-end out and dendrites are predominantly minus-end out. The microtubules are shown in green with their growing plus-end marked with a circle to represent what EB proteins look like when fused to a green fluorescent protein (GFP). Of note is the branch point microtubule orientation where there are no microtubules on the distal side of the branch point in relation to the cell body. Microtubules in the cell body are left out because their direction is typically random.

CAMSAP family member patronin helps minus-ends to actively grow into dendrites (Figure 6) (Feng et al., 2019). It was also demonstrated that this same microtubule regulator is required for minus-end out polarity in developed dendrites. So, it seems that patronin acts early to help populate developing dendrites with an abundance of minus-end out microtubules but also is a regulatory mechanism to maintain minus-end out polarity. Plus-end polymerization events were seen from these patronin minus-ends and this can explain how microtubules grow from the peripheral neurites, which much of the time is devoid of nucleation machinery (Feng et al., 2019). Growing minus-ends were also visualized in sensory axons of Zebrafish Rohan Beard (RB)

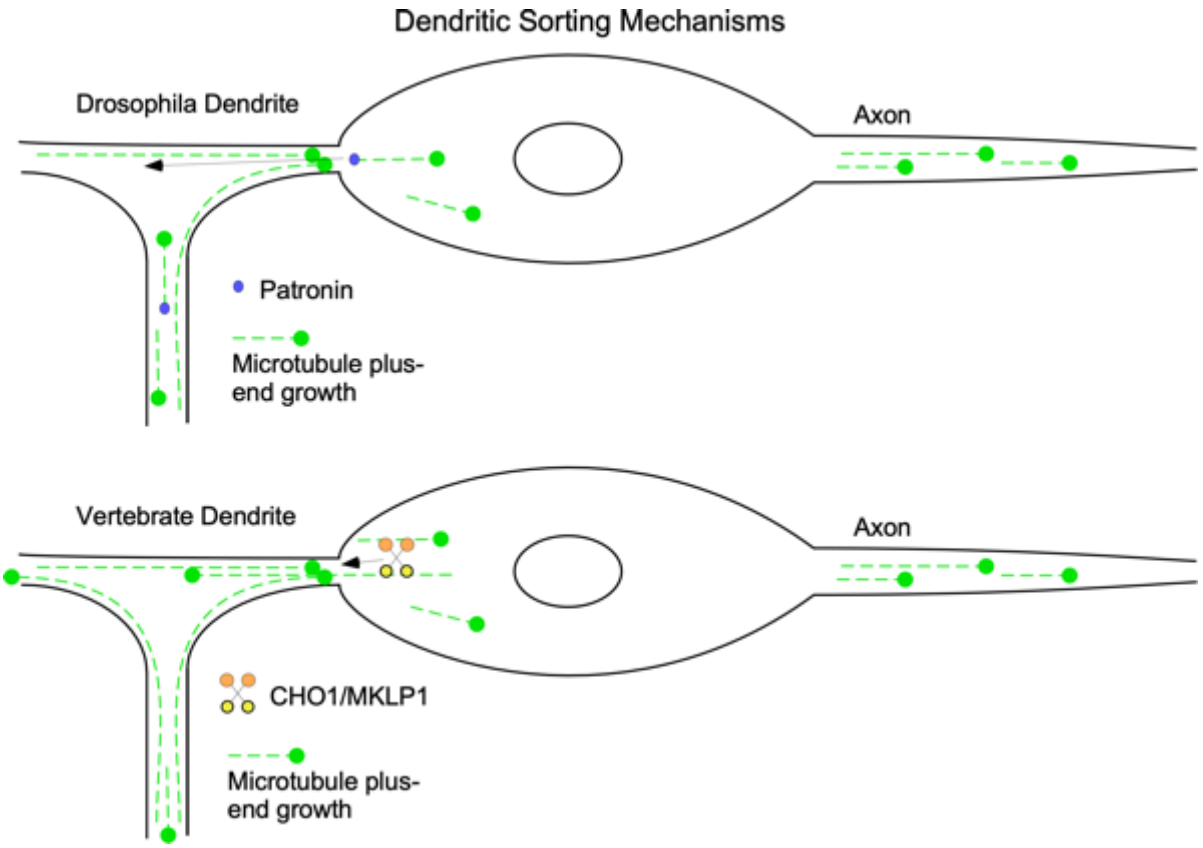

Figure 1-6. Ways of Populating Dendrites with Minus-end Out Microtubules in *Drosophil*a and Vertebrate Dendrites During Development: There have been two different mechanisms shown for transporting minus-end out microtubules in *Drosophila* and vertebrate dendrites. In *Drosophila* the minus-end binding proteins patronin has been shown to facilitate minus-end growth into dendrites during development. In developing vertebrate dendrites, the motor CHO/MLKP1 has been shown to transport small minus-end out microtubule fragments in dendrites. Neither of these mechanisms has been shown in the other system to function in populating dendrites with minus-end out microtubules. However in Zebra Fish growing minus-ends have been visualized in the dendrite-like processes (plus-end out) of RB neurons.

neurons. The finding that growing minus-ends help populate dendrites during development is important in the context of dendrites such as those in *Drosophila*.

In addition to these mechanisms that jockey for a role in establishing microtubule polarity, microtubule steering is one that acts as a positive feedback loop in *Drosophila* and helps to strengthen dendritic minus-end out microtubule polarity. Dendritic branch points act as a

region that challenges microtubule polarity (Figure 7). When a microtubule polymerizes into the branch point from the peripheral arbor there are typically two paths it can take. It could grow towards the cell body and maintain minus-end out polarity or it could grow away and this would cause mixed polarity (Mattie et al., 2010). Based on this challenge it was reasonable that a motor might be involved in directed microtubule growth. In mammalian cells part of the heterotrimeric Kinesin-2 protein interacts with the tumor suppressor proteins adenomatous polyposis coli 1 (Apc) (Jimbo et al., 2002). Normally Apc proteins are thought to function in Wnt signaling by regulating levels of β-catenin and when alleles of Apc are inactivated colorectal cancers manifest (Bienz & Clevers, 2000). Intriguingly, Apc has also been shown to act as a plus-tip protein in Xenopus kidney epithelial cells (Mimori-Kiyosue, Shiina, & Tsukita, 2000a). Through a two-hybrid assay it was found that *Drosophila* Apc binds to EB1 and Kap3 which confirms that interaction of these proteins is conserved (Mattie et al., 2010). Additionally, the subunits of Kinesin-2, Klp64D, Klp68D, and Kap3 were depleted using RNAi to test if they were involved in maintaining dendritic microtubule polarity. Results confirmed that Kinesin-2 was required for minus-end out microtubule polarity in *Drosophila* dendrites. Therefore, it was proposed that in *Drosophila* a complex which includes Apc and Apc2 as well as the plus-tip associated MAP end-binding protein 1 (EB1) helps facilitate a microtubule steering mechanism at branch points (Mattie et al., 2010). Apc is localized to branch points by Apc2 and subsequently is proposed to act as a link between the growing plus-end of a microtubule and the motor protein kinesin-2 which walks constitutively toward the plus-end of another microtubule (Figure 7). However, it remains to be determined whether this mechanism acts specifically at branch points or is constitutively guiding microtubules along the side of minus-end out microtubules within the dendrite.

Apc can bind to microtubules via its C-terminus and even though Apc2 lacks the same C-

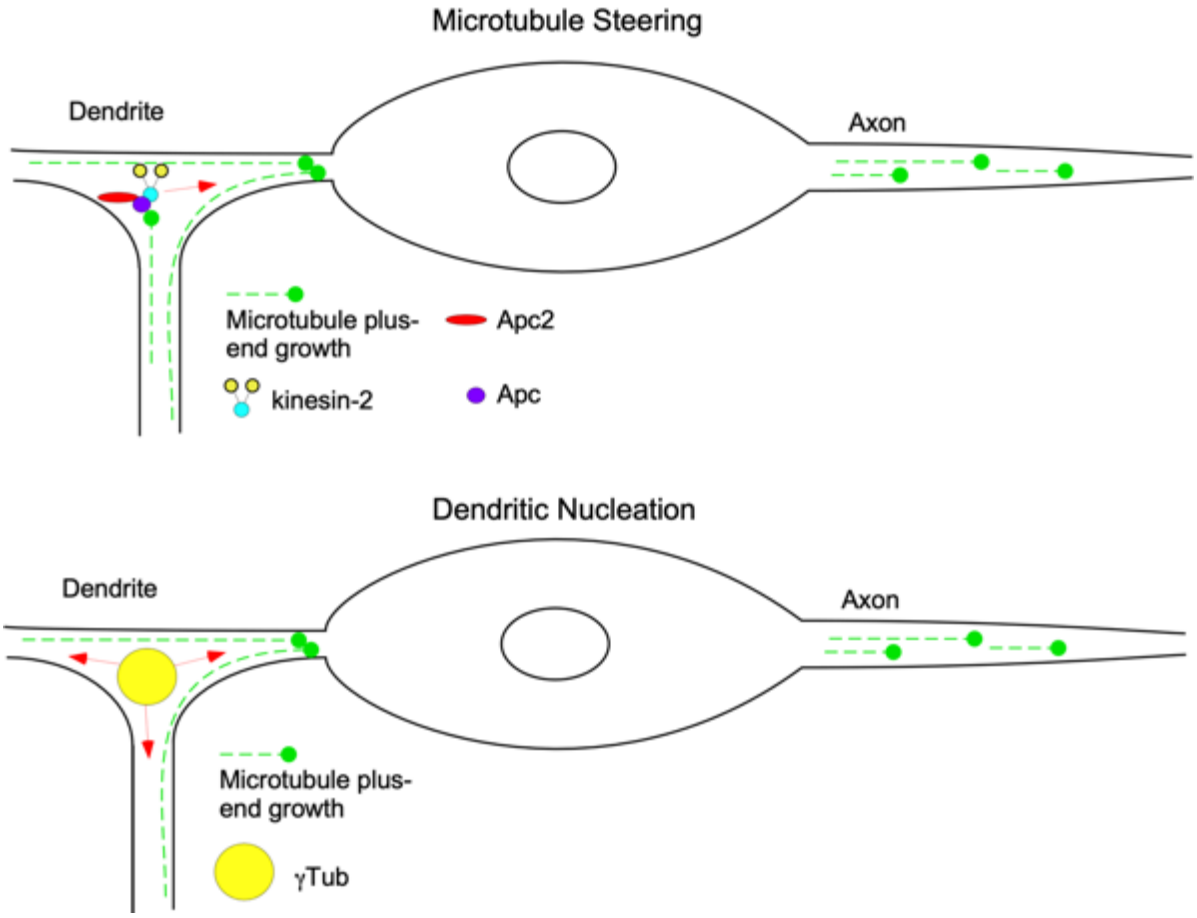

Figure 1-7. Mechanisms that regulate microtubule polarity in *Drosophila* dendrites: In addition to patronin two other modes of maintaining minus-end out polarity are shown. The top mechanism depicts the microtubule steering model involving Kinesin-2, Apc, Apc2 and Eb1. The second shows local positioning of nucleation sites at dendrite branch points. Both of these mechanisms have been implicated in maintaining microtubule organization in Drosophila dendrites. The steering model has been proposed to function at branch points but never specifically shown to act there. In addition, there is little known about how nucleation sites are enriched at branch points or how depletion of nucleation machinery results in mixed microtubule polarity.

terminus it has been shown to regulate the neuronal microtubule stability in axons by promoting acetylation of αTub (Mimori-Kiyosue et al., 2000a; Shintani et al., 2009). Apc has also been demonstrated in mouse dorsal root ganglion (DRG) neurons and chick retinal ganglion cells (RGC) to facilitate microtubule growth direction during axon pathfinding (Koester, Muller, & Pollerberg, 2007; Purro et al., 2008). Furthermore, Apc2 recruits Apc to branch points in *Drosophila* (Mattie et al., 2010). Apc2 has multifaceted roles in a variety of cellular contexts as it

has been shown to organize cortical actin in the *Drosophila* embryo by first localizing to the cortex using a Ser-Ala-Met-Pro (SAMP) motif and novel C-terminal domain. (Zhou, Kunttas-Tatli, Zimmerman, Zhouzheng, & McCartney, 2011). In *Drosophila*, the Arm domain repeats allow Apc2 to form higher order complexes once at the cortex (Zhou et al., 2011). In addition, truncated Apc proteins that lack the C-terminus have been shown to form complexes on mitochondria (Brocardo et al., 2008). Due to the variety of molecular partners Apc proteins have and since Apc2 has distinct localization to dendritic branch points it is therefore of significance to determine what localizes it to its proposed site of action in dendrites.

Local microtubule nucleation has also been proposed to contribute to dendritic microtubule organization (Figure 7). Evidence from different labs has shown that γTub localizes to sites outside of the cell body which suggests that local nucleation is regulated in axons and dendrites (Nguyen et al., 2011; Ori-McKenney et al., 2012; Sanchez-Huertas et al., 2016; Yalgin et al., 2015). In fly neurons γTub localizes to dendritic branch points. (Nguyen et al., 2014; Nguyen et al., 2011). From this study it was left unclear what organized nucleation machinery in dendrites.

As mentioned before Golgi outposts have been suggested to house nucleation machinery and by doing so control dendritic shape in *Drosophila* (Ori-McKenney et al., 2012). Overexpressed Golgi markers were suggested to be sites of microtubule events and during *in vitro* studies demonstrated γTub localizes to Golgi during microtubule growth assays. However, this study did not show any endogenous labeling of Golgi fragments and the inconsistency between outpost localization and γTub localization could not be explained. A follow-up study to this one meticulously tested a role for Golgi outpost organization of dendritic microtubule polarity. First, by reducing γTub it was shown to be required for both axonal and dendritic microtubule polarity (Nguyen et al., 2014). Endogenous γTub concentrates at dendrite branch points and microtubule

spawning events were enriched at the branch point compared to non-branch point regions. This validates the branch point as a probable site of microtubule nucleation. Additionally, rare Golgi outpost localization at branch points did not coincide with γTub localization. Finally, an experiment using fusions of kinesin-1 and *cis* or *trans* Golgi proteins was conducted to test whether γTub and microtubule polarity depended on the presence of Golgi outposts in dendrites. When outpost were dragged out of dendrites γTub localization was unaffected indicating that Golgi are completely dispensable for organizing nucleation machinery in dendrites (Nguyen et al., 2014). This study called into question one membrane structure but as previously stated other membranes have been shown to organize microtubule nucleation. It is therefore possible that microtubule nucleation is controlled by either complexes on the plasma membrane or another internal membrane bound organelle. So far evidence for this has not been demonstrated in neurons.

Populations of γTub have been shown in a variety of cellular contexts to transform regions or organelles into MTOCs. It is also interesting to posit how γTub nucleation is activated at distinct regions of localization. The most commonly known activator of nucleation is centrosomin (cnn) in Drosophila or CDK5RAP2 in mammals. Cnn contains a conserved γTuRC binding domain which not only binds to nucleating complexes but also activates microtubule nucleation (Choi, Liu, Sze, Dai, & Qi, 2010). This domain has been renamed the γTuRC-mediated nucleation activator (γTuNA) domain and a splice variant of cnn has been shown to be able to convert mitochondria into MTOCs (Chen, Buchwalter, Kao, & Megraw, 2017; Choi et al., 2010). cnn and other PCM components, such as pericentrin-like protein (Plp) interact through the cnn CM2 domain and help construct the PCM of the centrosome (Lerit et al., 2015). These two proteins have been suggested to regulate dendritic microtubules through control of nucleation (Ori-McKenney et al., 2012; Yalgin et al., 2015). In addition, reduced γTub results in mixed

microtubule polarity in *Drosophila* dendrites supporting its role in mediating minus-end out microtubule polarity (Nguyen et al., 2014). Therefore, which signaling pathways mediating how γTub is recruited and activated at dendrite branch points is a key question for investigation. Apc2/Apc hint at which signaling pathway may be modulating microtubule organization at branch points. These two proteins function in Wnt signaling and therefore may suggest a Wnt signaling pathway functions in dendrites to organize the microtubule cytoskeleton.

Wnt Signaling as a Modulator of the Cytoskeleton

Wnt signaling, which is divided into canonical and non-canonical categories, is involved in a myriad of biological processes including cell outgrowth and migration, fate determination, and establishment of cell polarity (Gao & Chen, 2010) (Figure 8). The molecule Wnt, for which Wnt signaling is named, is a small glycoprotein trafficked and modified by the secretory pathway and eventually released to act as an intercellular signaling molecule (Nusse & Clevers, 2017). Wnts are processed through the ER and Golgi which are locations where two key steps take place. First, Wnts are lipid modified by a palmitoyl transferase known as Porcupine (Rios-Esteves & Resh, 2013). This lipid modification is suggested to be important for membrane tethering but is critical for the second part of the Wnt protein journey. Second, lipid-modified Wnts are recognized by the chaperone protein Wntless which helps transport Wnts to the plasma membrane for export. After they are exported Wnts act as intercellular signaling molecules once they bind to a target receptor. Canonical Wnt signaling involves the seven-pass transmembrane receptor frizzled (fz), the obligate co-receptor low density lipoprotein receptor-related protein 5/6 (arrow or arr), heterotrimeric G-proteins, scaffolding proteins Axin and disheveled (dsh), Gsk3β (sgg), casein kinsase γ (Gilgamesh or gish), Apc, Apc2, and ultimately converges on the regulation of the transcription factor β-catenin (armadillo or arm) (Blagodatski, Poteryaev, &

Katanaev, 2014; Logan & Nusse, 2004). Canonical Wnt signaling works as a sequestration pathway. In the absence of extracellular Wnt, Axin forms what is known as the β-catenin destruction complex. The destruction complex targets β-catenin for degradation via phosphorylation by the proteins CK1 and GSK3β (Rao & Kuhl, 2010). However, when Wnts are present they bind to fz and arr at the membrane and recruit the destruction complex. This interaction occurs at multiple levels including direct binding of arr and Axin as well as through dsh recruitment via the dsh/Axin binding domain (DIX) (Fiedler, Mendoza-Topaz, Rutherford, Mieszczanek, & Bienz, 2011). By moving the destruction complex to the membrane degradation of β-catenin is spatially separated and the transcription factor is allowed to transit into the nucleus to regulate downstream gene targets. Protein assemblies at the membrane are known as signalosomes and are mediated by the interaction between dsh and Axin but also facilitated by LRP5/6 and fz (Hagemann et al., 2014). Some members of canonical Wnt signaling including Goα, fz2 and sgg have been shown to regulate microtubule stability through phosphorylation of the MAP futsch at the neuromuscular junction (NMJ) (Luchtenborg et al., 2014). Although this is not technically canonical Wnt signaling because it does not regulate β-catenin, members of canonical Wnt signaling are used in similar way. Just as with the mechanism at the NMJ other variants of Wnt signaling have been described.

The most classically studied non-canonical Wnt signaling pathway is known as the Planar Cell Polarity (PCP) Wnt signaling pathway (Axelrod, 2019). This pathway establishes asymmetry across an entire tissue such as in the Drosophila wing or human inner ear (Montcouquiol & Kelley, 2019; Vladar, Antic, & Axelrod, 2009). Within PCP signaling, an anterior and a posterior end of an individual epithelial cell is determined by the segregation of distinct protein signaling molecules and helps give rise to large scale organization across a tissue. The major signaling

mechanism within PCP involves fz along with the co-receptor Vang to initiate dsh mediated recruitment of actin regulators including RhoA and Rock (Figure 7). These help to produce a

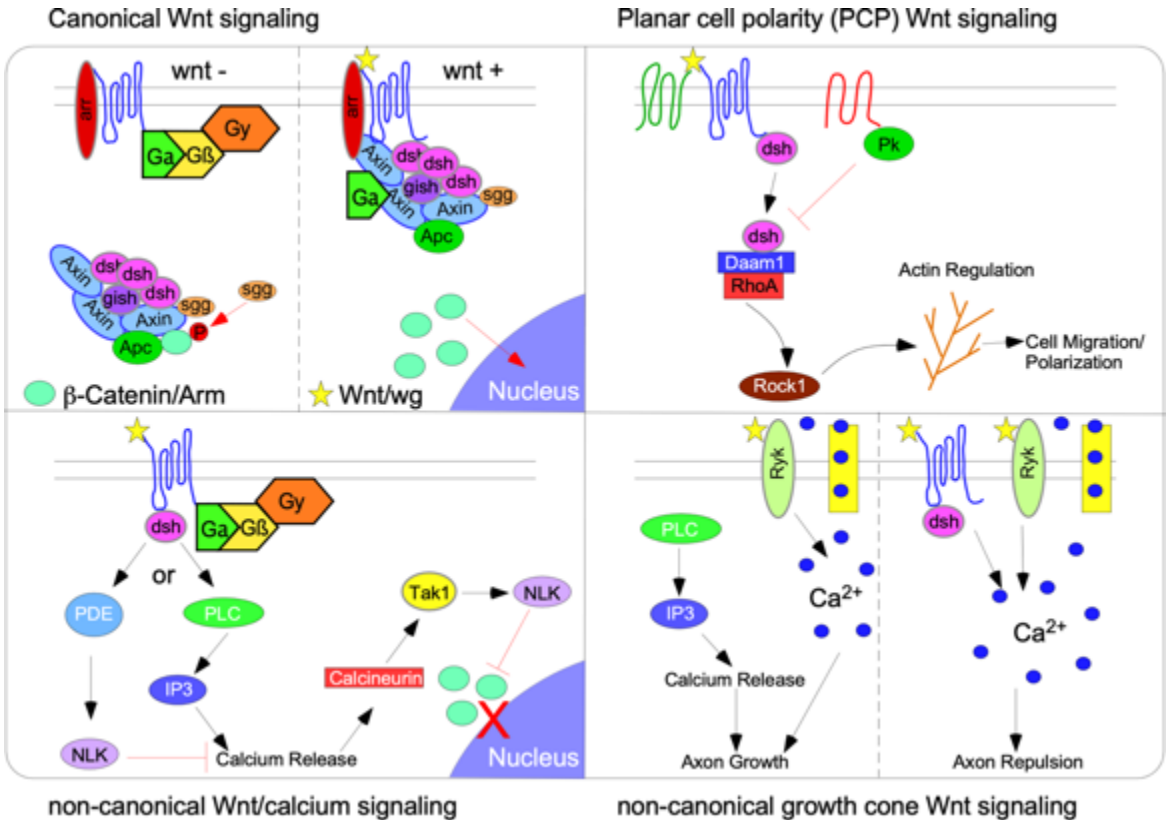

Figure 1-8. Canonical and non-canonical Wnt signaling pathways: Wnt signaling pathways are subdivided into canonical and non-canonical classifications. The classically studied canonical pathway converges downstream on the transcription factor β-catenin. Other examples shown include the planar cell polarity which establishes polarity across tissues, non-canonical calcium signaling, as well as a co-opted calcium signaling pathway that functions in axonal growth cones. In each of the examples given the extracellular Wnt ligand is noted with a yellow star.

patch of branched actin at the anterior side of the epithelial cell. However, in counteraction to this anterior signaling there is a negative regulation at the posterior end of a neighboring epithelial cell that acts to block dsh recruitment. In this way, differential recruitment of signaling molecules to the anterior and posterior sides of epithelial cell is established across an entire tissue. The regulation of the actin cytoskeleton is one way in which PCP modulates cellular cytoskeletal networks. Another role for PCP is to help establish microtubule directional bias through Prickle

isoforms in the Drosophila wing (Olofsson, Sharp, Matis, Cho, & Axelrod, 2014). Yet another role for PCP has been shown to help produce specialized cilium in other cell types such as mammalian multiciliated cells of the lungs (Vladar, Lee, Stearns, & Axelrod, 2015). These two examples showcase another connection between Wnt signaling and microtubules.

Recently, other Wnt signaling variants have been uncovered. One such pathway is a non-canonical Wnt signaling pathway that results in the release of Endoplasmic Reticulum (ER) sequestered calcium through PLC and IP3 (Figure7) (Saneyoshi, Kume, Amasaki, & Mikoshiba, 2002; Slusarski, Yang-Snyder, Busa, & Moon, 1997). The calcium released activates calcineurin to eventually block beta catenin's translocation into the nucleus independent of the destruction complex regulation of the same. In growing axons, a modified version of this pathway functions at the tip of the growth cone (Hutchins, Li, & Kalil, 2012). At the tip a dual regulation occurs wherein at high levels of internal calcium produced by calcium influx from channels opened by the Ryk receptor in addition to internal calcium release, axon growth is initiated. However, at lower internal cytoplasmic calcium levels the growth cone experiences a repulsive cue. Both of these seem to happen together to help with the directional growth of neuronal axons.

Although variants of Wnt signaling have been shown to function in neurons and help to modulate the microtubule plus-end or lattice stability, there has never been a connection between Wnt signaling and regulation of microtubule nucleation in neurons. The discovery that Apc and Apc2 engage in a microtubule polarity regulatory mechanism was surprising but not unprecedented. Apc and Apc2 both act in canonical Wnt signaling and the same proteins work together in the steering complex. In addition, two studies have linked the canonical Wnt signaling scaffolding protein Axin to the recruitment of γTub to the centrosome and spindle (Fumoto, Kadono, Izumi, & Kikuchi, 2009; He et al., 2016). With this in mind, it is unclear whether Axin performs a similar role and if this role is downstream of Wnt signaling in post mitotic cells such as neurons.

Endosomes and Wnt Signaling

Membranes, endosomes and Wnt signaling have been linked through various mechanisms (Brunt & Scholpp, 2018). Once bound to a ligand fz receptors are eventually internalized via clathrin mediated endocytosis into Rab5 early endosomes, which usually progress in one of three ways. One route is that the endosome may mature into a Rab7 late endosome which eventually fuses with the lysosome and degrades the proteins. Another route is through two types of recycling events. These can be slow through Rab11 endosomes or fast through Rab4 endosomes depending on a cell's need for receptor density at the plasma membrane (Brunt & Scholpp, 2018). With either recycling event the receptor is eventually brought back to the membrane to be able to bind another Wnt. The classic view of receptor internalization is to modulate the signaling pathway and shut off the signal. However, in some circumstances receptors do not stop signaling once internalized (Calebiro, Nikolaev, Persani, & Lohse, 2010). Whether cell surface receptors are involved in positioning nucleation sites remains to be determined. However, recycling endosomes have been shown to help recruit nucleation machinery to the spindle during mitosis (Hehnly & Doxsey, 2014). This implies that there is at least some connection between endosomes and γTub. Whether endosomes are involved in nucleation site recruitment in neurons remains to be seen.

Lingering Questions

It is clear that much has been discovered concerning the regulation of the microtubule cytoskeleton. However, many questions remain and because the microtubule cytoskeleton is vital to neuronal capabilities, we chose to focus on how microtubules are controlled in neurons. Additionally, due to the complex compartmentalization of neuronal cells we further subdivided

our study to examine how microtubule regulation occurs in dendrites. It was proposed that the steering complex functions at branch points but the mechanism had not been pinpointed to the branch point. Furthermore, the way in which Apc2, a key component to localize the steering complex member Apc to branch points, concentrated to branch points in the first place was left unknown. As stated before, it has been observed that microtubule nucleation machinery also enriches at branch points. However, the mechanism to localize these acentrosomal nucleation sites remains unknown. Due to the multiplicity of proteins involved in Apc2 branch point targeting we surmised that γTub might share some of the components to localize at the same location. Moreover, because nucleation sites are typically tethered to an MTOC we asked which site at the branch point might be acting as an organizing center.

Based on the results described in the chapters of this work, considerable contributions are made to the fields of neuronal cell biology and microtubule regulation. We verify that dendritic branch points function as hubs of microtubule regulation. The microtubule steering complex does not act by pre-bundling microtubules but acts specifically at branch points to resolve microtubule collisions. Additionally, Apc2 requires a diverse group of proteins to localize to branch points and γTub shares a common group with Apc2. This group includes members of canonical Wnt signaling. Finally, we help alleviate a longstanding debate within the field and reconcile previous results concerning Golgi outpost mediated nucleation in dendrites. We identify a population of specialized Rab5 endosomes that act as acentrosomal MTOCs and demonstrate these endosomes were mislabeled as Golgi fragments in previous studies.

References:

Akhmanova, A., & Steinmetz, M. O. (2019). Microtubule minus-end regulation at a glance. *J Cell Sci, 132*(11). doi:10.1242/jcs.227850

Alonso, A., Zaidi, T., Novak, M., Grundke-Iqbal, I., & Iqbal, K. (2001). Hyperphosphorylation induces self-assembly of tau into tangles of paired helical filaments/straight filaments. *Proc Natl Acad Sci U S A, 98*(12), 6923-6928. doi:10.1073/pnas.121119298

Ambrose, J. C., & Wasteneys, G. O. (2008). CLASP modulates microtubule-cortex interaction during self-organization of acentrosomal microtubules. *Mol Biol Cell, 19*(11), 4730-4737. doi:10.1091/mbc.E08-06-0665

Axelrod, J. D. (2019). Planar cell polarity signaling in the development of left-right asymmetry. *Curr Opin Cell Biol, 62*, 61-69. doi:10.1016/j.ceb.2019.09.002

Baas, P. W., Deitch, J. S., Black, M. M., & Banker, G. A. (1988). Polarity orientation of microtubules in hippocampal neurons: uniformity in the axon and nonuniformity in the dendrite. *Proc Natl Acad Sci U S A, 85*(21), 8335-8339. doi:10.1073/pnas.85.21.8335

Baas, P. W., & Lin, S. (2011). Hooks and comets: The story of microtubule polarity orientation in the neuron. *Dev Neurobiol, 71*(6), 403-418. doi:10.1002/dneu.20818

Baas, P. W., White, L. A., & Heidemann, S. R. (1987). Microtubule polarity reversal accompanies regrowth of amputated neurites. *Proc Natl Acad Sci U S A, 84*(15), 5272-5276. doi:10.1073/pnas.84.15.5272

Baas, P. W., & Yu, W. (1996). A composite model for establishing the microtubule arrays of the neuron. *Mol Neurobiol, 12*(2), 145-161. doi:10.1007/BF02740651

Babic, M., Russo, G. J., Wellington, A. J., Sangston, R. M., Gonzalez, M., & Zinsmaier, K. E. (2015). Miro's N-terminal GTPase domain is required for transport of mitochondria into axons and dendrites. *J Neurosci, 35*(14), 5754-5771. doi:10.1523/JNEUROSCI.1035-14.2015

Bienz, M., & Clevers, H. (2000). Linking colorectal cancer to Wnt signaling. *Cell, 103*(2), 311-320. doi:10.1016/s0092-8674(00)00122-7

Blagodatski, A., Poteryaev, D., & Katanaev, V. L. (2014). Targeting the Wnt pathways for therapies. *Mol Cell Ther, 2*, 28. doi:10.1186/2052-8426-2-28

Bodakuntla, S., Jijumon, A. S., Villablanca, C., Gonzalez-Billault, C., & Janke, C. (2019). Microtubule-Associated Proteins: Structuring the Cytoskeleton. *Trends Cell Biol, 29*(10), 804-819. doi:10.1016/j.tcb.2019.07.004

Brocardo, M., Lei, Y., Tighe, A., Taylor, S. S., Mok, M. T., & Henderson, B. R. (2008). Mitochondrial targeting of adenomatous polyposis coli protein is stimulated by truncating cancer mutations: regulation of Bcl-2 and implications for cell survival. *J Biol Chem, 283*(9), 5950-5959. doi:10.1074/jbc.M708775200

Brouhard, G. J., Stear, J. H., Noetzel, T. L., Al-Bassam, J., Kinoshita, K., Harrison, S. C., . . . Hyman, A. A. (2008). XMAP215 is a processive microtubule polymerase. *Cell, 132*(1), 79-88. doi:10.1016/j.cell.2007.11.043

Brunt, L., & Scholpp, S. (2018). The function of endocytosis in Wnt signaling. *Cell Mol Life Sci, 75*(5), 785-795. doi:10.1007/s00018-017-2654-2

Calebiro, D., Nikolaev, V. O., Persani, L., & Lohse, M. J. (2010). Signaling by internalized G-protein-coupled receptors. *Trends Pharmacol Sci, 31*(5), 221-228. doi:10.1016/j.tips.2010.02.002

Cao, L., Wang, L., Zheng, M., Cao, H., Ding, L., Zhang, X., & Fu, Y. (2013). Arabidopsis AUGMIN subunit8 is a microtubule plus-end binding protein that promotes microtubule reorientation in hypocotyls. *Plant Cell, 25*(6), 2187-2201. doi:10.1105/tpc.113.113472

Chaaban, S., & Brouhard, G. J. (2017). A microtubule bestiary: structural diversity in tubulin polymers. *Mol Biol Cell, 28*(22), 2924-2931. doi:10.1091/mbc.E16-05-0271

Chen, Buchwalter, R. A., Kao, L. R., & Megraw, T. L. (2017). A Splice Variant of Centrosomin Converts Mitochondria to Microtubule-Organizing Centers. *Curr Biol, 27*(13), 1928-1940 e1926. doi:10.1016/j.cub.2017.05.090

Chen, L., Nye, D. M., Stone, M. C., Weiner, A. T., Gheres, K. W., Xiong, X., . . . Rolls, M. M. (2016). Mitochondria and Caspases Tune Nmnat-Mediated Stabilization to Promote Axon Regeneration. *PLoS Genet, 12*(12), e1006503. doi:10.1371/journal.pgen.1006503

Chen, L., Stone, M. C., Tao, J., & Rolls, M. M. (2012). Axon injury and stress trigger a microtubule-based neuroprotective pathway. *Proc Natl Acad Sci U S A, 109*(29), 11842-11847. doi:10.1073/pnas.1121180109

Choi, Y. K., Liu, P., Sze, S. K., Dai, C., & Qi, R. Z. (2010). CDK5RAP2 stimulates microtubule nucleation by the gamma-tubulin ring complex. *J Cell Biol, 191*(6), 1089-1095. doi:10.1083/jcb.201007030

Cleveland, D. W., Hwo, S. Y., & Kirschner, M. W. (1977). Purification of tau, a microtubule-associated protein that induces assembly of microtubules from purified tubulin. *J Mol Biol, 116*(2), 207-225. doi:10.1016/0022-2836(77)90213-3

Cunha-Ferreira, I., Chazeau, A., Buijs, R. R., Stucchi, R., Will, L., Pan, X., . . . Hoogenraad, C. C. (2018). The HAUS Complex Is a Key Regulator of Non-centrosomal Microtubule Organization during Neuronal Development. *Cell Rep, 24*(4), 791-800. doi:10.1016/j.celrep.2018.06.093

Curcio, M., & Bradke, F. (2015). Microtubule Organization in the Axon: TRIM46 Determines the Orientation. *Neuron, 88*(6), 1072-1074. doi:10.1016/j.neuron.2015.12.006

Dehmelt, L., & Halpain, S. (2005). The MAP2/Tau family of microtubule-associated proteins. *Genome Biol, 6*(1), 204. doi:10.1186/gb-2004-6-1-204

del Castillo, U., Winding, M., Lu, W., & Gelfand, V. I. (2015). Interplay between kinesin-1 and cortical dynein during axonal outgrowth and microtubule organization in Drosophila neurons. *Elife, 4*, e10140. doi:10.7554/eLife.10140

Desai, A., & Mitchison, T. J. (1997). Microtubule polymerization dynamics. *Annu Rev Cell Dev Biol, 13*, 83-117. doi:10.1146/annurev.cellbio.13.1.83

Elliott, A., & Shaw, S. L. (2018). Update: Plant Cortical Microtubule Arrays. *Plant Physiol, 176*(1), 94-105. doi:10.1104/pp.17.01329

Ems-McClung, S. C., & Walczak, C. E. (2010). Kinesin-13s in mitosis: Key players in the spatial and temporal organization of spindle microtubules. *Semin Cell Dev Biol, 21*(3), 276-282. doi:10.1016/j.semcdb.2010.01.016

Feng, C., Thyagarajan, P., Shorey, M., Seebold, D. Y., Weiner, A. T., Albertson, R. M., . . . Rolls, M. M. (2019). Patronin-mediated minus end growth is required for dendritic microtubule polarity. *J Cell Biol, 218*(7), 2309-2328. doi:10.1083/jcb.201810155

Fiedler, M., Mendoza-Topaz, C., Rutherford, T. J., Mieszczanek, J., & Bienz, M. (2011). Dishevelled interacts with the DIX domain polymerization interface of Axin to interfere with its function in down-regulating beta-catenin. *Proc Natl Acad Sci U S A, 108*(5), 1937-1942. doi:10.1073/pnas.1017063108

Fu, M. M., McAlear, T. S., Nguyen, H., Oses-Prieto, J. A., Valenzuela, A., Shi, R. D., . . . Barres, B. A. (2019). The Golgi Outpost Protein TPPP Nucleates Microtubules and Is Critical for Myelination. *Cell, 179*(1), 132-146 e114. doi:10.1016/j.cell.2019.08.025

Fumoto, K., Kadono, M., Izumi, N., & Kikuchi, A. (2009). Axin localizes to the centrosome and is involved in microtubule nucleation. *EMBO Rep, 10*(6), 606-613. doi:10.1038/embor.2009.45

Gao, C., & Chen, Y. G. (2010). Dishevelled: The hub of Wnt signaling. *Cell Signal, 22*(5), 717-727. doi:10.1016/j.cellsig.2009.11.021

Goshima, G., Mayer, M., Zhang, N., Stuurman, N., & Vale, R. D. (2008). Augmin: a protein complex required for centrosome-independent microtubule generation within the spindle. *J Cell Biol, 181*(3), 421-429. doi:10.1083/jcb.200711053

Goshima, G., Wollman, R., Goodwin, S. S., Zhang, N., Scholey, J. M., Vale, R. D., & Stuurman, N. (2007). Genes required for mitotic spindle assembly in Drosophila S2 cells. *Science, 316*(5823), 417-421. doi:10.1126/science.1141314

Hagemann, A. I., Kurz, J., Kauffeld, S., Chen, Q., Reeves, P. M., Weber, S., . . . Scholpp, S. (2014). In vivo analysis of formation and endocytosis of the Wnt/beta-catenin signaling complex in zebrafish embryos. *J Cell Sci, 127*(Pt 18), 3970-3982. doi:10.1242/jcs.148767

Harterink, M., Edwards, S. L., de Haan, B., Yau, K. W., van den Heuvel, S., Kapitein, L. C., . . . Hoogenraad, C. C. (2018). Local microtubule organization promotes cargo transport in C. elegans dendrites. *J Cell Sci, 131*(20). doi:10.1242/jcs.223107

Harterink, M., Vocking, K., Pan, X., Soriano Jerez, E. M., Slenders, L., Freal, A., . . . Hoogenraad, C. C. (2019). TRIM46 Organizes Microtubule Fasciculation in the Axon Initial Segment. *J Neurosci, 39*(25), 4864-4873. doi:10.1523/JNEUROSCI.3105-18.2019

Hayden, J. H., Bowser, S. S., & Rieder, C. L. (1990). Kinetochores capture astral microtubules during chromosome attachment to the mitotic spindle: direct visualization in live newt lung cells. *J Cell Biol, 111*(3), 1039-1045. doi:10.1083/jcb.111.3.1039

He, X. Q., Song, Y. Q., Liu, R., Liu, Y., Zhang, F., Zhang, Z., . . . Wang, H. L. (2016). Axin-1 Regulates Meiotic Spindle Organization in Mouse Oocytes. *PLoS One, 11*(6), e0157197. doi:10.1371/journal.pone.0157197

Heald, R., & Khodjakov, A. (2015). Thirty years of search and capture: The complex simplicity of mitotic spindle assembly. *J Cell Biol, 211*(6), 1103-1111. doi:10.1083/jcb.201510015

Hehnly, H., & Doxsey, S. (2014). Rab11 endosomes contribute to mitotic spindle organization and orientation. *Dev Cell, 28*(5), 497-507. doi:10.1016/j.devcel.2014.01.014

Heidemann, S. R., Landers, J. M., & Hamborg, M. A. (1981). Polarity orientation of axonal microtubules. *J Cell Biol, 91*(3 Pt 1), 661-665. doi:10.1083/jcb.91.3.661

Hendershott, M. C., & Vale, R. D. (2014). Regulation of microtubule minus-end dynamics by CAMSAPs and Patronin. *Proc Natl Acad Sci U S A, 111*(16), 5860-5865. doi:10.1073/pnas.1404133111

Hill, S. E., Parmar, M., Gheres, K. W., Guignet, M. A., Huang, Y., Jackson, F. R., & Rolls, M. M. (2012). Development of dendrite polarity in Drosophila neurons. *Neural Dev, 7*, 34. doi:10.1186/1749-8104-7-34

Holy, T. E., & Leibler, S. (1994). Dynamic instability of microtubules as an efficient way to search in space. *Proc Natl Acad Sci U S A, 91*(12), 5682-5685. doi:10.1073/pnas.91.12.5682

Hutchins, B. I., Li, L., & Kalil, K. (2012). Wnt-induced calcium signaling mediates axon growth and guidance in the developing corpus callosum. *Sci Signal, 5*(206), pt1. doi:10.1126/scisignal.2002523

Jiang, K., Hua, S., Mohan, R., Grigoriev, I., Yau, K. W., Liu, Q., . . . Akhmanova, A. (2014). Microtubule minus-end stabilization by polymerization-driven CAMSAP deposition. *Dev Cell, 28*(3), 295-309. doi:10.1016/j.devcel.2014.01.001

Jiang, K., Toedt, G., Montenegro Gouveia, S., Davey, N. E., Hua, S., van der Vaart, B., . . . Akhmanova, A. (2012). A Proteome-wide screen for mammalian SxIP motif-containing microtubule plus-end tracking proteins. *Curr Biol, 22*(19), 1800-1807. doi:10.1016/j.cub.2012.07.047

Jimbo, T., Kawasaki, Y., Koyama, R., Sato, R., Takada, S., Haraguchi, K., & Akiyama, T. (2002). Identification of a link between the tumour suppressor APC and the kinesin superfamily. *Nat Cell Biol, 4*(4), 323-327. doi:10.1038/ncb779

Kadavath, H., Hofele, R. V., Biernat, J., Kumar, S., Tepper, K., Urlaub, H., . . . Zweckstetter, M. (2015). Tau stabilizes microtubules by binding at the interface between tubulin heterodimers. *Proc Natl Acad Sci U S A, 112*(24), 7501-7506. doi:10.1073/pnas.1504081112

Kalinina, I., Nandi, A., Delivani, P., Chacon, M. R., Klemm, A. H., Ramunno-Johnson, D., . . . Tolic-Norrelykke, I. M. (2013). Pivoting of microtubules around the spindle pole accelerates kinetochore capture. *Nat Cell Biol, 15*(1), 82-87. doi:10.1038/ncb2640

Kapitein, L. C., Schlager, M. A., Kuijpers, M., Wulf, P. S., van Spronsen, M., MacKintosh, F. C., & Hoogenraad, C. C. (2010). Mixed microtubules steer dynein-driven cargo transport into dendrites. *Curr Biol, 20*(4), 290-299. doi:10.1016/j.cub.2009.12.052

Khanal, I., Elbediwy, A., Diaz de la Loza, M. D. C., Fletcher, G. C., & Thompson, B. J. (2017). Correction: Shot and Patronin polarise microtubules to direct membrane traffic and biogenesis of microvilli in epithelia. *J Cell Sci, 130*(13), 2221. doi:10.1242/jcs.206912

Kilmartin, J. V. (2014). Lessons from yeast: the spindle pole body and the centrosome. *Philos Trans R Soc Lond B Biol Sci, 369*(1650). doi:10.1098/rstb.2013.0456

Kirschner, M., & Mitchison, T. (1986). Beyond self-assembly: from microtubules to morphogenesis. *Cell, 45*(3), 329-342. doi:10.1016/0092-8674(86)90318-1

Kleele, T., Marinkovic, P., Williams, P. R., Stern, S., Weigand, E. E., Engerer, P., . . . Misgeld, T. (2014). An assay to image neuronal microtubule dynamics in mice. *Nat Commun, 5*, 4827. doi:10.1038/ncomms5827

Koester, M. P., Muller, O., & Pollerberg, G. E. (2007). Adenomatous polyposis coli is differentially distributed in growth cones and modulates their steering. *J Neurosci, 27*(46), 12590-12600. doi:10.1523/JNEUROSCI.2250-07.2007

Lansbergen, G., Grigoriev, I., Mimori-Kiyosue, Y., Ohtsuka, T., Higa, S., Kitajima, I., . . . Akhmanova, A. (2006). CLASPs attach microtubule plus ends to the cell cortex through a complex with LL5beta. *Dev Cell, 11*(1), 21-32. doi:10.1016/j.devcel.2006.05.012

Leask, A., Obrietan, K., & Stearns, T. (1997). Synaptically coupled central nervous system neurons lack centrosomal gamma-tubulin. *Neurosci Lett, 229*(1), 17-20. doi:10.1016/s0304-3940(97)00412-6

Lee, H. H., Jan, L. Y., & Jan, Y. N. (2009). Drosophila IKK-related kinase Ik2 and Katanin p60-like 1 regulate dendrite pruning of sensory neuron during metamorphosis. *Proc Natl Acad Sci U S A, 106*(15), 6363-6368. doi:10.1073/pnas.0902051106

Lerit, D. A., Jordan, H. A., Poulton, J. S., Fagerstrom, C. J., Galletta, B. J., Peifer, M., & Rusan, N. M. (2015). Interphase centrosome organization by the PLP-Cnn scaffold is required for centrosome function. *J Cell Biol, 210*(1), 79-97. doi:10.1083/jcb.201503117

Lim, A., Rechtsteiner, A., & Saxton, W. M. (2017). Two kinesins drive anterograde neuropeptide transport. *Mol Biol Cell, 28*(24), 3542-3553. doi:10.1091/mbc.E16-12-0820

Logan, C. Y., & Nusse, R. (2004). The Wnt signaling pathway in development and disease. *Annu Rev Cell Dev Biol, 20*, 781-810. doi:10.1146/annurev.cellbio.20.010403.113126

Luchtenborg, A. M., Solis, G. P., Egger-Adam, D., Koval, A., Lin, C., Blanchard, M. G., . . . Katanaev, V. L. (2014). Heterotrimeric Go protein links Wnt-Frizzled signaling with ankyrins to regulate the neuronal microtubule cytoskeleton. *Development, 141*(17), 3399-3409. doi:10.1242/dev.106773

Magidson, V., O'Connell, C. B., Loncarek, J., Paul, R., Mogilner, A., & Khodjakov, A. (2011). The spatial arrangement of chromosomes during prometaphase facilitates spindle assembly. *Cell, 146*(4), 555-567. doi:10.1016/j.cell.2011.07.012

Maniar, T. A., Kaplan, M., Wang, G. J., Shen, K., Wei, L., Shaw, J. E., . . . Bargmann, C. I. (2011). UNC-33 (CRMP) and ankyrin organize microtubules and localize kinesin to polarize axon-dendrite sorting. *Nat Neurosci, 15*(1), 48-56. doi:10.1038/nn.2970

Mattie, F. J., Stackpole, M. M., Stone, M. C., Clippard, J. R., Rudnick, D. A., Qiu, Y., . . . Rolls, M. M. (2010). Directed microtubule growth, +TIPs, and kinesin-2 are required for uniform microtubule polarity in dendrites. *Curr Biol, 20*(24), 2169-2177. doi:10.1016/j.cub.2010.11.050

Milo, R., & Phillips, R. (2016). *Cell biology by the numbers*. New York, NY: Garland Science, Taylor & Francis Group.

Mimori-Kiyosue, Y., Shiina, N., & Tsukita, S. (2000a). Adenomatous polyposis coli (APC) protein moves along microtubules and concentrates at their growing ends in epithelial cells. *J Cell Biol, 148*(3), 505-518. doi:10.1083/jcb.148.3.505

Mimori-Kiyosue, Y., Shiina, N., & Tsukita, S. (2000b). The dynamic behavior of the APC-binding protein EB1 on the distal ends of microtubules. *Curr Biol, 10*(14), 865-868. doi:10.1016/s0960-9822(00)00600-x

Mitchison, T., & Kirschner, M. (1984). Dynamic instability of microtubule growth. *Nature, 312*(5991), 237-242. doi:10.1038/312237a0

Montcouquiol, M., & Kelley, M. W. (2019). Development and Patterning of the Cochlea: From Convergent Extension to Planar Polarity. *Cold Spring Harb Perspect Med*. doi:10.1101/cshperspect.a033266

Moores, C. A., & Milligan, R. A. (2006). Lucky 13-microtubule depolymerisation by kinesin-13 motors. *J Cell Sci, 119*(Pt 19), 3905-3913. doi:10.1242/jcs.03224

Moritz, M., Braunfeld, M. B., Sedat, J. W., Alberts, B., & Agard, D. A. (1995). Microtubule nucleation by gamma-tubulin-containing rings in the centrosome. *Nature, 378*(6557), 638-640. doi:10.1038/378638a0

Mustyatsa, V. V., Boyakhchyan, A. V., Ataullakhanov, F. I., & Gudimchuk, N. B. (2017). EB-Family Proteins: Functions and Microtubule Interaction Mechanisms. *Biochemistry (Mosc), 82*(7), 791-802. doi:10.1134/S0006297917070045

Nguyen, M. M., McCracken, C. J., Milner, E. S., Goetschius, D. J., Weiner, A. T., Long, M. K., . . . Rolls, M. M. (2014). Gamma-tubulin controls neuronal microtubule polarity independently of Golgi outposts. *Mol Biol Cell, 25*(13), 2039-2050. doi:10.1091/mbc.E13-09-0515

Nguyen, M. M., Stone, M. C., & Rolls, M. M. (2011). Microtubules are organized independently of the centrosome in Drosophila neurons. *Neural Dev, 6*, 38. doi:10.1186/1749-8104-6-38

Nusse, R., & Clevers, H. (2017). Wnt/beta-Catenin Signaling, Disease, and Emerging Therapeutic Modalities. *Cell, 169*(6), 985-999. doi:10.1016/j.cell.2017.05.016

Oddoux, S., Zaal, K. J., Tate, V., Kenea, A., Nandkeolyar, S. A., Reid, E., . . . Ralston, E. (2013). Microtubules that form the stationary lattice of muscle fibers are dynamic and nucleated at Golgi elements. *J Cell Biol, 203*(2), 205-213. doi:10.1083/jcb.201304063

Olofsson, J., Sharp, K. A., Matis, M., Cho, B., & Axelrod, J. D. (2014). Prickle/spiny-legs isoforms control the polarity of the apical microtubule network in planar cell polarity. *Development, 141*(14), 2866-2874. doi:10.1242/dev.105932

Ori-McKenney, K. M., Jan, L. Y., & Jan, Y. N. (2012). Golgi outposts shape dendrite morphology by functioning as sites of acentrosomal microtubule nucleation in neurons. *Neuron, 76*(5), 921-930. doi:10.1016/j.neuron.2012.10.008

Pack-Chung, E., Kurshan, P. T., Dickman, D. K., & Schwarz, T. L. (2007). A Drosophila kinesin required for synaptic bouton formation and synaptic vesicle transport. *Nat Neurosci, 10*(8), 980-989. doi:10.1038/nn1936

Pearson, C. G. (2014). Choosing sides--asymmetric centriole and basal body assembly. *J Cell Sci, 127*(Pt 13), 2803-2810. doi:10.1242/jcs.151761

Peng, L. X., Hsu, M. T., Bonomi, M., Agard, D. A., & Jacobson, M. P. (2014). The free energy profile of tubulin straight-bent conformational changes, with implications for microtubule assembly and drug discovery. *PLoS Comput Biol, 10*(2), e1003464. doi:10.1371/journal.pcbi.1003464

Petry, S., Groen, A. C., Ishihara, K., Mitchison, T. J., & Vale, R. D. (2013). Branching microtubule nucleation in Xenopus egg extracts mediated by augmin and TPX2. *Cell, 152*(4), 768-777. doi:10.1016/j.cell.2012.12.044

Purro, S. A., Ciani, L., Hoyos-Flight, M., Stamatakou, E., Siomou, E., & Salinas, P. C. (2008). Wnt regulates axon behavior through changes in microtubule growth directionality: a new role for adenomatous polyposis coli. *J Neurosci, 28*(34), 8644-8654. doi:10.1523/JNEUROSCI.2320-08.2008

Rao, & Kuhl, M. (2010). An updated overview on Wnt signaling pathways: a prelude for more. *Circ Res, 106*(12), 1798-1806. doi:10.1161/CIRCRESAHA.110.219840

Rao, Patil, A., Black, M. M., Craig, E. M., Myers, K. A., Yeung, H. T., & Baas, P. W. (2017). Cytoplasmic Dynein Transports Axonal Microtubules in a Polarity-Sorting Manner. *Cell Rep, 19*(11), 2210-2219. doi:10.1016/j.celrep.2017.05.064

Rieder, C. L., & Alexander, S. P. (1990). Kinetochores are transported poleward along a single astral microtubule during chromosome attachment to the spindle in newt lung cells. *J Cell Biol, 110*(1), 81-95. doi:10.1083/jcb.110.1.81

Rios, R. M. (2014). The centrosome-Golgi apparatus nexus. *Philos Trans R Soc Lond B Biol Sci, 369*(1650). doi:10.1098/rstb.2013.0462

Rios-Esteves, J., & Resh, M. D. (2013). Stearoyl CoA desaturase is required to produce active, lipid-modified Wnt proteins. *Cell Rep, 4*(6), 1072-1081. doi:10.1016/j.celrep.2013.08.027

Roll-Mecak, A., & Vale, R. D. (2008). Structural basis of microtubule severing by the hereditary spastic paraplegia protein spastin. *Nature, 451*(7176), 363-367. doi:10.1038/nature06482

Roostalu, J., Thomas, C., Cade, N. I., Kunzelmann, S., Taylor, I. A., & Surrey, T. (2020). The speed of GTP hydrolysis determines GTP cap size and controls microtubule stability. *Elife, 9*. doi:10.7554/eLife.51992

Sanchez, A. D., & Feldman, J. L. (2017). Microtubule-organizing centers: from the centrosome to non-centrosomal sites. *Curr Opin Cell Biol, 44*, 93-101. doi:10.1016/j.ceb.2016.09.003

Sanchez-Huertas, C., Freixo, F., Viais, R., Lacasa, C., Soriano, E., & Luders, J. (2016). Non-centrosomal nucleation mediated by augmin organizes microtubules in post-mitotic neurons and controls axonal microtubule polarity. *Nat Commun, 7*, 12187. doi:10.1038/ncomms12187

Sanders, A. A., & Kaverina, I. (2015). Nucleation and Dynamics of Golgi-derived Microtubules. *Front Neurosci, 9*, 431. doi:10.3389/fnins.2015.00431

Saneyoshi, T., Kume, S., Amasaki, Y., & Mikoshiba, K. (2002). The Wnt/calcium pathway activates NF-AT and promotes ventral cell fate in Xenopus embryos. *Nature, 417*(6886), 295-299. doi:10.1038/417295a

Satoh, D., Sato, D., Tsuyama, T., Saito, M., Ohkura, H., Rolls, M. M., . . . Uemura, T. (2008). Spatial control of branching within dendritic arbors by dynein-dependent transport of Rab5-endosomes. *Nat Cell Biol, 10*(10), 1164-1171. doi:10.1038/ncb1776

Segal, M., & Bloom, K. (2001). Control of spindle polarity and orientation in Saccharomyces cerevisiae. *Trends Cell Biol, 11*(4), 160-166. doi:10.1016/s0962-8924(01)01954-7

Sharp, D. J., Yu, W., Ferhat, L., Kuriyama, R., Rueger, D. C., & Baas, P. W. (1997). Identification of a microtubule-associated motor protein essential for dendritic differentiation. *J Cell Biol, 138*(4), 833-843. doi:10.1083/jcb.138.4.833

Shintani, T., Ihara, M., Tani, S., Sakuraba, J., Sakuta, H., & Noda, M. (2009). APC2 plays an essential role in axonal projections through the regulation of microtubule stability. *J Neurosci, 29*(37), 11628-11640. doi:10.1523/JNEUROSCI.2394-09.2009

Sloboda, R. D., Rudolph, S. A., Rosenbaum, J. L., & Greengard, P. (1975). Cyclic AMP-dependent endogenous phosphorylation of a microtubule-associated protein. *Proc Natl Acad Sci U S A, 72*(1), 177-181. doi:10.1073/pnas.72.1.177

Slusarski, D. C., Yang-Snyder, J., Busa, W. B., & Moon, R. T. (1997). Modulation of embryonic intracellular Ca2+ signaling by Wnt-5A. *Dev Biol, 182*(1), 114-120. doi:10.1006/dbio.1996.8463

Starr, D. A. (2017). Muscle Development: Nucleating Microtubules at the Nuclear Envelope. *Curr Biol, 27*(19), R1071-R1073. doi:10.1016/j.cub.2017.08.030

Stepanova, T., Slemmer, J., Hoogenraad, C. C., Lansbergen, G., Dortland, B., De Zeeuw, C. I., . . . Galjart, N. (2003). Visualization of microtubule growth in cultured neurons via the use of EB3-GFP (end-binding protein 3-green fluorescent protein). *J Neurosci, 23*(7), 2655-2664. Retrieved from https://www.ncbi.nlm.nih.gov/pubmed/12684451

Stiess, M., Maghelli, N., Kapitein, L. C., Gomis-Ruth, S., Wilsch-Brauninger, M., Hoogenraad, C. C., . . . Bradke, F. (2010). Axon extension occurs independently of centrosomal microtubule nucleation. *Science, 327*(5966), 704-707. doi:10.1126/science.1182179

Stone, M. C., Roegiers, F., & Rolls, M. M. (2008). Microtubules have opposite orientation in axons and dendrites of Drosophila neurons. *Mol Biol Cell, 19*(10), 4122-4129. doi:10.1091/mbc.E07-10-1079

Tanaka, K., Mukae, N., Dewar, H., van Breugel, M., James, E. K., Prescott, A. R., . . . Tanaka, T. U. (2005). Molecular mechanisms of kinetochore capture by spindle microtubules. *Nature, 434*(7036), 987-994. doi:10.1038/nature03483

Tao, J., Feng, C., & Rolls, M. M. (2016). The microtubule-severing protein fidgetin acts after dendrite injury to promote their degeneration. *J Cell Sci, 129*(17), 3274-3281. doi:10.1242/jcs.188540

Tas, R. P., Chazeau, A., Cloin, B. M. C., Lambers, M. L. A., Hoogenraad, C. C., & Kapitein, L. C. (2017). Differentiation between Oppositely Oriented Microtubules Controls Polarized Neuronal Transport. *Neuron, 96*(6), 1264-1271 e1265. doi:10.1016/j.neuron.2017.11.018

Tovey, C. A., & Conduit, P. T. (2018). Microtubule nucleation by gamma-tubulin complexes and beyond. *Essays Biochem, 62*(6), 765-780. doi:10.1042/EBC20180028

van Beuningen, S. F. B., Will, L., Harterink, M., Chazeau, A., van Battum, E. Y., Frias, C. P., . . . Hoogenraad, C. C. (2015). TRIM46 Controls Neuronal Polarity and Axon Specification by Driving the Formation of Parallel Microtubule Arrays. *Neuron, 88*(6), 1208-1226. doi:10.1016/j.neuron.2015.11.012

Vemu, A., Szczesna, E., Zehr, E. A., Spector, J. O., Grigorieff, N., Deaconescu, A. M., & Roll-Mecak, A. (2018). Severing enzymes amplify microtubule arrays through lattice GTP-tubulin incorporation. *Science, 361*(6404). doi:10.1126/science.aau1504

Villarroel-Campos, D., Henriquez, D. R., Bodaleo, F. J., Oguchi, M. E., Bronfman, F. C., Fukuda, M., & Gonzalez-Billault, C. (2016). Rab35 Functions in Axon Elongation Are Regulated by P53-Related Protein Kinase in a Mechanism That Involves Rab35 Protein Degradation and the Microtubule-Associated Protein 1B. *J Neurosci, 36*(27), 7298-7313. doi:10.1523/JNEUROSCI.4064-15.2016

Vladar, E. K., Antic, D., & Axelrod, J. D. (2009). Planar cell polarity signaling: the developing cell's compass. *Cold Spring Harb Perspect Biol, 1*(3), a002964. doi:10.1101/cshperspect.a002964

Vladar, E. K., Lee, Y. L., Stearns, T., & Axelrod, J. D. (2015). Observing planar cell polarity in multiciliated mouse airway epithelial cells. *Methods Cell Biol, 127*, 37-54. doi:10.1016/bs.mcb.2015.01.016

Vladar, E. K., & Stearns, T. (2007). Molecular characterization of centriole assembly in ciliated epithelial cells. *J Cell Biol, 178*(1), 31-42. doi:10.1083/jcb.200703064

Waschke, J., & Drenckhahn, D. (2000). Uniform apicobasal polarity of microtubules and apical location of gamma-tubulin in polarized intestinal epithelium in situ. *Eur J Cell Biol, 79*(5), 317-326. doi:10.1078/s0171-9335(04)70035-7

Weiner, A. T., Seebold, D. Y., Torres-Gutierrez, P., Folker, C., Swope, R. D., Kothe, G. O., . . . Rolls, M. M. (2020). Endosomal Wnt signaling proteins control microtubule nucleation in dendrites. *PLoS Biol, 18*(3), e3000647. doi:10.1371/journal.pbio.3000647

Weingarten, M. D., Lockwood, A. H., Hwo, S. Y., & Kirschner, M. W. (1975). A protein factor essential for microtubule assembly. *Proc Natl Acad Sci U S A, 72*(5), 1858-1862. doi:10.1073/pnas.72.5.1858

Woodruff, J. B., Wueseke, O., & Hyman, A. A. (2014). Pericentriolar material structure and dynamics. *Philos Trans R Soc Lond B Biol Sci, 369*(1650). doi:10.1098/rstb.2013.0459

Wu, J., & Akhmanova, A. (2017). Microtubule-Organizing Centers. *Annu Rev Cell Dev Biol, 33*, 51-75. doi:10.1146/annurev-cellbio-100616-060615

Yalgin, C., Ebrahimi, S., Delandre, C., Yoong, L. F., Akimoto, S., Tran, H., . . . Moore, A. W. (2015). Centrosomin represses dendrite branching by orienting microtubule nucleation. *Nat Neurosci, 18*(10), 1437-1445. doi:10.1038/nn.4099

Yu, W., Cook, C., Sauter, C., Kuriyama, R., Kaplan, P. L., & Baas, P. W. (2000). Depletion of a microtubule-associated motor protein induces the loss of dendritic identity. *J Neurosci, 20*(15), 5782-5791. Retrieved from https://www.ncbi.nlm.nih.gov/pubmed/10908619

Zebrowski, D. C., Vergarajauregui, S., Wu, C. C., Piatkowski, T., Becker, R., Leone, M., . . . Engel, F. B. (2015). Developmental alterations in centrosome integrity contribute to the post-mitotic state of mammalian cardiomyocytes. *Elife, 4*. doi:10.7554/eLife.05563

Zheng, Y., Wildonger, J., Ye, B., Zhang, Y., Kita, A., Younger, S. H., . . . Jan, Y. N. (2008). Dynein is required for polarized dendritic transport and uniform microtubule orientation in axons. *Nat Cell Biol, 10*(10), 1172-1180. doi:10.1038/ncb1777

Zhou, M. N., Kunttas-Tatli, E., Zimmerman, S., Zhouzheng, F., & McCartney, B. M. (2011). Cortical localization of APC2 plays a role in actin organization but not in Wnt signaling in Drosophila. *J Cell Sci, 124*(Pt 9), 1589-1600. doi:10.1242/jcs.073916

Zhu, X., & Kaverina, I. (2013). Golgi as an MTOC: making microtubules for its own good. *Histochem Cell Biol, 140*(3), 361-367. doi:10.1007/s00418-013-1119-4

Introduction to Chapter 2

Chapter 2 comprises a published story in the journal Cytoskeleton in January of 2016. It is shown in its unaltered form as the publication appears online. Supplemental figure 1 is provided as an addendum to the thesis for reference. I am the first author on the manuscript and there are supporting contributions by Michael Lanz and Daniel Goetschius. The formation of the manuscript was co-supervised by William Hancock and Melissa Rolls. The manuscript was written entirely by Melissa Rolls. The majority of the microtubule polarity experiments were performed by myself, Michael, and Daniel by combined effort to produce datasets. During data generation I first overlapped with Michael Lanz when we both worked as research technicians in Melissa Rolls' lab. During this time, Michael and I conducted the blind experiments that make up the major claims of the manuscript. Next, I overlapped with Daniel Goetschius in the same role. Daniel performed the imaging of the Jupiter construct to visualize stable microtubule tracks. By the end of my employment in the summer of 2015 most of the experiments were complete. I entered graduate school in the fall of 2015 and decided to spend my final lab rotation in the Rolls lab.

During my rotation I generated the final dataset which is the final figure of the manuscript. Once this dataset was complete, I then helped design all of the figures included in the manuscript and helped prepare it for submission. The story contributes to the overall thesis because it is a follow-up story to the first characterization of the microtubule steering complex by Dr. Floyd Mattie and describes the biological significance of regulator Apc2, which is the focus of chapter 3. The contribution to the field of neuronal microtubule polarity is that this chapter confirms the branch point as the unique site of microtubule steering and regulation left over as a remaining question following Dr. Mattie's thesis.

Chapter 2

Kinesin-2 and Apc function at dendrite branch points to resolve microtubule collisions.

Abstract

In Drosophila neurons, kinesin-2, EB1 and Apc are required to maintain minus-end-out dendrite microtubule polarity, and we previously proposed they steer microtubules at branch points. Motor-mediated steering of microtubule plus ends could be accomplished in two ways: 1) by linking a growing microtubule tip to the side of an adjacent microtubule as it navigates the branch point (bundling), or 2) by directing a growing microtubule after a collision with a stable microtubule (collision resolution). Using live imaging to distinguish between these two mechanisms, we found that reduction of kinesin-2 did not alter the number of microtubules that grew along the edge of the branch points where stable microtubules are found. However, reduction of kinesin-2 or Apc did affect the number of microtubules that slowed down or depolymerized as they encountered the side of the branch opposite to the entry point. These results are consistent with kinesin-2 functioning with Apc to resolve collisions. However, they do not pinpoint stable microtubules as the collision partner as stable microtubules are typically very close to the membrane. To determine whether growing microtubules were steered along stable ones after a collision, we analyzed the behavior of growing microtubules at dendrite crossroads where stable microtubules run through the middle of the branch point. In control neurons, microtubules turned in the middle of the crossroads. However, when kinesin-2 was reduced some

microtubules grew straight through the branch point and failed to turn. We propose that kinesin-2 functions to steer growing microtubules along stable ones following collisions.

Introduction

All neuronal mRNAs and most proteins are made in the cell body. These new materials must supply parts of the cell that may be hundreds of microns to more than a meter away. Neuronal microtubules serve as both the tracks and signposts for this long-distance transport. Cargo that is hitched to a motor protein in the cell body can be destined for either axons or dendrites. Motor proteins walk along microtubules towards either the plus or minus end; most kinesins walk towards the plus, or growing end, and dynein walks towards the minus end. Thus, microtubule polarity can be read like a signpost by motor proteins.

Axonal microtubules in animals including C. elegans, Drosophila, and mice have plus ends directed away from the cell body (Baas and Lin 2011; Rolls and Jegla 2015). This means that kinesins carry cargo from the site of synthesis in the cell body into the axon, and dynein is the major retrograde motor (Hirokawa et al. 2010). Dendrites are a little more complicated. In mammalian neurons, dendritic microtubules have mixed polarity with about half minus-end-out and half plus-end-out orientation (Baas et al. 1988; Stepanova et al. 2003). This means that either kinesins (Hirokawa et al. 2010; Jenkins et al. 2012) or dynein (Kapitein et al. 2010) can act as anterograde motors to take cargo into dendrites. In Drosophila, neurons start off with mixed microtubules in dendrites (Hill et al. 2012), but mature neurons have 90% or more minus-end-out microtubules (Stone et al. 2008). C. elegans neurons have similar internal organization with largely minus-end-out dendritic microtubules (Goodwin et al. 2012; Yan et al. 2013). This more extreme difference in axonal and dendritic polarity in invertebrate neurons emphasizes the importance of dynein as a dendritic motor; an interpretation that is supported by severe dendrite

growth and trafficking defects in dynein mutants (Liu et al. 2000; Satoh et al. 2008; Zheng et al. 2008). It also led us to think about the relationship between dendrite branching and microtubule organization.

Dendrites, including Drosophila dendrites with minus-end-out microtubules, are often highly branched. We realized that for uniform microtubule polarity to be maintained in branched dendrites, the direction of microtubule growth must be controlled at branch points; if microtubules were allowed to grow in any direction when they encountered a branch junction, some would grow away from the cell body and result in a plus-end-out microtubule. When we examined growing microtubules navigating branch points, we observed that almost all turned towards the cell body (Mattie et al. 2010). Based on phenotypic analysis, protein-protein interactions and protein localization we proposed a model for directed growth of microtubules through branch points. Reduction of any of the three subunits of kinesin-2, Klp64D, Klp68D or Kap3, resulted in mixed polarity in dendrites. Based on an interaction between Kap3 and Apc in mammalian cells (Jimbo et al. 2002), we tested whether the Drosophila homologs interact, and whether Apc was required for microtubule polarity. A summary of protein-protein interactions identified in our study is shown in Figure 1B. All of these proteins, Apc, Apc2 and EB1 are required to maintain polarity like kinesin-2 (Mattie et al. 2010). In addition Apc2-GFP localizes strongly to dendrite branch points (Figure 1A) and can recruit Apc there (Mattie et al. 2010). We therefore hypothesized that the microtubule plus end-binding protein (+TIP), EB1, links the end of growing microtubules to kinesin-2 through Apc. This would allow growing microtubules to be directed along stable ones, and since kinesins walk towards microtubule plus ends, the growing microtubules would be forced into the same orientation as existing microtubules.

Although this model is satisfying and fits with the phenotypic analysis, we were not able at that time to directly demonstrate that this complex functioned at branch points, and several important questions remained. First, the association of +TIPs with microtubule plus ends is very

transient (Chen et al. 2014; Dixit et al. 2009; Maurer et al. 2014), and so it was not clear that sufficient force could be transferred through this temporary cloud of +TIPs to steer one microtubule along another. In vitro reconstitution of microtubule steering using kinesins linked to +TIPs demonstrated that the proposed mechanism is sufficient to steer growing microtubules along stable ones (Chen et al. 2014; Doodhi et al. 2014). Second, the initial in vivo study left open two alternate mechanisms by which kinesin-2 might steer microtubules through branch points. The motor could pull the growing microtubule along the side of a stable one, bundling the two together in parallel orientation (Figure 1C). Alternately, the motor might only engage with a stable microtubule to determine the direction of growth after a collision (Figure 1C). In this study our goal was to determine whether we could pinpoint the activity of the kinesin-2-+TIP complex to branch points, and to determine whether this complex acts to bundle microtubules, to resolve collisions, or both.

Results

Microtubule turning and Apc-RFP comets are consistent with kinesin-2 and +TIP function at branch points.

Our first goal was to determine whether we could find direct evidence for kinesin-2 functioning with +TIPs at dendrite branch points. We previously showed that in the comb dendrite of ddaE neurons (Figure 1A), RNA hairpins targeting any of the three kinesin-2 subunits resulted in mixed polarity, and that mutant and RNAi phenotypes are similar (Mattie et al. 2010). These neurons are sensory neurons in the body wall of Drosophila that have a fairly simple and stereotyped branching pattern (Grueber et al. 2002). In addition, the close to right angle branches mean that they are more reliant on kinesin-2 to maintain polarity than dendrites with more acute

branch angles (Mattie et al. 2010). To determine whether mixed polarity in these dendrites is associated with misdirection of growing microtubules as they traverse branch points, we monitored the pattern of microtubule growth at branch points in control and Klp64D RNAi ddaE neurons. Growing microtubules were labeled with low levels of EB1-GFP; high levels of this transgene can have dominant-negative effects (Mattie et al. 2010). Timelapse movies of EB1-GFP comets moving through the comb dendrite were analyzed and comets that passed through a branch point were scored as either turning towards the cell body or away from the cell body. In control neurons, almost all microtubules grew towards the cell body at the branch point, while in Klp64D RNAi neurons more than half turned away from the cell body (Figure 2A and B). This result is consistent with kinesin-2 functioning at dendrite branch points.

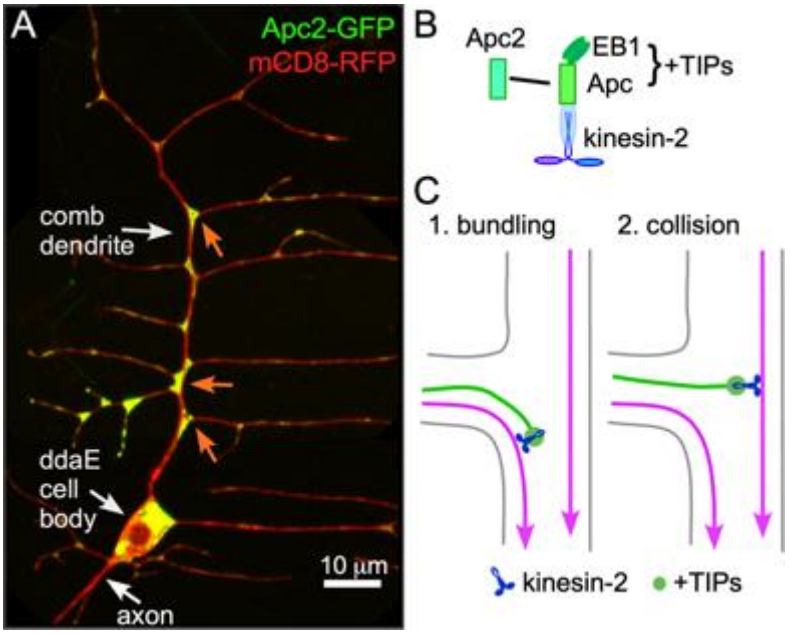

Figure 2-1. Dendrite branch points and microtubule steering.

The shape of the ddaE dendrite arbor and localization of Apc2-GFP is shown in A. The dorsal comb-shaped dendrite was used for imaging experiments. Apc2-GFP is highly concentrated at dendrite branch points (orange arrows). B. A summary of interactions between +TIPs and kinesin-2 is shown. C. Kinesin-2 and +TIPs could direct microtubule growth in two different ways: the complex could link the growing microtubule end to the sides of neighboring microtubules (bundling) or it could function when the growing ends of free microtubules collide with the side of a microtubule (collision). In either scenario the outcome would be that stable microtubules guide growing ones towards the cell body at dendrite branch points.

Drosophila Apc can bind to both kinesin-2 and EB1 (Mattie et al. 2010), potentially positioning it as the linker

between the growing plus end and the motor. We therefore imaged Apc-RFP to see if it might track microtubule plus ends. Without extra expression of Apc2, very little Apc-RFP is present in dendrites (Mattie et al. 2010). We therefore expressed Apc-RFP with Apc2-GFP. In some cases we could see spots of Apc-RFP moving through branch points at the speed expected for growing microtubules (Figure 2C). Although consistent with our model, these events were rare, so we wished to use other approaches to determine whether and how this complex functions at branch points.

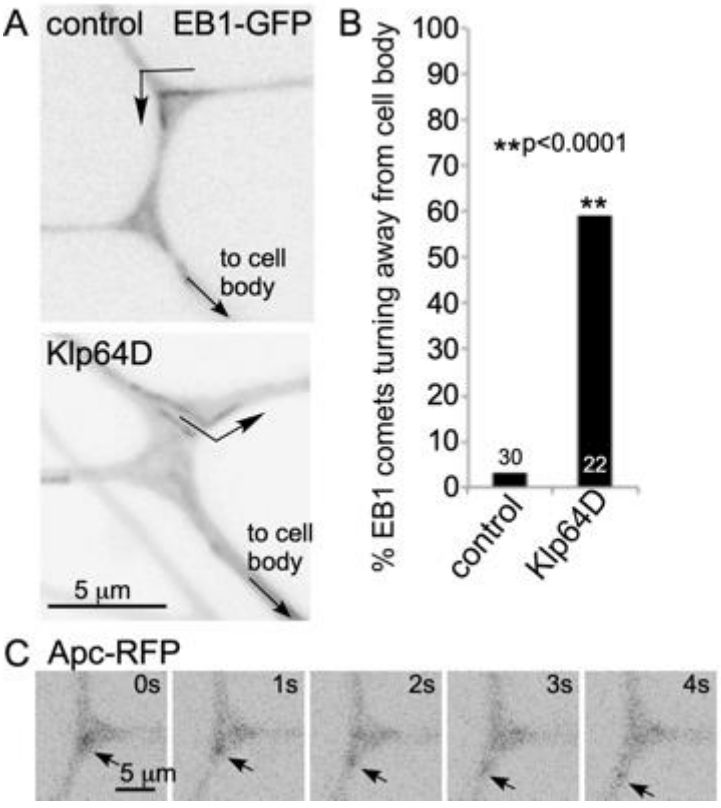

Figure 2-2. Behavior of tagged +TIPs at branch points.

A. EB1-GFP was used to track growing microtubule in the comb dendrite of ddaE in control (Rtnl2) RNAi and Klp64D RNAi neurons. Maximum projections of timeseries movies are shown and the tracks of individual microtubules through the branch points are marked with arrows. In all images the cell body is at the bottom. B. Comets were scored based on whether they turned towards the cell body or away from it at branch points. The numbers of the bars in the graph are the number of comets scored. A Fisher's exact test was performed to determine statistical significance. C. Apc-RFP was expressed with Apc2-GFP and live imaging of the RFP channel was performed. An example of an Apc-RFP comet moving through a branch point is shown.

Kinesin-2 does not influence the number of growing microtubules that cross branch points in smooth arcs.

One way that kinesin-2 and +TIPs could guide growing microtubules towards the cell body is by bundling the growing tip along existing microtubules (Figure 1C). To test this idea we first needed to map the pattern of stable regions of microtubules in branch points. We expressed Jupiter-RFP (Cabernard and Doe 2009), a microtubule-associated protein (MAP) and imaged its distribution in living ddaE neurons. Jupiter localizes similarly to other MAPs, including tau, Drosophila cells, and like these MAPs that bind to stable regions of microtubules is highly expressed in neurons (Karpova et al. 2006). Almost all branch points had microtubules running in smooth arcs along the outside edges and meeting in a sharp V at the cell body side of the branch (Figure 3A). This is

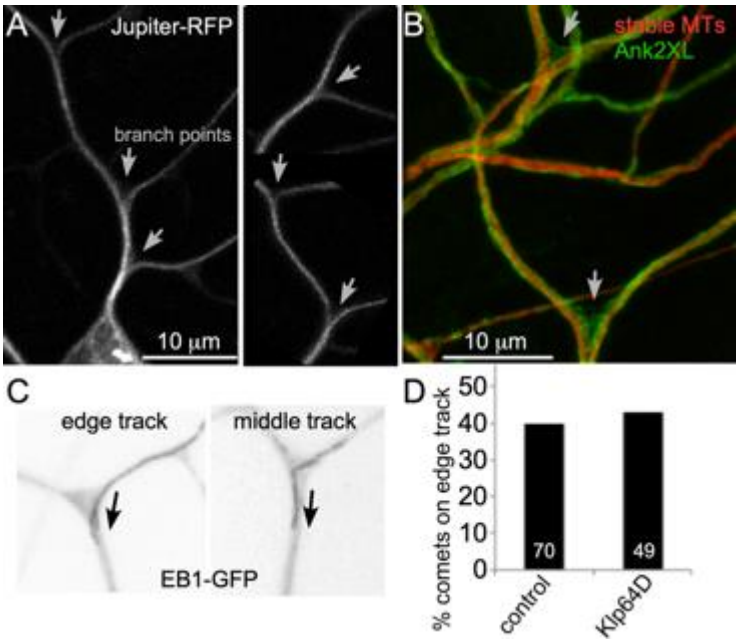

Figure 2-3. Kinesin-2 does not influence the number of microtubules that track the position of stable microtubules in branch points.

A and B. Stable microtubules in da neurons were visualized in live animals expressing Jupiter-RFP (A) or fixed animals stained with anti-futsch (B). Fixed animals were also stained with anti-Ank2XL antibodies to outline the cell by labeling the submembrane skeleton. C and D. Maximum projection images of EB1-GFP comets traveling through branch points were generated to determine whether they followed the edge of the branch where stable microtubules lie or go through the middle of the branch. Examples of both types of paths are shown in C. Based on these projections, comets in control (Rtnl2) RNAi and Klp64D RNAi neurons were classified as either tracking along the edge of the branch or not; the numbers in the graph are the ones that moved along the edge of the branch point and the remainder moved through the middle of the branch (D). Numbers of comets analyzed are indicated on the bars.

similar to the pattern of stable microtubules we previously observed with endogenous GFP-labeled tau (Stone et al. 2008). To ensure that this V pattern represented the overall distribution of stable microtubules and was not specific to the tagged Jupiter, we also performed immunostaining of fixed and fileted larvae. Because we were detecting endogenous futsch, a microtubule-associated protein that binds stable microtubules and is similar to MAP1B (Hummel et al. 2000), all neurons in the body wall are observed. Again, stable regions of microtubules can be seen to arc smoothly along the edges of branch points (Figure 3B). Co-staining for Ankyrin2 allowed us to visualize neuron shape. In many of the branch points, microtubules occupy only the edge leaving open space in the middle that does not contain stable microtubules (see the schematic in Figure 1C).

Using this information about the layout of stable microtubules in branch points, we classified EB1-GFP comets into i) those that took paths along the edge of the branch point where stable microtubules are found ii) and those that entered the middle of the branch away from stable microtubules. For this analysis we only considered comets that turned from a side branch into the main dendrite trunk of the ddaE comb dendrite. We distinguished these two classes based on time projections of comet movement through the branch point (Figure 3C). In control animals, about 40% of comets that passed through a branch point did so in a smooth arc along the outer edge, and this number was unchanged in Klp64D RNAi neurons (Figure 3D), although this RNAi had a strong effect on turning direction (Figure 2B). Thus kinesin-2 is not required for growing microtubules to travel along the outside of branch points where stable microtubules are found.

Kinesin-2 and Apc prevent microtubule growth from slowing when the microtubule encounters the edge of a branch point.

As we found no evidence that kinesin-2 guides growing microtubules along stable ones, we tested whether there were other parameters of microtubule growth through branch points that depended on the motor. One possibility we examined was that interaction with the motor might change the speed at which the microtubule grew through the branch point. We therefore generated kymographs to track individual comets through time and marked the point at which the comet contacted the opposite branch wall with a white line (Figures S1A and 4B). Comets moving at constant speed appear as a straight diagonal line on a kymograph, and changes in speed are seen as a change the angle of the line. The speed change for comets passing through a branch point was calculated from the difference in angles (Figure S1B). We separated the data into two pools based on the origin point of the comet: from a side branch versus within the main trunk of the comb dendrite. The set of comets originating from a side branch was also analyzed in Figure 3D; here we break down the behavior based on speed rather than path through the branch. The trajectory of comets within the main trunk tended to be quite straight, while the ones arising in the periphery typically had to turn more as they navigated the branch point. The majority of microtubules growing within the dendrite trunk did not change speed in branch points, and this did not change in Klp64D RNAi neurons (Figure S1B and 4A). However, for the set of microtubules that had to turn more as they entered the trunk from the periphery, the average speed decreased in Klp64D RNAi neurons (Figure S1B). When we binned microtubules into categories (no change, decrease in speed or increase in speed), we could see that the overall decrease in velocity was due to more comets slowing down in the branch points in Klp64D RNAi neurons than in control neurons (Figure 4A).

To understand where microtubules were slowing down in the absence of kinesin-2 we analyzed the position of stalling, which includes microtubules that slowed down and microtubules

that depolymerized. We used two different control RNAi hairpins, as well as RNAi hairpins that targeted kinesin-2 subunits and Apc. In all genotypes roughly 20% of comets that entered the branch point stalled in the middle (Figure 4C). In control neurons 15-20% of the comets that

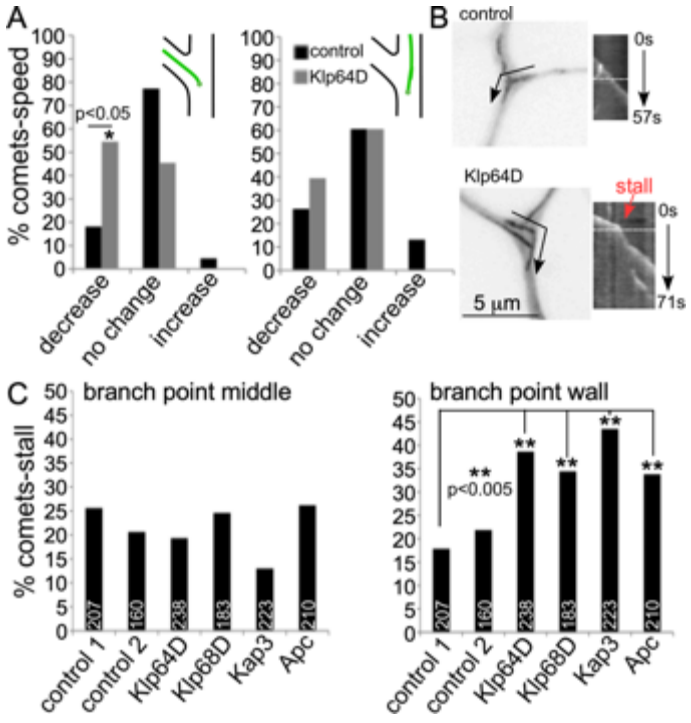

Figure 2-4. Kinesin-2 and Apc are required for a subset of microtubules to grow through branch points without stalling.

A. Speed changes of microtubules growing from peripheral processes were measured through branch points (left graph), and the same was done for microtubules in the main trunk (right graph). Numbers of microtubules analyzed for control RNAi (Rtnl1) and Klp64D RNAi were the same, 22 comets of each genotype were analyzed for the left graph, and 38 for the right graph. B. Examples of microtubule behavior seen with EB1-GFP comets are shown in time projections and kymographs. The white line indicates the time when the comet encountered the edge of the branch point opposite to the point of entry. C. EB1-GFP comet behavior was analyzed in six different RNAi conditions. Control 1 is Rtnl2 and control 2 is □-tubulin37C RNAi. Klp64D, Klp68D and Kap3 are the three subunits of kinesin-2. Comets that entered the branch point from a peripheral dendrite were categorized based on whether they changed speed, and for the ones that slowed this was further broken down into the position where the change occurred. The number of microtubules analyzed for each genotype is shown above the bars. A Fisher's exact test was used to determine statistical significance for each type of behavior. Only decrease at the edge was altered by reducing kinesin-2 and Apc. The significance shown on the graph is a comparison to control 1, but the differences were significant when compared to either control.

entered the branch stalled close near the wall of the branch point opposite to the side of entry (Figure 4C). However, when any of the kinesin-2 subunits or Apc was targeted by RNAi, this number increased to 35-45% of the total. This result suggests that kinesin-2 and Apc function when a growing microtubule collides with a structure near the wall of the branch point; in the absence of kinesin-2 more of these collisions result in slowed or terminated microtubule growth.

Kinesin-2 steers microtubules at dendrite crossroads.

In V-shaped branch points, stable microtubules run along the edge close to the plasma membrane. It was therefore not possible to distinguish between growing plus ends colliding with the side of stable microtubules versus with the membrane or submembrane skeleton. While most branches along the main trunk of the ddaE comb dendrite were V-shaped, some of these neurons also contained 4-way or crossroad branch points (Figure 5A). Jupiter-RFP labeled stable microtubules ran through the middle of these crossroads (Figure 5A). In branch points with this geometry the stable tracks are therefore spatially separated from the plasma membrane.

To further characterize the layout of microtubules in crossroad branch points, we took advantage of EB1 labeled with GFP at an internal site rather than at the C-terminus (EB1int-GFP). EB1 has a low affinity for the microtubule lattice (Berrueta et al. 1998; Morrison et al. 1998), and the C-terminally tagged EB1-GFP used to label growing plus ends also has low background fluorescence along stable microtubules. However, when we generated transgenic flies that expressed a different tagged version of EB1 with the GFP inserted into a loop before the C-terminus, microtubules were often labeled quite clearly. This labeling provided further confirmation that in crossroad branch points, microtubules often ran through the middle (Figure 5B). There were also often smaller bundles of microtubules that ran along the outside edge of the branch point as in V-shaped branch points (Figure 5B).

We hypothesized that if kinesin-2 acted to steer growing microtubules along stable ones after a collision, then EB1-GFP comets would turn in the middle of crossroads at the stable track.

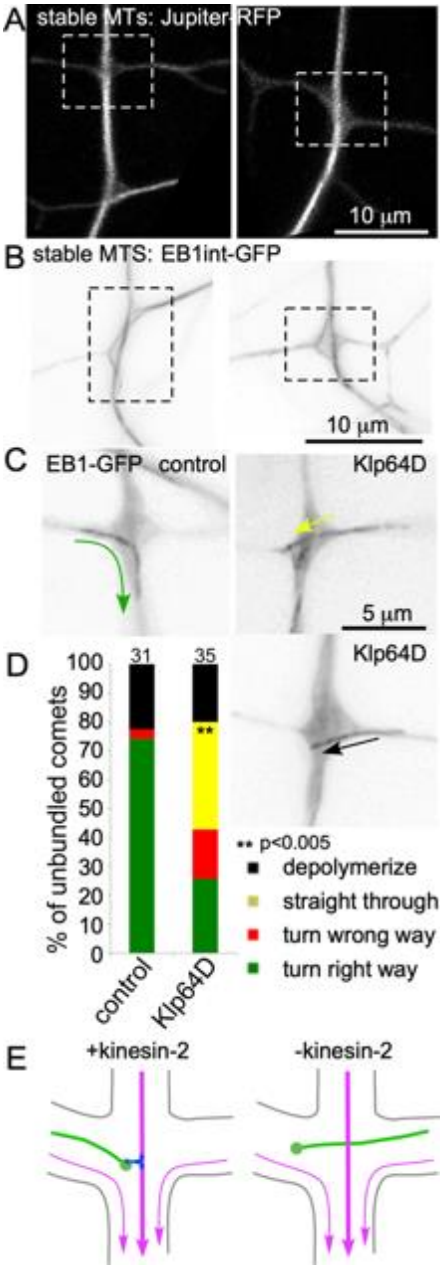

Figure 2-5. Microtubule behavior at dendrite crossroads.

The layout of stable microtubules at 4-way or crossroad branch points in ddaE comb dendrites was visualized in living animals either with Jupiter-RFP (A) or EB1int-GFP (B). C. Examples of EB1-GFP comet behavior at dendrite branch points are shown. The green arrow tracks a microtubule that turns towards the cell body; a yellow arrow indicates a microtubule that grows across the crossroad from one peripheral branch to the other, and the black arrow tracks a microtubule that depolymerizes in the branch point. The percentages of these types of behavior in control (Rtnl2) and Klp64D RNAi are shown in D. Only comets that entered the middle area of the branch were considered for this analysis. Numbers of comets analyzed for each genotype are shown above the bars. A chi-squared test was used to compare the distribution of all 4 outcomes between the two genotypes; the p value was less than 0.0001. In addition, a Fisher's exact test was used to specifically compare the "straight through" outcome between the two genotypes and the p vale was less than 0.005. E. Diagrams of the behavior of microtubules growing through crossroads are shown.

We selected dendrites that contained crossroads and performed live imaging of EB1-GFP. Of the microtubules that entered from a side process, and that did not hug the outside edge of the branch

point, many turned towards the cell body, often turning before reaching the far side of the branch point (Figure 5C and D). When we compared the behavior of EB1-GFP comets in crossroads of control neurons and Klp64D RNAi neurons, the most striking difference was a population of microtubules that grew straight through the crossroads only in the absence of Klp64D (Figure 5D). There was a corresponding reduction of microtubules that turned into the main branch. This result suggests that in the presence of kinesin-2 growing microtubules that encountered stable tracks in the middle of the crossroads can steer into the main dendrite trunk (Figure 5E). In the absence of kinesin-2, this encounter would be more likely to be non-productive and the microtubule would proceed straight through the crossroad (Figure 5E).

Discussion

In this study we analyzed stable and growing microtubules at dendrite branch points to determine how kinesin-2 and +TIPs contribute to dendritic microtubule organization. Our previous phenotypic analysis suggested that these proteins were likely to control microtubule polarity by controlling the direction of growth at branch points, but left open two modes of action: aligning parallel microtubules or resolving microtubule collisions. We found no evidence that kinesin-2 helps growing microtubules to bundle in parallel. Instead, we found that when kinesin-2 or Apc levels were reduced, more microtubules slowed or stopped growing when they encountered the back wall of the branch point. By taking advantage of crossroad branch points, we pinpointed the key difference in microtubule behavior in the absence of kinesin-2: fewer microtubules were directed along the bundles in the motor's absence, and instead microtubules grew straight through the intersections.

In many differentiated cells microtubules take on specific arrangements that are essential to cellular organization and function (Bartolini and Gundersen 2006). Lateral interactions

between microtubules are used in a number of different scenarios to generate aligned bundles. In mammalian neurons, tau and MAP2 generate microtubule bundles with characteristic spacing in axons and dendrites (Chen et al. 1992). As muscle cells differentiate, microtubules align into an array parallel with the long axis of the cell. An isoform of MAP4, oMAP4, is required for this alignment (Mogessie et al. 2015). Using in vitro experiments with purified oMAP4 and dynamic microtubules, it was shown that oMAP4 acts to zipper together microtubules that encounter one another at shallow angles, but not wider angles (Mogessie et al. 2015). Similar angle-dependent zippering has been observed in the plant cortical microtubule array (Dixit and Cyr 2004). This zippering behavior is quite distinct from that facilitated by kinesin and +TIP complexes, which allow microtubules that grow into one another at wide angles to become aligned (Chen et al. 2014; Doodhi et al. 2014). Our data support the idea that kinesin-2 works with +TIPs in vivo to resolve microtubule collisions rather than to mediate lateral interactions.

Motor proteins do, however, also mediate lateral interactions between microtubules in vivo. In neurons, kinesin-6 is important for arranging antiparallel microtubules characteristic of mammalian dendrites (Lin et al. 2012; Sharp et al. 1997; Yu et al. 2000). Kinesins-5 and -12 also regulate microtubules in mammalian neurons (Liu et al. 2010), probably by limiting sliding forces of microtubules against one another generated by other motors (Myers and Baas 2007). One of the motors that generates sliding forces during early neurite extension in Drosophila neurons is kinesin-1 (Lu et al. 2013), which is also important for microtubule organization in C. elegans neurons (Yan et al. 2013). In all of these examples of kinesin actions on neuronal microtubules, microtubules are lined up against one another either in parallel or anti-parallel, and the motors mediate lateral interactions. This type of motor activity is quite different from the resolution of collisions between non-aligned microtubules by kinesin-2.

The mode of kinesin-2 action at dendrite branch points is perhaps most similar to entry of growing microtubules into dendritic spines mediated by interactions between microtubules and

actin (Merriam et al. 2013). However, because motor proteins are quite ubiquitous regulators of microtubule organization, and because specific arrangements of microtubules are required in many cell types, we anticipate that guidance of growing microtubules by motors at the plus end will be discovered in other contexts as well.

Materials and Methods

Drosophila lines

Standard genetic methods were used to generate lines containing multiple transgenes. Transgenic lines used in this study include: UAS-Apc2-GFP and UAS-Dicer2 from the Bloomington Drosophila Stock Center, 221-Gal4 from Dr. Wes Grueber,

For EB1 comet assays in da neurons, line containing UAS-Dicer2; 221-Gal4, UAS-EB1-GFP/TM6 was crossed with RNAi lines from the Vienna Drosophila RNAi Center (VDRC). The RNAi lines used as controls were Rtnl2 RNAi (#33320) and γ-tubulin37C (a maternal γ-tubulin not expressed in somatic cells (Wiese 2008)) RNAi (#25271). We have previously validated these as controls (Chen et al. 2012; Mattie et al. 2010). Other RNAi lines from VDRC were: Klp64D (#45373), Klp68D (#27943), Kap3 (#45400), and Apc (#51469). Larvae were grown on standard fly media consisting of cornmeal, yeast, dextrose, sucrose, and agar. Caps of food with fly embryos were collected every 24h and aged 3 days at 25ºC. On the third day imaging experiments were performed.

Generation of EB1int-GFP transgenic flies

N-terminal and C-terminal fragments of Drosophila EB1 were amplified from cDNA. The N-terminal EB1 fragment (amino acids 1-257) was cloned into pUAST containing 3 copies of Emerald GFP with EcoRI and KpnI. The N-terminal part of EB1 replaced the first GFP coding sequence. The C-terminal EB1 fragment (amino acids 258-291) was then cloned using AgeI and XbaI to replace the third GFP. The result was the coding sequence of Emerald GFP inserted between amino acids 257 and 258 of EB1. Injections of the plasmid into Drosophila embryos to generate transgenics ere performed by BestGene.

Live imaging of Drosophila larvae

Third instar larvae were selected from their food cap and washed in PBS. They were then transferred to a circle of dried agarose on a microscope slide. Once a larva oriented with its dorsal side up and started to move, a 22x40 mm coverslip was anchored on top of it with sticky tape. Larvae were imaged with a Zeiss ImagerM2 with a Colibri LED light source, Zeiss LSM510 confocal microscope, or an Olympus FV1000 confocal microscope. Timeseries of ddaE neurons were acquired for 300 frames at one frame per second. After images were collected, they were analyzed in ImageJ. Each movie was inverted and aligned using the TurboReg plugin (http://bigwww.epfl.ch/thevenaz/turboreg/ (Thevenaz et al. 1998)) to reduce the impact of larva movement. Comets moving through branch points were selected for analysis.

Immunofluorescence of Drosophila larvae

Third instar larvae were dissected to generate body wall filets, and then fixed in 4% paraformaldehyde. Staining was performed as described (Koch et al. 2008) using rabbit anti-

Ank2XL at 1:1000. Microtubules were stained with the 22C10 primary antibody (1:100 mouse anti-futsch, from the Developmental Studies Hybridoma Bank). Goat secondary antibodies were obtained from Jackson ImmunoResearch.

Blind analysis of EB1 comet behavior.

Using Microsoft Excel, random IDs were assigned to each EB1 comet analyzed in the experiment in Figure 3B and C. From each comet, a maximum projection plot of the path through the branch point was generated in ImageJ, a line was drawn on this, and a kymograph was generated from the line (shown in Figure S1). The time when the comet encountered the far side of the branch point was indicated on the kymograph by deleting a frame, which then leaves a line at this point in the kymograph. The shape of the maximum projection path (edge track or middle track) was determined without knowing the genotype of the animal. Velocity measurements (Figures 4 and S1) were made using the kymographs (see Figure S1).

Measurement of comet speed

The velocity change was calculated from the slope of the line generated by the comet in a kymograph before and after it encountered the back of the branch point (see diagram in Figure S1). Each slope was calculated as an angle drawn using the line tool in ImageJ. In Excel, the formula, =((TAN(RADIANS(90-ABS(slope before))))/9.767)-((TAN(RADIANS(90-ABS(slope after))))/9.767) was used to convert the slopes into a velocity difference (Figure S1). Velocities were subsequently binned into categories: increase in velocity, a decrease, or no change (Figure 4A).

Position of stalling in a branch point

Every comet in the dendrite that entered a branch point along the main backbone of the ddaE comb was analyzed. The behavior of comets was binned into three categories: those that depolymerized or slowed at the back wall, those that depolymerized or slowed anywhere else in the branch point, and those that did not slow down as they traveled through the branch.

Analysis of comet behavior at crossroads

ddaE neurons containing 4-way branch points were selected at low magnification, and timelapse movies of EB1-GFP were captured in these cells. In the movies, comets that entered form the peripheral processes into the 4-way branch point were counted. As a first step comets were categorized into ones that stayed near the edge of the branch (edge track as in Figure 3) and comets that entered the middle of the branch. Only the ones that entered the middle of the branch were considered further. These were then categorized into one of the following groups: comets that turned toward the cell body, comets that turned away from the cell body, comets that remained free and continued into the opposite peripheral process, and those that depolymerized within the branch point.

Acknowledgements

We are grateful to members of the Rolls and Hancock labs for helpful discussions, in particular Matt Shorey and Yalei Chen. We are grateful to Dr. Hermann Aberle for the Ank2-XL antibody. The Bloomington Drosophila Stock Center and the Vienna Drosophila RNAi Center are both invaluable resources and provided key transgenic lines for this study. The Developmental Studies Hybridoma Bank is a similarly critical resource for monoclonal antibodies. ImageJ is an

extremely useful resource for analysis of microscope data. This work was funded by the National Institute of General Medical Sciences R01 GM100076 to WOH and MMR.

Conflict of Interest

None of the authors have any conflicts of interest.

References

Baas PW, Deitch JS, Black MM, Banker GA. 1988. Polarity orientation of microtubules in hippocampal neurons: uniformity in the axon and nonuniformity in the dendrite. Proc Natl Acad Sci U S A 85(21):8335-9.

Baas PW, Lin S. 2011. Hooks and comets: The story of microtubule polarity orientation in the neuron. Dev Neurobiol 71(6):403-18.

Bartolini F, Gundersen GG. 2006. Generation of noncentrosomal microtubule arrays. J Cell Sci 119(Pt 20):4155-63.

Berrueta L, Kraeft SK, Tirnauer JS, Schuyler SC, Chen LB, Hill DE, Pellman D, Bierer BE. 1998. The adenomatous polyposis coli-binding protein EB1 is associated with cytoplasmic and spindle microtubules. Proc Natl Acad Sci U S A 95(18):10596-601.

Cabernard C, Doe CQ. 2009. Apical/basal spindle orientation is required for neuroblast homeostasis and neuronal differentiation in Drosophila. Dev Cell 17(1):134-41.

Chen J, Kanai Y, Cowan NJ, Hirokawa N. 1992. Projection domains of MAP2 and tau determine spacings between microtubules in dendrites and axons. Nature 360(6405):674-7.

Chen L, Stone MC, Tao J, Rolls MM. 2012. Axon injury and stress trigger a microtubule-based neuroprotective pathway. Proc Natl Acad Sci U S A.

Chen Y, Rolls MM, Hancock WO. 2014. An EB1-kinesin complex is sufficient to steer microtubule growth in vitro. Curr Biol 24(3):316-21.

Dixit R, Barnett B, Lazarus JE, Tokito M, Goldman YE, Holzbaur EL. 2009. Microtubule plus-end tracking by CLIP-170 requires EB1. Proc Natl Acad Sci U S A 106(2):492-7.

Dixit R, Cyr R. 2004. Encounters between dynamic cortical microtubules promote ordering of the cortical array through angle-dependent modifications of microtubule behavior. Plant Cell 16(12):3274-84.

Doodhi H, Katrukha EA, Kapitein LC, Akhmanova A. 2014. Mechanical and geometrical constraints control kinesin-based microtubule guidance. Curr Biol 24(3):322-8.

Goodwin PR, Sasaki JM, Juo P. 2012. Cyclin-dependent kinase 5 regulates the polarized trafficking of neuropeptide-containing dense-core vesicles in Caenorhabditis elegans motor neurons. J Neurosci 32(24):8158-72.

Grueber WB, Jan LY, Jan YN. 2002. Tiling of the Drosophila epidermis by multidendritic sensory neurons. Development 129(12):2867-78.

Hill SE, Parmar M, Gheres KW, Guignet MA, Huang Y, Jackson FR, Rolls MM. 2012. Development of dendrite polarity in Drosophila neurons. Neural Dev 7:34.

Hirokawa N, Niwa S, Tanaka Y. 2010. Molecular motors in neurons: transport mechanisms and roles in brain function, development, and disease. Neuron 68(4):610-38.

Hummel T, Krukkert K, Roos J, Davis G, Klambt C. 2000. Drosophila Futsch/22C10 is a MAP1B-like protein required for dendritic and axonal development. Neuron 26(2):357-70.

Jenkins B, Decker H, Bentley M, Luisi J, Banker G. 2012. A novel split kinesin assay identifies motor proteins that interact with distinct vesicle populations. J Cell Biol 198(4):749-61.

Jimbo T, Kawasaki Y, Koyama R, Sato R, Takada S, Haraguchi K, Akiyama T. 2002. Identification of a link between the tumour suppressor APC and the kinesin superfamily. Nat Cell Biol 4(4):323-7.

Kapitein LC, Schlager MA, Kuijpers M, Wulf PS, van Spronsen M, MacKintosh FC, Hoogenraad CC. 2010. Mixed microtubules steer dynein-driven cargo transport into dendrites. Curr Biol 20(4):290-9.

Karpova N, Bobinnec Y, Fouix S, Huitorel P, Debec A. 2006. Jupiter, a new Drosophila protein associated with microtubules. Cell Motil Cytoskeleton 63(5):301-12.

Koch I, Schwarz H, Beuchle D, Goellner B, Langegger M, Aberle H. 2008. Drosophila ankyrin 2 is required for synaptic stability. Neuron 58(2):210-22.

Lin S, Liu M, Mozgova OI, Yu W, Baas PW. 2012. Mitotic motors coregulate microtubule patterns in axons and dendrites. J Neurosci 32(40):14033-49.

Liu M, Nadar VC, Kozielski F, Kozlowska M, Yu W, Baas PW. 2010. Kinesin-12, a mitotic microtubule-associated motor protein, impacts axonal growth, navigation, and branching. J Neurosci 30(44):14896-906.

Liu Z, Steward R, Luo L. 2000. Drosophila Lis1 is required for neuroblast proliferation, dendritic elaboration and axonal transport. Nat Cell Biol 2(11):776-83.

Lu W, Fox P, Lakonishok M, Davidson MW, Gelfand VI. 2013. Initial neurite outgrowth in Drosophila neurons is driven by Kinesin-powered microtubule sliding. Curr Biol 23(11):1018-23.

Mattie FJ, Stackpole MM, Stone MC, Clippard JR, Rudnick DA, Qiu Y, Tao J, Allender DL, Parmar M, Rolls MM. 2010. Directed Microtubule Growth, +TIPs, and Kinesin-2 Are Required for Uniform Microtubule Polarity in Dendrites. Curr Biol 20(24):2169-77.

Maurer SP, Cade NI, Bohner G, Gustafsson N, Boutant E, Surrey T. 2014. EB1 accelerates two conformational transitions important for microtubule maturation and dynamics. Curr Biol 24(4):372-84.

Merriam EB, Millette M, Lumbard DC, Saengsawang W, Fothergill T, Hu X, Ferhat L, Dent EW. 2013. Synaptic regulation of microtubule dynamics in dendritic spines by calcium, F-actin, and drebrin. J Neurosci 33(42):16471-82.

Mogessie B, Roth D, Rahil Z, Straube A. 2015. A novel isoform of MAP4 organises the paraxial microtubule array required for muscle cell differentiation. Elife 4:e05697.

Morrison EE, Wardleworth BN, Askham JM, Markham AF, Meredith DM. 1998. EB1, a protein which interacts with the APC tumour suppressor, is associated with the microtubule cytoskeleton throughout the cell cycle. Oncogene 17(26):3471-7.

Myers KA, Baas PW. 2007. Kinesin-5 regulates the growth of the axon by acting as a brake on its microtubule array. J Cell Biol 178(6):1081-91.

Rolls MM, Jegla TJ. 2015. Neuronal polarity: an evolutionary perspective. J Exp Biol 218(Pt 4):572-80.

Satoh D, Sato D, Tsuyama T, Saito M, Ohkura H, Rolls MM, Ishikawa F, Uemura T. 2008. Spatial control of branching within dendritic arbors by dynein-dependent transport of Rab5-endosomes. Nat Cell Biol 10(10):1164-71.

Sharp DJ, Yu W, Ferhat L, Kuriyama R, Rueger DC, Baas PW. 1997. Identification of a microtubule-associated motor protein essential for dendritic differentiation. J Cell Biol 138(4):833-43.

Stepanova T, Slemmer J, Hoogenraad CC, Lansbergen G, Dortland B, De Zeeuw CI, Grosveld F, van Cappellen G, Akhmanova A, Galjart N. 2003. Visualization of microtubule growth in cultured neurons via the use of EB3-GFP (end-binding protein 3-green fluorescent protein). J Neurosci 23(7):2655-64.

Stone MC, Roegiers F, Rolls MM. 2008. Microtubules Have Opposite Orientation in Axons and Dendrites of Drosophila Neurons. Mol Biol Cell 19(10):4122-9.

Thevenaz P, Ruttimann UE, Unser M. 1998. A pyramid approach to subpixel registration based on intensity. IEEE Trans Image Process 7(1):27-41.

Wiese C. 2008. Distinct Dgrip84 isoforms correlate with distinct gamma-tubulins in Drosophila. Mol Biol Cell 19(1):368-77.

Yan J, Chao DL, Toba S, Koyasako K, Yasunaga T, Hirotsune S, Shen K. 2013. Kinesin-1 regulates dendrite microtubule polarity in Caenorhabditis elegans. Elife 2:e00133.

Yu W, Cook C, Sauter C, Kuriyama R, Kaplan PL, Baas PW. 2000. Depletion of a microtubule-associated motor protein induces the loss of dendritic identity. J Neurosci 20(15):5782-91.

Zheng Y, Wildonger J, Ye B, Zhang Y, Kita A, Younger SH, Zimmerman S, Jan LY, Jan YN. 2008. Dynein is required for polarized dendritic transport and uniform microtubule orientation in axons. Nat Cell Biol 10(10):1172-80.

Introduction to Chapter 3

Chapter 3 is a manuscript that was published in G3: Genes|Genomes|Genetics in May 2018. It is provided as it is appears published online in its unaltered form. The manuscript contributes to the thesis by characterizing the molecular determinants of Apc2 localization at dendrite branch points. Since Apc2 is involved in the microtubule steering complex introduced in chapter 1 and described in chapter 2 it is an important continuation of this work. It is also important to the coherency of the thesis because it bridges the connection between the steering complex in chapter 2 with positioning of nucleation sites at branch points described in chapter 4. Chapter 3 provides the initial list of candidates that we rescreened to determine molecular determinants of γTub localization to dendrite branch points in chapter 4. In addition to the contribution to neuronal cell biology chapter 3 has contributed to cell biology in general because it demonstrates how many different cellular components influence Apc2 localization or function. This may translate to exploration of similar pathways in other cellular systems.

I am the first author on the manuscript and wrote a first draft which acted as the framework. I also created all figures used throughout the manuscript. Except for Figure 1, I contributed to data generation and analysis in all figures of the manuscript during my thesis work. Dylan Seebold, Nick Michael, Michelle Guignet, Chengye Feng, Brandon Follick, Brandon Yusko, Nathan Wasilko, and Pedro Torres contributed to experiments. Michelle and Nick produced the hypothesis generating data of figure 1. Brandon Follick produced an initial dataset for figure 3 but I redid the entire dataset to confirm his initial findings. Brandon Yusko and Nathan were responsible for a couple of the datapoints in the mitochondria screen and performed these during lab rotations. Chengye produced the Ankyrin dataset in figure 4. Nick produced the dataset in figure 5C. Dylan, Pedro and I produced the data for figures 6 and 7. For these figures I generated the majority of the data. Finally, Dylan and I created the schematic for figure 8.

Chapter 3

Identification of proteins required for precise positioning of Apc2 in dendrites

Abstract

In *Drosophila* neurons, uniform minus-end-out polarity in dendrites is maintained in part by kinesin-2-mediated steering of growing microtubules at branch points. Apc links the kinesin motor to growing microtubule plus ends and Apc2 recruits Apc to branch points where it functions. Because Apc2 acts to concentrate other steering proteins to branch points, we wished to understand how Apc2 is targeted. From an initial broad candidate RNAi screen, we found Miro (a mitochondrial transport protein), Ank2, Axin, spastin and Rac1 were required to position Apc2-GFP at dendrite branch points. YFP-Ank2-L8, Axin-GFP and mitochondria also localized to branch points suggesting the screen identified relevant proteins. By performing secondary screens, we found that energy production by mitochondria was key for Apc2-GFP positioning and spastin acted upstream of mitochondria. Ank2 seems to act independently from other players, except its membrane partner, Neuroglian (Nrg). Rac1 likely acts through Arp2/3 to generate branched actin to help recruit Apc2-GFP. Axin can function in a variety of wnt signaling pathways, one of which includes heterotrimeric G proteins and Frizzleds. Knockdown of G□s, G□o, Fz and Fz2, reduced targeting of Apc2 and Axin to branch points. Overall our data suggest that mitochondrial energy production, Nrg/Ank2, branched actin generated by Arp2/3 and Fz/G proteins/Axin function as four modules that control localization of the microtubule regulator Apc2 to its site of action in dendrite branch points.

Introduction

Many differentiated cells have special arrangements of microtubules that are quite different from the most familiar centrosomal organization found in rapidly dividing cells (BARTOLINI AND GUNDERSEN 2006; MUROYAMA AND LECHLER 2017; SANCHEZ AND FELDMAN 2017). Drosophila neurons are a particularly extreme example, and also a good model system for understanding how non-centrosomal microtubule arrays are established and maintained (ROLLS 2011). Like axons in other animals, those in Drosophila have all plus-end-out microtubules (BAAS AND LIN 2011). In stark contrast to the axon, dendritic microtubules are more than 90% minus-end-out (ROLLS *et al.* 2007; STONE *et al.* 2008). This arrangement, with minus ends away from the center of the cell, is very different from "standard" centrosomal microtubule organization in which minus ends are clustered centrally, and thus is particularly intriguing to investigate.

Several different mechanisms that contribute to maintenance of the minus-end-out microtubule array in Drosophila dendrites have been identified. First, local microtubule nucleation in dendrites is important for maintaining neuronal structure (ORI-MCKENNEY *et al.* 2012) and uniform polarity (NGUYEN *et al.* 2014). Second, directed growth of microtubules, or steering, at branch points prevents disruption of polarity by microtubule polymerization (MATTIE *et al.* 2010). This steering mechanism is the focus here.

Microtubule steering helps maintain minus-end-out polarity in branched dendrites by preventing a microtubule that grows into the branch point from turning away from the cell body at this junction and generating a plus-end-out microtubule (MATTIE *et al.* 2010; WEINER *et al.* 2016). Kinesin-2, a heterotrimeric motor consisting of the motor subunits Klp64D and Klp68D and accessory subunit Kap3, is linked to growing microtubules through binding of Kap3 to the +TIP protein Adenomatous polyposis coli (Apc), which in turn binds the core +TIP EB1 (MATTIE

et al. 2010). Kinesin-2 is then positioned on the microtubule plus end with its motor domain capable of engaging with stable microtubules (Figure 1A). If this happens, the plus end can be guided along the stable microtubule to maintain polarity at branch points (WEINER *et al.* 2016). Microtubule steering has been reconstituted in vitro by linking kinesin motors directly to +TIPs under conditions that allow microtubule polymerization (CHEN *et al.* 2014; DOODHI *et al.* 2014).

One aspect of the microtubule steering pathway that is not well understood is how the proteins that mediate it are localized to their sites of function at dendrite branch points. One clue is the interaction of Apc with Apc2. Drosophila Apc binds both kinesin-2 and EB1 and so can act as a bridge between the motor and plus end, but it also binds Apc2 (MATTIE *et al.* 2010). When tagged with GFP, Apc2 localizes strongly to dendrite branch points and can recruit Apc (MATTIE *et al.* 2010). None of the other proteins in the complex seems to be able to localize to branch points when overexpressed alone. The ability of Apc2 to self-associate (KUNTTAS-TATLI *et al.* 2014) may help it to act as a platform to recruit other proteins. Understanding how Apc2 is localized to branch points is thus central to determining how the steering complex (Figure 1) is concentrated where it functions.

Results

Identification of proteins that localize Apc2 to Dendrite Branch Points

Apc2-GFP localizes robustly to dendrite branch points of Drosophila sensory neurons and can recruit Apc-RFP (MATTIE *et al.* 2010). In addition, Apc proteins in general act as scaffolds in wnt signaling pathways and so have many known interacting partners (MCCARTNEY AND NATHKE 2008; NELSON AND NATHKE 2013). We therefore used Apc2-GFP localization as the readout to identify proteins involved in patterning microtubule regulators within dendrites

(Figure 1). Candidates selected to screen included proteins known to interact with Drosophila Apc2, like the formin diaphanous (dia) (WEBB *et al.* 2009), proteins known to work with Apc in wnt signaling including sgg (GSK3β) (CADIGAN AND PEIFER 2009), cytoskeletal regulators to reflect the interactions of Apc proteins with both actin and microtubules (DIKOVSKAYA *et al.* 2001), and mitochondria as there is evidence Apc can be targeted to them (BROCARDO *et al.* 2008).

The ddaE sensory neuron was chosen as a model system because it has a simple, stereotyped dendrite arbor (GRUEBER *et al.* 2002); has similar microtubule organization to Drosophila interneurons and motor neurons (STONE *et al.* 2008), and previous work on microtubule steering has been done in this cell type (MATTIE *et al.* 2010). To perform the candidate screen, females from a tester line containing UAS-Dicer2 (to promote neuronal RNAi (DIETZL *et al.* 2007)), UAS-mCD8-RFP (to outline the cell), UAS-Apc2-GFP and 221-Gal4 (to drive transgene expression in the ddaE neuron) were crossed to RNAi transgenes (Table 1). Many Drosophila RNAi lines (including GD and KK lines from VDRC and val1 and val10 lines from the TRiP collection at BDSC) generate RNA hairpins several hundred nucleotides long when transcribed and in the nervous system are typically supplemented with UAS-dicer2 as this enzyme seems limiting in neurons (DIETZL *et al.* 2007; NI *et al.* 2009). In contrast, the val20 lines in the TRiP collection generate shRNAs (NI *et al.* 2011) and so can be used without dicer2 in theory, however we tend to see more consistent phenotypes when dicer2 is included, so UAS-dicer2 was included in all RNAi experiments. Larval progeny were mounted on microscope slides and confocal images of ddaE neurons were acquired; one neuron was imaged per animal and approximately 10 neurons were imaged for each RNAi condition. Each branch point along the main trunk of the dorsal comb dendrite was scored as occupied by a bright Apc2-GFP patch or not occupied. All branch points from at least 10 individual neurons were pooled to generate a percent occupancy score. When control RNAi hairpins were expressed, about 90% of branch

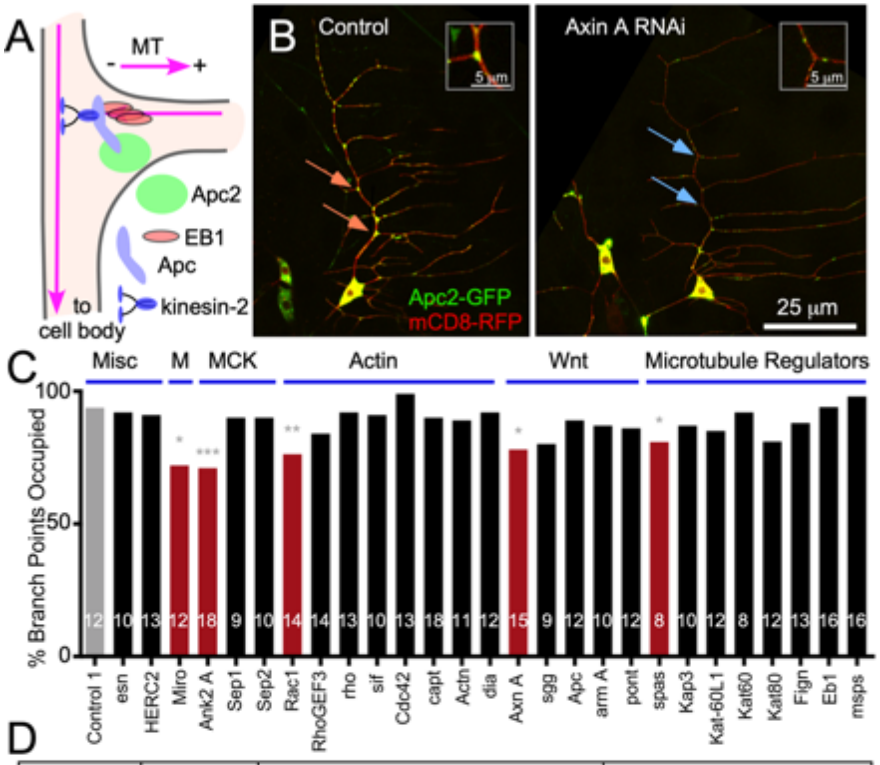

Name	VDRC #	Phenotype in ddaE	Reference
Miro	106683	fewer mitochondria in dendrites	Tao et al., 2012
Apc	51469	dendrite microtubule polarity	Mattie et al., 2010
spas	33110	axon regeneration	Stone et al., 2012
Kap3	45400	dendrite microtubule polarity	Mattie et al., 2010
kat-60L1	31598	dendrite pruning (ddaC)	Tao et al., 2012
Kat60	38368	axon regeneration	Stone et al., 2012
Fign	24746	dendrite degeneration	Tao et al., 2016
Eb1	24451	dendrite microtubule polarity	Mattie et al., 2010
msps	21982	dendrite stabilization	Chen et al., 2012

Figure 3-1. Several proteins are required to position Apc2-GFP at dendrite branch points.

(A) A schematic of the microtubule steering mechanism is shown. (B) Images of the ddaE neurons expressing mCD8-RFP and Apc2-GFP are shown for Rtnl2 RNAi (Control 1) (VDRC 33320) and Axin RNAi (VDRC 7748). Orange arrows indicate branch points with high Apc2 signal and blue arrows indicate branch points with low/no Apc2 signal. Insets show the top branch point indicated with an arrow in each panel. (C) Quantification Apc2-GFP branch point occupancy is shown for different RNAi conditions. Titles above the graph indicate which functional groups the RNAi lines belong and are abbreviated as Misc for miscellaneous, M for mitochondria, MCK for membrane cytoskeleton, Actin for actin regulators, Wnt for wnt signaling pathway members, and Microtubule Regulators. The grey bar indicates the control and red bars indicate genotypes that had significantly reduced Apc2 at branch points. Numbers of neurons analyzed are shown within the bars. A Fisher's Exact test was used to compare each genotype to the control. * $p<0.05$, ** $p<0.01$, *** $p<0.001$. (D) Table of RNAi lines previously shown to have phenotypes in ddaE neurons; the only exception is kat-60L1 which was tested in ddaC not ddaE. The stock number, phenotype, and published reference are noted.

points were scored as occupied (Figure 1B). Knockdown of Miro, spastin, Rac1, Axin and Ankyrin 2 (Ank2) significantly reduced the percentage of occupied branch points (Figure 1C). While screening we noticed that some of the genotypes resulted in ectopic Apc2-GFP localization, but as our goal was to identify branch point targeting mechanisms, we only scored Apc2 at branch points.

Based on the screen, we selected pathways for additional investigation. Miro links mitochondria to microtubule motors (GUO *et al.* 2005) and RNAi targeting Miro reduces the number of mitochondria in ddaE dendrites (TAO AND ROLLS 2011), so the reduction of branch point Apc2 in Miro RNAi neurons suggested mitochondria might be involved in Apc2 targeting. The reduction of Apc2 at branch points by Ank2 RNAi suggested the submembrane cytoskeleton might be involved. Of actin regulators tested, only Rac1 RNAi had a phenotype suggesting a specific type of actin arrangement could help recruit Apc2 to branch points. Similarly only one of the wnt pathway proteins tested, Axin, reduced Apc2 at branch points perhaps indicating only one part of the pathway, or a pathway variant, is involved. Of the microtubule regulators tested only spastin (spas) RNAi reduced Apc2 localization. While negative RNAi results are difficult to interpret without detailed analysis of protein levels or additional phenotypes, we have previously found phenotypes in ddaE neurons with some of the same RNAi lines used in this screen. For example, msps RNAi eliminates EB1-GFP comets in ddaE neurons (STONE *et al.* 2010) and Kap3 RNAi causes mixed polarity in ddaE dendrites (MATTIE *et al.* 2010). In fact, most of the RNAi lines used in this screen that target microtubule regulators have described phenotypes in these cells (Figure 1D and (TAO AND ROLLS 2011; STONE *et al.* 2012; TAO *et al.* 2016)). We therefore think that Apc2-GFP can still be localized to dendrite branch points under conditions where microtubules are partially disrupted and focused initially on the other regulators. Interestingly kinesin-2, of which Kap3 is a subunit, has previously been placed upstream of Apc targeting in mammalian axons (RUANE *et al.* 2016), but is not upstream in this context.

Tagged Axin, Ank2 and mitochondria localize to branch points.

To begin to determine whether the initial candidate screen identified important regulators of Apc2 dendrite localization, we tested whether any of the positive proteins themselves localized to branch points. To quantitatively assess concentration at branch points, regions of interest between branch points were manually outlined as were those within branch points. The ratio of branch point to non-branch point fluorescence was calculated for cytoplasmic GFP. On average cytoplasmic GFP was about 1.2 fold brighter at branch points than non-branch points, likely reflecting the larger cytoplasmic volume at branch points (Figure 2). A similar analysis of the tagged long exon of Ank2, YFP-Ank2-L8 (PIELAGE *et al.* 2008), indicated it was about two-fold brighter at dendrite branch points (Figure 2). Similarly, Axin-GFP (CLIFFE *et al.* 2003) was about 1.8-fold brighter at branch points (Figure 2). We also examined the distribution of mitochondria in dendrites. While they are fairly evenly distributed throughout the dendrite arbor, the majority of branch points do contain one or more GFP-labeled mitochondria (Figure 2D and 3D). Actin-GFP as well as other tagged actin-binding domains and regulatory proteins, including Arp3-GFP (Figure 2B) were not convincingly localized to branch points. We conclude that a subset of the hits from the initial candidate screen have a localization consistent with functioning to target Apc2 to dendrite branch points.

Mitochondrial function is required to position Apc2-GFP at branch points

As Miro was required for Apc2 localization and mitochondria localize to most branch points, we further investigated the relationship between mitochondria and Apc2 positioning. We considered two models for the role of mitochondria. In one model, mitochondria might act as a physical docking platform for Apc2, as suggested for some cancer-associated human Apc

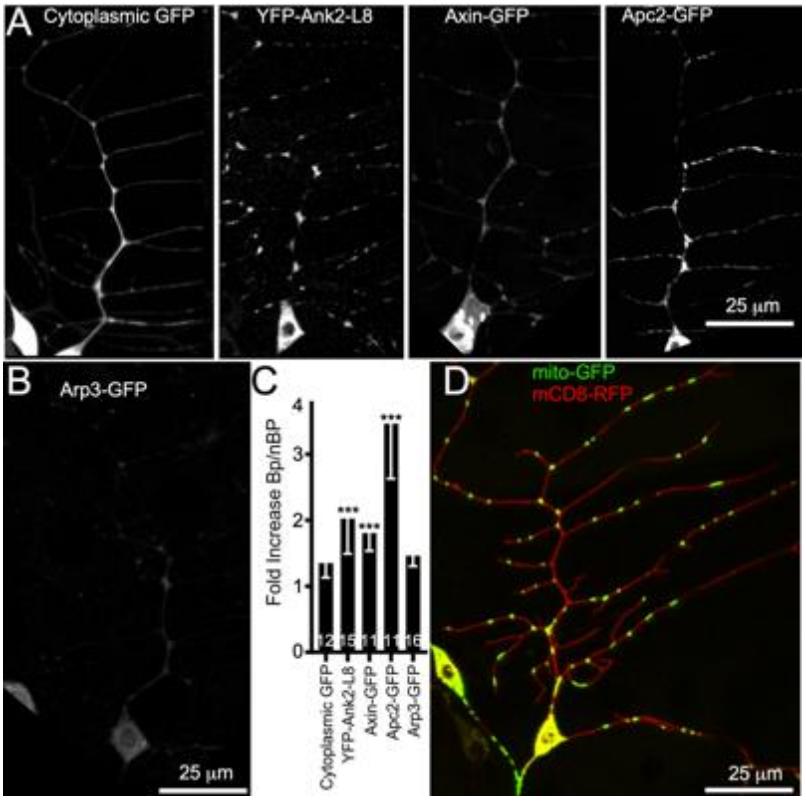

Figure 3-2. Localization of markers to branch points compared to a non-localized soluble control.

(A and B) Representative single channel images of markers used in localization experiments are shown. For comparison a cytoplasmic GFP that fills the dendrite is included. (C) Quantification of fold increase (to allow comparison across markers the branch point average was divided by non-branch point rather than subtracted) in localization between branch point and non-branch point areas of fluorescent markers. Compared to cytoplasmic GFP all except Arp3-GFP are enriched at branch points. Error bars indicate standard deviation. A linear regression was used to determine statistical significance. * $p<0.05$, ** $p<0.01$, *** $p<0.001$ (D) Representative image of mito-GFP distribution in a ddaE neuron.

truncation mutants (BROCARDO *et al.* 2008). In a second model, mitochondria could function primarily as a local source of ATP. To test whether mitochondrial ATP production might be important in this context, we knocked down two proteins that play roles in oxidative phosphorylation. SesB is an ADP/ATP antiporter that allows exchange of ATP and ADP across the inner membrane of the mitochondrion and ATP synthase beta (ATPsynβ) is a subunit of the complex that generates ATP from ADP. Targeting transcripts that encode either of these proteins by RNAi reduced the occupancy of branch points by Apc2-GFP (Figure 3A and B). This result suggests that energy production by mitochondria is important for Apc2 localization (Figure 3E).

In addition to investigating how mitochondria might be involved in Apc2 positioning, we wished to determine whether any of the other factors we identified in our initial screen might influence Apc2 localization indirectly by acting upstream of mitochondrial positioning. We generated a tester line that contained mito-GFP (UAS-Dicer2, UAS-mCD8-RFP; 221-Gal4, UAS-mito-GFP) and crossed it to RNAi lines that reduced Apc2 localization including lines targeting Axin, Rac1 and Miro. In control ddaE neurons about 80% of branch points along the main backbone of the comb dendrite contained mitochondria (Figure 3C and D). This occupancy is slightly lower than that of Apc2-GFP, consistent with the idea that mitochondria do not act directly as a platform for Apc2. Proteins known to be involved in mitochondrial transport into dendrites reduced dendritic branch point localization of mito-GFP as expected: Miro is required for mitochondrial transport into axons and dendrites (GUO *et al.* 2005; TAO AND ROLLS 2011;

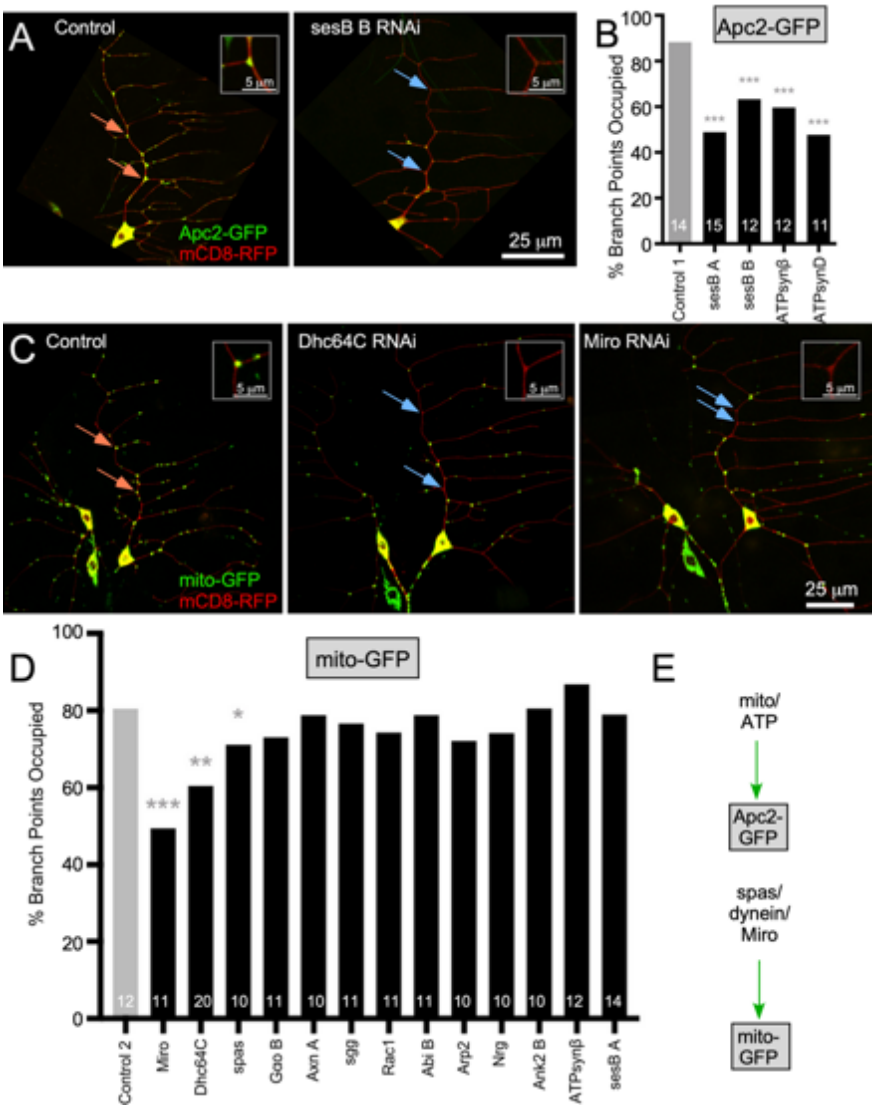

Figure 3-3. Mitochondrial energy production contributes to Apc2-GFP positioning at branch points.

(A) Example images of ddaE neurons expressing Apc2-GFP and mCD8-RFP are shown for control 1 RNAi (VDRC 33320) and sesB RNAi (BL36661). Orange arrows indicate high Apc2 signal and blue indicate low signal. Insets are the top ones indicated with arrows. (B) Quantification of branch point occupancy of Apc2-GFP with RNAi knockdowns. Numbers of neurons analyzed are shown within the bars. A Fisher's Exact test was used to assess whether conditions were different from the control. (C) Example images of ddaE neurons expressing mito-GFP and mCD8-RFP are shown with Control 1 RNAi (VDRC 33320), Dhc64C RNAi (VDRC 28054), and Miro RNAi (VDRC 106683). Example branch points that contain one or more mitochondria are indicated with orange arrows, and ones without mitochondria are shown with blue arrows. (D) The percentage of branch points occupied by mitochondria along the main comb dendrite is shown in the graph. A logistic regression was used to identify conditions likely to be different from the control. * $p<0.05$, ** $p<0.01$, *** $p<0.001$. (E) A summary diagram of data in the figure is shown.

BABIC *et al.* 2015), and dynein (Dhc64C) is required to transport mitochondria into dendrites in Drosophila (SATOH *et al.* 2008). Knockdown of spastin also reduced branch point localization of mitochondria, and the RNAi line used here is one we have previously shown has phenotypes similar to mutants (STONE *et al.* 2012). Spastin could influence mitochondrial positioning either through its role in microtubule organization or through its role in ER positioning, as both functions can be important in Drosophila neurons (SHERWOOD *et al.* 2004; RAO *et al.* 2016), and mitochondria are closely linked to the ER and microtubules (LABBE *et al.* 2014). We conclude that the effects of Miro and spastin on Apc2-GFP localization are likely due to their role in localization of mitochondria to dendrite branch points. However, other proteins like Axin and Ank2 probably influence Apc2 localization independently from mitochondria.

Ank2 works with Neuroglian to position Apc2 at branch points

The initial screen suggested a requirement for Ank2 in Apc2-GFP localization to dendrite branch points (Figure 1). Ank2 has been described to function in the axon near the cell body (YAMAMOTO *et al.* 2006; JEGLA *et al.* 2016) and in more distal axons and terminals (KOCH *et al.* 2008; PIELAGE *et al.* 2008; STEPHAN *et al.* 2015), but not dendrites. However, the localization of YFP-Ank2-L8 was consistent with a dendritic role (Figure 2A).

To confirm the involvement of Ank2 in Apc2 positioning in dendrites, we took several approaches. First, we retested Ank2 RNAi (Figure 4A and B). Second, we used two different mutant alleles of *Ank2* and crossed these to the Apc2 tester line to generate animals with one normal copy of the *Ank2* gene and one mutant copy; Apc2-GFP was reduced at branch points in both backgrounds (Figure 4B). Finally, we targeted Neuroglian (Nrg) by RNAi. Nrg is a

membrane protein partner of Ank2 in other contexts (BOULEY *et al.* 2000; YAMAMOTO *et al.* 2006).

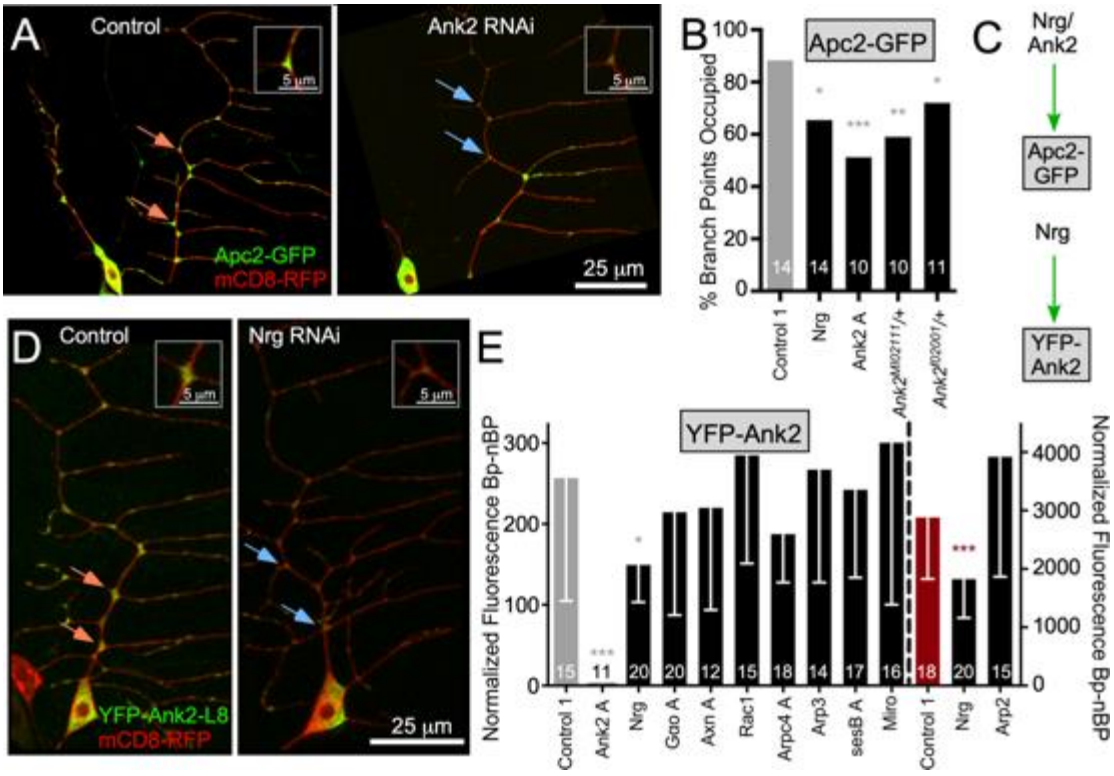

Figure 3-4. Ank2 and Neuroglian help position Apc2-GFP at branch points.

(A) Example images of Apc2-GFP and mCD8-RFP in ddaE neurons with Control1 RNAi (VDRC 33320) or UAS-Ank2 RNAi (VDRC 107369) are shown. (B) Quantification of Apc2-GFP localization is shown in the graph; numbers on the bars are neurons analyzed. The control dataset is the same one used in Figure 3B. A Fisher's Exact test was used to determine statistical significance. Throughout the figure orange arrows indicate branch points with high fluorescence and blue arrows low fluorescence. Insets show top examples. (C) The diagram summarizes data in the figure. (D) Images depicting UAS-YFP-Ank2L8 distribution in ddaE neurons with either Control 1 RNAi (VDRC 33320) or Nrg RNAi (VDRC 107991). (E) Quantification of YFP-Ank2L8 intensity at branch points compared to non-branch points is shown. The grey bar indicates control cells imaged on an Olympus FluoView 1000 and the red bar indicates the same control genotype imaged on a Zeiss LSM800. All data to the left of the dashed line was collected with the Olympus microscope, while data to the right was collected with the LSM800. The axes to the left and right are for the two different microscopes. Error bars are standard deviation. Comparisons were made between data collected on a single microscope, and the color of the star indicates which control is used for comparison. A linear regression was used to determine statistical significance. * $p<0.05$, ** $p<0.01$, *** $p<0.001$

Nrg RNAi also reduced Apc2-GFP branch point occupancy. Thus, multiple lines of evidence indicate that Nrg and Ank2 are required to position Apc2 (Figure 4C). Note that neither Nrg RNAi nor one Ank2 RNAi reduced mitochondrial localization to branch points (Figure 3D).

Drosophila Ank2 is expressed primarily in neurons (BOULEY *et al.* 2000) and contains extremely long exons that generate giant L and XL isoforms (KOCH *et al.* 2008; PIELAGE *et al.* 2008). These giant Ank2 isoforms have a common evolutionary origin and overlapping function with vertebrate giant ankyrins (JEGLA *et al.* 2016). The *Ank2^{f02001}* allele is a characterized P element insertion in the exon that encodes the L region, and it specifically reduces this splice form (KOCH *et al.* 2008; PIELAGE *et al.* 2008). Similarly the RNAi line labeled Ank2 A targets the L region. In contrast, the *Ank2^{MI02111}* transposon insertion disrupts the conserved ankyrin core and so reduces all isoforms (see Supplemental Table and FlyBase). The fact that one copy of the *Ank2^{f02001}* allele and the Ank2 A RNAi reduced Apc2 branch point localization (Figure 4B) suggested that the L form is involved in this Ank2 function. The exon that encodes the region specific to the L form is the one contained in YFP-Ank2-L8.

To determine whether Ank2 was likely to act downstream of any of the other proteins required for Apc2 localization, we generated a tester line with 221-Gal4, mCD8-RFP, YFP-Ank2-L8 and Dicer2 and crossed flies from this line to a variety of RNAi transgenic flies. For all genotypes images were acquired at the same microscope settings (within each data set) and the average intensity between branch points was subtracted from that at branch points (Figure 4D and E). As a control, the Ank2 A RNAi line that targets the coding sequence for the L region was used and it completely eliminated fluorescence of YFP-Ank2-L8 (Figure 4E). Nrg RNAi also reduced YFP-Ank2-L8 signal at branch points (Figures 4D and E) consistent with Nrg and Ank2 working together. None of the other RNAi lines tested reduced the branch point localization of YFP-Ank2-L8 (Figure 4C and D), although in other scenarios G proteins and fz can act through Ank2 (LUCHTENBORG *et al.* 2014). Based on this data, the simplest model is that Nrg helps

concentrate Ank2-L at branch points, and Nrg and Ank2-L function to position Apc2 independently of mitochondria and other regulators (Figure 4C).

Regulators of branched actin are required for Apc2-GFP branch point localization

Along with Ank2 and mitochondria, our initial Apc2 localization screen indicated that the small GTPase Rac1 helps recruit Apc2 to branch points (Figure 1C). While Rac1 can regulate many different signaling cascades, its classic role is to stimulate generation of branched actin formation by the Arp2/3 complex through activation of the WAVE complex (BOSCO *et al.* 2009; DERIVERY AND GAUTREAU 2010). We therefore tested Arp2/3 and WAVE complex members for a role in Apc2-GFP targeting to branch points. Arp2/3 complex members tested included Arp1, Arpc4, Arp2 and Arp3. The majority of RNAi lines that targeted these proteins reduced Apc2 GFP localization at dendrite branch points (Figure 5A and B). There were several RNAi lines that did not have an effect (Figure 5B), perhaps because they did not knock their targets down as efficiently as some of the others. We tested Abi as a representative of the WAVE complex and it also reduced Apc2-GFP branch point localization (Figure 5B). Thus generation of branched actin by Arp2/3 nucleation seems to be required for Apc2-GFP targeting in dendrites (Figure 5D). To confirm that Rac1 is involved in Apc2-GFP localization, we expressed constitutively GDP-bound $Rac1_{N17}$ and constitutively GTP-bound $Rac1_{V12}$ (LUO *et al.* 1994). Both forms of Rac1 dramatically reduced branch point occupancy by Apc2-GFP (Figure 5A and C), but also had strong effects on dendrite architecture (Figure 5A). We conclude that cycling of Rac1 between GTP and GDP bound forms is likely important for Apc2 localization, but that Rac1 also affects the dendritic cytoskeleton more broadly.

Based on this data, the simplest model is that a patch of branched actin is generated at the branch point itself. To see if we could get any direct evidence for this, we expressed tagged actin

and Arp2/3 complex members in the ddaE neuron. While all of the markers tested were present at branch points, for most it was not clear if they were more concentrated at branch points than soluble GFP. For example, Arp3-GFP (HUDSON AND COOLEY 2002) can be seen in dendrites

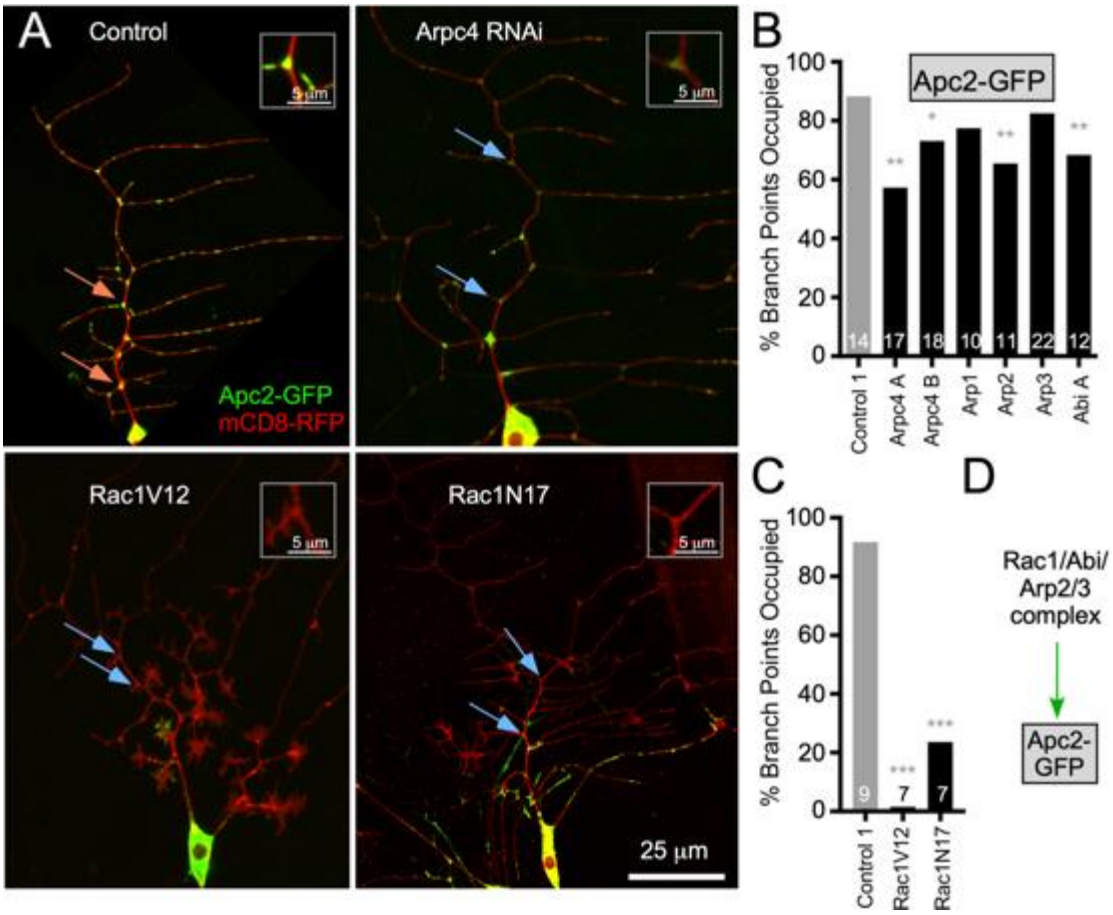

Figure 3-5. Arp2/3 complex members help recruit Apc2-GFP to branch points.

(A) Example images of Apc2-GFP and mCD8-RFP in ddaE neurons with Control 1 (VDRC 33320) RNAi or Arpc4 RNAi (BL41888). See supplemental table for a full listing of all the RNAi line numbers. Lower images show Apc2-GFP with overexpressed Rac1V12 (GTP-bound) and Rac1N17 (GDP-bound). (B) Quantification of Apc2-GFP branch point occupancy with Arp2/3 complex RNAis; the control is the same as in Figure 3B. Numbers on the graph are numbers of cells analyzed and a logistic regression was used to determine significance, * $p<0.05$, ** $p<0.01$, *** $p<0.001$. (C) The Apc2-GFP tester line was crossed to the control 1 RNAi (same genotype as in B, but different set of animals) or UAS-controlled Rac1 mutants. Numbers of animals tested for each condition are shown in the bars, and a logistic regression was used to analyze the data. The p values are indicated as in B. (D) A summary of results in the figure is diagrammed. In all panels orange arrows indicate occupied branch points and blue ones show branch points scored as unoccupied.

(Figure 2B), but is not significantly enriched at branch points compared to control soluble GFP (Figure 2C). We were therefore not able to screen for players acting upstream of branched actin, or get more direct evidence that branched actin is generated locally to recruit Apc2-GFP.

A subset of wnt signaling proteins acts through Axin to localize Apc2 to dendrite branch points

In our initial screen Axin RNAi reduced localization of Apc2-GFP to dendrite branch points (Figure 1). Axin is a scaffolding protein that plays a central role in wnt signaling (CADIGAN AND PEIFER 2009; NUSSE AND CLEVERS 2017), so we tested other proteins linked to wnt signaling for a role in Apc2-GFP localization. In the initial screen RNAi lines targeting armadillo (β-catenin) and sgg (GSK3β), key players in canonical wnt signaling, did not have phenotypes (Figure 1). We retested sgg RNAi, and also used a mutant, sggS9A, which eliminates a negative regulatory phosphorylation site and makes the kinase more active (HAZELETT *et al.* 1998). Again, the RNAi had no phenotype, but overexpression of sggS9A reduced Apc2 branch point localization (Figure 6B) suggesting sgg might at least be able to negatively regulate proteins involved in Apc2 localization in dendrites. Two different RNAi lines targeting each of the wnt receptors frizzled (fz) and frizzled2 (fz2) reduced Apc2-GFP localization (Figure 6B); they also appeared to increase branching of distal dendrites, but did not affect morphology of the main dendrite trunk where quantitation was performed. For fz the two large RNAi hairpins target different regions of the gene, and for fz2 both target the same region although they were generated independently (Supplemental Figure 1). Although best known for their role regulating β-catenin destruction, frizzleds are 7-transmembrane domain proteins and can function as G-protein coupled receptors (KOVAL *et al.* 2011), transduce fz signals in the wing (KATANAEV *et al.* 2005) and interact with Axin (EGGER-ADAM AND KATANAEV 2010). We therefore tested several

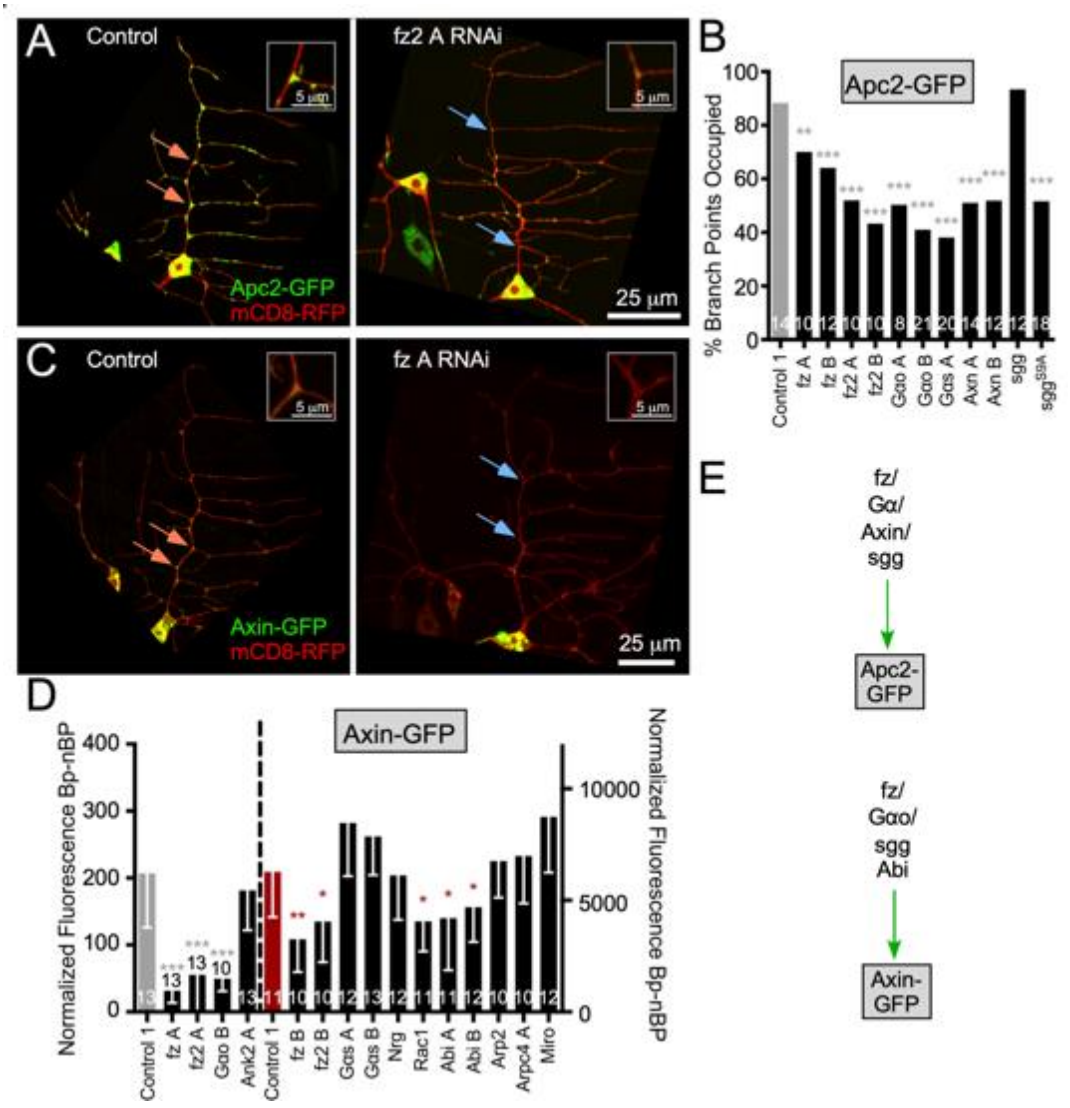

Figure 3-6. Wnt signaling proteins localize Apc2 and Axin to dendrite branch points.

(A) Example images of ddaE neurons expressing Apc2-GFP and mCD8-GFP with Control 1 (VDRC 33320) RNAi or fz A RNAi (VDRC 105493). (B) Quantification of Apc2-GFP branch point occupancy with RNAi knockdown of wnt signaling proteins compared to the same control dataset used in Figure 3B. A Fisher's Exact test was used to determine significance ** $p<0.01$, *** $p<0.001$. (C) Images of Axin-GFP in ddaE neurons with Control 1 (VDRC 33320) RNAi or fz A RNAi (VDRC 105493). (D) Quantification of Axin-GFP intensity at branch points minus intensity between branch points is shown in the graph. Grey and red controls indicate imaging done on an Olympus Fluoview 1000 (grey) or Zeiss LSM800 (red). Dashed line separates two halves of the graph. A linear regression was used to determine statistical significance, * $p<0.05$, ** $p<0.01$, *** $p<0.001$; stars are color-coded to indicate the appropriate control. Error bars are standard deviation. Throughout the image panels orange arrows point out branch points with high fluorescence, and blue ones low fluorescence. (E) A summary of results in the figure is shown.

G-protein alpha subunits as well. Reduction of Gαo and Gαs by RNAi reduced Apc2-GFP localization to dendrite branch points (Figure 6B). Thus core elements of a wnt signaling pathway variant are involved in Apc2-GFP localization.

To determine which candidates might act upstream of Axin in the Apc2 localization pathway, we generated a tester line that contained UAS-dicer2, UAS-mCD8-RFP; 221-Gal4, UAS-Axin-GFP and crossed this to RNAi transgenic flies. Two different RNAi lines targeting fz and fz2 reduced Axin-GFP localization to branch points (Figure 6D). Targeting Gαo, but not Gαs, also reduced Axin targeting. Thus, frizzleds may work through Gαo to regulate Axin in this context as suggested by studies in other Drosophila tissues (EGGER-ADAM AND KATANAEV 2010). In contrast, Miro, Ank2 and Nrg RNAi did not reduce Axin localization suggesting that Nrg/Ank2 and local mitochondrial function are not required upstream of Axin. We could not make a conclusion about whether branched actin regulates Axin positioning because of mixed results: RNAis targeting Arp2/3 components did not have a phenotype in this assay, despite being required for Apc2-GFP localization (Figure 5B), however, RNAis targeting Rac1 and Abi (two independent RNAis targeting different gene regions; see Supplemental Figure 1), upstream regulators of Arp2/3, did affect Axin localization. Both Rac1 and Abi have roles outside Arp2/3 regulation so it is possible they are acting in some other way, or that Axin-GFP localization is slightly more resistant to perturbation by changes in actin than Apc2 localization. A summary diagram of results in the figure is shown in panel 6E.

To confirm the involvement of a variant wnt signaling pathway, we used mutant and dominant negative approaches in addition to RNAi. *Df(3L)fz2* is a small deficiency that disrupts the *fz2* and *rept* genes (BHANOT *et al.* 1999; IHRY AND BASHIRULLAH 2014). The fz_{R52} allele has an early stop codon and is a strong loss of function mutant that makes very little protein (JONES *et al.* 1996) and fz_{F31} allele is a point mutation P278S (JONES *et al.* 1996) and has a relatively weak

phenotype for both canonical and planar cell polarity wnt signaling (POVELONES *et al.* 2005). Heterozygosity for either *fz* allele or the *fz2* deficiency reduced Axin-GFP localization to branch

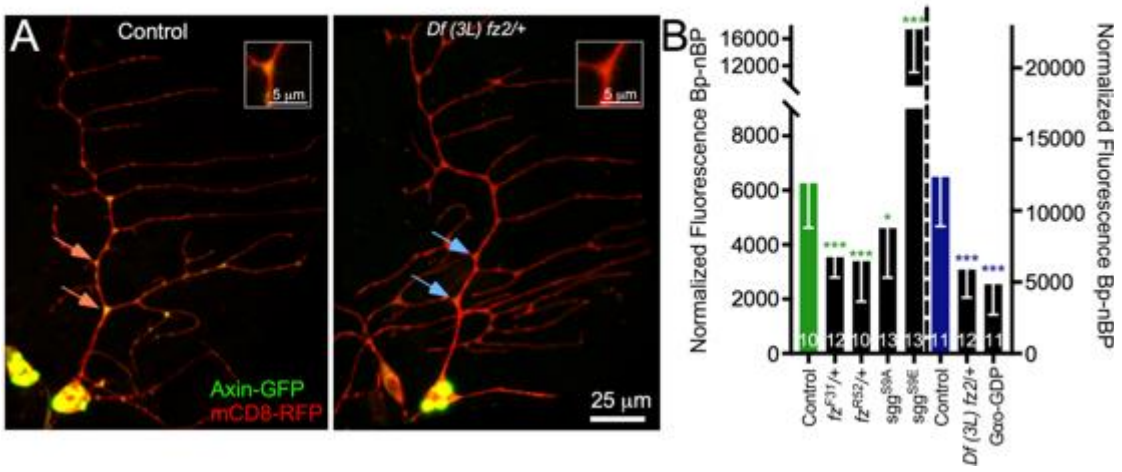

Figure 3-7. Dominant negative and mutant approaches confirm the role of GαO, fz and sgg in Axin targeting.

(A) Example images of ddaE neurons expressing Axin-GFP and mCD8-RFP with Control (yw) or Df (3L) fz2 (BL 6754). Orange arrows point out branch points with high fluorescence, and blue ones low fluorescence. (B). Quantification of Axin-GFP branch point intensity compared to non-branch point intensity is shown. The green bar indicates control taken on an inverted LSM800. The blue bar indicates the same control taken on an upright LSM800; absolute fluorescence values vary based on the particular microscope. A dashed line separates the bars that correspond to the left or right axis respectively. A linear regression was used to determine statistical significance, * $p<0.05$, ** $p<0.01$, *** $p<0.001$ and error bars are standard deviation.

points (Figure 7). We also used a GDP-bound form of Gαo (KATANAEV *et al.* 2005) to confirm the involvement of this G protein in Axin localization, and observed a reduction of Axin-GFP at branch points. As for Apc2-GFP, the activated sggS9A reduced Axin-GFP localization (Figure 7), and expression of the constitutively inhibited sggS9E (BOUROUIS 2002) increased Axin-GFP localization again suggesting a negative role for sgg.

Based on the results so far, we have identified four regulatory modules that cooperate to position Apc2-GFP to dendrite branch points: 1) local ATP production by mitochondria, 2) Nrg/Ank2, 3) branched actin, and 4) fz/Gαo/Axin. The data also suggest that these modules likely act independently with the following possible exceptions: 1) we could not determine whether any of the modules act upstream of actin, and 2) we could not exclude that actin acts upstream of Axin.

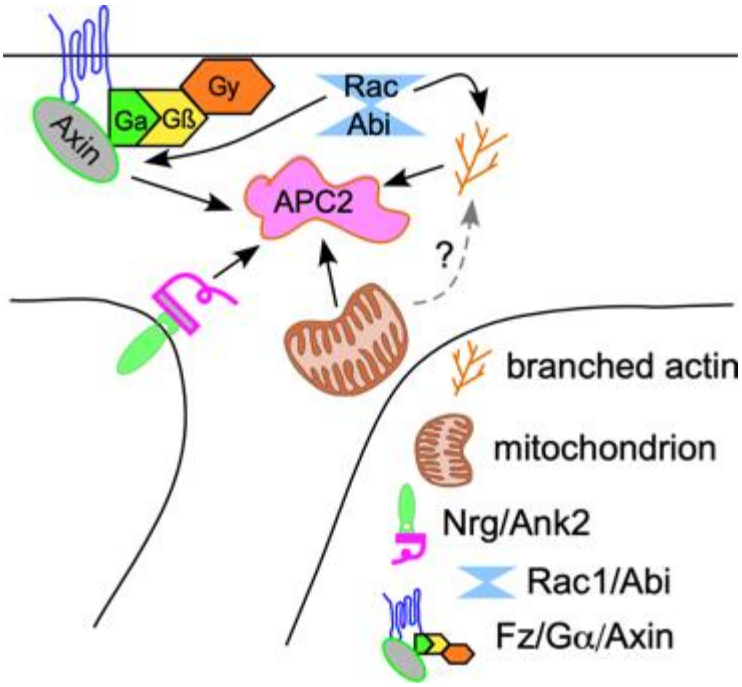

Figure 3-8. Summary of proteins involved in Apc2-GFP localization to dendrite branch points. The figure is a model that assembles the different proteins/organelles required to position Apc2-GFP at dendrite branch point. The small summary diagrams in figures throughout represent the dependencies that were used to generate this model.

Discussion

Generation of a minus-end-out microtubule array in Drosophila dendrites involves activity of both plus and minus end regulators at dendrite branch points (MATTIE *et al.* 2010; NGUYEN *et al.* 2014). To understand how these regulators are concentrated at branch points, we began with Apc2-GFP as it can recruit Apc and is very robustly targeted (MATTIE *et al.* 2010). We started by sampling a variety of candidates, from Apc interactors to representatives of different cytoskeletal systems. Positives in this screen spread across different groups of proteins, rather than pinpointing a single regulatory pathway (Figure 1). Tagged versions of several of the proteins that emerged from the initial screen, including Axin and Ank2,

also localized to dendrite branch points. After extensive secondary screening to validate the initial screen and order hits into dependency groups, we propose that they can be put into four functional modules, each of which is required for Apc2-GFP concentration at dendrite branch points (Figure 8).

Of these, the one that made the most intuitive sense was Rac1/Abi/Arp2/3. In Drosophila neuroblasts, Apc2 is localized at the cell cortex (AKONG *et al.* 2002), which tends to be a region rich in actin. Cortical actin is nucleated by Arp2/3 and formins (BOVELLAN *et al.* 2014), though in dendrites we only found a role for Arp2/3 in Apc2 localization. Actin has also been linked more directly to Apc2 localization in several other contexts. During the syncytial divisions of early Drosophila embryos, Apc2 localizes with actin dynamically (MCCARTNEY *et al.* 2001). In this case, however, armadillo (β-catenin) was proposed to link actin to Apc2 (MCCARTNEY *et al.* 2001) and we do not have evidence for a role for armadillo here. Apc2 also localizes to the cortex of Drosophila S2 cells in culture, but in this case Axin is not thought to play an upstream role (ZHOU *et al.* 2011) so it is unclear whether the link between Apc2 and actin is mechanistically similar in dendrites and the cortex of other cells. Alternatively, Arp2/3 could influence Apc2 localization through its role in endocytosis (GALLETTA AND COOPER 2009). This idea is particularly appealing because mammalian Apc can bind the clathrin adaptor AP-2 mu1 subunit (MATSUI *et al.* 2008). A potential role for endocytosis is also worth considering because ankyrins also interact with endocytic machinery, either directly through binding proteins that regulate endocytosis, or indirectly by helping to organize a submembrane spectrin network that opposes endocytosis (BENNETT AND LORENZO 2016). The neuronal ankyrin, Ank2, was also a hit in our initial screen, and Nrg, a plasma membrane protein partner of Ank2, acts upstream of Ank2. In general ankyrins link membrane proteins to the submembrane spectrin network, which can be regionally specialized as in the axon initial segment (AIS). In the AIS in Drosophila Ank2 and Neuroglian are required to establish a plasma membrane diffusion barrier that helps pattern

membrane proteins (JEGLA *et al.* 2016). So an alternate potential role to regulation of endocytosis for Ank2 and Neuroglian, is making a region of the plasma membrane distinct, as they do at the axon initial segment (JEGLA *et al.* 2016). However, while we identified the plasma membrane proteins fz and fz2, as well as lipid anchored heterotrimeric G proteins, as regulators of Apc2 localization, we do not think that Ank2 acts by partitioning any of these players within branch points because they act upstream of Axin localization and Ank2 does not.

In addition to the Arp2/3 and Ank2/Nrg modules, mitochondria are important for Apc2 localization. Both actin polymerization activated by Arp2/3 and cycling of heterotrimeric G proteins are potential energy consumers. However, as mitochondria did not affect Axin localization, but heterotrimeric G proteins did, actin is more likely to be the target of ATP production by mitochondria. Alternatively there could be yet another process occurring at the branch point that requires local energy production.

The fourth module acts through Axin to position Apc2. While Axin itself was not a surprise as it binds Apc2 (ROBERTS *et al.* 2011), the involvement of heterotrimeric G proteins and frizzleds upstream of Axin was not expected. First, it was surprising that plasma membrane proteins, Neuroglian, fz and fz2, would be involved in positioning Apc2, a cytosolic protein involved in steering microtubules. Second, it is only quite recently that frizzleds have been accepted to function as GPCRs (KOVAL *et al.* 2011; NICHOLS *et al.* 2013), so the involvement of heterotrimeric G proteins was not a given. Third, although frizzleds, G proteins and Axin have been linked in Drosophila, this work has been done primarily in epithelial cells (KATANAEV *et al.* 2005; EGGER-ADAM AND KATANAEV 2010) and there was no evidence that this pathway also might function in dendrites. However, the data strongly indicates that frizzleds, Gαo and Gαs act to position Apc2, and all except Gαs likely act through Axin as they are required for its positioning. The ability of activated and inactive forms of sgg (GSK3β) to modulate localization of Apc2-GFP and Axin-GFP are consistent with a subset of wnt signaling proteins playing a role

in branch point localization as sgg can bind Axin (KREMER *et al.* 2010) as well as other wnt signaling proteins. However, we do not have evidence that sgg is normally involved in branch point localization at this point because the RNAi that targets sgg had no effect in any of the assays. Based on the data, this wnt pathway variant seems to have Apc2 localization as its output. The only known dendritic function of Apc2 is microtubule steering. So, in contrast to canonical wnt signaling, which regulates transcription through β-catenin, this pathway seems to act locally to regulate the cytoskeleton.

Methods

Drosophila Stocks and Expression System

Drosophila stocks were obtained in large part from either Vienna Drosophila Resource Center (VDRC) or Bloomington Drosophila Stock Center (BDSC). RNAi lines from the BDSC are part of the TRiP collection; we thank the TRiP at Harvard Medical School (NIH/NIGMS R01-GM084947) for providing transgenic RNAi fly stocks used in this study. Specific RNAi lines, as well as overexpression and mutant alleles, are detailed in the Supplemental Table. The 221-Gal4 driver was used to express transgenes in Class I dendritic arborization sensory neurons. UAS-Dicer2 was included in all RNAi experiments. For whole brain imaging experiments, expression was pan-neuronally driven with elav-Gal4. Stocks with mutant fz alleles including *fz*^{F31} and *fz*^{R52} were a gift from Dr. Paul Adler at the University of Virginia. Constitutively active UAS-Gαs-GTP and inactive UAS-Gαo-GDP were provided by Dr. Andrew Tomlinson at Columbia University Medical Center. UAS-YFP-Ank2L8 was given to us by Dr. Jan Pielage (Technische Universitat Kaiserslautern). UAS-sggS9A and UAS-sggS9E were obtained from the BDSC. Tester lines for screens included: 1) UAS-dicer2, mCD8-RFP; 221-Gal4, Apc2-GFP, 2)

UAS-dicer2, UAS-mCD8-RFP; 221-Gal4, Mito-GFP, 3) UAS-dicer2, UAS-mCD8-RFP; 221-Gal4, UAS-YFP-Ank2L8, 4) UAS-dicer2, UAS-mCD8-RFP; 221-Gal4, UAS-Axin-GFP. Components from each of these lines can be obtained from BDSC. Additional fly lines used were UAS-Arp3-GFP and elav-Gal4, also available at BDSC.

Confocal Fluorescent *In vivo* Microscopy

After mating virgin female flies from tester lines (see *Drosophila* Stocks) with RNAi male flies (crosses kept at 25$_{o}$C), embryos were collected on caps filled with standard media every 24 hours. Caps were incubated with embryos/larvae for 3 days at 25$_{o}$C and used to harvest third instar animals for imaging on the third day. Individual larvae were placed on a microscope slide with a circular piece of dried agar in the middle with a little bit of water. Animals were allowed to move until they were dorsal side up, and then a cover slip was taped down on top of them. 10x objectives were used to locate larvae under the microscope. 60x Oil (NA 1.42) (Olympus) and 63x Oil (NA 1.4) (Zeiss) objectives were used to locate dendritic arborization neurons in the central hemisegments on either side of the animal. For UAS-Apc2-GFP localization, larvae were imaged on an Olympus Fluoview 1000. For the rest of the fluorescent markers including UAS-Mito-GFP, UAS-YFP-Ank2L8, UAS-Arp3-GFP, and UAS-Axin-GFP larvae were imaged on an Olympus Fluoview 1000 or a Zeiss LSM800 scanning confocal microscope.

Fluorescence Quantification Methods

Images were prepared and quantified using the image processing software Fiji. Maximum projection stacked images were used for quantitation of markers at branch points. UAS-Apc2-

GFP and UAS-Mito-GFP experiments were scored with a qualitative binary method. For examples of branch points that were scored as “positive” see branch points indicated with orange arrows throughout the figures, and for those scored as “negative” see examples with blue arrows. For the rest of the markers a relative pixel intensity measurement was used to calculate mean branch point intensity and non-branch point intensity within the main trunk of the comb dendrite. These non-branch point values were then subtracted from branch point to determine the branch point intensity over background. For each marker a set of microscope conditions (laser power, gain, pinhole) was chosen and the same setting were used throughout. The values on the y axes are fluorescence intensity with these settings. For some experiments two y axes are present, and the graph is divided by a dotted line to indicate where the left and right axes apply. The data on each side of the line was collected with a different microscope. Typically the left side is with an Olympus FV1000 and the right side with a Zeiss LSM800. It was necessary to change microscopes in the middle of some of the data sets because the Olympus was destroyed by a flood.

Statistical Methods

A Fisher’s Exact test to compare each condition to the control was used for UAS-Apc2-GFP screens. Linear or logistic regressions were performed for all other experiments using GraphPad Prism 6 software. Logistic regressions were used because they are the standard for testing differences between probabilities like Apc2-GFP occupancy. Three different control data sets were generated for Apc2-GFP and agree very closely with one another (Figure 1C, 3B and 5C). For many of the graphs the control data from 3B was used. Linear regressions are appropriate for comparing a group to the same control, and so these were used for continuous data sets. Statistical tests were chosen with help from Haley Brittingham as part of her Masters

work in Statistics at Penn State. See individual figure legends for statistical test used. Statistical significance is noted as * $p<0.05$, ** $p<0.01$, *** $p<0.001$. All error bars show the standard deviation as this is an intuitive representation of variability. Where no error bars are present the data is categorical.

Data Availability

Drosophila strains are available upon request. The Supplemental Table contains a list of all fly lines used, and lines with multiple transgenes are listed in the materials and methods. Example raw image files are also available on request.

Acknowledgements

We are grateful to Dr. Paul Adler, Dr. Mariann Bienz, Dr. Andrew Tomlinson and Dr. Jan Pielage for providing various fly strains. Stocks obtained from the Bloomington Drosophila Stock Center (NIH P40OD018537) were used in this study. Vienna Drosophila Resource Center also provided valuable fly stocks. We used FlyBase release FB2017_06 (GRAMATES *et al.* 2017) as a reference throughout and include GBrowse images in the Supplemental Data. We are also thankful for the support and input of all Rolls lab members. We are especially grateful for the input from Matthew Shorey and Dr. Gregory Kothe. We also very much appreciate Haley Brittingham, a Masters student in Applied Statistics at Penn State, for consulting with us about appropriate statistical tests. This work was funded in part from NIH grant R01 GM08511 to MMR.

References

Akong, K., B. M. McCartney and M. Peifer, 2002 Drosophila APC2 and APC1 have overlapping roles in the larval brain despite their distinct intracellular localizations. Dev Biol 250**:** 71-90.

Baas, P. W., and S. Lin, 2011 Hooks and comets: The story of microtubule polarity orientation in the neuron. Dev Neurobiol 71**:** 403-418.

Babic, M., G. J. Russo, A. J. Wellington, R. M. Sangston, M. Gonzalez *et al.*, 2015 Miro's N-terminal GTPase domain is required for transport of mitochondria into axons and dendrites. J Neurosci 35**:** 5754-5771.

Bartolini, F., and G. G. Gundersen, 2006 Generation of noncentrosomal microtubule arrays. J Cell Sci 119**:** 4155-4163.

Bennett, V., and D. N. Lorenzo, 2016 An Adaptable Spectrin/Ankyrin-Based Mechanism for Long-Range Organization of Plasma Membranes in Vertebrate Tissues. Curr Top Membr 77**:** 143-184.

Bhanot, P., M. Fish, J. A. Jemison, R. Nusse, J. Nathans *et al.*, 1999 Frizzled and Dfrizzled-2 function as redundant receptors for Wingless during Drosophila embryonic development. Development 126**:** 4175-4186.

Bosco, E. E., J. C. Mulloy and Y. Zheng, 2009 Rac1 GTPase: a "Rac" of all trades. Cell Mol Life Sci 66**:** 370-374.

Bouley, M., M. Z. Tian, K. Paisley, Y. C. Shen, J. D. Malhotra *et al.*, 2000 The L1-type cell adhesion molecule neuroglian influences the stability of neural ankyrin in the Drosophila embryo but not its axonal localization. J Neurosci 20**:** 4515-4523.

Bourouis, M., 2002 Targeted increase in shaggy activity levels blocks wingless signaling. Genesis 34**:** 99-102.

Bovellan, M., Y. Romeo, M. Biro, A. Boden, P. Chugh *et al.*, 2014 Cellular control of cortical actin nucleation. Curr Biol 24**:** 1628-1635.

Brocardo, M., Y. Lei, A. Tighe, S. S. Taylor, M. T. Mok *et al.*, 2008 Mitochondrial targeting of adenomatous polyposis coli protein is stimulated by truncating cancer mutations: regulation of Bcl-2 and implications for cell survival. J Biol Chem 283**:** 5950-5959.

Cadigan, K. M., and M. Peifer, 2009 Wnt signaling from development to disease: insights from model systems. Cold Spring Harb Perspect Biol 1**:** a002881.

Chen, Y., M. M. Rolls and W. O. Hancock, 2014 An EB1-kinesin complex is sufficient to steer microtubule growth in vitro. Curr Biol 24**:** 316-321.

Cliffe, A., F. Hamada and M. Bienz, 2003 A role of Dishevelled in relocating Axin to the plasma membrane during wingless signaling. Curr Biol 13**:** 960-966.

Derivery, E., and A. Gautreau, 2010 Generation of branched actin networks: assembly and regulation of the N-WASP and WAVE molecular machines. Bioessays 32**:** 119-131.

Dietzl, G., D. Chen, F. Schnorrer, K. C. Su, Y. Barinova *et al.*, 2007 A genome-wide transgenic RNAi library for conditional gene inactivation in Drosophila. Nature 448**:** 151-156.

Dikovskaya, D., J. Zumbrunn, G. A. Penman and I. S. Nathke, 2001 The adenomatous polyposis coli protein: in the limelight out at the edge. Trends Cell Biol 11**:** 378-384.

Doodhi, H., E. A. Katrukha, L. C. Kapitein and A. Akhmanova, 2014 Mechanical and geometrical constraints control kinesin-based microtubule guidance. Curr Biol 24**:** 322-328.

Egger-Adam, D., and V. L. Katanaev, 2010 The trimeric G protein Go inflicts a double impact on axin in the Wnt/frizzled signaling pathway. Dev Dyn 239**:** 168-183.

Galletta, B. J., and J. A. Cooper, 2009 Actin and endocytosis: mechanisms and phylogeny. Curr Opin Cell Biol 21**:** 20-27.

Gramates, L. S., S. J. Marygold, G. D. Santos, J. M. Urbano, G. Antonazzo *et al.*, 2017 FlyBase at 25: looking to the future. Nucleic Acids Res 45**:** D663-D671.

Grueber, W. B., L. Y. Jan and Y. N. Jan, 2002 Tiling of the Drosophila epidermis by multidendritic sensory neurons. Development 129**:** 2867-2878.

Guo, X., G. T. Macleod, A. Wellington, F. Hu, S. Panchumarthi *et al.*, 2005 The GTPase dMiro is required for axonal transport of mitochondria to Drosophila synapses. Neuron 47**:** 379-393.

Hazelett, D. J., M. Bourouis, U. Walldorf and J. E. Treisman, 1998 decapentaplegic and wingless are regulated by eyes absent and eyegone and interact to direct the pattern of retinal differentiation in the eye disc. Development 125**:** 3741-3751.

Hudson, A. M., and L. Cooley, 2002 A subset of dynamic actin rearrangements in Drosophila requires the Arp2/3 complex. J Cell Biol 156**:** 677-687.

Ihry, R. J., and A. Bashirullah, 2014 Genetic control of specificity to steroid-triggered responses in Drosophila. Genetics 196**:** 767-780.

Jegla, T., M. M. Nguyen, C. Feng, D. J. Goetschius, E. Luna *et al.*, 2016 Bilaterian Giant Ankyrins Have a Common Evolutionary Origin and Play a Conserved Role in Patterning the Axon Initial Segment. PLoS Genet 12**:** e1006457.

Jones, K. H., J. Liu and P. N. Adler, 1996 Molecular analysis of EMS-induced frizzled mutations in Drosophila melanogaster. Genetics 142**:** 205-215.

Katanaev, V. L., R. Ponzielli, M. Semeriva and A. Tomlinson, 2005 Trimeric G protein-dependent frizzled signaling in Drosophila. Cell 120**:** 111-122.

Koch, I., H. Schwarz, D. Beuchle, B. Goellner, M. Langegger *et al.*, 2008 Drosophila ankyrin 2 is required for synaptic stability. Neuron 58**:** 210-222.

Koval, A., V. Purvanov, D. Egger-Adam and V. L. Katanaev, 2011 Yellow submarine of the Wnt/Frizzled signaling: submerging from the G protein harbor to the targets. Biochem Pharmacol 82**:** 1311-1319.

Kremer, S. A., N. Erdeniz, W. Peterson-Nedry, E. A. Swanson and M. Wehrli, 2010 In vivo analysis in Drosophila reveals differential requirements of contact residues in Axin for interactions with GSK3beta or beta-catenin. Dev Biol 337**:** 110-123.

Kunttas-Tatli, E., D. M. Roberts and B. M. McCartney, 2014 Self-association of the APC tumor suppressor is required for the assembly, stability, and activity of the Wnt signaling destruction complex. Mol Biol Cell 25**:** 3424-3436.

Labbe, K., A. Murley and J. Nunnari, 2014 Determinants and functions of mitochondrial behavior. Annu Rev Cell Dev Biol 30**:** 357-391.

Luchtenborg, A. M., G. P. Solis, D. Egger-Adam, A. Koval, C. Lin *et al.*, 2014 Heterotrimeric Go protein links Wnt-Frizzled signaling with ankyrins to regulate the neuronal microtubule cytoskeleton. Development 141**:** 3399-3409.

Luo, L., Y. J. Liao, L. Y. Jan and Y. N. Jan, 1994 Distinct morphogenetic functions of similar small GTPases: Drosophila Drac1 is involved in axonal outgrowth and myoblast fusion. Genes Dev 8**:** 1787-1802.

Matsui, C., S. Kaieda, T. Ikegami and Y. Mimori-Kiyosue, 2008 Identification of a link between the SAMP repeats of adenomatous polyposis coli tumor suppressor and the Src homology 3 domain of DDEF. J Biol Chem 283**:** 33006-33020.

Mattie, F. J., M. M. Stackpole, M. C. Stone, J. R. Clippard, D. A. Rudnick *et al.*, 2010 Directed Microtubule Growth, +TIPs, and Kinesin-2 Are Required for Uniform Microtubule Polarity in Dendrites. Curr Biol 20**:** 2169-2177.

McCartney, B. M., D. G. McEwen, E. Grevengoed, P. Maddox, A. Bejsovec *et al.*, 2001 Drosophila APC2 and Armadillo participate in tethering mitotic spindles to cortical actin. Nat Cell Biol 3**:** 933-938.

McCartney, B. M., and I. S. Nathke, 2008 Cell regulation by the Apc protein Apc as master regulator of epithelia. Curr Opin Cell Biol 20**:** 186-193.

Muroyama, A., and T. Lechler, 2017 Microtubule organization, dynamics and functions in differentiated cells. Development 144**:** 3012-3021.

Nelson, S., and I. S. Nathke, 2013 Interactions and functions of the adenomatous polyposis coli (APC) protein at a glance. J Cell Sci 126**:** 873-877.

Nguyen, M. M., C. J. McCracken, E. S. Milner, D. J. Goetschius, A. T. Weiner *et al.*, 2014 Gamma-tubulin controls neuronal microtubule polarity independently of Golgi outposts. Mol Biol Cell 25**:** 2039-2050.

Ni, J. Q., L. P. Liu, R. Binari, R. Hardy, H. S. Shim *et al.*, 2009 A Drosophila resource of transgenic RNAi lines for neurogenetics. Genetics 182**:** 1089-1100.

Ni, J. Q., R. Zhou, B. Czech, L. P. Liu, L. Holderbaum *et al.*, 2011 A genome-scale shRNA resource for transgenic RNAi in Drosophila. Nat Methods 8**:** 405-407.

Nichols, A. S., D. H. Floyd, S. P. Bruinsma, K. Narzinski and T. J. Baranski, 2013 Frizzled receptors signal through G proteins. Cell Signal 25**:** 1468-1475.

Nusse, R., and H. Clevers, 2017 Wnt/beta-Catenin Signaling, Disease, and Emerging Therapeutic Modalities. Cell 169**:** 985-999.

Ori-McKenney, K. M., L. Y. Jan and Y. N. Jan, 2012 Golgi outposts shape dendrite morphology by functioning as sites of acentrosomal microtubule nucleation in neurons. Neuron 76**:** 921-930.

Pielage, J., L. Cheng, R. D. Fetter, P. M. Carlton, J. W. Sedat *et al.*, 2008 A presynaptic giant ankyrin stabilizes the NMJ through regulation of presynaptic microtubules and transsynaptic cell adhesion. Neuron 58**:** 195-209.

Povelones, M., R. Howes, M. Fish and R. Nusse, 2005 Genetic evidence that Drosophila frizzled controls planar cell polarity and Armadillo signaling by a common mechanism. Genetics 171**:** 1643-1654.

Rao, K., M. C. Stone, A. T. Weiner, K. W. Gheres, C. Zhou *et al.*, 2016 Spastin, atlastin, and ER relocalization are involved in axon but not dendrite regeneration. Mol Biol Cell 27**:** 3245-3256.

Roberts, D. M., M. I. Pronobis, J. S. Poulton, J. D. Waldmann, E. M. Stephenson *et al.*, 2011 Deconstructing the sscatenin destruction complex: mechanistic roles for the tumor suppressor APC in regulating Wnt signaling. Mol Biol Cell 22**:** 1845-1863.

Rolls, M. M., 2011 Neuronal polarity in Drosophila: Sorting out axons and dendrites. Dev Neurobiol 71**:** 419-429.

Rolls, M. M., D. Satoh, P. J. Clyne, A. L. Henner, T. Uemura *et al.*, 2007 Polarity and compartmentalization of Drosophila neurons. Neural Development 2**:** 7.

Ruane, P. T., L. F. Gumy, B. Bola, B. Anderson, M. J. Wozniak *et al.*, 2016 Tumour Suppressor Adenomatous Polyposis Coli (APC) localisation is regulated by both Kinesin-1 and Kinesin-2. Sci Rep 6**:** 27456.

Sanchez, A. D., and J. L. Feldman, 2017 Microtubule-organizing centers: from the centrosome to non-centrosomal sites. Curr Opin Cell Biol 44**:** 93-101.

Satoh, D., D. Sato, T. Tsuyama, M. Saito, H. Ohkura *et al.*, 2008 Spatial control of branching within dendritic arbors by dynein-dependent transport of Rab5-endosomes. Nat Cell Biol 10**:** 1164-1171.

Sherwood, N. T., Q. Sun, M. Xue, B. Zhang and K. Zinn, 2004 Drosophila spastin regulates synaptic microtubule networks and is required for normal motor function. PLoS Biol 2**:** e429.

Stephan, R., B. Goellner, E. Moreno, C. A. Frank, T. Hugenschmidt *et al.*, 2015 Hierarchical microtubule organization controls axon caliber and transport and determines synaptic structure and stability. Dev Cell 33**:** 5-21.

Stone, M. C., M. M. Nguyen, J. Tao, D. L. Allender and M. M. Rolls, 2010 Global up-regulation of microtubule dynamics and polarity reversal during regeneration of an axon from a dendrite. Mol Biol Cell 21**:** 767-777.

Stone, M. C., K. Rao, K. W. Gheres, S. Kim, J. Tao *et al.*, 2012 Normal Spastin Gene Dosage Is Specifically Required for Axon Regeneration. Cell Rep.

Stone, M. C., F. Roegiers and M. M. Rolls, 2008 Microtubules Have Opposite Orientation in Axons and Dendrites of Drosophila Neurons. Mol Biol Cell 19**:** 4122-4129.

Tao, J., C. Feng and M. M. Rolls, 2016 The microtubule-severing protein fidgetin acts after dendrite injury to promote their degeneration. J Cell Sci 129**:** 3274-3281.

Tao, J., and M. M. Rolls, 2011 Dendrites have a rapid program of injury-induced degeneration that is molecularly distinct from developmental pruning. J Neurosci 31**:** 5398-5405.

Webb, R. L., M. N. Zhou and B. M. McCartney, 2009 A novel role for an APC2-Diaphanous complex in regulating actin organization in Drosophila. Development 136**:** 1283-1293.

Weiner, A. T., M. C. Lanz, D. J. Goetschius, W. O. Hancock and M. M. Rolls, 2016 Kinesin-2 and Apc function at dendrite branch points to resolve microtubule collisions. Cytoskeleton (Hoboken) 73**:** 35-44.

Yamamoto, M., R. Ueda, K. Takahashi, K. Saigo and T. Uemura, 2006 Control of axonal sprouting and dendrite branching by the Nrg-Ank complex at the neuron-glia interface. Curr Biol 16**:** 1678-1683.

Zhou, M. N., E. Kunttas-Tatli, S. Zimmerman, F. Zhouzheng and B. M. McCartney, 2011 Cortical localization of APC2 plays a role in actin organization but not in Wnt signaling in Drosophila. J Cell Sci 124**:** 1589-1600.

Introduction to Chapter 4

Chapter 4 is a published manuscript at PLOS Biology as of March 12th 2020. The current version is the manuscript without submitted revisions. The chapter fits into the thesis as the hypothesis generating experiments are adapted from chapter 3. The same candidate proteins tested for a role in Apc2 localization are tested for a role in γTub targeting to branch points. The Wnt signaling proteins are found to overlap between these two microtubule regulators and so ties together the two chapters.

Golgi outposts are currently the only proposed site for acentrosomal nucleation in dendrites. However, the proof is inherently flawed and so this site has been called into question. In chapter 4 we provide a signaling pathway for positioning nucleation sites at dendrite branch points. We identify how Golgi outposts were misidentified and are actually early endosomes. This settles a long-standing dispute within the field and it will undoubtably open up new areas of exploration within neuronal cell biology but also generally within the cell biology community.

I am the first author on the manuscript and there are supporting contributions by Dylan Seebold, Pedro Torres, Christin Folker, Rachel Swope, Gregory Kothe, Jessica Stoltz, Madaleine Zalenski, Christopher Kozlowski, Dylan Barbera, Mit Patel, Pankajam Thyagarajan, Matthew Keegan, Kana Behari, and Song Song. Jeffrey Axelrod provided mentorship to Song Song for her contribution and expertise with regard to Wnt signaling. Melissa Rolls contributed to writing of the manuscript and managed the project. Dylan Seebold contributed to a few of the datasets in figures 1, 3 and 4. Pedro helped with a couple of the datasets in figure 3 and helped image the data in figure 8. Christin generated the data in the beginning of figure 4. Rachel Swope characterized the UAS-dsh-GFP construct and developed the dataset for it in figure 2. Gregory Kothe and Jessica Stoltz generated the Axin targeting construct used in figure 8 and supplemental figure 7. Madaeleine generated some of the data in the Rab screen of figure 5. Christopher and

Dylan Barbara performed the initial polarity experiments in figure 3 for G-proteins. I redid the experiments which are shown in the figure. Pankajam imaged the γTub-sfGFP construct in supplemental figure 2. Matthew performed the initial wntless RNAi experiments in figure 5 and then I confirmed the findings which are shown in the figure. Kana made the line for looking at Rab5 localization and screening with RNAi. Song created the dsh-clover construct used in figure 6 and supplemental figure 4. I conducted and analyzed the vast majority of the experiments and these were done during my thesis work. In addition, I created all figures throughout and contributed to the writing of the manuscript.

Chapter 4

Endosomal Wnt signaling proteins control microtubule nucleation in dendrites

Abstract

Dendrite microtubules are polarized with minus-end-out orientation. Nucleation sites concentrate at dendrite branch points, but how they localize is not known. Using Drosophila, we found that canonical Wnt signaling proteins regulate localization of the core nucleation protein γTubulin (γTub). Reduction of frizzleds, arrow (LRP5/6), dishevelled, casein kinase Iγ, G proteins and Axin reduced γTub-GFP at branch points and two functional readouts of dendritic nucleation confirmed a role for Wnt signaling proteins. Both dsh and Axin localized to branch points, with dsh upstream of Axin. Moreover, tethering Axin to mitochondria was sufficient to recruit ectopic γTub-GFP and increase microtubule dynamics in dendrites. At dendrite branch points Axin and dsh colocalized with early endosomal marker Rab5 and new microtubule growth initiated at puncta marked with fz, dsh, Axin and Rab5. We propose that in dendrites canonical Wnt signaling proteins are housed on early endosomes and recruit nucleation sites to branch points.

Introduction

Neurons extend long branched processes from a central cell body. This shape is incompatible with a centrosomal microtubule organizing center (MTOC). Mature neurons are therefore among the ranks of differentiated cells that have non-centrosomal microtubule arrays (Bartolini and Gundersen 2006, Muroyama and Lechler 2017, Sanchez and Feldman 2017, Tillery, Blake-Hedges et al. 2018). It is particularly important to understand how neuronal

microtubules are organized because the distance between the primary site of synthesis in the cell body to functional sites in axons and dendrites can be large, and therefore place heavy demands on microtubule-based transport. In humans, slight disruptions in microtubule regulators or motors can manifest as neurodegenerative disease (Gunawardena and Goldstein 2004, Chevalier-Larsen and Holzbaur 2006) underscoring neuronal reliance on perfectly orchestrated microtubule-based transport.

If neuronal microtubules are not anchored to the centrosome, how are they organized? In all neurons so far examined, axonal microtubules have their dynamic plus ends oriented away from the cell body (plus-end-out) (Baas and Lin 2011). In dendrites of vertebrate neurons, microtubules are mixed (Baas, Deitch et al. 1988, Burton 1988, Yau, Schatzle et al. 2016). In invertebrate neurons (Drosophila and C. elegans), axons have the same plus-end-out microtubule organization as vertebrates (Rolls, Satoh et al. 2007, Stone, Roegiers et al. 2008, Goodwin, Sasaki et al. 2012, Maniar, Kaplan et al. 2012), but mature dendrites have almost all minus-end-out microtubules (Rolls, Satoh et al. 2007, Stone, Roegiers et al. 2008, Goodwin, Sasaki et al. 2012). In immature Drosophila dendrites, microtubules are mixed and only gradually resolve to the minus-end-out mature arrangement (Hill, Parmar et al. 2012). Thus, although the final arrangement of microtubules in vertebrate and invertebrate dendrites is somewhat different, they are the same during dendrite development.

While the arrangement of neuronal microtubules is clearly non-centrosomal, the source of axonal and dendritic microtubules has been controversial. Two major models for generating axonal and dendritic microtubules have been proposed. The first is that neuronal microtubules are nucleated at the centrosome, or perhaps elsewhere in the cell body, and then released for transport/sliding into axons and dendrites (Baas and Yu 1996). This model has substantial support, including recent analyses with newer techniques. For example, live imaging of microtubules with plus-tip tracking proteins and photoconvertible αTubulin has provided

evidence for directional transport of microtubules into and out of developing axons in mammalian (Rao, Patil et al. 2017) and Drosophila (del Castillo, Winding et al. 2015) neurons.

The second model is that nucleation sites are found outside the cell body and microtubules are generated locally in axons and dendrites. Evidence for this model came from the observation that centrosomal γTubulin (γTub) decreases gradually over time and centrosome ablation does not disrupt axon formation (Stiess, Maghelli et al. 2010). Similarly, the centriole is not surrounded by γTub in Drosophila neurons in vivo, and it is dispensable for neuronal microtubule organization (Nguyen, Stone et al. 2011). One way to reconcile these two models is to assume that both are important, and that very early in neuronal development microtubule sliding can dominate, while later in development and in mature neurons microtubules are primarily locally nucleated.

In some cell types the Golgi complex recruits nucleation sites (Sanders and Kaverina 2015), and small Golgi outposts can be found in both mammalian and Drosophila dendrites (Horton and Ehlers 2003, Ye, Zhang et al. 2007). Thus, it was proposed that the Golgi might act as a non-centrosomal MTOC in dendrites (Ori-McKenney, Jan et al. 2012). However, subsequent analysis of γTub and Golgi outposts, including a strategy to deplete Golgi from dendrites, called this proposal into question (Nguyen, McCracken et al. 2014).

Within Drosophila dendrites, γTub is concentrated at branch points (Nguyen, McCracken et al. 2014). In a previous study, we identified proteins that localize a different microtubule regulator, Apc2, to branch points (Weiner, Seebold et al. 2018). We reasoned that some or all of this machinery might be used to position γTub to the same region. We therefore tested whether any of these proteins acts upstream of γTub-GFP in dendrites. Surprisingly, a subset of Wnt signaling proteins was required to localize γTub-GFP to dendrite branch points, to regulate dendritic microtubule polarity, and to nucleate microtubules in dendrites in response to axon

injury. The required proteins include the seven transmembrane domain frizzled proteins (Wnt receptors), arrow (a Wnt co-receptor) heterotrimeric G proteins, dishevelled, casein kinase Iγ and Axin. Axin seems to be the key output protein of this pathway as it was sufficient to recruit γTub to ectopic sites in dendrites. Within branch points, frizzled, Axin and dsh were found on puncta that colocalized with Rab5. In addition, new EB1 comets at polymerizing microtubule plus-ends initiated from puncta marked with fz, dsh, Axin and Rab5. We propose that Wnt signaling proteins localize to early endosomes at dendrite branch points and function there to control local microtubule nucleation. While it has previously been shown that Wnt signaling proteins can function from endosomes (Seto and Bellen 2006), identification of microtubule nucleation as an output of endosomal Wnt proteins is quite unexpected.

Results

A subset of canonical Wnt signaling proteins is required for γTubulin concentration at dendrite branch points

To understand how γTub is concentrated at dendrite branch points, we expressed γTub-GFP in a model Drosophila cell, the dorsal dendritic arborization (dda) E neuron. γTub-GFP localizes similarly to endogenous γTub (Nguyen, McCracken et al. 2014) and can rescue phenotypes in mutant animals (Chen, Stone et al. 2012). The ddaE cell is found in the larval body wall where it helps sense body position to facilitate coordinated movement (Hughes and Thomas 2007). Microtubule organization in this cell type has been described in previous studies (Stone, Roegiers et al. 2008, Mattie, Stackpole et al. 2010, Nguyen, McCracken et al. 2014, Yalgin, Ebrahimi et al. 2015), and the stereotyped shape of its large dorsal dendrite makes it easy to

consistently assay protein localization. A soluble protein is about 1.2 fold brighter at branch points (BP) than non-branch points (nBP), while γTub-GFP is over two-fold brighter in this

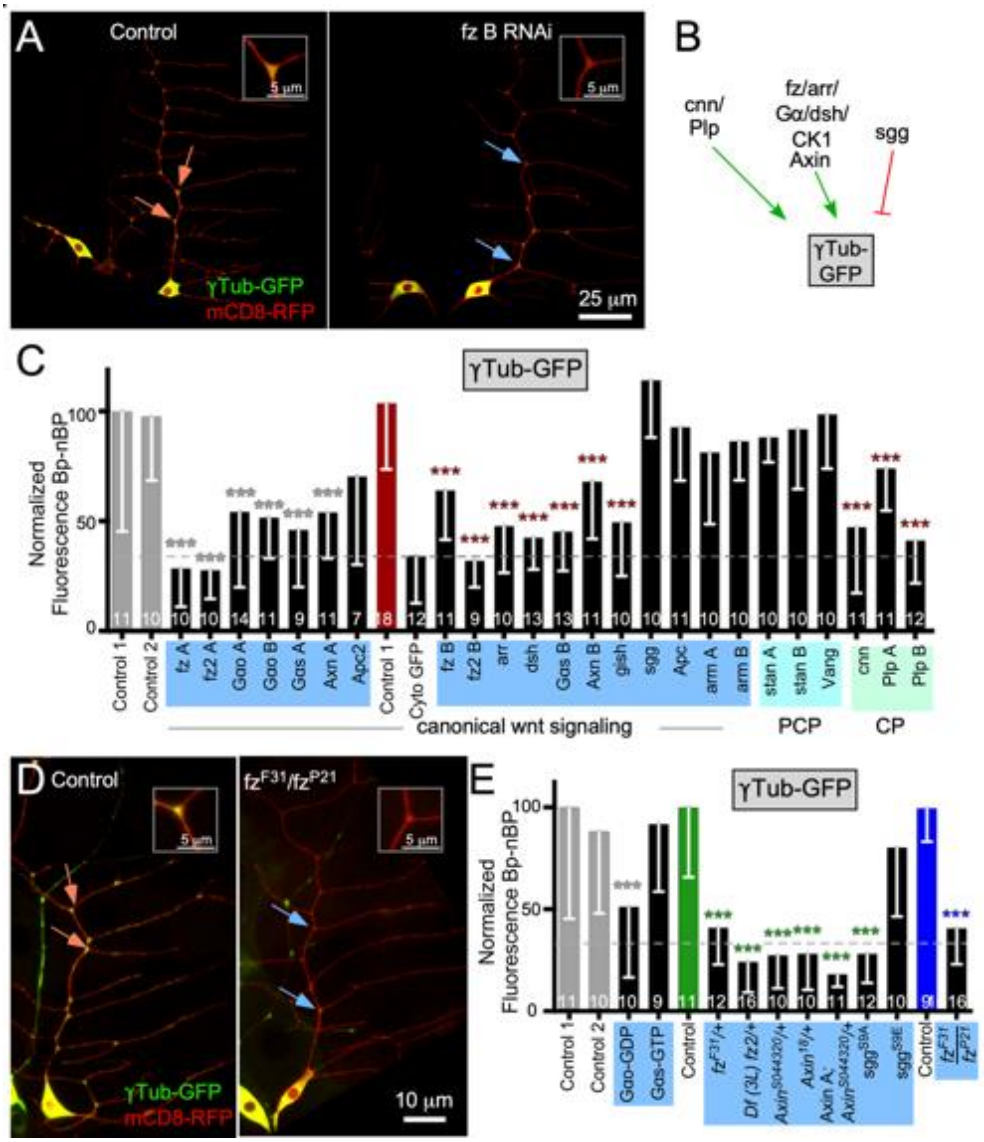

Figure 4-1. A candidate screen to identify proteins that target γTub-GFP to dendrite branch points.

(A) Example images of UAS-γTub-GFP localization in ddaE neurons expressing UAS-Rtnl2 RNAi (Control 1) (VDRC 33320) and UAS-fz B RNAi (VDRC 43075) hairpins. Membranes were marked with UAS-mCD8-RFP to see cell shape. Scale bar is 25 µm. Orange arrows indicate branch points with high γTub-GFP signal and blue arrows indicate branch points with low γTub-GFP signal. Insets in the top corner of each image show the top branch point highlighted with an arrow in each image (B) Diagram summarizing data in the Figure is shown.

See also Figure S1 for information about branch point and non-branch point quantitation. (C) Quantification of γTub-GFP at branch points is shown in larvae expressing different RNAi hairpins. Control 1 is Rtnl2 RNAi, as Rtnl2 is thought to be a pseudogene. Control 2 is γTub37C RNAi. This isoform of γTub is maternally deposited and not expressed in somatic cells like neurons. Values were generated by subtracting mean non-branch point (nBP) fluorescence from branch point (BP) fluorescence for each cell; normalized fluorescence values are shown. Normalization values were generated by making the control value equal to 100. The normalization constant was then used to normalize each sample from every other genotype. Additionally, each sample in the control is also normalized to this value. A dashed line indicates where a soluble GFP control is used to show baseline BP localization due to the difference in size and shape from nBp regions. This dashed line will continue throughout the rest of the figures that show γTub-GFP or Axin-GFP. Shaded colors over x-axis names indicate which functional groups the RNAi lines belong to and are noted as pink for mitochondria (Figure S1), yellow for Ankyrin2 and Neuroglian (Figure S1), purple for branched-actin regulators (Figure S1), blue for wnt signaling and green for centrosomal proteins. Color codes will follow throughout the rest of the figures. Grey bars are controls done on an Olympus FluoView1000; the same control data sets are shown Figure S1 for reference. The red bars indicate a control performed on a Zeiss LSM800; the same control data set is shown in Figure S1. (D) Examples images of *yw* (control) and fz_{F31}/fz_{P21} animals expressing UAS-γTub-GFP and UAS-mCD8-RFP with the promoter IGI-Gal4 to drive expression in Class I da neurons. Orange arrows indicate branch points with high γTub-GFP signal and blue arrows indicate branch points with low γTub-GFP signal. Insets in the top corner of each image indicate the top branch point marked in each image. (E) Quantification of Bp-nBP fluorescence as carried out before. Throughout the figures data from the Olympus is on the left and data from the Zeiss are on the right. Refer to Supplemental Table 1 for all genotypes. Sample sizes are shown within the bars. Error bars indicate standard deviation. A linear regression was used to determine statistical significance. * $p<0.05$, ** $p<0.01$, *** $p<0.001$.

region (Nguyen, McCracken et al. 2014) indicating it is likely to be actively recruited. We therefore constructed a tester line, UAS-dicer2, UAS-mCD8-RFP; 221-Gal4, UAS-γTub-GFP (Figure 1A), in which we could perform RNAi and assay γTub-GFP in whole, living larvae. When this tester line was crossed to a control RNAi line, GFP fluorescence was higher within branch points than between them (Figure 1A, and S1). To make sure that this represented active targeting rather than larger volume of branch points, we compared γTub-GFP signal to cytoplasmic GFP signal (Figure S1F). While cytoplasmic GFP signal is slightly higher at branch points than non-branch points, γTub-GFP is much higher (Figure S1G). The difference between

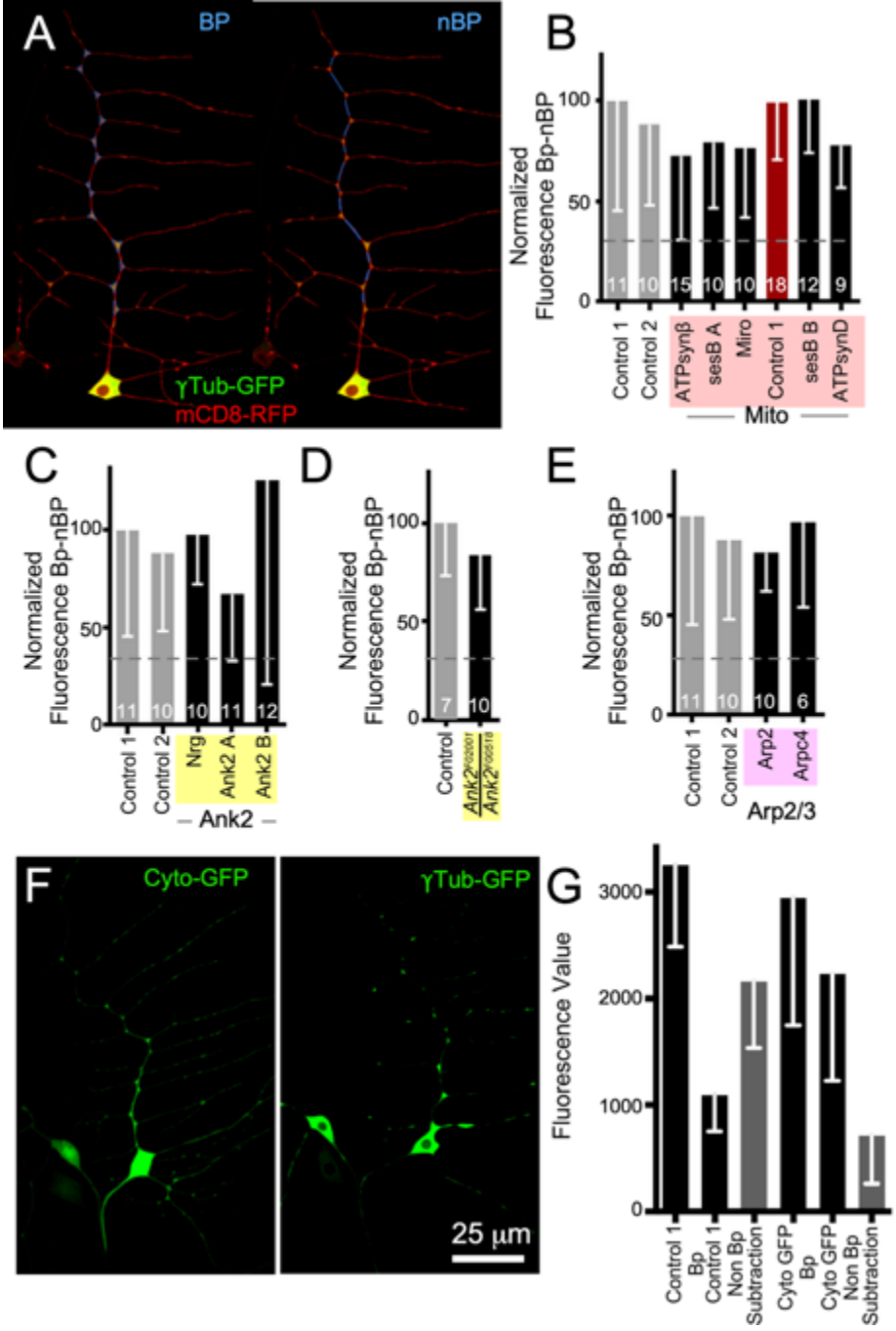

Figure 4-S1. Candidate screen for proteins required for γTub-GFP localization to dendrite branch points.

(A) Example images of γTub-GFP and mCD8-RFP in ddaE neurons are shown with branch point (left) and non-branch point (right) regions outlined. Outlines were drawn manually in Fiji and the measuring tool was then used to measure fluorescence in each region. These values were then averaged for each cell. The branch point was outlined until it began to taper and this was the cut off point for where the non-branch point areas began. (B-E) Quantification of γTub-GFP at branch points is shown in larvae expressing different RNAi hairpins. Control 1 is Rtnl2 RNAi, as Rtnl2 is thought to be a pseudogene. Control 2 is γTub37C RNAi. This isoform of γTub is maternally deposited and not expressed in somatic cells like neurons. Values were generated by subtracting mean non-branch point (nBP) fluorescence from branch point (BP) fluorescence for each cell; normalized fluorescence values are shown. Shaded colors over x-axis names indicate which functional groups the RNAi lines belong to and are noted as pink for mitochondria, yellow for Ankyrin2 and Neuroglian, and purple for branched-actin regulators.

(F) Representative images showing a soluble cytoplasmic GFP (left) and UAS-γTub-GFP (right) under 221 GAL4. (G) Raw quantification of fluorescence showing BP and nBP values. Grey bars indicate the subtraction of nBP from BP that was used to create the control normalization value in Figs 1, 5, and S4.

cytoplasmic GFP at branch points (Bp) vs non-branch points (nBp) represents the lowest expected value for γTub-GFP when active targeting is removed, and is indicated by a dotted line on graphs (Figure 1C and E). The γTub-GFP tester line was validated as a screening tool by crossing it to lines with RNAi transgenes targeting centrosomin (cnn) and Pericentrin-like protein (Plp), proteins previously implicated in dendritic microtubule nucleation (Ori-McKenney, Jan et al. 2012, Yalgin, Ebrahimi et al. 2015). Compared to control, cnn and Plp RNAi resulted in less γTub-GFP at branch points (Figure 1C). Note that these effects are cell-autonomous as UAS-RNAi hairpins were expressed with 221-Gal4 in a small subset of neurons that includes ddaE.

The branch point localization of γTub-GFP is reminiscent of another microtubule regulator, Apc2 (Mattie, Stackpole et al. 2010). We previously identified proteins required for Apc2 localization to branch points (Weiner, Seebold et al. 2018) and hypothesized that some of these may also target γTub-GFP. Reduction of mitochondria and actin regulators as well as Wnt signaling proteins disrupted Apc2-GFP localization (Weiner, Seebold et al. 2018). RNAi lines that targeted proteins in the Wnt signaling group, but not the other groups, reduced γTub-GFP at dendrite branch points (Figure 1A-C and S1B-E). Of Wnt signaling proteins, those broadly involved in multiple signaling pathways including frizzleds, dishevelled (dsh), casein kinase 1γ/gish and heterotrimeric G proteins (Davidson, Wu et al. 2005, Katanaev and Tomlinson 2006, Cadigan and Peifer 2009, Koval, Purvanov et al. 2011, Gault, Olguin et al. 2012, Devenport 2014) had phenotypes (Figure 1A and C). In addition, phenotypes occurred upon reduction of a subset of proteins specific to canonical Wnt signaling including the scaffolding protein Axin (Cadigan and Peifer 2009) and arrow (arr), the Drosophila LRP5/6 ortholog (Cadigan and Peifer

2009, MacDonald and He 2012). Knockdown of proteins specific to Planar Cell Polarity (PCP) (Devenport 2014, Humphries and Mlodzik 2017) did not reduce γTub-GFP at branch points (Figure 1C). Surprisingly, canonical Wnt signaling proteins Apc and armadillo (β-catenin/arm) did not seem to play a role at branch points (Figure 1C). As it is difficult to make firm conclusions from negative RNAi data, we examined expression of arm in the ddaE neuron using a GFP-tagged arm minigene (arm promoter driving full length arm) that is fully functional and rescues a null arm mutant (Orsulic and Peifer 1996). Arm-GFP was readily visible at borders of epithelial cells, but was not detectable in neurons (Figure S2A). In contrast, a GFP insertion in the *gish* gene yielded visible fluorescence in neuronal nuclei and dendrites as well as epithelial cells (Figure S2B). Axin expression in ddaE neurons was confirmed using a validated (Wang, Tacchelly-Benites et al. 2016) antibody (Figure S2C), and concentration of endogenous γTubulin at dendrite branch points was validated with a functional γTubulin-sfGFP, which is tagged at the endogenous locus (Tovey, Tubman et al. 2018) (Figure S2D). Thus, while we confirmed expression of γTubulin, Axin and gish in ddaE neurons, we could not detect expression or function of arm, the key transcriptional output of Wnt signaling, in these cells.

To confirm that a specific subset of canonical Wnt signaling proteins was required for γTub-GFP localization in dendrites, we used additional genetic approaches. Animals heterozygous for the hypomorphic fz_{F31} allele (Povelones, Howes et al. 2005) had strongly reduced γTub-GFP at dendrite branch points (Figure 1E); the dotted line indicates the baseline signal expected from cytosolic GFP. Similar results were obtained with a small deficiency that removes the entire *fz2* gene and one neighboring gene (*rept*) (Bhanot, Fish et al. 1999) and in animals heterozygous for two different strong loss of function *Axin* alleles, $Axin_{18}$ (Wang, Tacchelly-Benites et al. 2016) and $Axin_{s044320}$ (Hamada, Tomoyasu et al. 1999). Combining Axin RNAi with a mutant allele (Axin A; $Axin_{s044320}$/+) also reduced γTub-GFP at branch points to

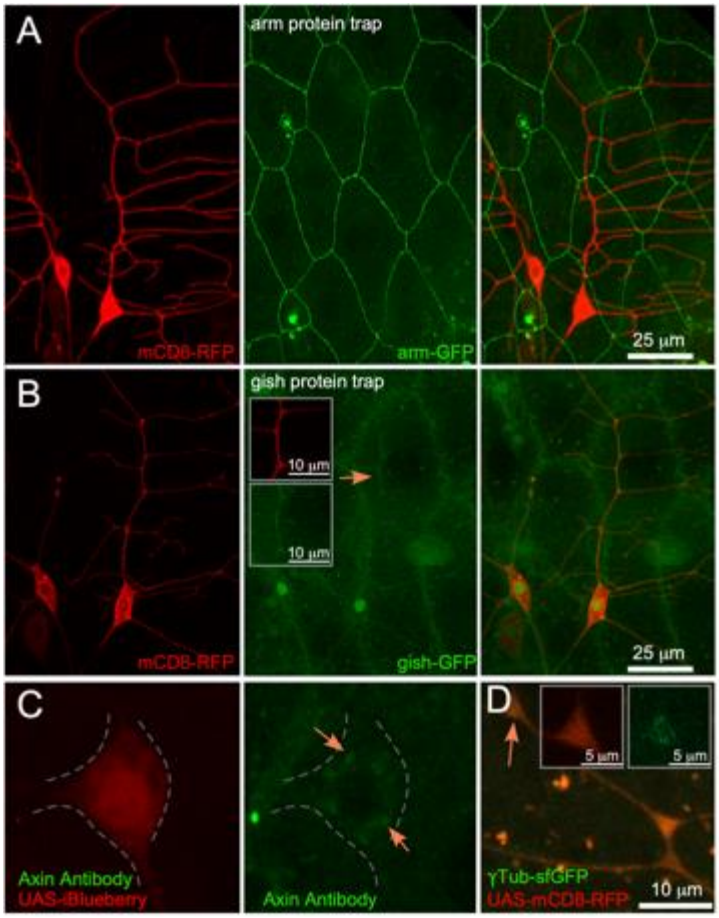

Figure 4-S2. Endogenous arm, gish, Axin and γTub localization in neurons

(A and B) Example images from a region of a 3rd instar larval body wall are shown from animals expressing UAS-mCD8-RFP under the control of 221 GAL4 and either arm-GFP or gish-GFP under the control of their native promoters. (C) An example image from a filleted larva, immunostained with an antibody against Axin. Cell shape marker is the cytoplasmic marker UAS-iBlueberry pseudocolored in red for viewing convenience. Scale bar is 10 μm. (D) Example image from the main trunk of a comb dendrite from an animal expressing UAS-mCD8-RFP under the control of 221 GAL4 and a CRISPR tagged γTub-sfGFP at the endogenous locus. An orange arrow points to the branch point shown in the insets. Scale bar is 10 μm and 5 μm for insets.

baseline. To confirm a role for Gαo, we overexpressed a dominant-negative GDP bound mutant (Katanaev, Ponzielli et al. 2005) and this reduced γTub-GFP (Figure 1E). A constitutively active Gαs-GTP (Wolfgang, Roberts et al. 1996) had no effect (Figure 1E). Finally, we used two sgg (GSK3β) transgenes that contain mutations of a conserved regulatory phosphorylation site. The S9A version cannot be inhibited by phosphorylation and so is constitutively active, while the S9E version mimics the inactive phosphorylated form (Hazelett, Bourouis et al. 1998, Bourouis 2002). The active, but not inactive, mutant reduced γTub-GFP localization to branch points (Figure 1E) suggesting an antagonistic role for sgg in the pathway. To test γTub-GFP localization in *fz* homozygotes

(*fz*$_{F31}$/*fz*$_{P21}$, *fz*$_{P21}$ is a strong loss of function allele (Jones, Liu et al. 1996, Povelones, Howes et al. 2005)), we used a different Gal4 driver that expresses in Class I neurons, IG1-Gal4 and generated control data in a matched background. As expected, γTub-GFP was strongly reduced at branch points (Figure 1D and E). We conclude from this data that fz, fz2, dsh, CK1γ, Gαo, Gαs, and Axin, as well as cnn and Plp, positively regulate γTub localization while sgg may negatively regulate it (Figure 1B). We did not find any evidence that arm or PCP-specific proteins participate in localizing γTub.

Arrow and frizzleds act upstream of dsh, and dsh upstream of Axin, at dendrite branch points

Consistent with a role in localizing γTubulin, a functional tagged Axin transgene (Cliffe, Hamada et al. 2003)) concentrates at dendrite branch points (Figure 2A and (Weiner, Seebold et al. 2018). We previously showed fz, fz2 and Gαo are necessary for Axin-GFP branch point localization (Weiner, Seebold et al. 2018). After finding that other Wnt signaling proteins act

upstream of γTub localization, we wished to confirm that they also play a role in Axin targeting.

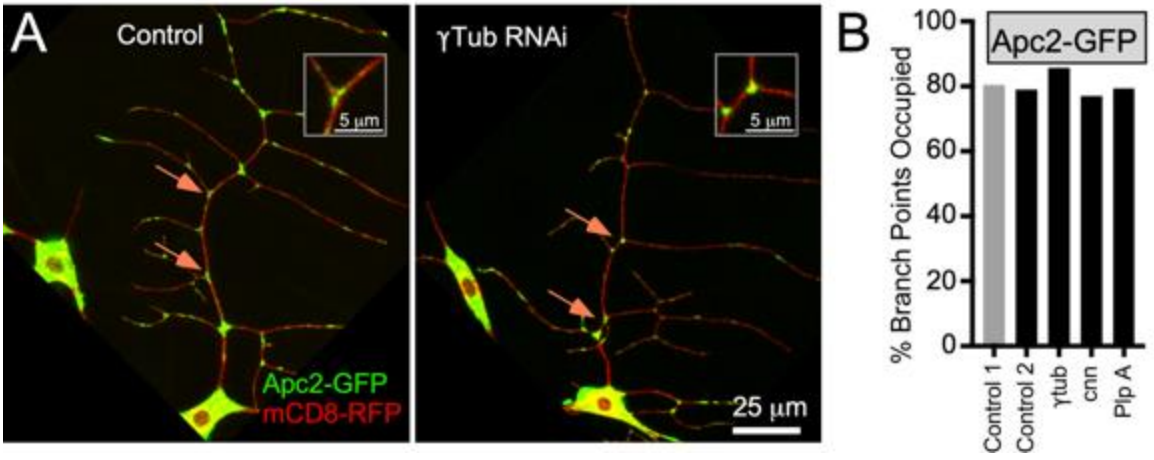

Figure 4-S3. Related to Figure 3. RNAis targeting γTub, cnn and Plp do not affect Apc2-GFP localization to branch points.

(A) Example image of Apc2-GFP and mCD8-RFP in ddaE neurons expressing UAS-Rtnl2 RNAi (Control 1) (VDRC 33320) and UAS-γTub23C RNAi (VDRC 19130) hairpins are shown. Orange arrows indicate branch points with high Apc2-GFP signal, scored as occupied. Insets in the top corner of each image indicate the top branch point indicated by an arrow. (B) Quantification of Apc2-GFP branch point occupancy is shown in neurons expressing different RNAi hairpins. A logistic regression was used to determine statistical significance. * $p<0.05$, ** $p<0.01$, *** $p<0.001$

Indeed, the same Wnt signaling proteins required for γTub positioning were required for Axin-GFP targeting. Dsh, gish and arrow, but not Apc and Apc2, reduced Axin at branch points (Figure 2A and B). Unlike γTub, cnn and Plp RNAi did not affect Axin localization (Figure 2B). Similarly, cnn and Plp RNAi did not affect Apc2-GFP localization (Figure S3), suggesting these centrosomal proteins are specifically required upstream of γTub.

Although a role for Axin in dendritic localization of γTub was unexpected, there is some precedent for a relationship between Axin and γTub. In cultured mammalian cells and mouse oocytes, Axin localizes to the centrosome and is required for γTub recruitment (Fumoto, Kadono

et al. 2009, He, Song et al. 2016). We therefore examined Axin localization in dividing Drosophila neuroblasts and found that Axin-GFP was concentrated at centrosomes marked with EB1-RFP (Figure 2C and Movie 1).

We next tested whether dsh, the other Wnt signaling scaffold involved in γTub-GFP localization, had a similar distribution to Axin. Dsh-GFP under UAS control localized to puncta present at over 90% of branch points (Figure 2D and E). Axin-GFP also clustered in puncta, although more diffuse background was also seen with this marker (Figure 2A). To rule out that the dsh localization pattern was due to overexpression, we examined dsh-Clover, a derivative of an EGFP-tagged functional transgene expressed using its own regulatory sequences (Axelrod 2001) tagged with the brighter Clover (Lam, St-Pierre et al. 2012) fluorescent protein (Figure S4). dsh-Clover localized to puncta in neurons and in the surrounding epidermal cells (Figure S4B and C). Because the UAS version was easier to image in neurons, we generated a tester line with this transgene. While RNAi targeting Axin did not reduce dsh-GFP at branch points, the reduction of

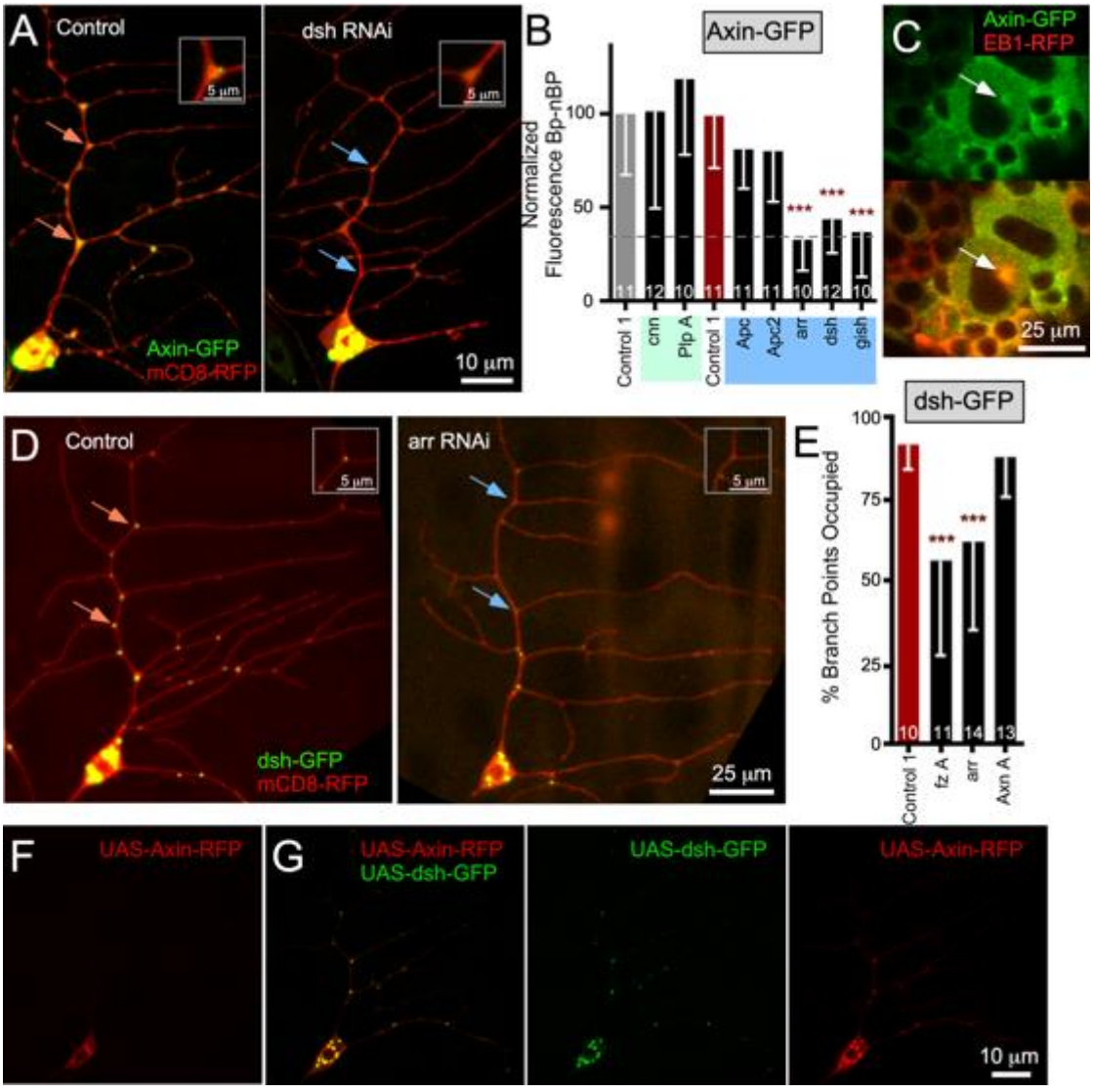

Figure 4-2. arr and fz act upstream of dsh, which is sufficient to recruit Axin to branch points

(A) Example images of ddaE neurons expressing UAS-Axin-GFP, UAS-mCD8-RFP and either UAS-Rtnl2 RNAi (Control1) (VDRC 33320) or UAS-dsh RNAi (VDRC 101525) transgenes. Orange arrows indicate branch points with high Axin-GFP signal and blue arrows indicate branch points with low signal. Insets in the top corner of each image indicate the top branch point indicated in each image (B) Quantification Axin-GFP BP-nBP normalized fluorescence in ddaE neurons expressing different RNAi hairpins. (C) UAS-Axin-GFP and UAS-EB1-RFP were expressed using the pan neuronal driver elav Gal4. Live first instar larvae were mounted for imaging and movies of neuroblasts in the brain were acquired (see Supplemental Movie 1). Still images from movies are shown. Centrosomes were identified as the site of EB1-GFP comet initiation and are identified with white arrows. (D) Example images of dsh-GFP and mCD8-RFP in neurons also expressing UAS-Rtnl2 RNAi (Control1) (VDRC 33320) and UAS-arr

RNAi (BDSC 31473) transgenes. Orange arrows indicate branch points with high Tub-GFP signal and blue arrows indicate branch points with low γTub-GFP signal; insets are as in other figures. (E) Quantification of dsh-GFP localization at branch points. Branch point occupancy was scored if there was a discrete dsh punctum present at each branch point along the main branch of the comb dendrite. The number of cells (one per animal) is shown on the bars. Error bars indicate standard deviation. A linear regression was used to determine statistical significance. * $p<0.05$, ** $p<0.01$, *** $p<0.001$. (F) Representative image of UAS-Axin-RFP. (G) Panel of images showing UAS-Axin-RFP expressed with UAS-dsh-GFP using 221 Gal4. Scale bar is 10 μm.

the membrane proteins frizzled and arrow did (Figure 2D and E). This data suggests that dsh acts downstream of frizzled and arrow, but upstream of Axin at branch points.

To further confirm that dsh is upstream of Axin in dendrites, we used an RFP-tagged Axin transgene that is largely diffuse on its own (Figure 2F). When expressed with dsh-GFP, Axin-RFP was recruited to puncta at dendrite branch points and in the cell body that were labeled with GFP (Figure 2G). This data indicates that in dendrites Wnt receptors fz and arrow act upstream of dsh, which in turn acts upstream of Axin.

Wnt signaling proteins are required for normal microtubule polarity in dendrites

So far we have used γTub-GFP as a proxy for nucleation sites. As a first functional test of a role for Wnt signaling proteins in controlling dendritic nucleation, we took advantage of the polarity phenotype generated by loss of γTub. Strong reduction of γTub23C (the somatic γTub) generates mixed polarity in ddaE dendrites, shifting the percentage of plus-end-out microtubules from about ten to 25 (Nguyen, McCracken et al. 2014). We hypothesized that reduction of γTub at branch points would phenocopy the *γTub* phenotype and disrupt dendrite microtubule polarity. We used the direction of EB1-GFP comet movement (Stepanova, Slemmer et al. 2003) as a readout of microtubule polarity. As expected, in control neurons about ten percent of microtubules were plus-end-out (Figure 3B and D). In many genetic backgrounds in which γTub-

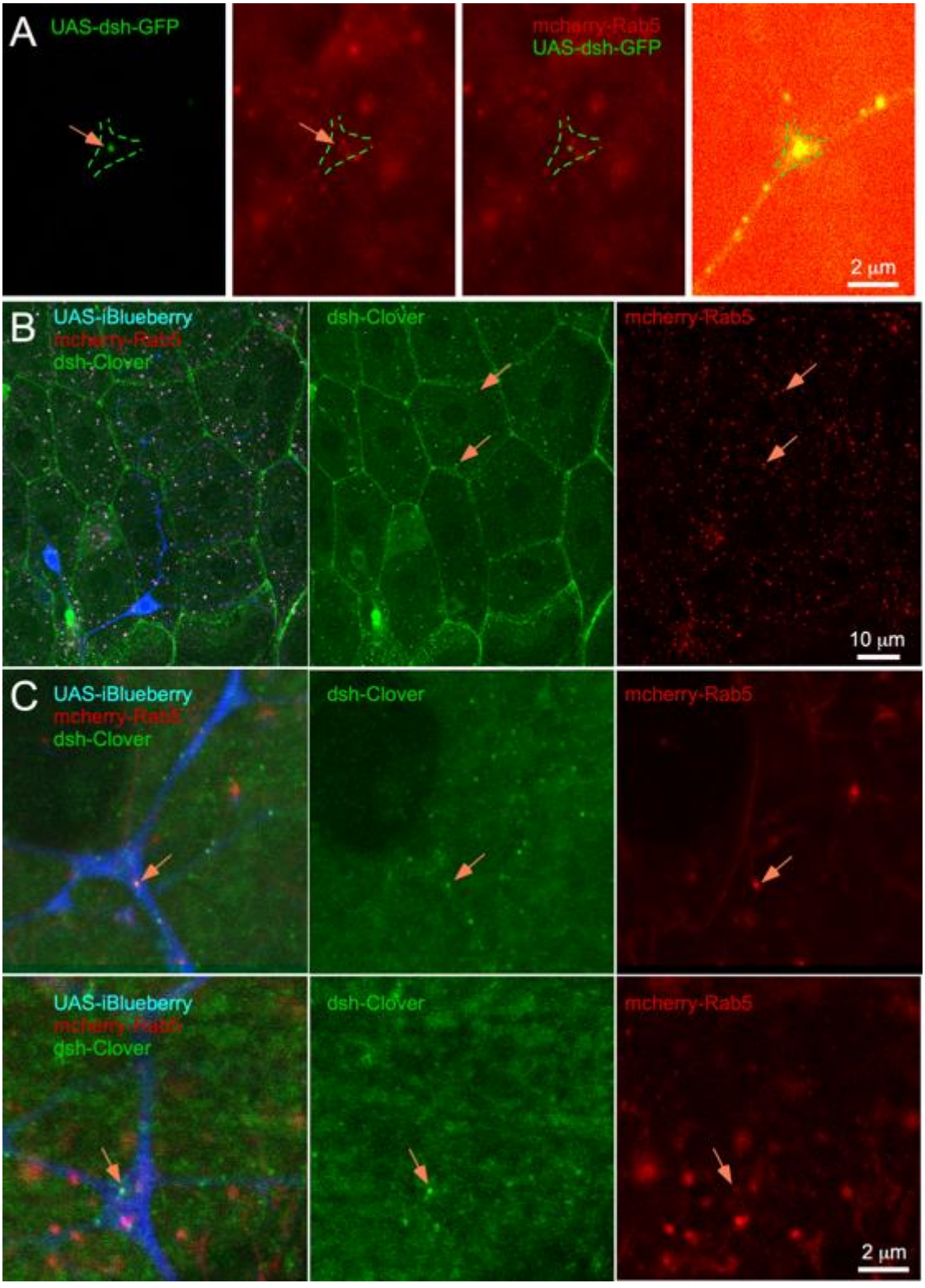
A
UAS-dsh-GFP
mcherry-Rab5
UAS-dsh-GFP
2 μm
B
UAS-iBlueberry
mcherry-Rab5
dsh-Clover
dsh-Clover
mcherry-Rab5
10 μm
C
UAS-iBlueberry
mcherry-Rab5
dsh-Clover
dsh-Clover
mcherry-Rab5
UAS-iBlueberry
mcherry-Rab5
dsh-Clover
dsh-Clover
mcherry-Rab5
2 μm

Figure 4-S4. dsh localizes to endogenous Rab5 early endosomes.

(A) Example image of endogenous mcherry-Rab5 and UAS-dsh-GFP. Since there is no membrane marker the panel on the right was enhanced and used as a template to draw the outline of the dendrite branch point. Scale bar is 2 μm. (B) Example image of endogenous mcherry-Rab5 and dsh-Clover localization in the body wall of a *Drosophila* larvae. The cytoplasmic marker UAS-iBlueberry is used for cell shape. The orange arrows are used to point to colocalization events between mcherry-Rab5 and dsh-Clover in the epithelial cells. The middle and right panels show the green and red channels with orange arrows indicating colocalization. Scale bar is 10 μm (C) Two example images of a section of dendrite where the colocalization between mcherry-Rab5 and dsh-Clover can be seen in the branch point of the neuron. The orange arrow indicates the colocalization. The middle and right panels show the green and red channels with orange arrows indicating colocalization. Scale bar is 2 μm.

GFP was reduced at branch points, polarity was more mixed (Figure 3 and Movie 2), and was comparable to that in $\gamma Tub_{A14\text{-}9}/\gamma Tub_{A15\text{-}2}$ mutant animals (Nguyen, McCracken et al. 2014). In contrast to other assays, inactive sgg had a phenotype here, suggesting that sgg may have a positive function in maintaining dendritic microtubule polarity not necessarily related to nucleation (Figure 3C). Not all of the genetic backgrounds that reduced γTub-GFP localization resulted in changes in dendrite microtubule polarity. For example, the *fz* heterozygous mutant animals had reduced γTub-GFP at dendrite branch points (Figure 1E) but had normal microtubule polarity, as did cnn and plp RNAi (Figure 3D and E). One explanation consistent with our previous results is that γTub function must be strongly reduced to affect microtubule polarity (Chen, Stone et al. 2012, Nguyen, McCracken et al. 2014). We therefore wished to use a more sensitive functional assay to further test the requirement of candidate proteins in nucleation.

Wnt signaling proteins are required to increase microtubule dynamics in response to axon injury

Axon severing results in increased microtubule dynamics (number of growing plus ends) in parts of the neuron remaining connected to the cell body in Drosophila (Stone, Nguyen et al. 2010) and mammals (Kleele, Marinkovic et al. 2014). This increase in dynamics is dependent on

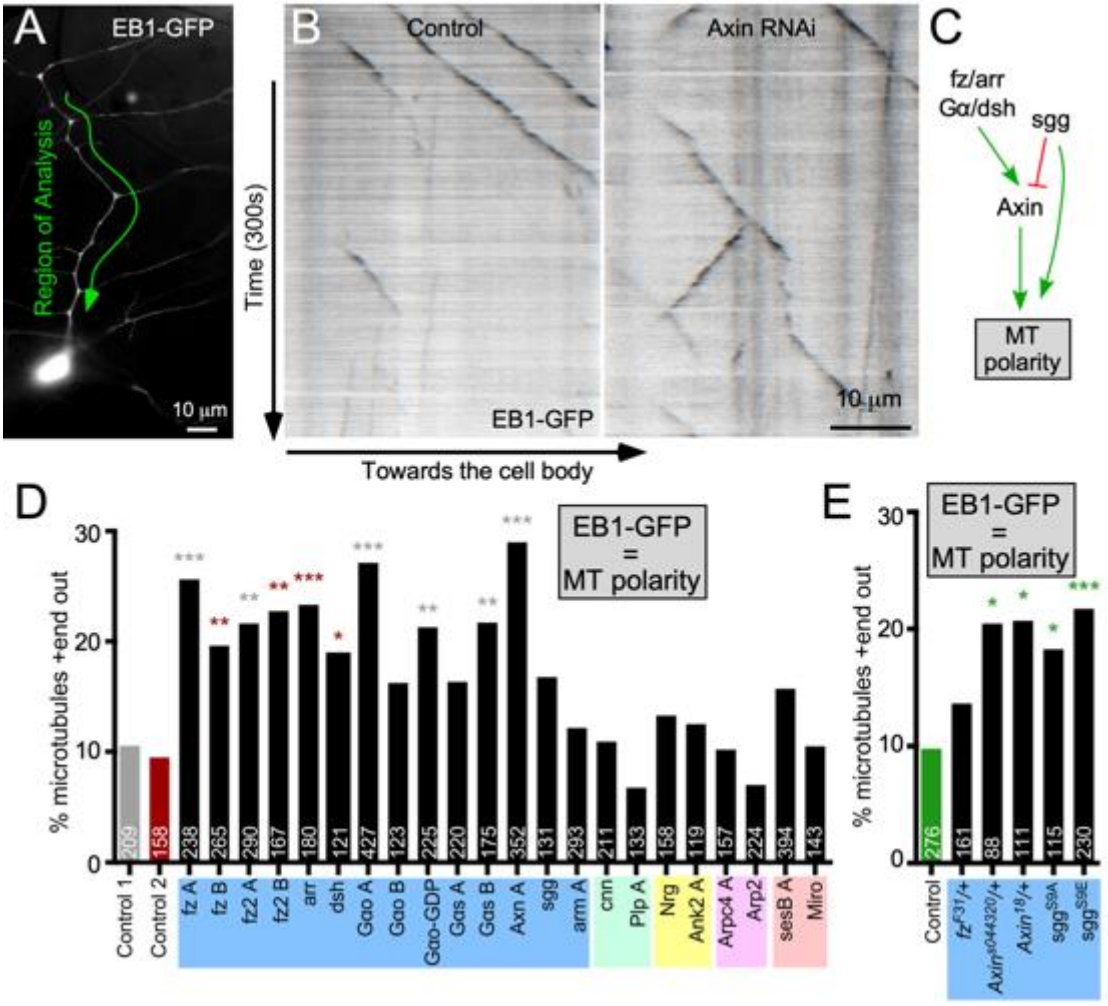

Figure 4-3. Wnt signaling proteins are required for minus-end-out microtubule polarity in dendrites. (A) An overview of the ddaE neuron dendrite arbor is shown. The main trunk of the ddaE neuron used for EB1-GFP movies is highlighted. (B) 300s movies of EB1-GFP were acquired in the ddaE dorsal dendrites and kymographs were generated in Fiji. Cells also expressed either UAS-Rtnl2 RNAi (Control1) (VDRC 33320) (left) or UAS-Axin RNAi (VDRC 7748) (right). (C) A summary of data in earlier figures as well as some previous data (Weiner, Seebold et al. 2018) is shown. (D) Quantification of EB1-GFP comet direction in the main trunk of the ddaE dendrite in animals expressing hairpin RNAis. The percentage of microtubules oriented plus-end out is plotted as a summed value across all cells for each genotype. The numbers on each bar are total EB1-GFP comets counted, and at least 15 cells were analyzed for each genotype, with one cell per animal. Data in panel D was collected by two different individuals; the grey bar shows control data from one individual and the red bar is from the other individual. Experimental genotypes analyzed by an individual were compared to their own control data and significance stars are color-coded to indicate the comparisons. (E) Quantification of microtubule polarity from mutant and dominant negative strains compared to control data without an RNAi transgene. A logistic regression was used to determine significance. * $p<0.05$, ** $p<0.01$, *** $p<0.001$

microtubule nucleation (Chen, Stone et al. 2012). Unlike polarity in uninjured neurons, increased microtubule dynamics after axon injury is affected by loss of one copy of *γTub23C* or by RNAi targeting γTub (Chen, Stone et al. 2012) and so is more sensitive to partial reduction of nucleation.

Before using this as a nucleation assay, we wished to confirm that the injury response relies on classical microtubule nucleation through the γTub Ring Complex (γTuRC). The γTuRC contains Grip91 and 84 that together make the γTub small complex (γTuSC), as well as four additional subunits, Grip71, Grip75, Grip128, and Grip163, that bring together γTuSCs to form the γTuRC. We used RNAi to reduce γTuRC proteins in neurons and assayed microtubule dynamics in dendrites immediately after axon injury and 24h later. Right after injury, microtubule plus end number was similar in all genetic backgrounds (Figure 4A and B). At 24h after injury, when the number of growing plus ends in control dendrites was more than two-fold elevated compared to uninjured neurons (Figure 4A and B), neurons expressing RNAi hairpins targeting some of the γTuRC components did not increase microtubule dynamics to the same extent (Figure 4A and B). The Grip84 RNAi line did not reduce dynamics in response to injury and may be ineffective. We conclude that the injury-induced increase in microtubule dynamics in dendrites depends on γTuRC and is thus a functional assay for classic microtubule nucleation.

To test whether reduction of γTub-GFP in dendrites predicts reduced ability to nucleate microtubules in response to stress, we assayed microtubule dynamics in the ddaE comb dendrite 8h after axon injury in different genetic backgrounds (Figure 4C and Movie 3). Consistent with γTub localization results (Figure S1) and the microtubule polarity assay (Figure 3D) disruption of branched actin (Arpc4, Arp2 RNAi), mitochondria (Miro, ATPsynβ RNAi) or Nrg/Ank2 did not block the increase in microtubule dynamics after injury (Figure 4E). However, reducing any of the proteins that were required for γTub localization to dendrite branch points reduced

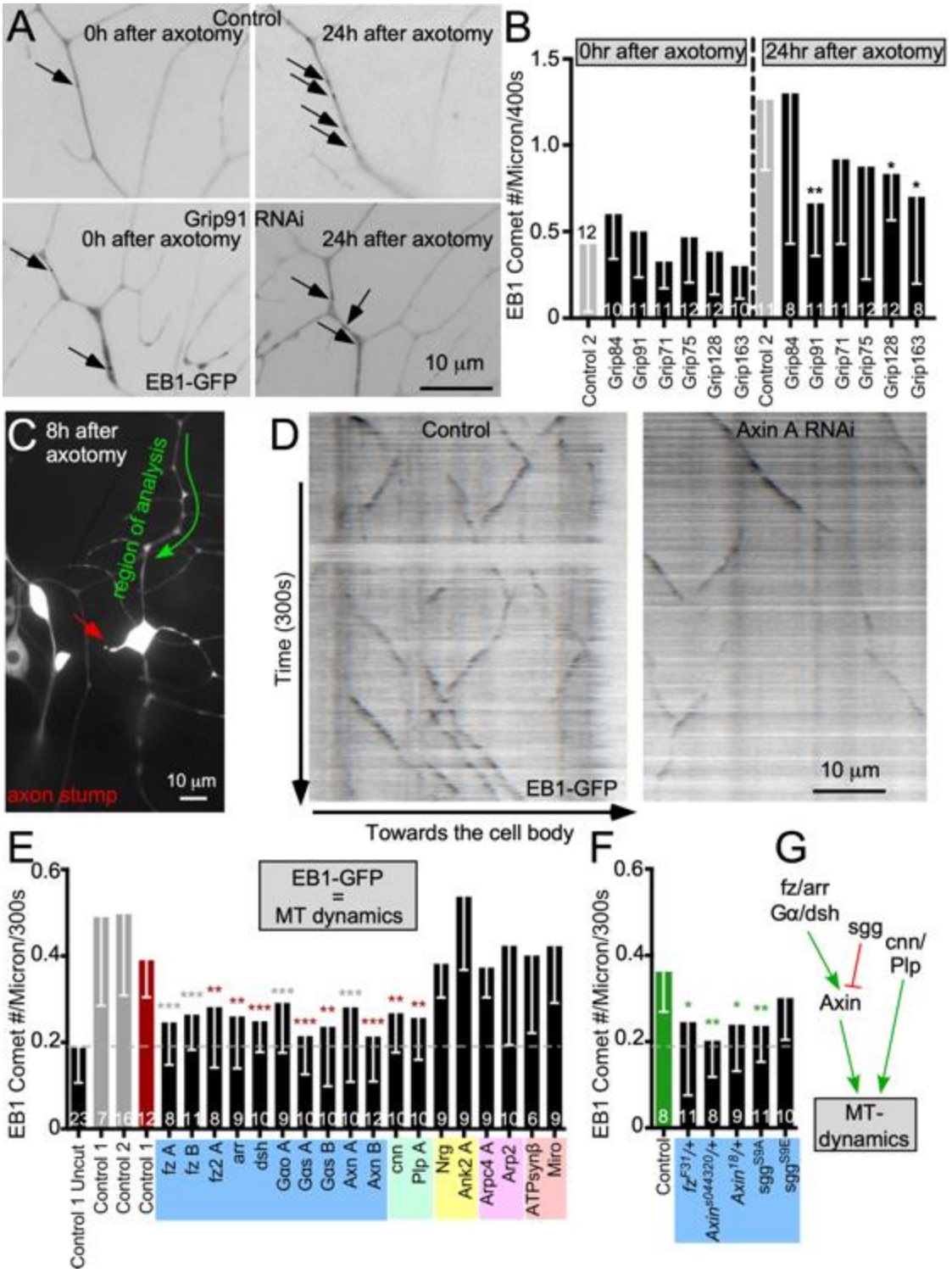

Figure 4-4. Wnt signaling proteins are required for microtubule dynamics induced by axon injury. (A) UAS-EB1-GFP was expressed in ddaE neurons with different RNAi hairpins. Axons were severed with a pulsed UV laser and 400s, 1 frame per 2s, movies were acquired immediately after injury and 24h after injury in the dendrite. Individual frames from the movies

are shown. (B) Quantification of EB1-GFP comets per micron and 400s for all knockdowns immediately following injury and 24 hours after injury are shown in different RNAi backgrounds. Dashed line separates 0h from 24h measurements. Number of cells analyzed is noted on each bar. A linear regression was used to determine statistical significance. * $p<0.05$, ** $p<0.01$, *** $p<0.001$ (C) An overview of a ddaE neuron 8 hours after axon injury is shown. The axon stump is indicated with a red arrow. (D) Fiji generated kymographs depicting microtubule dynamics 8 hours post axotomy in UAS-Rtnl2 RNAi (Control1) (VDRC 33320) (left) and UAS-Axin RNAi (VDRC 7748) (right) are shown. (E) Quantification of microtubule dynamics (comet number per micron and 300s) in animals in different knockdown conditions is shown. A dashed line indicates baseline, uninjured, control microtubule dynamics. This dashed line will continue throughout the figures that show microtubule dynamics. Grey and red control data was generated by two different individuals and experimental data were compared to the control by the same individual as indicated by star color. (F) Quantification of microtubule dynamics in non-RNAi genetic backgrounds is shown. Error bars indicate standard deviation. A linear regression was used to determine statistical significance. * $p<0.05$, ** $p<0.01$, *** $p<0.001$ (G) A schematic summarizing the data in panels E and F is shown.

microtubule dynamics in dendrites after axon injury (Figure 4D, E and F). Microtubule polarity changes were also observed in response to injury (Figure 4D) as expected (Stone, Nguyen et al. 2010). These changes are not dependent on microtubule nucleation (Chen, Stone et al. 2012), and so were not tracked in this assay.

As predicted, injury-induced nucleation was more sensitive to reduction in proteins that target γTub than the polarity assay. We conclude that not only are fz/arr/dsh/Gα/Axin, cnn and Plp required to position γTub at dendrite branch points, but also that disruption of γTub localization has functional consequences for microtubule nucleation in dendrites (Figure 4G).

Axin and dsh localize to Rab5 endosomes in dendrites.

The involvement of membrane proteins in γTub localization suggested that either the plasma membrane or an organelle might be used as a platform to organize nucleation sites. We examined Golgi and endosome markers in ddaE neurons and found that endosomes localized to most branch points, while clear spots of Golgi were only seen occasionally in proximal branch

points (Figure S5A). RNAi transgenes targeting lava lamp (lva), a protein required for Golgi transport into Drosophila dendrites (Ye, Zhang et al. 2007), chb, the Drosophila CLASP (CLASPs in mammalian cells help microtubules grow from the Golgi (Efimov, Kharitonov et al. 2007)), and CLIP-190, which is a binding partner of lva (Sisson, Field et al. 2000) did not alter γTub-GFP at branch points (Figure S5B). In contrast, Rab5 RNAi, but not knockdown of other Rabs, reduced γTub-GFP localization (Figure 5A and B). Endocytosis is required for efficient Wnt secretion and involves the cargo chaperone wntless (Brunt and Scholpp 2018). However, wntless RNAi did not have a phenotype (Figure 5B) suggesting the Rab5 phenotype is not because of reduced ligand generated by the neuron.

To determine whether Wnt signaling proteins localize to dendritic endosomes, we co-expressed tagged fz, Axin and dsh with Rab4, Rab5 and Rab11. Unlike tagged Axin and dsh, fz-EGFP was observed throughout the plasma membrane as well as defined puncta at branch points (Figure 5C). Fz, dsh and Axin puncta colocalized with Rab5, but not Rab4 or 11 (Figure 5C-H and S5D). To make sure that colocalization was not due to overexpression of tagged transgenes, we used mCherry-Rab5 (Lund, DeLotto et al. 2010) and dsh-Clover controlled by their own regulatory sequences (Figure S4). A subset of mCherry-Rab5 puncta aligned with dsh-GFP expressed in neurons (Figure S4A). In epidermal cells, dsh-Clover was seen enriched at cell boundaries as well as at intracellular puncta (Figure S4B). The intracellular puncta colocalized with mCherry-Rab5. In neurons dsh-Clover puncta aligned with mCherry-Rab5 puncta (Figure S4C). A functional role for Rab5 in control of nucleation was supported by failure to upregulate microtubule dynamics after axon injury in Rab5 RNAi neurons (Figure 5I).

To try to understand why the Golgi complex rather than endosomes was previously implicated in dendritic nucleation (Ori-McKenney, Jan et al. 2012, Yalgin, Ebrahimi et al. 2015),

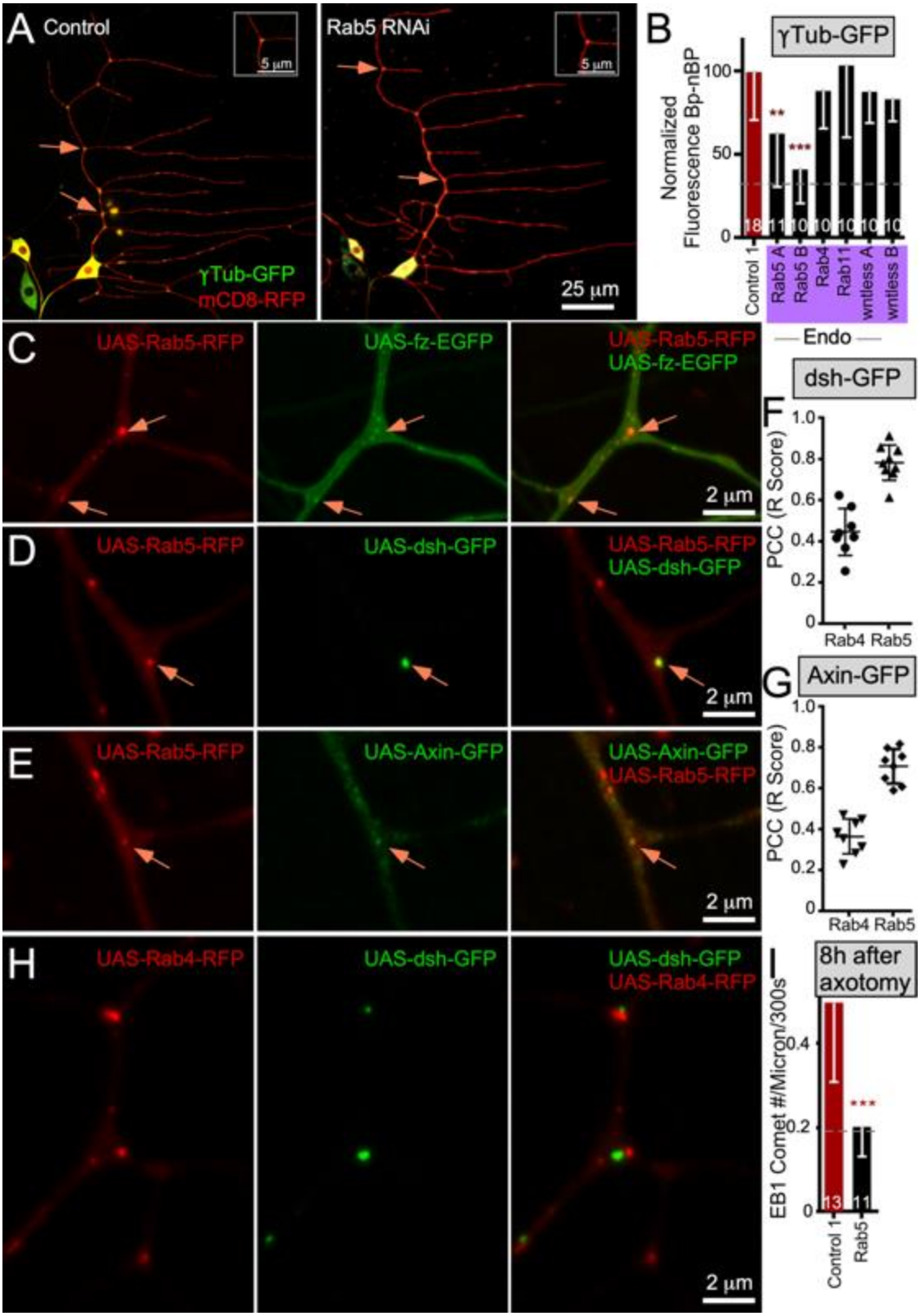
A
Control
5 μm
γTub-GFP
mCD8-RFP
Rab5 RNAi
5 μm
25 μm
B
γTub-GFP
Normalized Fluorescence Bp-nBP
100
50
0
**
***
18
11
10
10
10
10
Control 1
Rab5 A
Rab5 B
Rab4
Rab11
wntless A
wntless B
Endo
C
UAS-Rab5-RFP
UAS-fz-EGFP
UAS-Rab5-RFP
UAS-fz-EGFP
2 μm
D
UAS-Rab5-RFP
UAS-dsh-GFP
UAS-Rab5-RFP
UAS-dsh-GFP
2 μm
E
UAS-Rab5-RFP
UAS-Axin-GFP
UAS-Axin-GFP
UAS-Rab5-RFP
2 μm
F
dsh-GFP
PCC (R Score)
1.0
0.8
0.6
0.4
0.2
0
Rab4
Rab5
G
Axin-GFP
PCC (R Score)
1.0
0.8
0.6
0.4
0.2
0
Rab4
Rab5
H
UAS-Rab4-RFP
UAS-dsh-GFP
UAS-dsh-GFP
UAS-Rab4-RFP
2 μm
I
8h after axotomy
EB1 Comet #/Micron/300s
0.4
0.2
0
***
13
11
Control 1
Rab5

Figure 4-5. Wnt signaling proteins localize to Rab5 endosomes

(A) Example images of UAS-γTub-GFP localization in ddaE neurons expressing UAS-Rtnl2 RNAi (Control 1) (VDRC 33320) and UAS-Rab5 RNAi (VDRC 34096) hairpins. Membranes were marked with UAS-mCD8-RFP to see cell shape. Scale bar is 25 μm. Orange arrows indicate branch points with high γTub-GFP signal and blue arrows indicate branch points with low γTub-GFP signal. Insets in the top corner of each image show the top branch point highlighted with an arrow in each image. (B) Quantification of □Tub-GFP at branch points is shown in larvae expressing different RNAi hairpins targeting endosomal proteins or a wnt secretion protein wntless. Values were generated by subtracting mean non-branch point (nBP) fluorescence from branch point (BP) fluorescence for each cell; normalized fluorescence values are shown. Sample sizes are shown within the bars. Error bars indicate standard deviation. A linear regression was used to determine statistical significance. * $p<0.05$, ** $p<0.01$, *** $p<0.001$. (C-E) Example colocalization image of UAS-Rab5-RFP co-expressed with UAS-fz-eGFP, UAS-dsh-GFP, or UAS-Axin-GFP. The orange arrows point to puncta of colocalization between the two markers in each case. Scale bar is 2 μm. (F and G) Plot of Pearson Correlation Coefficient between UAS-Rab4-RFP or UAS-Rab5-RFP with either UAS-dsh-GFP or UAS-Axin-GFP. The y-axis indicates the R score with 1 being positive correlation, zero meaning no correlation and -1 meaning negative correlation. (H) Examples images of UAS-Rab4-RFP co-expressed with UAS-dsh-GFP. (I) Quantification of microtubule dynamics (comet number per micron and 300s) following laser axotomy in control animals or animals expressing UAS-Rab5 RNAi (VDRC 34096). Error bars indicate standard deviation. A linear regression was used to determine statistical significance. * $p<0.05$, ** $p<0.01$, *** $p<0.001$

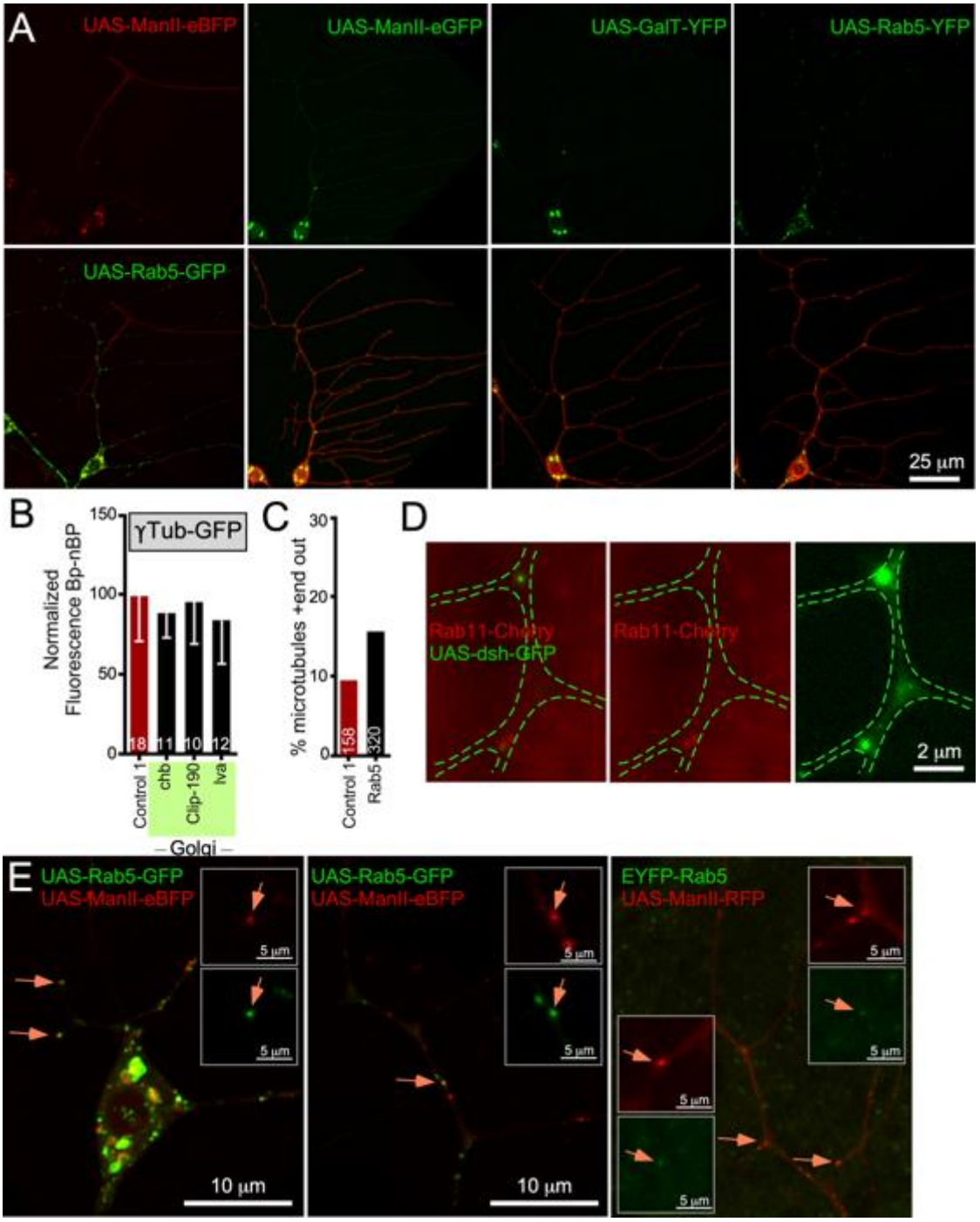

Figure 4-S5. The Golgi is not required for γTub-GFP localization and other Rabs do not colocalize with dsh-GFP.

(A) Three examples of dendritic localization of Golgi markers including UAS-ManII-eBFP, UAS-ManII-eGFP and UAS-GalT-YFP, and one example of the early endosomal marker UAS-Rab5-YFP. The UAS-ManII-eBFP (psedocolored) is coexpressed with UAS-Rab5-GFP. All other markers have the cell shape marker UAS-mCD8-RFP coexpressed for localization

reference. (B) Quantification of γTub-GFP at branch points is shown in larvae expressing different RNAi hairpins targeting Golgi associated proteins. Values were generated by subtracting mean non-branch point (nBP) fluorescence from branch point (BP) fluorescence for each cell; normalized fluorescence values are shown. The number of cells (one per animal) is shown on the bars. Error bars indicate standard deviation. A linear regression was used to determine statistical significance. * $p<0.05$, ** $p<0.01$, *** $p<0.001$. (C) Quantification of EB1-GFP comet direction in the main trunk of the ddaE dendrite in animals expressing hairpin RNAis. The percentage of microtubules oriented plus-end out is plotted as a summed value across all cells for each genotype. The numbers on each bar are total EB1-GFP comets counted, and at least 15 cells were analyzed for each genotype, with one cell per animal. A logistic regression was used to determine significance. * $p<0.05$, ** $p<0.01$, *** $p<0.001$. (D) Example image of endogenous Rab11-cherry and UAS-dsh-GFP. Since there is no membrane marker the panel on the right was enhanced and used as a template to draw the outline of the dendrite branches. Scale bar is 2 μm. (E) Examples images of either EYFP-Rab5 or UAS-Rab5-GFP co-expressed with UAS-ManII-eBFP. The orange arrows point to puncta of colocalization between the two markers in each case. Insets in the top corner of each image show the example highlighted with an arrow in each image. For EYFP-Rab5 the bottom arrow correlates with the bottom left insets. Scale bar is 10 μm.

we examined tagged versions of ManII, the major Golgi marker used in the previous studies. Different tagged ManII transgenes were present in zero to one large puncta in dendrites (Figure S5A), as well as many smaller spots that could be seen with higher laser power (Figure S5E). Some of these smaller spots colocalized with Rab5-GFP (Figure S5E) suggesting leakage of markers between organelles. To make sure that it was not the endosomal marker leaking into Golgi, we used a fly line that has the start codon of the *Rab5* gene replaced with the EYFP coding sequence (Dunst, Kazimiers et al. 2015). ManII-RFP was seen in puncta labeled with endogenous EYFP-Rab5 (Figure S4E) indicating that the ManII, not Rab5, is mislocalized in these cells. Therefore, it is possible that the structures assumed to be Golgi outposts in other studies were actually early endosomes into which overexpressed ManII had leaked. In summary, the data suggests that Wnt signaling proteins can be found on a subset of early endosomes in dendrites.

New growing plus ends can initiate at early endosomes in dendrites.

The finding that dsh and Axin localized to endosomes in dendrites implicated these as potential sites of nucleation. We used formation of new comets by EB1-GFP as a readout of nucleation. While new comets can be a result of catastrophe rescue, within branch points comet formation has been linked to nucleation (Nguyen, McCracken et al. 2014). In movies of tagged protein pairs, we captured EB1 comets initiating from puncta labeled with Rab5 as well as each of the Wnt signaling markers that colocalized with Rab5 (Figure 6 and Movies 4-10). In addition to UAS-driven transgenes, Rab5 and dsh under endogenous control were seen as sites of comet initiation (Figure 6B and F and Movies 5 and 9). EYFP-Rab5 has the fluorescent protein coding sequence inserted at the start codon of the genomic Rab5 (Dunst, Kazimiers et al. 2015). In some of the movies EB1 was in the same channel as the other marker, but it was easy to distinguish endosomes and microtubule plus ends based on their behavior. In some examples including that in Figure 6A and Movie 4, the endosome was pulled along by the newly growing microtubule providing strong support for association of the microtubule with the endosome. These events are consistent with recruitment of nucleation machinery to Rab5 endosomes by Wnt signaling proteins.

To further test whether a specific type of signaling endosome is involved in dendritic microtubule nucleation, we coexpressed EB1-GFP, dsh-GFP and Rab5-RFP. We counted dsh and Rab5 puncta in branch points of 25 cells and found that all dsh puncta overlapped with Rab5 puncta, but that some Rab5 puncta did not contain dsh signal. When we quantitated the overlap, we found that 60% of Rab5 puncta colocalized with dsh (Figure 7A and B). Thus, dsh is found at a subset of endosomal structures marked with Rab5. Based on the involvement of dsh in γTub localization, we hypothesized that only Rab5 structures with dsh should be sites of comet initiation. Indeed, when we examined 5-minute movies of dendrite arbors from 25 cells, we

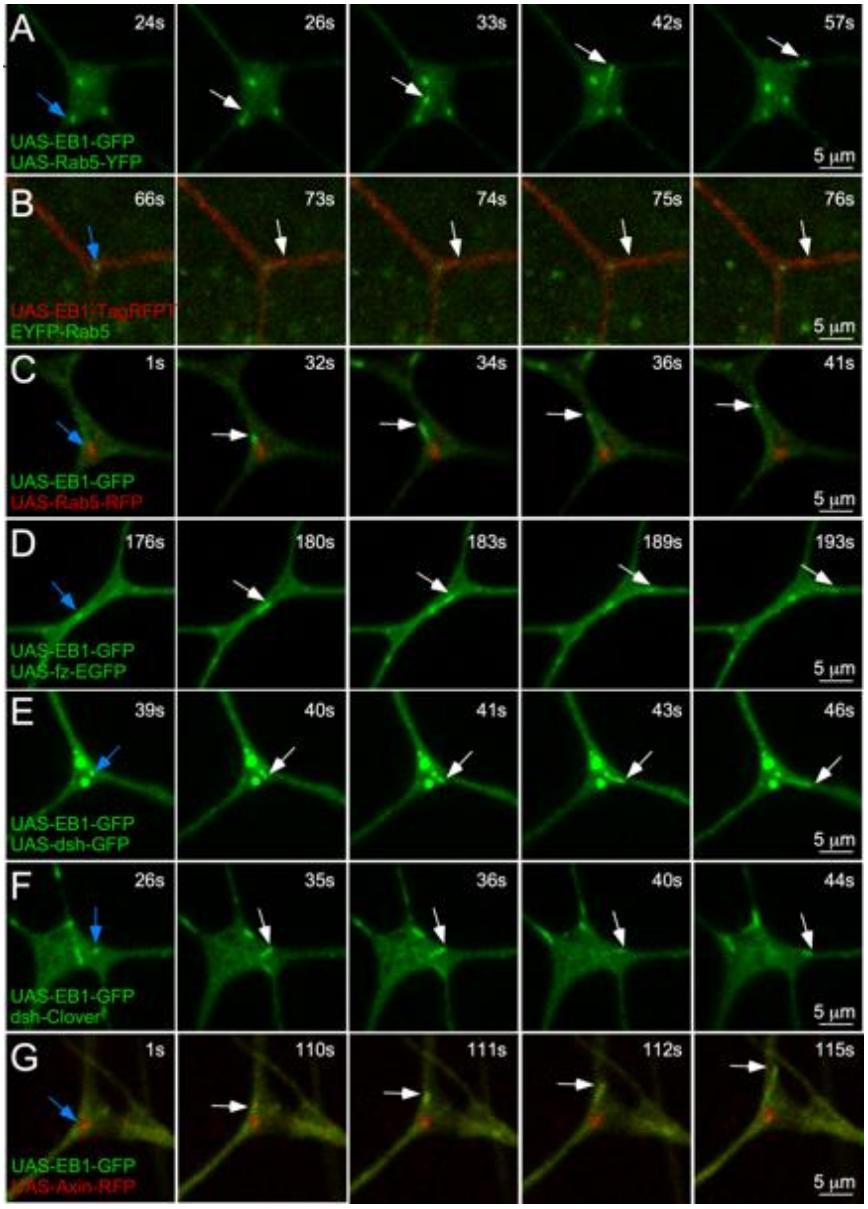

Figure 4-6. Microtubules can initiate off early endosomes and wnt proteins in dendrites

(A-G) Example five frame stills of microtubule comet formation off either Rab5 endosomes or Wnt proteins. UAS-Rab5-GFP or UAS-Rab5-RFP are shown co-expressed with UAS-EB1-GFP. In addition, UAS-EB1-TagRFPT is shown expressed with endogenous EYFP-Rab5. UAS-fz-eGFP is shown co-expressed with UAS-EB1-TagRFPT. Finally, UAS-dsh-GFP, endogenous dsh-Clover, and UAS-Axin-RFP are shown with UAS-EB1-GFP. In all examples the first frame includes a blue arrow to show the endosome or wnt proteins that the microtubule comet will initiate off. Subsequent frames track movement of the microtubule with a white arrow. Time stamp at the top right corner correlates to the time point in the corresponding Supplemental Movies 5-8. Scale bar is 5 µm.

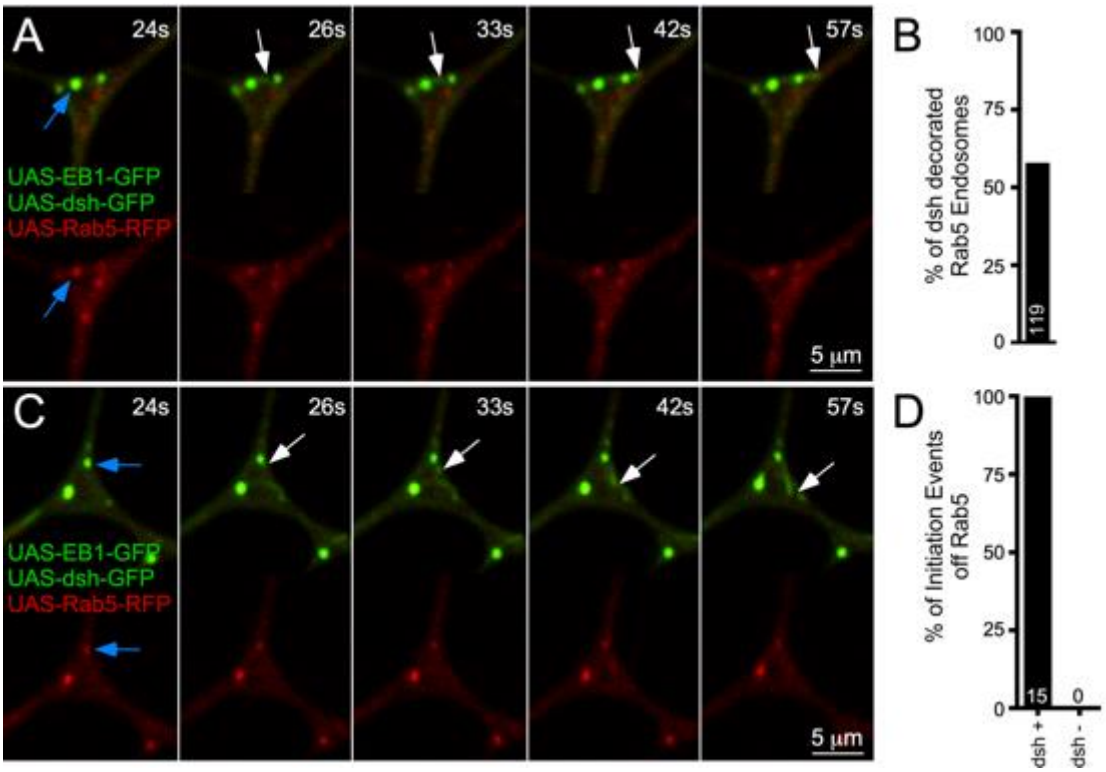

Figure 4-7. Microtubules initiate from dsh decorated early endosomes

(A and C) Frames from two representative videos of a class I neuron expressing UAS-EB1-GFP, UAS-dsh-GFP and UAS-Rab5-RFP. Top panels are the merged image and bottom is the UAS-Rab5-RFP. A blue arrow is used to show the endosome from which an EB1 comet will initiate from in subsequent frames indicated with white arrows to track movement. Time stamp at the top right corner correlates to the time point in the corresponding Supplemental Movies 9 and 10. Scale bar is 5 µm. (B) Quantification of percentage of Rab5 endosomes that are labeled with UAS-dsh-GFP. Sample size is shown in the bar and indicates total number of Rab5-RFP puncta that were counted in branch points during 25 300s videos. (D) Quantification of EB1 comet events that initiate from dsh positive or negative Rab5 endosomes during the same 300s videos. Samples size which represents total comet number is shown in the bar.

identified 15 comets that initiated at Rab5-labeled puncta, and all of these also contained dsh signal (Figure 7 and Movies 11 and 12). We conclude that new microtubules can initiate at a subset of endosomes that contains Wnt signaling proteins.

Axin is sufficient to localize γTub to ectopic cellular sites

While we observed localization of fz, dsh and Axin to endosomes, we were not normally able to observe distinct puncta of γTub even with endogenously tagged γTub (Figure S2D) and antibody staining of γTub (Nguyen, McCracken et al. 2014). The one exception to diffuse γTub was when we overexpressed it with tagged Axin. By itself, γTub-RFP was diffuse in the cell body (Figure 8A), but when paired with Axin-GFP it was recruited to very defined puncta (Figure 8A). We therefore hypothesized that Axin might be sufficient to recruit γTub to specific intracellular locations, but that at branch points this was normally too transient to detect above diffuse background. To test whether Axin was sufficient to localize γTub, we used a short sequence from the ActA protein of Listeria monocytogenes that targets the outer mitochondrial membrane in mammalian (Pistor, Chakraborty et al. 1994) and Drosophila (Gates, Mahaffey et al. 2007) cells to generate an Axin fusion protein that we predicted would be targeted to mitochondria (Figure 8B). When expressed in ddaE neurons with mito-GFP, Axin-RFP-ActA colocalized with mitochondria; this pattern was particularly noticeable in the linear tips of the dorsal comb dendrite (Figure 8D and F). In contrast, Axin-GFP was present at very low levels in this region and did not align with mitochondria (Figure 8C and E). Since we were able to target Axin to mitochondria, we asked whether γTub-GFP would be concentrated around mitochondria. In the absence of mitochondrial Axin, γTub-GFP fluorescence was not strongly correlated with mitochondria (Figure 8G, I, and K). However, when mitochondria were coated with Axin-RFP-ActA, γTub-GFP fluorescence much more closely followed the pattern of RFP fluorescence such that all γTub-GFP peaks in the regions analyzed were associated with RFP peaks (Figure 8F, H, and J). To more quantitatively assess colocalization across multiple cells, we generated Pearson's

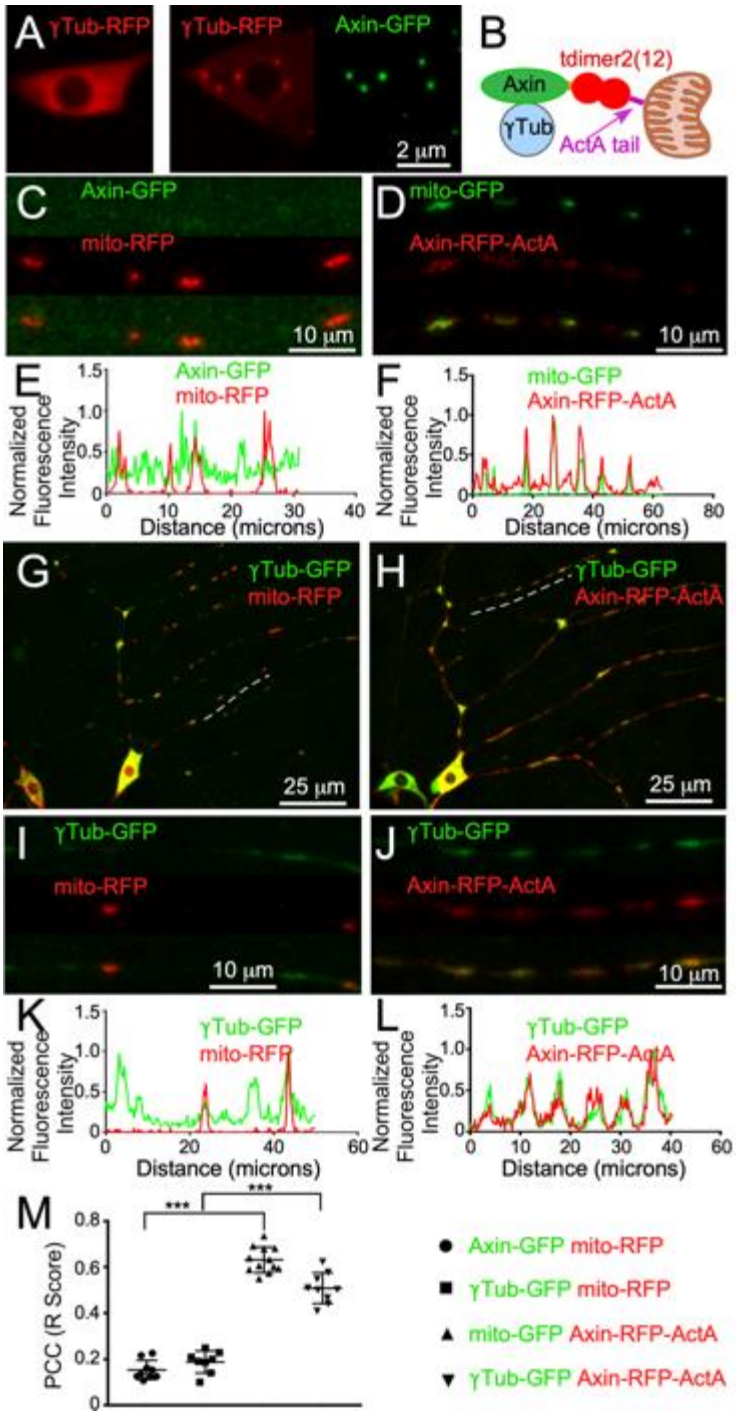

Figure 4-8. Axin is sufficient to localize γTub to ectopic cellular sites.

(A) Images show the localization of UAS-γTub-RFP in the cell body of a ddaE neuron when expressed alone (left) or when co-expressed with UAS-Axin-GFP (right) using the 221-Gal4 driver. Scale bar is 2 μm. (B) A diagram of the chimeric protein used to tag Axin with RFP (tdimer2(12)) and target it to mitochondria is shown. (C-D) Example images of enlarged regions within the secondary ddaE dendrites in cells expressing a mitochondrial marker and either UAS-Axin-GFP or UAS-Axin-RFP-ActA. Scale bar is 10 μm (E-F) Fluorescence intensity measurements from line traces of the dendrite regions shown in B and C. (G-H) UAS-γTub-GFP was co-expressed with either UAS-mito-RFP or UAS-Axin-RFP-ActA using 221Gal4. Overview images of the entire ddaE dendrite arbor are shown. Scale bar is 25 μm (I-J) Enlarged images of the regions within the secondary ddaE dendrites, indicated by the dashed lines in G and H. Scale bar is 10 μm (K-L) Normalized fluorescence measurements from line tracings of the regions in G and H. (M) A plot of the Pearson Correlation Coefficient for the four conditions (see the key to the right of the graph). The y-axis indicates the R score with 1 being a positive correlation, zero meaning no correlation, and -1 indicating a negative correlation.

Correlation Coefficients from the comb dendrite for each set of markers (Figure 8M). This analysis was consistent with line tracings. From this data we conclude that Axin is sufficient to recruit γTub to specific sites in Drosophila neurons.

In addition to Wnt signaling proteins, cnn is required to position γTub at branch points (Figure 1C), and seems to act in parallel to or downstream of Axin (Figure 2B). If it acts with γTub downstream of Axin, we hypothesized that Axin-RFP-ActA might also recruit cnn-GFP to mitochondria. Indeed, when we paired these two markers, we found that cnn-GFP could be relocalized to mitochondria (Figure S6).

As cnn can activate microtubule nucleation (Choi, Liu et al. 2010, Chen, Buchwalter et al. 2017), we hypothesized that ectopic γTub and cnn on mitochondria might convert mitochondria into nucleation sites. We therefore combined Axin-RFP-ActA with EB1-GFP to determine whether comets would initiate at mitochondria. In control neurons, more comet initiation, or spawning events, occurred at branch points compared to between branch points in control neurons (Figure S7A and B). When one copy of an *Axin* null allele was introduced into the background, spawning at branch points was reduced (Figure S7A and B). Neurons expressing mito-RFP had a similar pattern of spawning to neurons expressing only EB1-GFP (Figure S7C and D) while ectopic mitochondrial Axin increased spawning at branch points and between them (Figure S7C and D). The increase in comet initiation both at branch points and between them is consistent with localization of mitochondria to 80% of branch points (Weiner, Seebold et al. 2018) as well as to intervening regions (Figure 8G). On rare occasions we saw multiple spawning events initiating from the region within a dendrite where Axin-RFP-ActA was concentrated (Movie 13). We conclude that Axin is necessary for normal dendritic microtubule dynamics, and sufficient to increase microtubule dynamics when ectopically expressed.

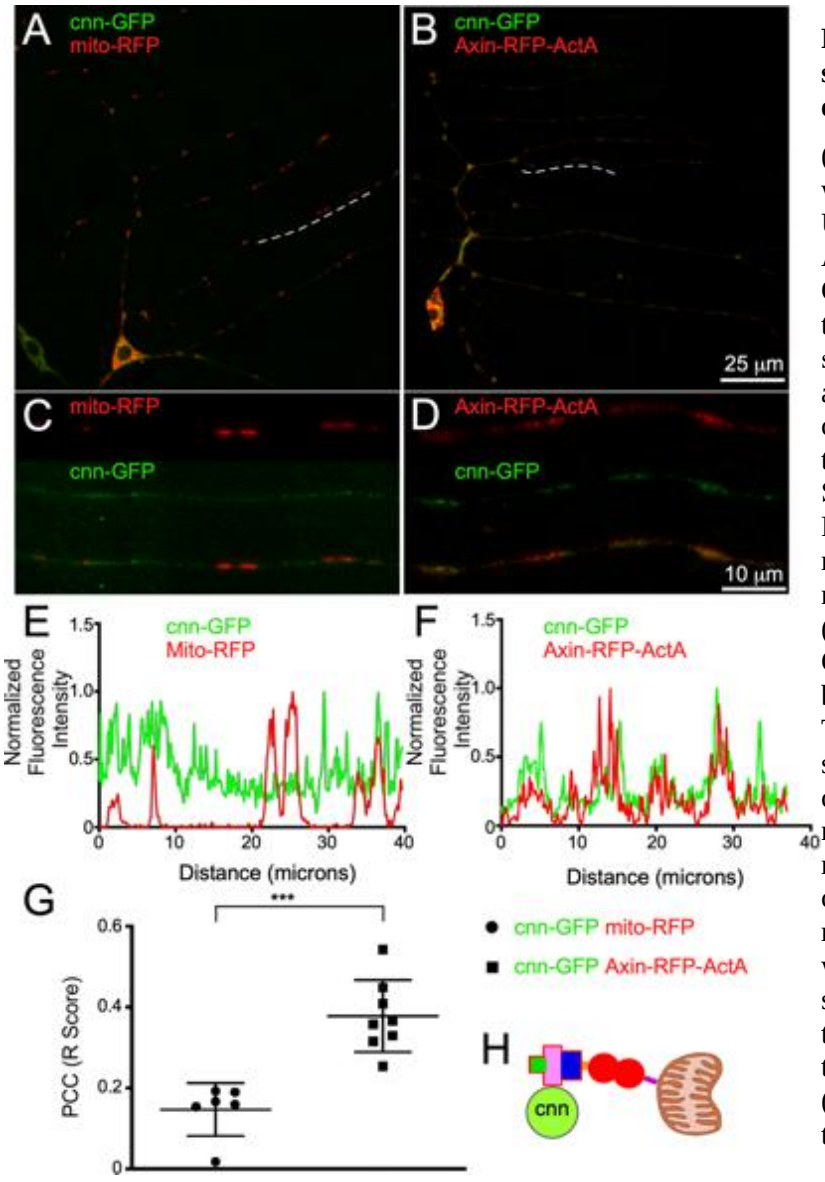

Figure 4-S6. Axin is sufficient to recruit cnn to ectopic cellular sites

(A and B) UAS-cnn-GFP was coexpressed with either UAS-mito-RFP or UAS-Axin-RFP-ActA using 221-Gal4. Overview images of the entire dendrite arbor are shown. Scale is 25 µm. (C and D) Regions within the comb dendrite indicated by the dashed lines in A and B. Scale is 10 µm. (E and F) Fluorescence intensity measurements from the regions shown in C and D. (G) A plot of Pearson Correlation Coefficient between the two conditions. The y-axis indicates the R score with 1 being positive correlation, zero meaning no correlation and -1 meaning negative correlation. The key to the right of the graph indicates which conditions match the symbols. (H) A diagram of the chimeric protein used to tag Axin with RFP (tdimer2(12)) and target it to mitochondria is shown.

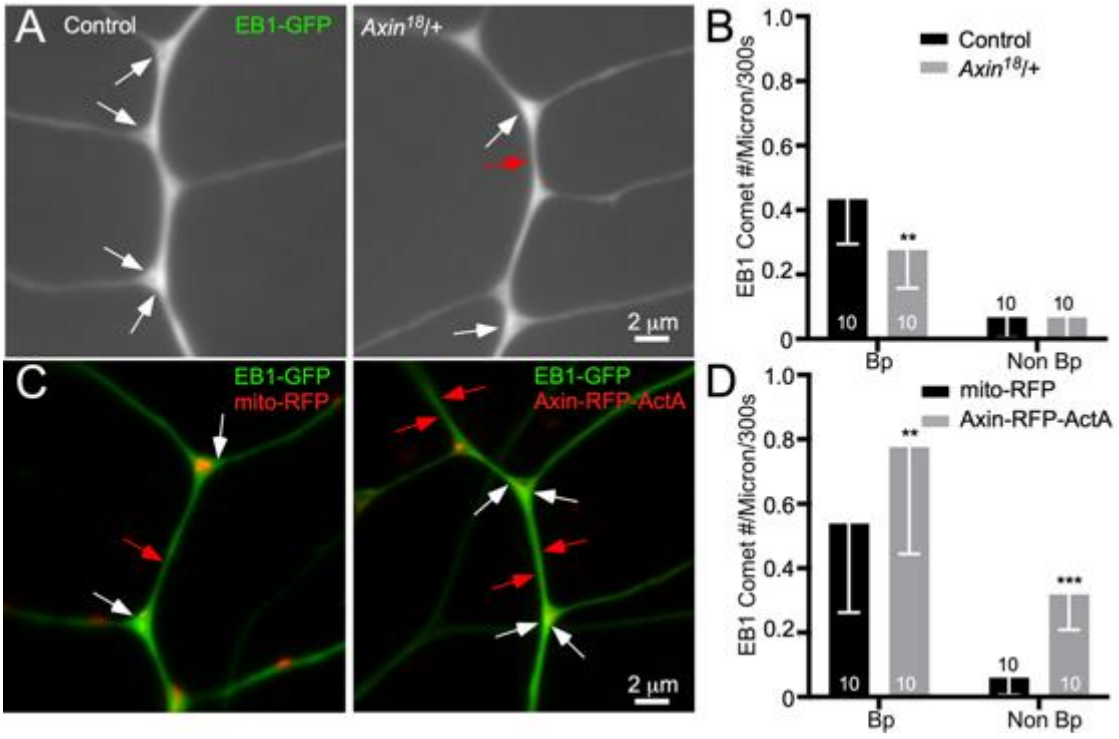

Figure 4-S7. Analysis of microtubule spawning events in dendrites with reduced and ectopic Axin.

(A) Example images compiled from EB1-GFP movies of the main comb dendrite trunk were generated using a summed projection of all 300 frames. Movies were acquired in control (*yw*) and *Axin*$_{18}$/+ mutant backgrounds. White arrows indicate spawning events at branch points and red arrows indicate comets that spawn from non-branch point regions during the 300 second movie. (B) Quantification of number of EB1 comets per micron for the entire 300 second movie is shown. (C) UAS-EB1-GFP was co-expressed with either RFP tagged mitochondria or the chimeric UAS-Axin-RFP-ActA. Summed example images are shown. Arrows follow the same scheme as the top two panels. (D) Quantification of number of EB1 comets per micron for the entire 300 second movie is shown. Sample size shown in or above the bars represents number of cells imaged. Error bars indicate standard deviation. A linear regression was used to determine statistical significance. * $p<0.05$, ** $p<0.01$, *** $p<0.001$

Discussion

It was particularly intriguing to find integral membrane signaling proteins required for non-centrosomal microtubule nucleation. Although Wnt signaling has been linked to microtubule plus-end regulation in axon growth cones (Purro, Ciani et al. 2008) and regulation of microtubule stability and spindle orientation (Salinas 2007), the only connection to the minus end is localization of some cytoplasmic Wnt signaling proteins like Axin to the centrosome in dividing cells (Fumoto, Kadono et al. 2009, Mbom, Nelson et al. 2013). Through our findings here we demonstrate that a Wnt signaling pathway acts upstream of microtubule nucleation. Not only were many canonical Wnt signaling proteins required for γTub-GFP to accumulate at branch points, but Axin and dsh themselves concentrated at branch points. In addition, the scaffolding protein Axin was able to recruit γTub-GFP to mitochondria when tethered to them. Moreover, reduction of Wnt signaling proteins phenocopied loss of γTub in two functional nucleation assays. While we consistently found that partial loss of function (RNAi or heterozygous mutants) for fz, fz2, arr, dsh, Gao, Gas, and Axin, reduced γTub localization and/or function, we could not find any evidence that β-catenin/armadillo, the key transcription factor that is the output of canonical Wnt signaling, was involved. In addition, an arm protein trap showed clear expression in epidermal cells, but was not seen in da neurons. Because Axin itself was sufficient to recruit γTub, there was no strong rationale for a transcriptional regulator to mediate signaling between fz/arr and microtubule nucleation. We propose that canonical Wnt signaling proteins are co-opted in dendrites to directly recruit nucleation complexes to endosomes. Because this is a variant of canonical Wnt signaling that unexpectedly seems not to involve β-catenin, we term this pathway apocryphal Wnt signaling in reference to the Apocrypha, ancient writings found in only

some versions of the Bible.

The involvement of arrow as well as dishevelled and Axin suggests that a signalosome might be involved in dendritic Wnt signaling. Signalosomes form when wnt ligands bind to fz and LRP5/6 at the plasma membrane triggering recruitment and multimerization of dishevelled and Axin (Gammons and Bienz 2017). The normal output of signalosome formation is release of β-catenin from the destruction complex and its subsequent stabilization and transit to the nucleus to activate transcription (Gammons and Bienz 2017).

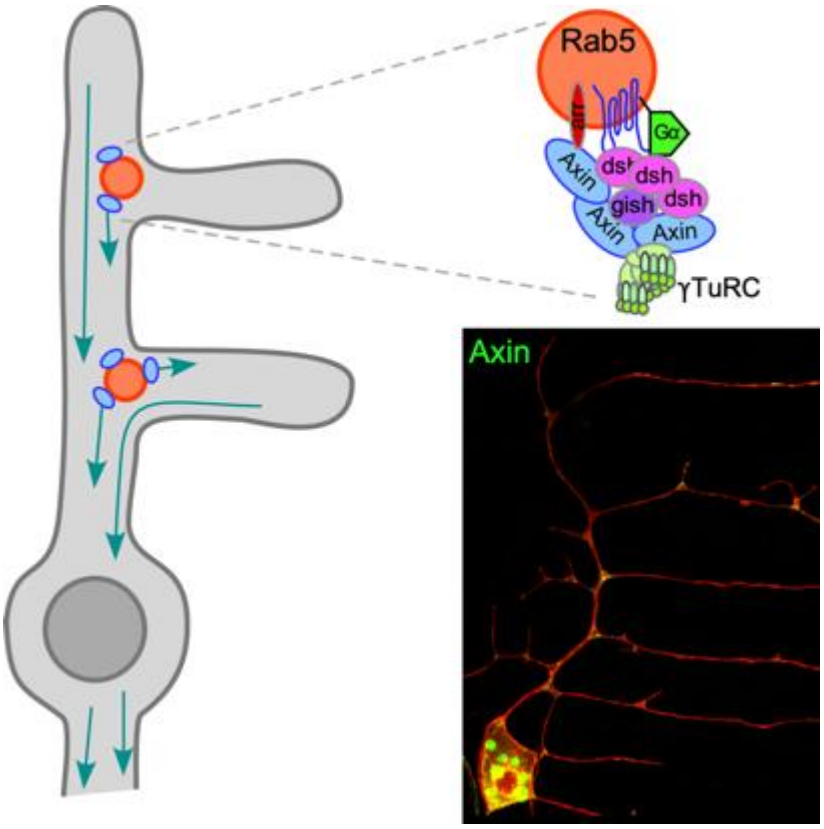

Figure 4-9 Model depicting how early endosomes recruit Wnt signaling proteins and nucleation machinery to dendrite branch points. A super resolution overview of a sensory neuron expressing mCD8-RFP and Axin-GFP is given for context.

Signalosomes assemble at the plasma membrane (Bilic, Huang et al. 2007, Hagemann, Kurz et al. 2014). Endocytosis generally seems to promote Wnt signaling (Brunt and Scholpp 2018) although in many contexts the signalosome itself is disassembled upon endocytosis (Hagemann, Kurz et al. 2014, Brunt and Scholpp 2018). It is not clear whether signalosomes persist after endocytosis, though in some Drosophila cells dsh and arrow are localized to endosomes (Seto and Bellen 2006). In dendrites puncta of frizzled, dsh and Axin colocalized with Rab5 (Figure 5)

suggesting that a stable signaling complex is present on endosomes in mature neurons. The initiation of comets from these puncta indicates that endosomes are likely the key site where Wnt signaling proteins promote nucleation. Colocalization of tagged Golgi proteins with Rab5 suggests that the previous association between Golgi markers and nucleation could have been due to leakage into endosomes. In addition, the identification of plasma membrane proteins acting upstream of γTub in dendrites suggests a more general role for the Golgi in the cell body by controlling secretion of arr and fz.

Wnt signaling receptors have been classically studied at the plasma membrane where they bind extracellular ligands that can be both autocrine or paracrine in nature. A requirement for arrow and frizzleds upstream of γTub in dendrites suggests that a Wnt ligand is likely involved. Failure of neuronal wntless knockdown to reduce γTub-GFP at branch points (Figure 5B) favors the hypothesis that the ligand may be secreted from a neighboring cell. In the embryo wg/Wnt-1 is made in a patch of epithelial cells adjacent to developing dendritic arborization neurons and helps pattern dendrite orientation in ddaE (Li, Wang et al. 2016). It would be very interesting if surrounding cells influenced the microtubule cytoskeleton in mature neurons through frizzled and arrow at the plasma membrane. This signaling pathway is particularly intriguing in the context of regeneration or during neurodegenerative disease. During axon regeneration, the initial injury response involves a nucleation-dependent increase in microtubule dynamics which serves a neuroprotective role. Modulating the Wnt signaling pathway described here could induce neuroprotection in dendrites, as that is where the pathway locally functions. Furthermore, we have discovered that the pathway is required during dendrite regeneration to position nucleation sites in regrowing dendrites via the frizzled co-receptor Ror (Nye, Albertson, co-submitted). Interestingly, GPCRs represent 33% of all FDA approved drug targets, and, as part of this family, frizzleds present a possible target (Hauser, Attwood et al. 2017).

One interesting remaining question is why dsh, Axin and γTub become concentrated at dendrite branch points. Several different mechanisms could lead to this distribution. First, endocytosis could be particularly active at branch points. A ligand might bind to frizzled/arrow distributed evenly on the plasma membrane, but then be activated by endocytosis only at branch points. The unique curvature of the plasma membrane at branch points could provide a milieu particularly favorable for endocytosis. Second, signaling endosomes coated with Axin and dsh could form randomly throughout the cell and be transported by motor proteins that release them at branch points. In this case the motor linkage would need to respond to a cue specific to branch points; one such cue could be curved microtubules. Third, the larger surface area of the dendrite available for interaction with surrounding cells at branch points could mean that uniform endocytosis of ligand could result in higher concentrations at branch points.

Local microtubule nucleation also occurs in axons (Nguyen, McCracken et al. 2014, Sanchez-Huertas, Freixo et al. 2016, Cunha-Ferreira, Chazeau et al. 2018). As Rab5 endosomes are present throughout axons, it will be interesting to determine whether Wnt signaling proteins can be recruited to axonal early endosomes, and whether they recruit nucleation proteins in this part of the cell. It is also possible that a link between Wnt signaling, endosomes and nucleation could exist more broadly in other cell types. Indeed, the localization of Axin to centrosomes (Fumoto, Kadono et al. 2009, He, Song et al. 2016) suggests that even in mitotic cells parts of this relationship are conserved. Intriguingly, endosomal membranes are concentrated around the centrosome (Das, Hehnly et al. 2014) and Rab5 reduction disrupts mitosis (Capalbo, D'Avino et al. 2011, Serio, Margaria et al. 2011, Das, Hehnly et al. 2014), so it is possible that Wnt signaling proteins, endosomes and nucleation function together at centrosomes.

Methods

Drosophila genetics and lines.

Many stocks used in this study were from the Vienna Drosophila Resource Center or Bloomington Drosophila Stock Center (NIH P40OD018537). Refer to Supplemental Table 1 for information on specific strains used as well as how they are referred to in Figures. RNAi experiments were performed by crossing Drosophila strains with UAS-controlled hairpins to tester lines that included 221-Gal4 to drive expression in Class I dendritic arborization neurons, fluorescently tagged markers and UAS-Dcr2 to increase RNAi knockdown efficiency (Dietzl, Chen et al. 2007). Of the two dorsal class I neurons the ddaE cell was chosen for analysis as the shape of its dorsal comb-like dendrite makes it particularly sensitive to perturbation of microtubule polarity (Mattie, Stackpole et al. 2010). In whole brain imaging experiments expression was driven pan-neuronally with elav-Gal4. The mutant frizzled stock, *fz*^{F31} was graciously sent by Dr. Paul Adler at the University of Virginia and *fz*^{P21} was kindly sent by Dr. Yashi Ahmed at Dartmouth University. Constitutively active Gαs and inactive Gαo fly lines were given to us by Dr. Andrew Tomlinson at Columbia University Medical Center. Tester lines for screens include (UAS-Dcr2, mCD8-RFP; 221-Gal4, Apc2-GFP), (UAS-Dcr2, UAS-mCD8-RFP; 221-Gal4, UAS-Axin-GFP), (UAS-Dcr2, UAS-mCD8-RFP; 221-Gal4, UAS-dsh-GFP) (UAS-Dcr2, UAS-mCD8-RFP; 221-Gal4, UAS-γtub-GFP), (UAS-Dcr2, UAS-mCD8-RFP; 221-Gal4, UAS-Rab5-GFP) (UAS-Dcr2; 221-Gal4, UAS-EB1-GFP). Additional fly lines used were: (221-Gal4, UAS-Mito-GFP), (221-Gal4, UAS-γTub-GFP), (221-Gal4, UAS-fz-EGFP), (221-Gal4, UAS-Axin-GFP) (IG1-Gal4, UAS-mCD8-RFP/cyo; FzR52/TM6), (UAS-gTub-GFP/cyo; FzP21/TM6), (UAS-Mito-RFP), (UAS-Axin-RFP-ActA), (UAS-dsh-GFP), (dsh-Clover) (mcherry-Rab5), (UAS-RAb4-mRFP), (Rab11-cherry), (UAS-ManII-EBFP), (UAS-ManII-

EGFP), (UAS-GalT-YFP), (UAS-Rab5-GFP), (UAS-Rab5-YFP) and (elav-Gal4, EB1-RFP). Control genotypes were matched for UAS-driven transgene number with experimental genotypes. For all RNAi and overexpression experiments the tester lines were crossed either to Rtnl2 (Control 1) or γTub37C (Control 2) RNAi lines (see Supplemental Table 1 for stock numbers used). These two targets were chosen for controls as neither is expected to be expressed in neurons. Rtnl2 is thought to be a pseudogene and γTub37C is the maternal γTub, as opposed to γTub23C, the somatic γTub referred to throughout the manuscript as γTub. For mutant experiments tester lines we crossed to *yw* flies (Control) that did not contain any UAS-driven transgenes.

Confocal *In vivo* Microscopy

After mating virgin female flies from tester lines with RNAi male flies, embryos were collected on 35mm caps filled with Drosophila corn meal media every 24 hours. Caps with embryos/larvae were incubated for 3 days at 25^{o}C and live *Drosophila* 3rd instar larvae were collected for mounting from these caps. After rinsing with water, individual larvae were mounted on a microscope slide with a circular piece of dried agar in the middle. Larvae were placed on the dried agar and whole mounted ventral side down by applying sub-lethal pressure with a 22x40 mm cover slip, which was then secured with tape. 10x objectives were used to locate larvae under the microscope. 60x Oil (NA 1.42) (Olympus) and 63x Oil (NA 1.4) (Zeiss) objectives were used to find ddaE neurons in segments a2-a4. For UAS-Apc2-GFP localization larvae were imaged on an Olympus FluoView1000. For the rest of the fluorescent markers including UAS-Mito-GFP, UAS-Mito-RFP, UAS-Axin-GFP and UAS-γTub-GFP larvae were imaged on an Olympus FluoView1000 or a Zeiss LSM800 as indicated in the figures. Markers including UAS-Rab4-mRFP, Rab11-cherry, mcherry-Rab5, UAS-ManII-EGFP, UAS-ManII-EBFP, UAS-GalT-YFP

and UAS-iBlueberry were imaged exclusively on the Zeiss LSM800. The UAS-dsh-GFP, UAS-Rab5-GFP and experiments showing EB1 comets originating off Rab5 endosomes or wnt signaling protein puncta were imaged on the Zeiss LSM800. These markers include UAS-Rab5-YFP, UAS-Rab5-tdTomato, EYFP-Rab5, UAS-fz-EGFP and dsh-Clover. The LSM800 is built on an AxioImager.Z2 and is operated with Zeiss Zen Blue software.

Larval Brain Imaging

Transgenic elav-Gal4, EB1-RFP flies were crossed with either flies expressing UAS-Apc2-GFP or UAS-Axin-GFP. Embryos were grown at 25_{o} for one day and 1_{st} instar larvae were mounted using the same protocol as 3_{rd} instar. The brain was located using the 10x objective of an Olympus FluoView1000 microscope. One of the lobes was then examined using a 60x oil (NA 1.42) objective. Actively dividing neuroblasts were identified the presence of a radial EB1-RFP aster and their relatively large size compared to surrounding mother ganglion cells. Movies were acquired by collecting images every second for up to 350 seconds.

Plasmid Construction

To generate Axin targeted to mitochondria the region that encodes the short C-terminal ActA mitochondrial targeting sequence (Pistor, Chakraborty et al. 1994) was synthesized by Genscript and cloned via Clone EZ Technology downstream of tDimer-Red12 (RFP) (Campbell, Tour et al. 2002) in pUAST to create a carboxyl-terminal fusion. The synthesized sequence was as follows:

agatctagattaattcttgcaatgttagctattggcgtgttctctttaggggcgtttatcaaaattattcaattaagaaaaaataattaa

The resulting vector pUAST-RFP-ActA was then linearized with SpeI and KpnI and gel isolated. Herculase from Agilent (Catalog #600675) and the following primers were used to PCR amplify the long isoform of Axin from Drosophila cDNA FI19317 (stock # 1647293) obtained from the Drosophila Genomics Resource Center (https://dgrc.bio.indiana.edu/product/View?product=1647293):

Axin5' primer:

ctcgagggcgcgccaactagtATGAGTGGCCATCCATCGGGAATCCGGAAACATGATGATAATG AG

Axin3' primer:

aggccggccacgcgtggtaccATCGGATGGCTTGACAAGACCCATCGCTTTGTC

The PCR product was gel isolated and cloned by In-Fusion (Clontech Catalog# 639646 In-Fusion® HD Cloning System) into SpeI-KpnI linearized pUAST-RFP-ActA to create pUAST-Axin-RFP-ActA. To generate a pUAST-Axin-RFP vector lacking the ActA sequence, tDimer-Red12 (RFP) was subcloned from the original pUAST-RFP construct as an FseI-PsiI fragment, which was gel isolated and used to replace the FseI-PsiI fragment in pUAST-Axin-RFP-ActA by ligation. In addition to Axin-RFP-ActA, the plasmid for pUAS-tdtomato-Rab5 was obtained from addgene. This construct was a gift from Matthew Scott's Lab and generated in the manuscript Zhang et. al. 2007.

pCasper4-Dsh::Clover2 was made by replacing EGFP of pCasper4-Dsh::EGFP (Axelrod 2001) (Axelrod, 2001) with Clover2, a derivative of Clover (Shaner, Lin et al. 2008). In detail, the last 713bp of Dsh coding sequence together with EGFP was cut out by XhoI/XbaI double digestion. Then the same 713bp of Dsh coding sequence without stop codon was cloned back into the XhoI/XbaI digested pCasper4-Dsh::EGFP to make a pCasper4-Dsh, introducing an XbaI site immediately following the Dsh coding sequence. Then the 717bp clover2 (with stop codon)

fragment was cloned into the XbaI site in pCasper4-Dsh. The Clover2 fragment was PCR amplified from the vector pNCS-Clover2 (Michael Lin lab at Stanford).

UAS-dsh::GFP was generated by cloning the dsh cDNA from EcoRI in the 5' UTR to EcoRI in the 3' UTR into pUAST (Axelrod, Miller et al. 1998). The GFP coding sequence was added by fusing the SnaBI site near the 3' end of dsh to ClaI near the 5' end of GFP by filled in blunt ligation, in pBS+beta. This fusion sequence was cloned into pCS2+, where it was placed after the beta-globin 5'UTR, and the GFP was substituted with EGFP. A fragment containing part of the beta-globin 5' UTR, part of the dsh 5' UTR, dsh cDNA::EGFP, followed by SV40 polyA, was cloned back into pUAST to generate the plasmid for injection. Plasmid injections into Drosophila embryos were performed by BestGene, and transgene insertion sites were mapped to chromosomes using standard segregation techniques with balancer chromosomes.

pUAST-γTub-TagRFPT was generated by first digesting GFP from the pUAST-γTub-GFP plasmid created in our previous publication (Nguyen, Stone et al. 2011) and digesting TagRFPT from pUAST-EB1-RFPT also previously generated in our lab (Feng et al., 2019) using at EcoRI and KpnI sites. TagRFPT was then ligated into the pUAST-γTub backbone. The product was then confirmed with diagnostic digest and sent to BestGene for plasmid injections into Drosophila embryos. Transgene insertion sties were mapped to chromosomes using standard segregation techniques with balancer chromosomes.

Microtubule Polarity Assay

Movies of EB1-GFP in the dorsal comb dendrite of the ddaE neuron were acquired with an AxioCam M2 or AxioCam 506 on a Zeiss ImagerM2 microscope running Zen Blue in live *Drosophila* 3rd instar larvae. A Colibri2 LED illumination system was used to excite GFP with 470 nm light and a 63X 1.4 NA objective was used. Movies were acquired for 300 frames at a

rate of one frame per second. After acquisition the Template Matching and Slice Alignment plugins in Fiji were used for stabilization. EB1-GFP comets visible for at least three frames were classified as growing towards or away from the cell body. The main trunk of the comb dendrite, distal to the first branch point, was used for analysis. Kymographs were generated using a built-in Fiji plugin. Data from each cell of a given genotype were pooled to generate total numbers of comets moving towards or away from the cell body. Statistical analysis was conducted using logistic regression.

Spawning Assay and Quantification

EB1-GFP movies were acquired at one frame per second for 300s. For movies without mitochondrial movies were taken with a Zeiss widefield microscope. When EB1-GFP was paired with mito-RFP or Axin-RFP-ActA movies were acquired on a Zeiss LSM800 microscope. For all movies the main trunk of the comb dendrite was used for analysis. Spawning events were characterized as emergence of an EB1 comet that covers a distance of at least 1 micron. Events that began before the movie started were not counted as a spawn event. Comet events that started off view and polymerized into the region of interest were also not counted. The same parameters were used for comets originating form labeled endosomes or Wnt proteins. Length measurements were performed in Fiji with the segmented line tool for non-branch point areas along the main trunk. For branch points length was calculated by drawing a line from the start of the taper on the side of the branch furthest from the cell body to the end of the taper closest to the cell body. Total comet counts were then divided by total length of branch point or non-branch point alike to produce a normalized value of comet number per micron per 300s.

Axon Injury Microtubule Dynamics Assay

A Micro-Point pulsed UV laser (Andor Technology) focused through the 63X objective of a Zeiss LSM800 microscope was used to make a precise cut to the proximal axon of a ddaE neuron in a 3rd instar larvae. Larvae were then incubated at 20oC for eight hours and the comb dendrite of the injured cell was imaged. EB1-GFP movies were acquired in the same way as for the microtubule polarity assay. Images were stabilized using the Template matching and Slice Alignment plugin in Fiji. Total comet number was then counted in Fiji and normalized to the length of dendrite region analyzed. This produced a value of microtubule comets per micron. Kymographs were generated using a built-in Fiji plugin. Statistics were generated using a linear regression model.

EB1 Comet Initiation off Endosomes Assays

Videos were acquired at one frame per second for 300s on a Zeiss LSM800 microscope. Only branch points in focus during the duration of the video were used for quantification. Comets that originated *de novo* at branch points off of either Rab5 or Wnt proteins were counted. Comets were not counted if they originated from a growing minus-end. They also were not counted if the comet was a result of a discernable catastrophe/rescue event. For the experiment involving dsh decorated Rab5 endosomes the same stipulations were followed. Total number of Rab5 puncta were counted and divided into two categories. These consisted of dsh positive and dsh negative Rab5 endosomes. Percentage of dsh decorated Rab5 endosomes was calculated using Fiji and comet events were also visualized with the software.

Fillet Prep and Immunostaining

3rd instar larvae expressing UAS-mcd8-RFP;221 Gal4 to label class I Da neurons were dorsally filleted in Schneiders Media using dissection scissors after pinning both head and tail down with .10mm steel insect Pins. After making a longitudinal incision between the primary trachea the gut and trachea were carefully removed leaving only muscle and skin. Following this removal four additional pins were used to carefully stretch and pin the larval body wall down. Immediately following this the media was removed and 4% PFA was used to fix the larvae for 30 minutes. After fixation, cells in the larvae were permeabilized in 3% PBS TX100 for 15 minutes. After this the fillets were moved to blocking solution of 10% NGS, 2%BSA, and .2% TX100 in PBS for 1 hour. Following this, larvae were incubated overnight at 4 degrees in a 1:100 solution of an antibody targeting Axin generated and described in Wang et. al. 2016. The following day the Axin antibody was washed off 5 times for 5 minutes each. The fillets were then exposed to a secondary 488 goat anti guinea antibody for 2 hours. Lastly the secondary antibody was washed off 5 times for 5 minutes each and then larvae were imaged using a Zeiss LSM800 microscope using the same mounting procedure as the live larvae.

Fluorescence Intensity Quantification Methods

For branch point intensity measurements z-stack images were acquired with either an Olympus or Zeiss confocal microscope as noted on each graph and images were prepared and quantified using the image processing software Fiji (ImageJ). Maximum projection stacked images were used for all localization analyses. UAS-Apc2-GFP was measured in a binary manner by scoring each branch point as Apc2-GFP present or absent. Similarly, for UAS-dsh-GFP any branch point that had a distinct punctum of GFP was counted as present. For UAS-γTub-GFP and

UAS-Axin-GFP the regions between branch points (nBP) and within branch points (BP) along the dorsal comb dendrite were manually outlined and average pixel intensities were measured (Supplemental Figure 1). Typically, 8-12 branch points and nBP regions were outlined in each cell, and a single average BP and nBP value was generated for the cell. These two values were then subtracted from each other to determine how much more fluorescence accumulated at the branch point than in between. Refer to Supplemental Figure 1 for images showing an example image with manual BP and nBP outlines. The raw average of BP-nBP for each control was normalized to 100 by dividing 100 by the average. This generated a normalization value that was then multiplied to each sample of the genotypes being compared to the control. The original control values were also multiplied by this normalization value. This generated an average for the control close to 100 but not exactly due to the rounding errors excel.

For mitochondrial colocalization experiments an overview z-stack image using sequential channel scanning was collected on a Zeiss LSM800 Imager.Z2 running Zen Blue and maximum intensity projections were generated using Fiji. Secondary dendrites emerging from the trunk of the dorsal comb dendrite of the ddaE neuron were chosen as regions for analysis because mitochondria are found along their length, but little Axin normally concentrates there. A segmented line was generated along one of these dendrites and fluorescent intensity line tracings were made using Fiji for both red and green channels. To normalize these intensities the values along the line were divided by the highest pixel value, and these values were plotted. For the correlation analysis the Fiji plugin JACoP was used to calculate a Pearson's Coefficient (R score) (Bolte and Cordelieres 2006). This coefficient was calculated for the entire comb dendrite between red and green channels for each of the four conditions.

Statistical Methods

Multiple linear regression analysis was used to compare conditions against a control for all localization experiments and for microtubule dynamics. This analysis calculates p values the same way as ANOVA, but allowed us to specify which condition was the control. A logistic regression was used to compare polarity assay conditions to a control since this is a pooled dataset. GraphPad Prism 6 software was used to carry out statistical analyses. See individual figure legends for statistical test used. Statistical significance is noted as * $p<0.05$, ** $p<0.01$, *** $p<0.001$. Statistical methods were carried out after consulting with Haley Brittingham a Masters student in the Penn State Statistics Department. In all figures with error bars they represent standard deviation.

Acknowledgements

We are grateful to Dr. Paul Adler, Dr. Mariann Bienz, Dr. Gary Struhl and Dr. Andrew Tomlinson for providing fly strains. We also would like to thank Dr. Yashi Ahmed for fly strains and the Axin Antibody. We would like to thank Dr. Paul Conduit for giving us the γTub-sfGFP fly line. Stocks obtained from the Bloomington Drosophila Stock Center (NIH P40OD018537) were used in this study, as were those from the Vienna Drosophila Resource Center. We are also thankful for the support and input of all Rolls lab members. We are especially grateful for the input from Matthew Shorey. We also very much appreciate Haley Brittingham, a Masters student in Applied Statistics at Penn State, for consulting with us about appropriate statistical tests. We are also grateful for the funding received for this project from the NIH R01 GM085115.

Author contributions

Alexis T. Weiner helped write the paper, created figures, performed experiments and analyzed data throughout and generated the UAS-γTub-TagRFPT. Dylan Y. Seebold performed experiments in all assays. Pedro Torres-Gutierrez performed a subset of localization experiments, microtubule polarity assays throughout and mitochondrial colocalization experiments. Gregory O. Kothe designed and created the UAS-Axin-RFP-ActA and UAS-Axin-RFP plasmids. Jessica G. Stoltz helped create the UAS-Axin-RFP-ActA plasmid under guidance of GOK. Christin Folker performed the Grip RNAi injury experiments. Christopher Kozlowski, Mit A. Patel and Dylan J. Barbera performed microtubule polarity experiments. Rachel D. Swope constructed the dsh tester line, carried out the RNAi screen in this background and helped acquired images/videos for mitochondria targeting and EB1 comet initiation assays. Pankajam Thyagarajan imaged the γTub-sfGFP and characterized it in dendrites. Madeleine Zalenski performed Rab RNAi to test for a role in γTub localization. Matthew Keegan tested a role for wntless in γTub localization. Kana Behari generated and validated transgenic fly lines. Song Song and Jeffrey D. Axelrod generated and validated tagged dsh lines. Melissa M. Rolls supervised all aspects of the project including experimental design, data analysis and writing the paper.

References

Axelrod, J. D. (2001). Unipolar membrane association of Dishevelled mediates Frizzled planar cell polarity signaling. *Genes Dev, 15*(10), 1182-1187. doi:10.1101/gad.890501

Axelrod, J. D., Miller, J. R., Shulman, J. M., Moon, R. T., & Perrimon, N. (1998). Differential recruitment of Dishevelled provides signaling specificity in the planar cell polarity and Wingless signaling pathways. *Genes Dev, 12*(16), 2610-2622.

Baas, P. W., Deitch, J. S., Black, M. M., & Banker, G. A. (1988). Polarity orientation of microtubules in hippocampal neurons: uniformity in the axon and nonuniformity in the dendrite. *Proc Natl Acad Sci U S A, 85*(21), 8335-8339.

Baas, P. W., & Lin, S. (2011). Hooks and comets: The story of microtubule polarity orientation in the neuron. *Dev Neurobiol, 71*(6), 403-418. doi:10.1002/dneu.20818

Baas, P. W., & Yu, W. (1996). A composite model for establishing the microtubule arrays of the neuron. *Mol Neurobiol, 12*(2), 145-161.

Bartolini, F., & Gundersen, G. G. (2006). Generation of noncentrosomal microtubule arrays. *J Cell Sci, 119*(Pt 20), 4155-4163.

Bhanot, P., Fish, M., Jemison, J. A., Nusse, R., Nathans, J., & Cadigan, K. M. (1999). Frizzled and Dfrizzled-2 function as redundant receptors for Wingless during Drosophila embryonic development. *Development, 126*(18), 4175-4186.

Bilic, J., Huang, Y. L., Davidson, G., Zimmermann, T., Cruciat, C. M., Bienz, M., & Niehrs, C. (2007). Wnt induces LRP6 signalosomes and promotes dishevelled-dependent LRP6 phosphorylation. *Science, 316*(5831), 1619-1622. doi:10.1126/science.1137065

Bolte, S., & Cordelieres, F. P. (2006). A guided tour into subcellular colocalization analysis in light microscopy. *J Microsc, 224*(Pt 3), 213-232. doi:10.1111/j.1365-2818.2006.01706.x

Bourouis, M. (2002). Targeted increase in shaggy activity levels blocks wingless signaling. *Genesis, 34*(1-2), 99-102. doi:10.1002/gene.10114

Brunt, L., & Scholpp, S. (2018). The function of endocytosis in Wnt signaling. *Cell Mol Life Sci, 75*(5), 785-795. doi:10.1007/s00018-017-2654-2

Burton, P. R. (1988). Dendrites of mitral cell neurons contain microtubules of opposite polarity. *Brain Res, 473*(1), 107-115.

Cadigan, K. M., & Peifer, M. (2009). Wnt signaling from development to disease: insights from model systems. *Cold Spring Harb Perspect Biol, 1*(2), a002881. doi:10.1101/cshperspect.a002881

Campbell, R. E., Tour, O., Palmer, A. E., Steinbach, P. A., Baird, G. S., Zacharias, D. A., & Tsien, R. Y. (2002). A monomeric red fluorescent protein. *Proc Natl Acad Sci U S A, 99*(12), 7877-7882.

Capalbo, L., D'Avino, P. P., Archambault, V., & Glover, D. M. (2011). Rab5 GTPase controls chromosome alignment through Lamin disassembly and relocation of the NuMA-like protein Mud to the poles during mitosis. *Proc Natl Acad Sci U S A, 108*(42), 17343-17348. doi:10.1073/pnas.1103720108

Chen, J. V., Buchwalter, R. A., Kao, L. R., & Megraw, T. L. (2017). A Splice Variant of Centrosomin Converts Mitochondria to Microtubule-Organizing Centers. *Curr Biol, 27*(13), 1928-1940 e1926. doi:10.1016/j.cub.2017.05.090

Chen, L., Stone, M. C., Tao, J., & Rolls, M. M. (2012). Axon injury and stress trigger a microtubule-based neuroprotective pathway. *Proc Natl Acad Sci U S A, 109*(29), 11842-11847. doi:10.1073/pnas.1121180109

Chevalier-Larsen, E., & Holzbaur, E. L. (2006). Axonal transport and neurodegenerative disease. *Biochim Biophys Acta, 1762*(11-12), 1094-1108. doi:10.1016/j.bbadis.2006.04.002

Choi, Y. K., Liu, P., Sze, S. K., Dai, C., & Qi, R. Z. (2010). CDK5RAP2 stimulates microtubule nucleation by the gamma-tubulin ring complex. *J Cell Biol, 191*(6), 1089-1095. doi:10.1083/jcb.201007030

Cliffe, A., Hamada, F., & Bienz, M. (2003). A role of Dishevelled in relocating Axin to the plasma membrane during wingless signaling. *Curr Biol, 13*(11), 960-966.

Cunha-Ferreira, I., Chazeau, A., Buijs, R. R., Stucchi, R., Will, L., Pan, X., . . . Hoogenraad, C. C. (2018). The HAUS Complex Is a Key Regulator of Non-centrosomal Microtubule Organization during Neuronal Development. *Cell Rep, 24*(4), 791-800. doi:10.1016/j.celrep.2018.06.093

Das, S., Hehnly, H., & Doxsey, S. (2014). A new role for Rab GTPases during early mitotic stages. *Small GTPases, 5*. doi:10.4161/sgtp.29565

Davidson, G., Wu, W., Shen, J., Bilic, J., Fenger, U., Stannek, P., . . . Niehrs, C. (2005). Casein kinase 1 gamma couples Wnt receptor activation to cytoplasmic signal transduction. *Nature, 438*(7069), 867-872. doi:10.1038/nature04170

del Castillo, U., Winding, M., Lu, W., & Gelfand, V. I. (2015). Interplay between kinesin-1 and cortical dynein during axonal outgrowth and microtubule organization in Drosophila neurons. *Elife, 4*, e10140. doi:10.7554/eLife.10140

Devenport, D. (2014). The cell biology of planar cell polarity. *J Cell Biol, 207*(2), 171-179. doi:10.1083/jcb.201408039

Dietzl, G., Chen, D., Schnorrer, F., Su, K. C., Barinova, Y., Fellner, M., . . . Dickson, B. J. (2007). A genome-wide transgenic RNAi library for conditional gene inactivation in Drosophila. *Nature, 448*(7150), 151-156.

Dunst, S., Kazimiers, T., von Zadow, F., Jambor, H., Sagner, A., Brankatschk, B., . . . Brankatschk, M. (2015). Endogenously tagged rab proteins: a resource to study membrane trafficking in Drosophila. *Dev Cell, 33*(3), 351-365. doi:10.1016/j.devcel.2015.03.022

Efimov, A., Kharitonov, A., Efimova, N., Loncarek, J., Miller, P. M., Andreyeva, N., . . . Kaverina, I. (2007). Asymmetric CLASP-Dependent Nucleation of Noncentrosomal Microtubules at the trans-Golgi Network. *Dev Cell, 12*(6), 917-930.

Fumoto, K., Kadono, M., Izumi, N., & Kikuchi, A. (2009). Axin localizes to the centrosome and is involved in microtubule nucleation. *EMBO Rep, 10*(6), 606-613. doi:10.1038/embor.2009.45

Gammons, M., & Bienz, M. (2017). Multiprotein complexes governing Wnt signal transduction. *Curr Opin Cell Biol, 51*, 42-49. doi:10.1016/j.ceb.2017.10.008

Gates, J., Mahaffey, J. P., Rogers, S. L., Emerson, M., Rogers, E. M., Sottile, S. L., . . . Peifer, M. (2007). Enabled plays key roles in embryonic epithelial morphogenesis in Drosophila. *Development, 134*(11), 2027-2039. doi:10.1242/dev.02849

Gault, W. J., Olguin, P., Weber, U., & Mlodzik, M. (2012). Drosophila CK1-gamma, gilgamesh, controls PCP-mediated morphogenesis through regulation of vesicle trafficking. *J Cell Biol, 196*(5), 605-621. doi:10.1083/jcb.201107137

Goodwin, P. R., Sasaki, J. M., & Juo, P. (2012). Cyclin-dependent kinase 5 regulates the polarized trafficking of neuropeptide-containing dense-core vesicles in Caenorhabditis elegans motor neurons. *J Neurosci, 32*(24), 8158-8172. doi:10.1523/JNEUROSCI.0251-12.2012

Gunawardena, S., & Goldstein, L. S. (2004). Cargo-carrying motor vehicles on the neuronal highway: transport pathways and neurodegenerative disease. *J Neurobiol, 58*(2), 258-271.

Hagemann, A. I., Kurz, J., Kauffeld, S., Chen, Q., Reeves, P. M., Weber, S., . . . Scholpp, S. (2014). In vivo analysis of formation and endocytosis of the Wnt/beta-catenin signaling complex in zebrafish embryos. *J Cell Sci, 127*(Pt 18), 3970-3982. doi:10.1242/jcs.148767

Hamada, F., Tomoyasu, Y., Takatsu, Y., Nakamura, M., Nagai, S., Suzuki, A., . . . Akiyama, T. (1999). Negative regulation of Wingless signaling by D-axin, a Drosophila homolog of axin. *Science, 283*(5408), 1739-1742.

Hauser, A. S., Attwood, M. M., Rask-Andersen, M., Schioth, H. B., & Gloriam, D. E. (2017). Trends in GPCR drug discovery: new agents, targets and indications. *Nat Rev Drug Discov, 16*(12), 829-842. doi:10.1038/nrd.2017.178

Hazelett, D. J., Bourouis, M., Walldorf, U., & Treisman, J. E. (1998). decapentaplegic and wingless are regulated by eyes absent and eyegone and interact to direct the pattern of retinal differentiation in the eye disc. *Development, 125*(18), 3741-3751.

He, X. Q., Song, Y. Q., Liu, R., Liu, Y., Zhang, F., Zhang, Z., . . . Wang, H. L. (2016). Axin-1 Regulates Meiotic Spindle Organization in Mouse Oocytes. *PLoS One, 11*(6), e0157197. doi:10.1371/journal.pone.0157197

Hill, S. E., Parmar, M., Gheres, K. W., Guignet, M. A., Huang, Y., Jackson, F. R., & Rolls, M. M. (2012). Development of dendrite polarity in Drosophila neurons. *Neural Dev, 7*, 34. doi:10.1186/1749-8104-7-34

Horton, A. C., & Ehlers, M. D. (2003). Dual modes of endoplasmic reticulum-to-Golgi transport in dendrites revealed by live-cell imaging. *J Neurosci, 23*(15), 6188-6199.

Hughes, C. L., & Thomas, J. B. (2007). A sensory feedback circuit coordinates muscle activity in Drosophila. *Mol Cell Neurosci, 35*(2), 383-396. doi:S1044-7431(07)00086-3 [pii]
10.1016/j.mcn.2007.04.001

Humphries, A. C., & Mlodzik, M. (2017). From instruction to output: Wnt/PCP signaling in development and cancer. *Curr Opin Cell Biol, 51*, 110-116. doi:10.1016/j.ceb.2017.12.005

Jones, K. H., Liu, J., & Adler, P. N. (1996). Molecular analysis of EMS-induced frizzled mutations in Drosophila melanogaster. *Genetics, 142*(1), 205-215.

Katanaev, V. L., Ponzielli, R., Semeriva, M., & Tomlinson, A. (2005). Trimeric G protein-dependent frizzled signaling in Drosophila. *Cell, 120*(1), 111-122. doi:10.1016/j.cell.2004.11.014

Katanaev, V. L., & Tomlinson, A. (2006). Multiple roles of a trimeric G protein in Drosophila cell polarization. *Cell Cycle, 5*(21), 2464-2472.

Kleele, T., Marinkovic, P., Williams, P. R., Stern, S., Weigand, E. E., Engerer, P., . . . Misgeld, T. (2014). An assay to image neuronal microtubule dynamics in mice. *Nat Commun, 5*, 4827. doi:10.1038/ncomms5827

Koval, A., Purvanov, V., Egger-Adam, D., & Katanaev, V. L. (2011). Yellow submarine of the Wnt/Frizzled signaling: submerging from the G protein harbor to the targets. *Biochem Pharmacol, 82*(10), 1311-1319. doi:10.1016/j.bcp.2011.06.005

Lam, A. J., St-Pierre, F., Gong, Y., Marshall, J. D., Cranfill, P. J., Baird, M. A., . . . Lin, M. Z. (2012). Improving FRET dynamic range with bright green and red fluorescent proteins. *Nat Methods, 9*(10), 1005-1012. doi:10.1038/nmeth.2171

Li, X., Wang, Y., Wang, H., Liu, T., Guo, J., Yi, W., & Li, Y. (2016). Epithelia-derived wingless regulates dendrite directional growth of drosophila ddaE neuron through the Fz-Fmi-Dsh-Rac1 pathway. *Mol Brain, 9*(1), 46. doi:10.1186/s13041-016-0228-0

Lund, V. K., DeLotto, Y., & DeLotto, R. (2010). Endocytosis is required for Toll signaling and shaping of the Dorsal/NF-kappaB morphogen gradient during Drosophila embryogenesis. *Proc Natl Acad Sci U S A, 107*(42), 18028-18033. doi:10.1073/pnas.1009157107

MacDonald, B. T., & He, X. (2012). Frizzled and LRP5/6 receptors for Wnt/beta-catenin signaling. *Cold Spring Harb Perspect Biol, 4*(12), 1-23. doi:10.1101/cshperspect.a007880

Maniar, T. A., Kaplan, M., Wang, G. J., Shen, K., Wei, L., Shaw, J. E., . . . Bargmann, C. I. (2012). UNC-33 (CRMP) and ankyrin organize microtubules and localize kinesin to polarize axon-dendrite sorting. *Nat Neurosci, 15*(1), 48-56. doi:10.1038/nn.2970

Mattie, F. J., Stackpole, M. M., Stone, M. C., Clippard, J. R., Rudnick, D. A., Qiu, Y., . . . Rolls, M. M. (2010). Directed Microtubule Growth, +TIPs, and Kinesin-2 Are Required for Uniform Microtubule Polarity in Dendrites. *Curr Biol, 20*(24), 2169-2177. doi:S0960-9822(10)01516-2 [pii]
10.1016/j.cub.2010.11.050

Mbom, B. C., Nelson, W. J., & Barth, A. (2013). beta-catenin at the centrosome: discrete pools of beta-catenin communicate during mitosis and may co-ordinate centrosome functions and cell cycle progression. *Bioessays, 35*(9), 804-809. doi:10.1002/bies.201300045

Muroyama, A., & Lechler, T. (2017). Microtubule organization, dynamics and functions in differentiated cells. *Development, 144*(17), 3012-3021. doi:10.1242/dev.153171

Nguyen, M. M., McCracken, C. J., Milner, E. S., Goetschius, D. J., Weiner, A. T., Long, M. K., . . . Rolls, M. M. (2014). Gamma-tubulin controls neuronal microtubule polarity independently of Golgi outposts. *Mol Biol Cell, 25*(13), 2039-2050. doi:10.1091/mbc.E13-09-0515

Nguyen, M. M., Stone, M. C., & Rolls, M. M. (2011). Microtubules are organized independently of the centrosome in Drosophila neurons. *Neural Dev, 6*, 38. doi:10.1186/1749-8104-6-38

Ori-McKenney, K. M., Jan, L. Y., & Jan, Y. N. (2012). Golgi outposts shape dendrite morphology by functioning as sites of acentrosomal microtubule nucleation in neurons. *Neuron, 76*(5), 921-930. doi:10.1016/j.neuron.2012.10.008

Orsulic, S., & Peifer, M. (1996). An in vivo structure-function study of armadillo, the beta-catenin homologue, reveals both separate and overlapping regions of the protein required for cell adhesion and for wingless signaling. *J Cell Biol, 134*(5), 1283-1300.

Pistor, S., Chakraborty, T., Niebuhr, K., Domann, E., & Wehland, J. (1994). The ActA protein of Listeria monocytogenes acts as a nucleator inducing reorganization of the actin cytoskeleton. *EMBO J, 13*(4), 758-763.

Povelones, M., Howes, R., Fish, M., & Nusse, R. (2005). Genetic evidence that Drosophila frizzled controls planar cell polarity and Armadillo signaling by a common mechanism. *Genetics, 171*(4), 1643-1654. doi:10.1534/genetics.105.045245

Purro, S. A., Ciani, L., Hoyos-Flight, M., Stamatakou, E., Siomou, E., & Salinas, P. C. (2008). Wnt regulates axon behavior through changes in microtubule growth directionality: a new role for adenomatous polyposis coli. *J Neurosci, 28*(34), 8644-8654.

Rao, A. N., Patil, A., Black, M. M., Craig, E. M., Myers, K. A., Yeung, H. T., & Baas, P. W. (2017). Cytoplasmic Dynein Transports Axonal Microtubules in a Polarity-Sorting Manner. *Cell Rep, 19*(11), 2210-2219. doi:10.1016/j.celrep.2017.05.064

Rolls, M. M., Satoh, D., Clyne, P. J., Henner, A. L., Uemura, T., & Doe, C. Q. (2007). Polarity and compartmentalization of Drosophila neurons. *Neural Development, 2*, 7.

Salinas, P. C. (2007). Modulation of the microtubule cytoskeleton: a role for a divergent canonical Wnt pathway. *Trends Cell Biol, 17*(7), 333-342. doi:10.1016/j.tcb.2007.07.003

Sanchez, A. D., & Feldman, J. L. (2017). Microtubule-organizing centers: from the centrosome to non-centrosomal sites. *Curr Opin Cell Biol, 44*, 93-101. doi:10.1016/j.ceb.2016.09.003

Sanchez-Huertas, C., Freixo, F., Viais, R., Lacasa, C., Soriano, E., & Luders, J. (2016). Non-centrosomal nucleation mediated by augmin organizes microtubules in post-mitotic neurons and controls axonal microtubule polarity. *Nat Commun, 7*, 12187. doi:10.1038/ncomms12187

Sanders, A. A., & Kaverina, I. (2015). Nucleation and Dynamics of Golgi-derived Microtubules. *Front Neurosci, 9*, 431. doi:10.3389/fnins.2015.00431

Serio, G., Margaria, V., Jensen, S., Oldani, A., Bartek, J., Bussolino, F., & Lanzetti, L. (2011). Small GTPase Rab5 participates in chromosome congression and regulates localization of the centromere-associated protein CENP-F to kinetochores. *Proc Natl Acad Sci U S A, 108*(42), 17337-17342. doi:10.1073/pnas.1103516108

Seto, E. S., & Bellen, H. J. (2006). Internalization is required for proper Wingless signaling in Drosophila melanogaster. *J Cell Biol, 173*(1), 95-106. doi:10.1083/jcb.200510123

Shaner, N. C., Lin, M. Z., McKeown, M. R., Steinbach, P. A., Hazelwood, K. L., Davidson, M. W., & Tsien, R. Y. (2008). Improving the photostability of bright monomeric orange and red fluorescent proteins. *Nat Methods, 5*(6), 545-551. doi:10.1038/nmeth.1209

Sisson, J. C., Field, C., Ventura, R., Royou, A., & Sullivan, W. (2000). Lava lamp, a novel peripheral golgi protein, is required for Drosophila melanogaster cellularization. *J Cell Biol, 151*(4), 905-918.

Stepanova, T., Slemmer, J., Hoogenraad, C. C., Lansbergen, G., Dortland, B., De Zeeuw, C. I., . . . Galjart, N. (2003). Visualization of microtubule growth in cultured neurons via the use of EB3-GFP (end-binding protein 3-green fluorescent protein). *J Neurosci, 23*(7), 2655-2664.

Stiess, M., Maghelli, N., Kapitein, L. C., Gomis-Ruth, S., Wilsch-Brauninger, M., Hoogenraad, C. C., . . . Bradke, F. (2010). Axon extension occurs independently of centrosomal microtubule nucleation. *Science, 327*(5966), 704-707. doi:science.1182179 [pii] 10.1126/science.1182179

Stone, M. C., Nguyen, M. M., Tao, J., Allender, D. L., & Rolls, M. M. (2010). Global up-regulation of microtubule dynamics and polarity reversal during regeneration of an axon from a dendrite. *Mol Biol Cell, 21*(5), 767-777. doi:E09-11-0967 [pii] 10.1091/mbc.E09-11-0967

Stone, M. C., Roegiers, F., & Rolls, M. M. (2008). Microtubules Have Opposite Orientation in Axons and Dendrites of Drosophila Neurons. *Mol Biol Cell, 19*(10), 4122-4129.

Tillery, M. M. L., Blake-Hedges, C., Zheng, Y., Buchwalter, R. A., & Megraw, T. L. (2018). Centrosomal and Non-Centrosomal Microtubule-Organizing Centers (MTOCs) in Drosophila melanogaster. *Cells, 7*(9). doi:10.3390/cells7090121

Tovey, C. A., Tubman, C. E., Hamrud, E., Zhu, Z., Dyas, A. E., Butterfield, A. N., . . . Conduit, P. T. (2018). gamma-TuRC Heterogeneity Revealed by Analysis of Mozart1. *Curr Biol, 28*(14), 2314-2323 e2316. doi:10.1016/j.cub.2018.05.044

Wang, Z., Tacchelly-Benites, O., Yang, E., & Ahmed, Y. (2016). Dual Roles for Membrane Association of Drosophila Axin in Wnt Signaling. *PLoS Genet, 12*(12), e1006494. doi:10.1371/journal.pgen.1006494

Weiner, A. T., Seebold, D. Y., Michael, N. L., Guignet, M., Feng, C., Follick, B., . . . Rolls, M. M. (2018). Identification of Proteins Required for Precise Positioning of Apc2 in Dendrites. *G3 (Bethesda), 8*(5), 1841-1853. doi:10.1534/g3.118.200205

Wolfgang, W. J., Roberts, I. J., Quan, F., O'Kane, C., & Forte, M. (1996). Activation of protein kinase A-independent pathways by Gs alpha in Drosophila. *Proc Natl Acad Sci U S A, 93*(25), 14542-14547.

Yalgin, C., Ebrahimi, S., Delandre, C., Yoong, L. F., Akimoto, S., Tran, H., . . . Moore, A. W. (2015). Centrosomin represses dendrite branching by orienting microtubule nucleation. *Nat Neurosci, 18*(10), 1437-1445. doi:10.1038/nn.4099

Yau, K. W., Schatzle, P., Tortosa, E., Pages, S., Holtmaat, A., Kapitein, L. C., & Hoogenraad, C. C. (2016). Dendrites In Vitro and In Vivo Contain Microtubules of Opposite Polarity and Axon Formation Correlates with Uniform Plus-End-Out Microtubule Orientation. *J Neurosci, 36*(4), 1071-1085. doi:10.1523/JNEUROSCI.2430-15.2016

Ye, B., Zhang, Y., Song, W., Younger, S. H., Jan, L. Y., & Jan, Y. N. (2007). Growing dendrites and axons differ in their reliance on the secretory pathway. Cell, 130(4), 717-72

Chapter 5

Discussion and Follow Up

Drosophila Dendritic Microtubule Organization

Neuron shape and size is unsuited to a centralized MTOC in the cell body. Although microtubules are capable of growing long distances, they cannot continuously grow from a cell body through the entire length of axons and dendrites. Additionally, microtubule polarity in axons and dendrites is different such that minus-ends organized in the cell body would not be able to support minus-end out polarity in dendrites. Therefore, the evolutionary need for local control of microtubules has led to the emergence of specialized neuronal control mechanisms in both axons and dendrites. In this work we have confirmed the location of the microtubule steering mechanism at dendrite branch points. In addition, we have shown the molecular constituents required for the localization of the protein Apc2. Lastly, we have discovered a co-opted canonical Wnt signaling pathway without the need for the transcriptional activity of beta catenin. This pathway acts as a master regulator of both the steering component Apc2 and the core microtubule nucleator γTub. We have shown the pathway converges on the scaffolding protein Axin and it is sufficient to recruit γTub. Through this connection we have demonstrated for the first time that Wnt signaling proteins can have a regulatory effect not only on the plus-end of microtubules but also on the microtubule minus-end in neurons. We have termed this divergent Wnt signaling pathway Apocryphal Wnt signaling because it leaves out the fundamental output of canonical Wnt signaling harkening back to the books of the Apocrypha left out of the Bible. Additionally, this pathway functions from a subset of unique Rab5 endosomes that house the signaling machinery and initiate microtubule nucleation. The identification of Rab5 endosomes as

nucleation sites offers up a site of acentrosomal microtubule organization that has yet to be uncovered.

These results solidify one and add an additional mechanism of microtubule control in *Drosophila* dendrites. If we add these to our current understanding so far mechanisms controlling microtubule polarity in *Drosophila* dendrites include microtubule steering through Kinesin-2, minus-end out growth via patronin, and local nucleation via Wnt signaling proteins at branch points from Rab5 endosomes (Figure 1) (Feng et al., 2019; Mattie et al., 2010; Weiner, Lanz,

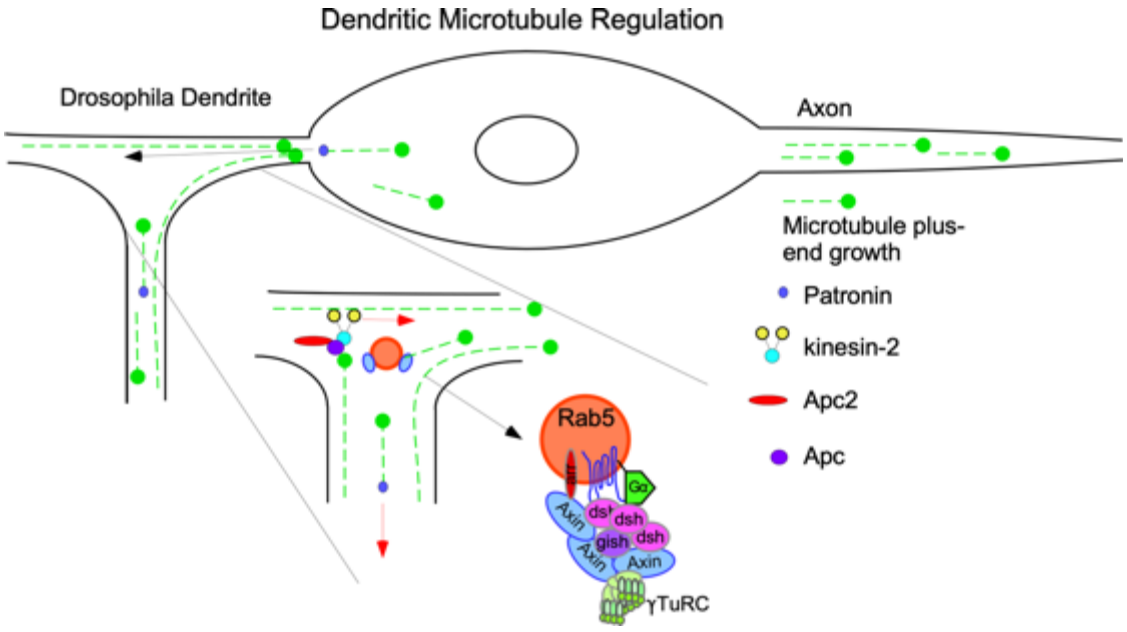

Figure 5-1. *Drosophila* Dendritic Microtubule Regulation: Model showing regulatory mechanisms governing microtubule polarity in *Drosophila* dendrites. Three distinct mechanism function in *Drosophila* dendrites. Two of them including microtubule steering through Apc, Eb1 and Kinesin-2, and microtubule enucleation off of Wnt signaling endosomes are mechanisms that function specifically at branch points. The third mechanism which contributes to overall microtubule polarity is minus-end growth mediated by patronin. These growing minus-ends are seen throughout the dendrite and are thought to populate the most distal regions with minus-end out microtubules. Red arrows indicate direction of that mechanism in terms of both steering and minus-end growth.

Goetschius, Hancock, & Rolls, 2016; Weiner et al., 2020) (Figure 1). Since *Drosophila* dendrites are initially mixed (Hill et al., 2012) it begs the question of how microtubules resolve to become minus-end out. Based on these results and others we can start to form a model. First during initial

neurite outgrowth plus-ends can enter dendrites creating dominant plus-end out polarity. Second minus end growth facilitated by patronin can grow microtubule minus-ends into dendrites creating a mixed microtubule phase (Feng et al., 2019) (Figure 1). Around the same time local nucleation sites are placed at branch points on Wnt signaling endosomes which contributes to minus-end out polarity (Nguyen et al., 2014; Weiner et al., 2020). These two early mechanisms help to shift the balance of minus-end out microtubules and a mechanism such as steering mediated by the complex of Apc/Eb1/Kinesin-2 helps to enforce and push this bias even more by reading out the polarity (Mattie et al., 2010; Weiner et al., 2016). However, these mechanisms cannot fully answer how complete minus-end out polarity is established and maintained.

For instance, even in the presence of these mechanisms, what prevents plus-ends from entering the dendrite from the cell body and continuously supplying dendrites with plus-end out microtubules? Indeed, there is a section between the cell body and first branch point that would not be subject to steering. Therefore, it is possible that a quality control mechanism exists at the cell body-dendrite interface where microtubule plus-ends are prohibited from entering the dendrite (Figure 2). In fact, similar mechanisms have been shown in mammalian hippocampal cell culture that act on both cargo and microtubules (Karasmanis et al., 2018). Similarly, what prevents microtubules generated at branch points from exiting distal sites of the branch point? If they were allowed to do so they would contribute to plus-end out polarity. It is possible that in the same manner that a sorting mechanism may exist at the cell body exit, a checkpoint may exist at the branch point. Such a checkpoint would possibly rely on positive and negative regulators of microtubule growth (Figure 2). Possible regulators may include motor proteins that recognize parallel or antiparallel microtubules. For example, the motor Kinesin-5 has been shown to exert both crosslinking and sliding action on microtubules (Leary et al., 2019). Therefore, it is possible this motor recognizes and limits antiparallel microtubules when a microtubule grows out toward one of the distal sites. It is also possible that this protein could recognize parallel microtubules

and crosslink them on the proximal exit thus promoting microtubule polymerization and maintaining minus-end out polarity. Another positive regulator for the branch point could be the homologue of the axonal microtubule bundling protein TRIM46. In flies, Trim9 displays most homology and could possibly facilitate a similar function as a microtubule regulator at branch points. Potential negative regulators could be those such as the class of Kinesin-13 microtubule depolymerases. Investigating this proposed mechanism would give a much more rounded

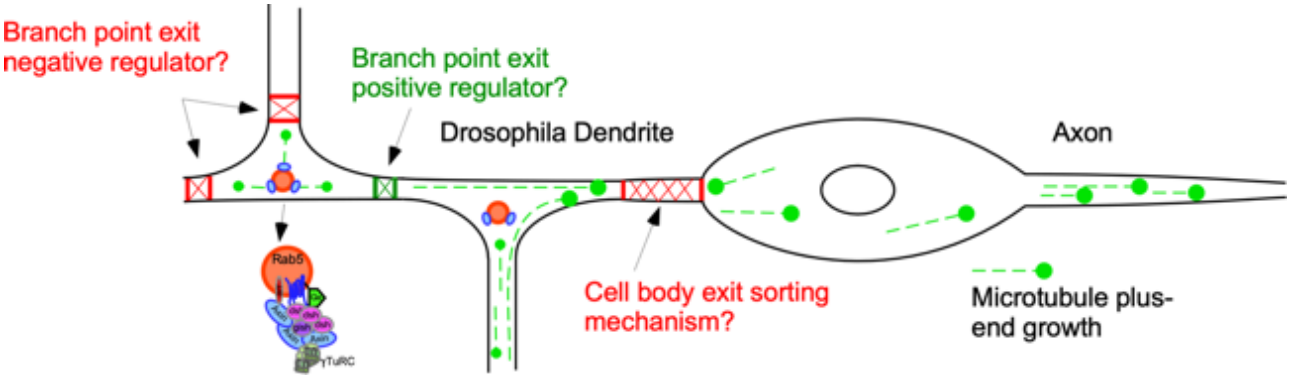

Figure 5-2. Lingering Questions Concerning *Drosophila* Dendritic Microtubule Regulation: Two major questions left are how microtubules generated in the cell body do not enter the dendrite and disrupt minus-end out microtubule polarity. One hypothesis is that there is a negative regulator that blocks plus-end entry into dendrites. Another similar unknown is how microtubules generated at branch points do not populate distal regions at random with plus-end out microtubules. Similarly, to the cell body there could be negative regulators that act on microtubules growing toward the distal exits. Additionally, there could be a positive regulator of microtubule growth at the branch point exit closest to the cell body.

explanation for how microtubule polarity is established and maintained. While these mechanisms shed light on microtubule polarity in *Drosophila* dendrites, how does this fit with vertebrate dendritic polarity organization?

Consistencies Between Vertebrate and *Drosophila* Dendritic Microtubule Control

Some of mechanisms underlying vertebrate dendrite microtubule organization include transporting microtubules via sliding (Baas & Yu, 1996), a role for a patronin family member in coordination with Kinesin-14 to stabilize microtubule minus-ends (Cao et al., 2020), HAUS/Augmin control of microtubules polarity (Cunha-Ferreira et al., 2018), and limiting retrograde microtubules via Kinesin-5 mediated microtubule stabilization (Figure 3) (Freixo et al., 2018). But how do these overlap with what has been discovered in *Drosophila* dendrites? Microtubule sliding has not been confirmed in *Drosophila* dendrites but it is possible that this could act in parallel to minus-end growth mediated by patronin to populate dendrites with minus-end out microtubules early in development. CAMPSAP2, one of the three mammalian homologues to *Drosophila* patronin has a function in regulating microtubule organization in vertebrate dendrites. However, it differs from minus-end growth mediated by patronin (Feng et al., 2019). In vertebrates CAMSAP2 has been shown to immobilize microtubule minus-ends by recruiting the Kinesin-14 motor KIFC3 (Cao et al., 2020). It is quite possible that another of the CAMSAP family members helps facilitate minus-end growth in vertebrates since growing minus-ends have been visualized in Zebra fish (Feng et al., 2019). With regard to the role of the HAUS/Augmin complex one study has touched on a possible role for Augmin activity in *Drosophila* dendrites, although the evidence is not substantial. When centrosomin, one of the key components of localizing nucleation machinery to dendrites, was depleted the *Drosophila* protein wee Augmin compensated for this loss and produced additional microtubules through recruitment of nucleation machinery (Yalgin et al., 2015). Therefore, augmin has been hinted at having a conserved role for controlling microtubules in dendrites but more detailed analysis needs to be conducted. Lastly, there has not been evidence when it comes to a role for the tetrameric motor Kinesin-5 in controlling

microtubules within *Drosophila* dendrites. Microtubule steering has also not been confirmed in vertebrates even though studies have investigated the role of APC proteins in vertebrate dendrites

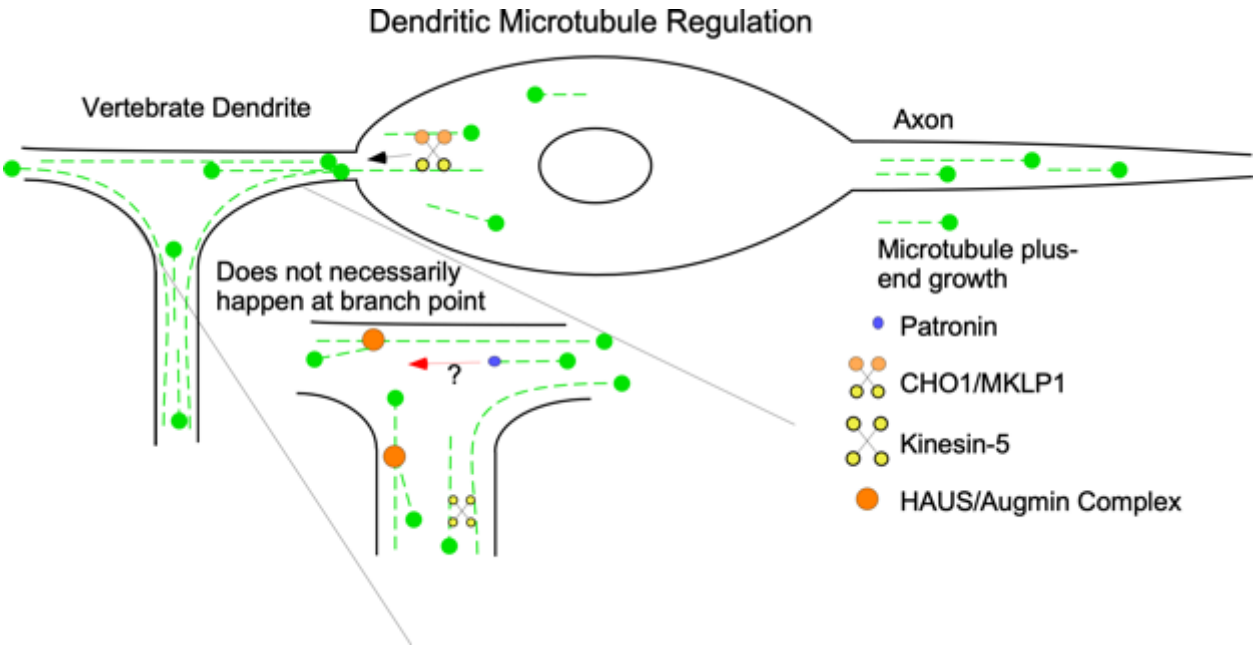

Figure 5-3. Vertebrate Dendritic Microtubule Control: Microtubule regulation in vertebrate dendrites has suggested roles for the motors CHO1/MLKP1 and Kinesin-5. CHO1/MLKP1 mediates sliding of minus-end out microtubule fragments from the cell body into the dendrites during development. Kinesin-5 helps to stabilize microtubules minimizing the amount of dynamic retrograde microtubules. The HAUS/Augmin complex contributes to dynamic microtubules by recruiting nucleation machinery and to the side of existing microtubules. Lastly, growing minus-ends have been shown in vertebrate dendrites lending to the possibility that CAMSAP/patronin mediated minus-end growth is conserved between *Drosophila* and vertebrate neurons. Whether this growth contributes to both plus-end and minus-end out microtubule growth has yet to be determined.

and found vertebrate APC2 is required for dendritic development through regulating microtubule dynamics (Kahn et al., 2018). One caveat about this study is that *Drosophila* and vertebrate APC proteins arose during an independent duplication event and the function of each set has not been shown to be equivalent. If steering does not function in vertebrate dendrites then it could be one way in which mixed microtubule polarity exists within these structures and why there is more extreme minus-end out polarity in *Drosophila*. Another explanation could be that vertebrate dendrites simply employ different regulatory mechanisms and are able to develop and function at

a 50/50 mixed state. Clearly much more needs to be investigated to know which regulatory mechanisms are conserved between *Drosophila* and vertebrate dendrites as well as what the ancestral state of microtubule polarity may have been. One thing is clear and that is we know at least two mechanisms are conserved.

It seems that microtubule minus-end growth is conserved but this needs functional analysis to confirm if patronin is involved. This also was only shown in RB sensory axons. Additionally, local nucleation via γTub is essential for microtubule organization across invertebrate and vertebrate neurons. Now we confirm the *Drosophila* dendritic branch point as a hub of microtubule organization including microtubule steering and endosomal microtubule nucleation. It would be interesting to know if vertebrate branch points are hubs for microtubule organization as well. It would also be interesting to know if similar mechanisms are utilized in the axon since we also observe localization of Rab5 endosomes throughout that compartment in *Drosophila* (Figure 4) (Weiner et al., 2020). Additionally, we see rare occurrences of branched axons in *Drosophila* sensory neurons. However, in most neuronal subtypes branched axons are normal. Therefore, do the same steering and nucleation mechanisms detailed here exist at this region? In any case, the investigation into the multifaceted control of neuronal microtubules must continue and the connection between surface signaling molecules and microtubules continues to unravel.

Implications and Follow-Up

Possibly one of the most intriguing findings was that the small GTPase Rac and the wave regulatory complex protein Abi were not only responsible for Apc2 localization but also Axin. Both Rac and Abi are well known for their role in mediating branched actin formation through the Arp2/3 complex (Havrylenko et al., 2015). Since Arp2/3 components were required for Apc2

localization the connection between these upstream regulators and Apc2 makes sense. However, the relationship between these and Axin is surprising. The activation of Rac alongside the other GTPase Rho has been found downstream of fz and dsh in PCP Wnt signaling but this variant does

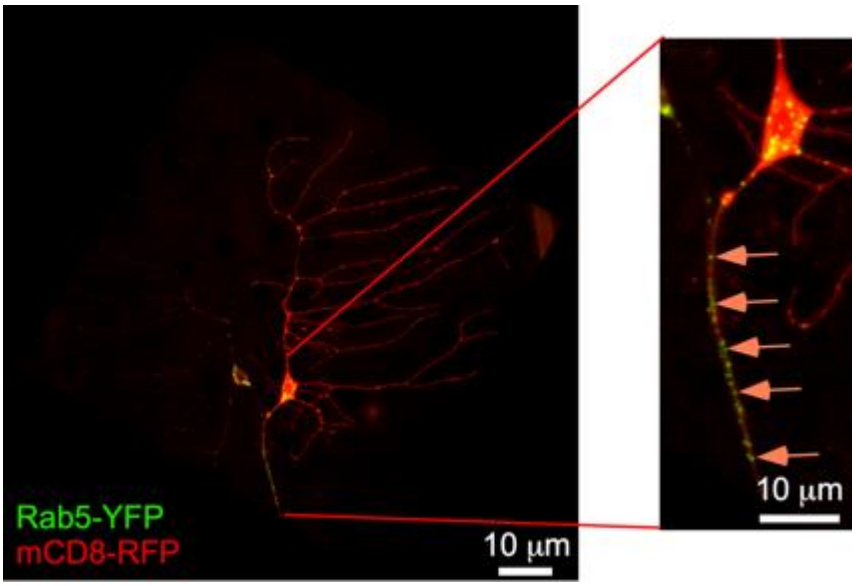

Figure 5-4. In addition to dendrite branch points Rab5 endosomes localize along the length of the axon: Rab5 endosomes are were visualized along the length of the axon in Class I sensory neurons. This localization pattern raises the question whether similar proteins that are localized to a subset of Rab5 endosomes in dendrites are localized to a subpopulation of these axonal endosomes.

not include Axin. Therefore, the data detailed in the Apc2 screen suggests that this relationship is novel and may warrant future study. It is possible that activated Rac not only regulates branched actin but is also important in setting up the proper scaffolding. Indeed, members of the Rac pathway have been found to act as scaffolds for Wnt signaling. For example, of the Rac GEFs, DOCK4 was shown to interact with members of the destruction complex including sgg, Apc, and Axin (Upadhyay et al., 2008). Thus, it seems that the relationship between Wnt signaling and actin regulation is not specific to PCP. From investigations into Apc2 localization it also seems that the relationship between actin regulation and microtubule organization may be as closely tied as some recent studies have shown. Axonal remodeling is downstream of Rac activation and actin

cytoskeletal remodeling. In addition to this, it has been shown in mammalian cell culture that the plus-tip tracking protein navigator (NAV) complexes with the Rho GEF Trio to activate Rac during neurite extension (van Haren et al., 2014) . Ultimately, the actin cytoskeleton is remodeled via a microtubule-linked complex. These two examples demonstrate how intricate the interplay between cytoskeletal elements can be and thus the regulation of Axin by upstream actin regulators in neurons may just be one more facet of that relationship.

Apocryphal Wnt signaling has far reaching implications for a number of processes in neurons. One in particular is the vastly unexplored questions of dendrite regeneration. For hundreds of years neurobiologists have studied axon regeneration because they form macroscopic nerve bundles. However, dendrites are typically much smaller and are shielded by the skull or spinal cord in the central nervous system. The tractable *Drosophila* sensory nervous system provides a space in which dendrite regeneration can be studied without the drawbacks of mammalian systems. Recently, as a companion story to chapter 4 we detailed a role for this Wnt signaling pathway in positioning nucleation sites at branch points during dendrite regeneration (Nye et al., 2020). All members of the pathway and γTub are required for robust dendrite regeneration. One additional player that was uncovered in this story is the fz co-receptor or orphan receptor tyrosine kinase Ror. Ror adds another wrinkle to the mechanism because there is already one co-receptor (arr) involved in the mechanism. This creates an intriguing scenario because there are multiple receptors and co-receptors involved in this mechanism.

Both fz and fz2 have always been described as functionally redundant (Bhanot et al., 1999). It would be interesting if one of the co-receptors arr or Ror were specific to one of the two receptors. The existence of the two receptors and two co-receptors offers up a tantalizing opportunity for exploration. It may be since neurons place such heavy demands on cytoskeletal regulation that parallel pathways have been developed to accomplish the same localization of γTub (Figure 5). Lending to this idea are two G-proteins that help localize γTub to branch points.

Gαo and Gαs have been shown to have different physiological roles (Syrovatkina, Alegre, Dey, & Huang, 2016). Classically in neurons, Gαs contributes to the production of cAMP through

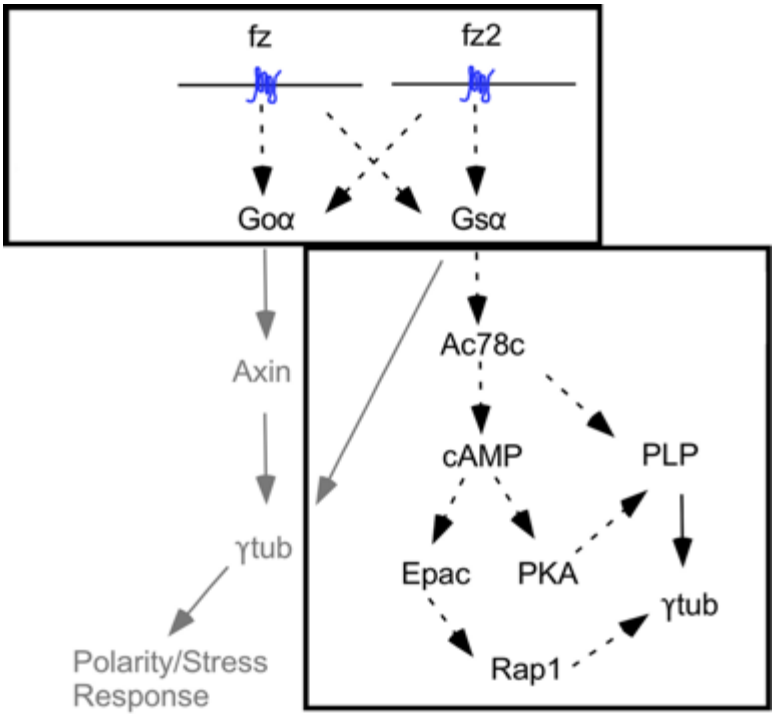

Figure 5-5. Proposed model of how two GPCRs and two G-proteins function in distinct mechanisms: fz and fz2 both localize Axin and this is presumably through Goα since Gsα does not localize γTub through Axin. Detailed is a proposed mechanism by which Gsα may function to position γTub at branch points in parallel to Goα. Gsα is classically known to activate adenylyl cyclases and these can lead to the production of cAMP a signal that can activate PKA. PKA can be positioned by a group of proteins with distinct docking locations. One of which is PLP which has been implicated in γTub localization in neurons at branch points. This could explain how cAMP downstream of Gsα signaling mediates γTub localization independent of Axin.

activation of adenylyl cyclases (Ronnett & Moon, 2002). cAMP has been shown to be a critical signaling molecule for the proper positioning of PLP through its A protein kinase anchoring protein domain (AKAP450) which helps induce local protein kinase A activity (Collado-Hilly & Coquil, 2009). It would be interesting if the positioning of PLP at branch points was independent of endosomal activity and thus a parallel mechanism to position γTub. On the other hand, Gαo

has been shown in a few studies to participate in all Wnt signaling pathways (Katanaev & Tomlinson, 2006). The role of Gαo is easier to fit into Apocryphal Wnt signaling, as it has been shown to have a regulatory impact on the localization of Axin (Egger-Adam & Katanaev, 2010). However, this G-protein has been shown to be able to signal from both fz and fz2 and so further convolutes the involvement of multiple receptors (Katanayeva, Kopein, Portmann, Hess, & Katanaev, 2010).

Another lingering question is how unregulated microtubule nucleation might influence microtubule polarity. Microtubule polarity defects occur with the reduction or loss of γTub at branch points and this suggests that it may be possible that when γTub is present there is a regulated direction to the nucleation event. This suggests that nucleation sites might be positioned on endosomes in the direction that would allow for minus-end out polarity instead of free floating where they may nucleate randomly in all directions. In other cell contexts it has been shown that branched actin interacts with endosomes through annexins and can be used to tether them in place or induce signaling changes (Grewal, Koese, Rentero, & Enrich, 2010). This may be one such mechanism that could account for correct microtubule growth direction. However, this is unlikely due to preliminary data from our lab. We have observed that microtubule spawning events are fairly random and at least 40% of microtubules grow toward one of the peripheral exits after spawning at the branch point (unpublished). These plus-end out microtubules do not successfully exit the branch point most likely due to an additional regulatory mechanism (unpublished). Therefore, it is just as possible that in the absence of local nucleation at branch points that other microtubule minus-end regulator activity is enhanced. If this is the case then one possible explanation is that severing enzymes may become more active to compensate for loss of nucleation and to create more microtubule mass. Once severed, existing microtubule polarity may be thrown off due to the newly generated microtubules direction being governed by feedback mechanisms such as the steering complex directing microtubules toward the wrong direction

on misoriented microtubules (Figure 6). A third explanation could be that when γTub is not localized properly to branch points that nucleation sites may be incorrectly positioned at non-branch point regions (Figure 6). In this scenario branch point specific mechanisms would not be

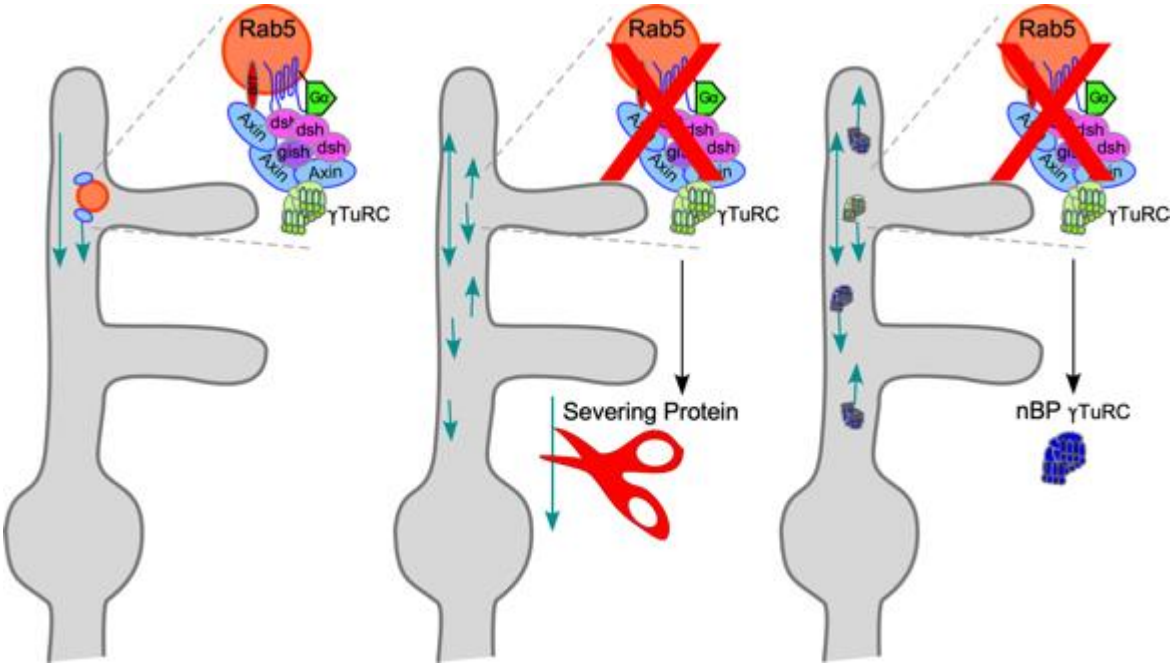

Figure 5-6. Two Possibly Ways that Reduced Branch Point Nucleation Results in Mixed Polarity: First the mechanism of localizing γTub by Wnt signaling endosomes is shown on the left. The middle and right show two possible explanations for how mixed polarity might result from a reduction in γTub at branch points. The middle one show that severing proteins might be upregulated. If this happens to increase microtubule number then the increase in microtubules might overwhelm steering or other branch point mechanisms. The second possibility might involve result in nucleation sites at non-branch point areas. If this happens it is possible that nucleation events away from the cell body would not be governed by branch point regulation.

able to act on the direction of the newly nucleated microtubule. If this were true it would help substantiate a case for branch point mechanisms that control plus-end out microtubules.

Signaling from endosomes has been described in many cellular contexts (Barford, Deppmann, & Winckler, 2017; Pavlos & Friedman, 2017). Possibly one of the most well-known instances of signaling endosomes comes from work done on the family of Rho GTPases (Phuyal & Farhan, 2019). This family includes many famously studied proteins such as Rac1 and Cdc42

and these are known to be recruited to endosomes. Once recruited they act as switches to help initiate a series of phosphorylation events that regulates actin formation spatially to enhance local signaling in processes such as the cell cycle and cell migration (Tebar, Enrich, Rentero, & Grewal, 2018). In mice, the p18 localizes MEK1 to late endosomes and helps enable the phosphorylation of MEK/ERK pathway targets (Nada et al., 2009). In human cells, mTOR signaling has been shown to be initiated from lysosomes (Betz & Hall, 2013). Not

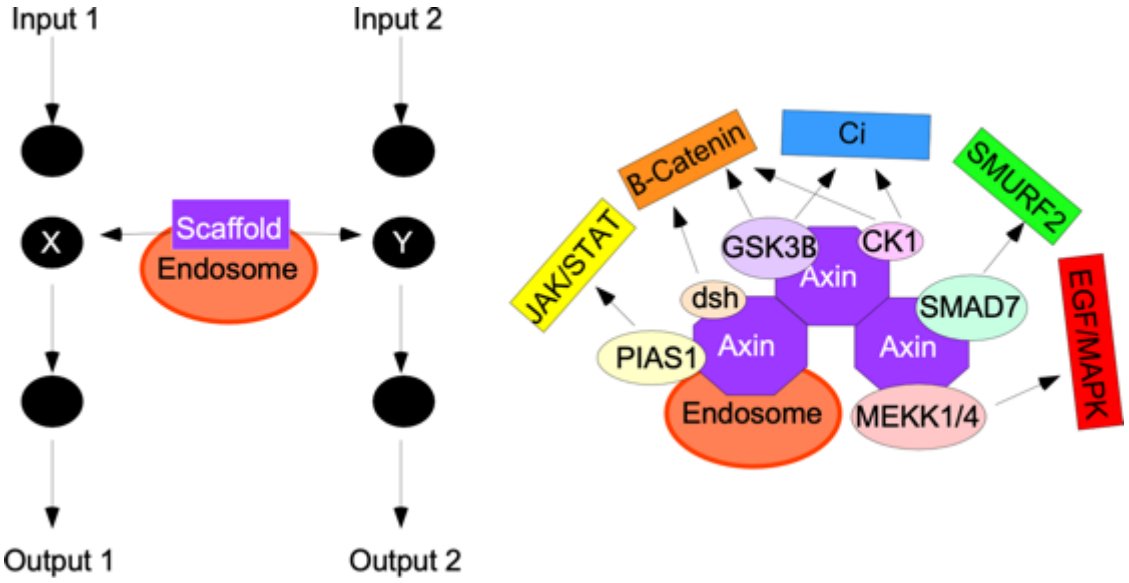

Figure 5-7. Endosomal scaffolds, signaling outputs, and Axin as a prime example: Protein scaffolds can localize to endosomes. When they do the signaling outputs can numerous. Shown on the lft is an example of a general scaffold that may have two different input signals that are mediated by that scaffolds promiscuous binding nature and produce two different outputs. A real example is provided on the right where Axin is one such promiscuous scaffold. From an endosome it can help regulate Jak/STAT, β-catenin, Ci, SMURF2, and EGF signaling.

surprisingly, most of these interactions are facilitated by cytoplasmic scaffolds. Interestingly, Axin is a scaffold known to localize to endosomes following internalization of the destruction complex from the plasma membrane. When internalized, Axin is normally shunted toward degradation but it can also continue to function as an effector of Hedgehog (Hh) signaling, regulation of JAK/STAT signaling, TGF-B through the E3 ligase SMURF2, and EGF pathways

through MEKK 1 and 4 (Luo & Lin, 2004; Palfy, Remenyi, & Korcsmaros, 2012; Zhang, Neo, Wang, Han, & Lin, 1999) (Figure 7). In the current study we expand the diversity of roles Axin plays. Here we demonstrate that Axin has a role on early signaling endosomes, most likely after internalization of fz receptors, by recruiting γTub to endosomes and helping to organize nucleation sites at dendrite branch points.

The idea that endosomes can be spatially docked in cells is not uncommon. Molecular motors have been shown to precisely sort endosomes where they are needed (Hunt & Stephens,

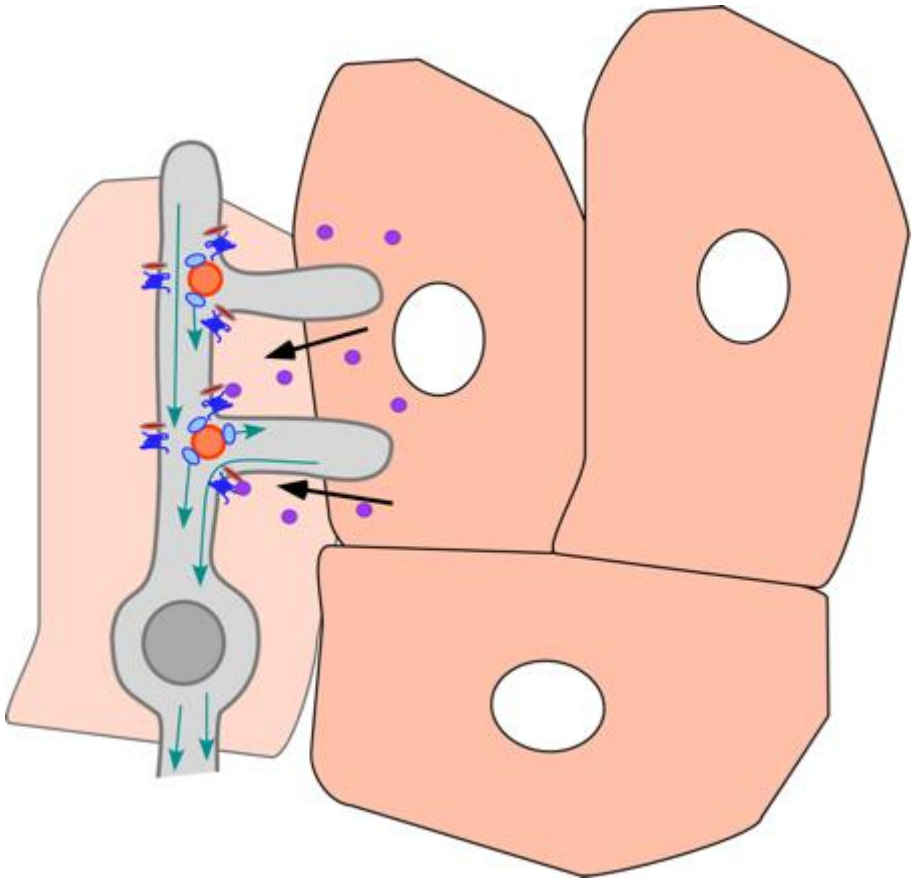

Figure 5-8. Paracrine signaling from epithelial cells to sensory neurons: Proposed model of Wnt secretion from neighboring epithelial cells providing the ligand source for fz receptors at the neuronal branch point. Since autocrine signaling is not the source of Wnt this may be the most likely scenario due to the close proximity the dendrites have to the epithelial cell layer. Ligand is shown as purple circles and directions of arrows indicate secretion from epithelial cells to neurons.

2011). This is just one instance of the close relationship between microtubules and endosomes. However, the connection between microtubule nucleation from an endosome has never been found. Epithelial cell membranes have been shown to dock microtubule minus-ends but endosomal membranes have not (Toya & Takeichi, 2016). Therefore, the regulation of microtubule minus-ends by proteins found on endosomal membranes is novel. It opens up an entire new field of study to explore how this process may occur in the some of the most fundamental areas of biology. Do endosomes regulate microtubule nucleation during cell division? Is the same relationship between Wnt signaling proteins on endosomes and microtubule minus-end regulation found in other cell types? The most intriguing question may be where does the ligand, if there is one involved at all, come from? Is it possible that a surrounding cell could modulate the neuronal cytoskeleton (Figure 8)? This last question may be the most fascinating because microtubule upregulation is γTub dependent after an injury to the axon. Thus, it may be possible that in sensory neurons the surrounding cellular populations help in the neuronal injury response. Within the same class of cells studied here it has been shown that a posterior patch of skin cells are a ligand source for a slightly different Wnt signaling pattern during development (Li et al., 2016). It is unclear whether more Wnt signaling complexes are endocytosed to increase nucleation site number or if inactive γTuRCs are activated. It could be just as possible that the response to injury may be cell autonomous and only in this circumstance would a knockdown of neuronal Wnt have a phenotype. If this were the case then two scenarios could exist in which one would be maintaining normal homeostasis by surrounding epithelial cells and the other would be that in a state of crisis the neuron excretes ligand to facilitate the injury response.

Preliminarily, we have found epithelial cells may be the source of Wnt ligand. Using the epithelial cell promoter A58 we have knocked down the chaperone wntless which is required for all Wnt secretion. By reducing wntless we take a broad approach before identifying which specific ligand may be used in Apocryphal Wnt signaling. When wntless was reduced in neurons

we saw no change in γTub enrichment but when reduced in the skin we find that γTub is reduced significantly at branch points of sensory neurons (Figure 9). This suggests that the ligand source for maintaining normal homeostasis may be the surrounding skin proximal to the sensory dendrites. However, this experiment is slightly flawed in that both skin and neurons have overexpressed γTub-GFP and mcd8-RFP. It would be more ideal to take advantage of the multiple binary expression systems in Drosophila. In addition to the UAS there are the qUAS and LexA systems that work under the same concept. In this way we could drive expression in the

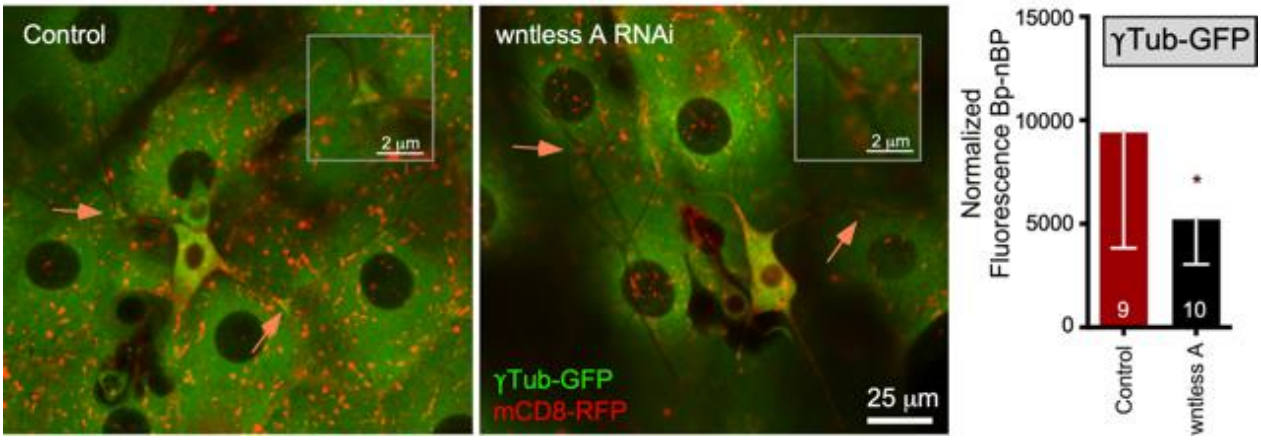

Figure 5-9. Maintenance of γTub at sensory neuron branch points depends on epithelial secreted Wnt: A58-GAL4 was used to drive UAS-mCD8-RFP, UAS-γTub-GFP and UAS-wntless RNAi or control RNAi in skin and class IV sensory neurons. Previously we have found that knocking down wnt secretion in the neuron does not affect γTub at branch points. Shown here when wntless is reduced in surrounding skin cells the level of branch point localized γTub is significantly reduced.

skin using our UAS-wntless RNAi but have qUAS or LexA driven γTub-GFP in the neurons of interest. Using this approach, we could eliminate any confounding background signal and cleanly answer whether skin cell produced Wnt provides the signal necessary to localize nucleation machinery to branch points in sensory neurons.

If there is no ligand involved in the endocytosis of these Rab5 endosomal Wnt signaling complexes then how do these complexes form? Not all Wnt signaling pathways require a Wnt. In non-canonical PCP signaling the role for a Wnt ligand is contentious (Chen et al., 2008; Wu & Mlodzik, 2008). The pathway described in this work includes canonical Wnt signaling members but does not need β-catenin and so cannot be classified as such. It is possible that Apocryphal Wnt signaling does not need a Wnt. There is some evidence that pools of GPCRs can signal from Golgi and endosomes without those receptors ever being at the plasma membrane

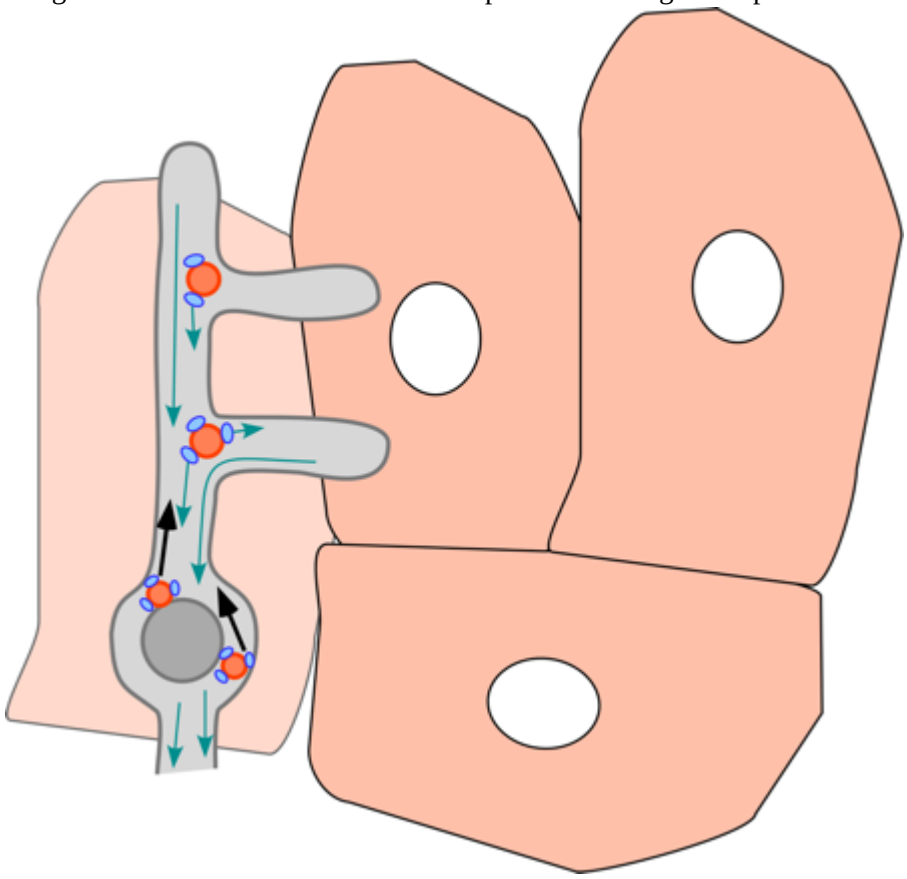

Figure 5-10. Endosomal signaling complexes might be assembled cell inside the cell: Proposed model where no Wnt ligand is involved in the formation of Wnt signaling complexes on endosomes. Instead these complexes are assembled in the neuron and trafficked to dendrite branch points where they regulate microtubule nucleation.

(Irannejad et al., 2017). Therefore, it is possible that the entire complex forms in the cell body where integral membrane proteins are processed into vesicles (Figure 10). Once the receptor is on

the vesicle it recruits the rest of the complex. Motor-mediated transport by dynein could preferentially localize these endosomes into dendrites but it could be just as likely that kinesin would mediate transport into axons. If this is the case then it is worth exploring if the same mechanisms regulate nucleation in axons as well.

The site specificity of this regulatory process makes the branch point an intriguing region for investigation. What makes the branch point unique such that endosomes are found there in

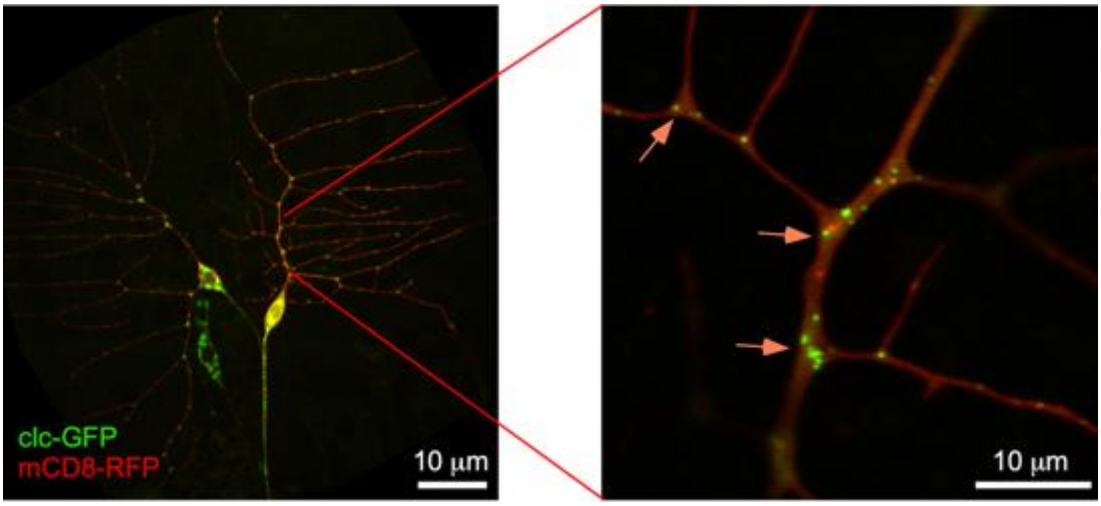

Figure 5-11. Clathrin activity is predominantly branch point specific in dendrites: The light chain of clathrin labeled with GFP (clc-GFP) was expressed in class I neurons using the 221-GAL4 driver. mCD8-GFP marks the cell membrane for reference. Clathrin dynamics were observed via time lapse images and clc-GFP puncta were locally observed at branch points. An overview is provided to the left and a region of the dendrite is shown to the right with arrows pointing to accumulations of clc-GFP puncta at branch points.

greater abundance than other regions of the dendrite? It is possible that clathrin mediated endocytosis occurs at the branch point specifically and if this is the case then what causes endocytic machinery to localize to branch point membranes? Branch point shape hints at a possible answer. Due to being a junction point the membrane of the branch point is curved. The curvature of the membrane in this region could recruit proteins known as Bin, Amphiphysin, Rv

(BAR) proteins. It has been shown that this BAR domain containing family of proteins do not require any upstream molecules or lipid modifiers (Ren et al., 2019). Due to domain binding structure they simply are attracted to curved membranes and then the recruitment of lipid modifier and actin regulators follows (Carman & Dominguez, 2018). This is intriguing because that could mean a BAR protein may recruit endocytic machinery to dendrite branch points and allow for site specific endocytosis. This could explain how signaling endosomes form at branch points to mediate branch point microtubule nucleation. So far, we have preliminarily been able to visualize a tagged clathrin light chain construct and show that dynamic populations of clathrin exist as branch points (Figure 11). These populations do not exist in the non-branch point regions

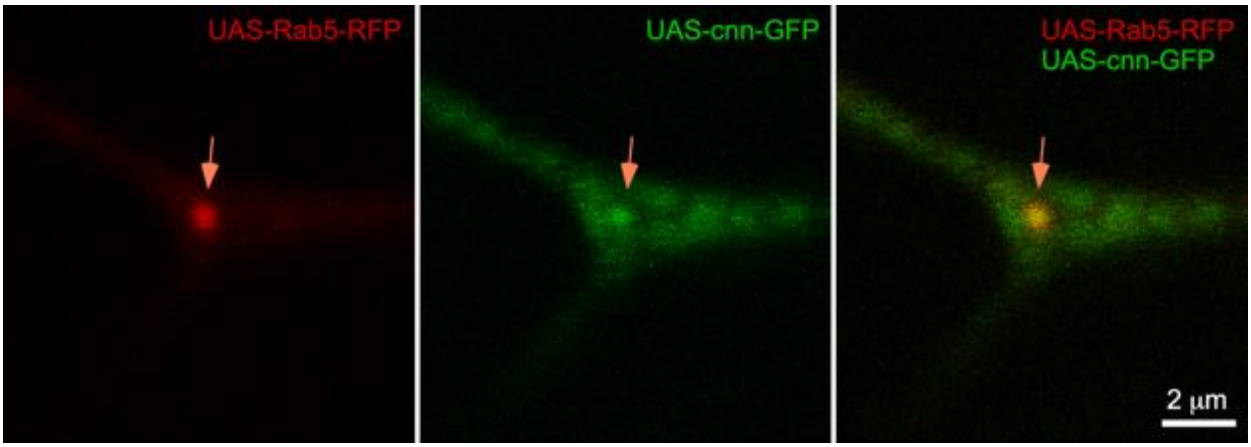

Figure 5-12. cnn enriches at Rab5 endosomes at branch points: Rab5 tagged with RFP was co-expressed with cnn-GFP in class I neurons. Colocalization was seen dendrite branch points. An example is shown where the arrow points to a Rab5-RFP endosome on the left, cnn-GFP puncta in the middle and the merged channel on the right.

of the dendrite. Since branch points seem to be a hotspot of clathrin activity this could indicate that local endocytosis does occur there uniquely compared to other regions of the dendrite.

An additional lingering question is the role of cnn. In one special context cnn can transform a subpopulation of Rab5 endosomes into active MTOCs? A splice form of cnn which

transforms mitochondria into MTOCs is expressed exclusively in the *Drosophila* spermatids and so that specific splice form is unlikely to facilitate its unique function here (Chen, Buchwalter, Kao, & Megraw, 2017). We have shown that cnn is required for γTub localization at branch points and that like γTub, Axin is sufficient to recruit cnn ectopically. It remains to be found whether Axin binds directly to γTub or it is through another protein like cnn that γTub localizes to branch points. Preliminarily, we have found that a tagged cnn also localizes to Rab5 endosomes (Figure 12). This raises the possibility that cnn is not only required for the localization of γTub but that it may also be an activator of nucleation at the endosome. The activation of nucleation machinery remains understudied and one that has only recently begun to be investigated.

Ultimately, this work uncovers a new site of microtubule organization in neurons. It adds significant contributions to two major microtubule maintenance mechanisms: microtubule steering and local microtubule nucleation. This work establishes a novel role for Wnt signaling and reveals the site of signaling at Rab5 endosomes. Whatever future insights are yet to be revealed, the case has been made for branch points as hubs of microtubule organization. In addition, a strong case has been made to add endosomes to the ranks of acentrosomal MTOCs. This work has a broad impact because it is quite possible that endosomes organize microtubules in other cell types as well.

References

Baas, P. W., & Yu, W. (1996). A composite model for establishing the microtubule arrays of the neuron. *Mol Neurobiol, 12*(2), 145-161. doi:10.1007/BF02740651

Barford, K., Deppmann, C., & Winckler, B. (2017). The neurotrophin receptor signaling endosome: Where trafficking meets signaling. *Dev Neurobiol, 77*(4), 405-418. doi:10.1002/dneu.22427

Betz, C., & Hall, M. N. (2013). Where is mTOR and what is it doing there? *J Cell Biol, 203*(4), 563-574. doi:10.1083/jcb.201306041

Bhanot, P., Fish, M., Jemison, J. A., Nusse, R., Nathans, J., & Cadigan, K. M. (1999). Frizzled and Dfrizzled-2 function as redundant receptors for Wingless during Drosophila embryonic development. *Development, 126*(18), 4175-4186. Retrieved from https://www.ncbi.nlm.nih.gov/pubmed/10457026

Cao, Y., Lipka, J., Stucchi, R., Burute, M., Pan, X., Portegies, S., . . . Hoogenraad, C. C. (2020). Microtubule Minus-End Binding Protein CAMSAP2 and Kinesin-14 Motor KIFC3 Control Dendritic Microtubule Organization. *Curr Biol, 30*(5), 899-908 e896. doi:10.1016/j.cub.2019.12.056

Carman, P. J., & Dominguez, R. (2018). BAR domain proteins-a linkage between cellular membranes, signaling pathways, and the actin cytoskeleton. *Biophys Rev, 10*(6), 1587-1604. doi:10.1007/s12551-018-0467-7

Chen, Antic, D., Matis, M., Logan, C. Y., Povelones, M., Anderson, G. A., . . . Axelrod, J. D. (2008). Asymmetric homotypic interactions of the atypical cadherin flamingo mediate intercellular polarity signaling. *Cell, 133*(6), 1093-1105. doi:10.1016/j.cell.2008.04.048

Chen, Buchwalter, R. A., Kao, L. R., & Megraw, T. L. (2017). A Splice Variant of Centrosomin Converts Mitochondria to Microtubule-Organizing Centers. *Curr Biol, 27*(13), 1928-1940 e1926. doi:10.1016/j.cub.2017.05.090

Collado-Hilly, M., & Coquil, J. F. (2009). Ins(1,4,5)P3 receptor type 1 associates with AKAP9 (AKAP450 variant) and protein kinase A type IIbeta in the Golgi apparatus in cerebellar granule cells. *Biol Cell, 101*(8), 469-480. doi:10.1042/BC20080184

Cunha-Ferreira, I., Chazeau, A., Buijs, R. R., Stucchi, R., Will, L., Pan, X., . . . Hoogenraad, C. C. (2018). The HAUS Complex Is a Key Regulator of Non-centrosomal Microtubule Organization during Neuronal Development. *Cell Rep, 24*(4), 791-800. doi:10.1016/j.celrep.2018.06.093

Egger-Adam, D., & Katanaev, V. L. (2010). The trimeric G protein Go inflicts a double impact on axin in the Wnt/frizzled signaling pathway. *Dev Dyn, 239*(1), 168-183. doi:10.1002/dvdy.22060

Feng, C., Thyagarajan, P., Shorey, M., Seebold, D. Y., Weiner, A. T., Albertson, R. M., . . . Rolls, M. M. (2019). Patronin-mediated minus end growth is required for dendritic microtubule polarity. *J Cell Biol, 218*(7), 2309-2328. doi:10.1083/jcb.201810155

Freixo, F., Martinez Delgado, P., Manso, Y., Sanchez-Huertas, C., Lacasa, C., Soriano, E., . . . Luders, J. (2018). NEK7 regulates dendrite morphogenesis in neurons via Eg5-dependent microtubule stabilization. *Nat Commun, 9*(1), 2330. doi:10.1038/s41467-018-04706-7

Grewal, T., Koese, M., Rentero, C., & Enrich, C. (2010). Annexin A6-regulator of the EGFR/Ras signalling pathway and cholesterol homeostasis. *Int J Biochem Cell Biol, 42*(5), 580-584. doi:10.1016/j.biocel.2009.12.020

Havrylenko, S., Noguera, P., Abou-Ghali, M., Manzi, J., Faqir, F., Lamora, A., . . . Plastino, J. (2015). WAVE binds Ena/VASP for enhanced Arp2/3 complex-based actin assembly. *Mol Biol Cell, 26*(1), 55-65. doi:10.1091/mbc.E14-07-1200

Hill, S. E., Parmar, M., Gheres, K. W., Guignet, M. A., Huang, Y., Jackson, F. R., & Rolls, M. M. (2012). Development of dendrite polarity in Drosophila neurons. *Neural Dev, 7*, 34. doi:10.1186/1749-8104-7-34

Hunt, S. D., & Stephens, D. J. (2011). The role of motor proteins in endosomal sorting. *Biochem Soc Trans, 39*(5), 1179-1184. doi:10.1042/BST0391179

Irannejad, R., Pessino, V., Mika, D., Huang, B., Wedegaertner, P. B., Conti, M., & von Zastrow, M. (2017). Functional selectivity of GPCR-directed drug action through location bias. *Nat Chem Biol, 13*(7), 799-806. doi:10.1038/nchembio.2389

Kahn, O. I., Schatzle, P., van de Willige, D., Tas, R. P., Lindhout, F. W., Portegies, S., . . . Hoogenraad, C. C. (2018). APC2 controls dendrite development by promoting microtubule dynamics. *Nat Commun, 9*(1), 2773. doi:10.1038/s41467-018-05124-5

Karasmanis, E. P., Phan, C. T., Angelis, D., Kesisova, I. A., Hoogenraad, C. C., McKenney, R. J., & Spiliotis, E. T. (2018). Polarity of Neuronal Membrane Traffic Requires Sorting of Kinesin Motor Cargo during Entry into Dendrites by a Microtubule-Associated Septin. *Dev Cell, 46*(2), 204-218 e207. doi:10.1016/j.devcel.2018.06.013

Katanaev, V. L., & Tomlinson, A. (2006). Multiple roles of a trimeric G protein in Drosophila cell polarization. *Cell Cycle, 5*(21), 2464-2472. doi:10.4161/cc.5.21.3410

Katanayeva, N., Kopein, D., Portmann, R., Hess, D., & Katanaev, V. L. (2010). Competing activities of heterotrimeric G proteins in Drosophila wing maturation. *PLoS One, 5*(8), e12331. doi:10.1371/journal.pone.0012331

Leary, A., Sim, S., Nazarova, E., Shulist, K., Genthial, R., Yang, S. K., . . . Vogel, J. (2019). Successive Kinesin-5 Microtubule Crosslinking and Sliding Promote Fast, Irreversible Formation of a Stereotyped Bipolar Spindle. *Curr Biol, 29*(22), 3825-3837 e3823. doi:10.1016/j.cub.2019.09.030

Li, X., Wang, Y., Wang, H., Liu, T., Guo, J., Yi, W., & Li, Y. (2016). Epithelia-derived wingless regulates dendrite directional growth of drosophila ddaE neuron through the Fz-Fmi-Dsh-Rac1 pathway. *Mol Brain, 9*(1), 46. doi:10.1186/s13041-016-0228-0

Luo, W., & Lin, S. C. (2004). Axin: a master scaffold for multiple signaling pathways. *Neurosignals, 13*(3), 99-113. doi:10.1159/000076563

Mattie, F. J., Stackpole, M. M., Stone, M. C., Clippard, J. R., Rudnick, D. A., Qiu, Y., . . . Rolls, M. M. (2010). Directed microtubule growth, +TIPs, and kinesin-2 are required for uniform microtubule polarity in dendrites. *Curr Biol, 20*(24), 2169-2177. doi:10.1016/j.cub.2010.11.050

Nada, S., Hondo, A., Kasai, A., Koike, M., Saito, K., Uchiyama, Y., & Okada, M. (2009). The novel lipid raft adaptor p18 controls endosome dynamics by anchoring the MEK-ERK pathway to late endosomes. *EMBO J, 28*(5), 477-489. doi:10.1038/emboj.2008.308

Nguyen, M. M., McCracken, C. J., Milner, E. S., Goetschius, D. J., Weiner, A. T., Long, M. K., . . . Rolls, M. M. (2014). Gamma-tubulin controls neuronal microtubule polarity independently of Golgi outposts. *Mol Biol Cell, 25*(13), 2039-2050. doi:10.1091/mbc.E13-09-0515

Nye, D. M. R., Albertson, R. M., Weiner, A. T., Hertzler, J. I., Shorey, M., Goberdhan, D. C. I., . . . Rolls, M. M. (2020). The receptor tyrosine kinase Ror is required for dendrite regeneration in Drosophila neurons. *PLoS Biol, 18*(3), e3000657. doi:10.1371/journal.pbio.3000657

Palfy, M., Remenyi, A., & Korcsmaros, T. (2012). Endosomal crosstalk: meeting points for signaling pathways. *Trends Cell Biol, 22*(9), 447-456. doi:10.1016/j.tcb.2012.06.004

Pavlos, N. J., & Friedman, P. A. (2017). GPCR Signaling and Trafficking: The Long and Short of It. *Trends Endocrinol Metab, 28*(3), 213-226. doi:10.1016/j.tem.2016.10.007

Phuyal, S., & Farhan, H. (2019). Multifaceted Rho GTPase Signaling at the Endomembranes. *Front Cell Dev Biol, 7*, 127. doi:10.3389/fcell.2019.00127

Ren, C., Yuan, Q., Braun, M., Zhang, X., Petri, B., Zhang, J., . . . Wu, D. (2019). Leukocyte Cytoskeleton Polarization Is Initiated by Plasma Membrane Curvature from Cell Attachment. *Dev Cell, 49*(2), 206-219 e207. doi:10.1016/j.devcel.2019.02.023

Ronnett, G. V., & Moon, C. (2002). G proteins and olfactory signal transduction. *Annu Rev Physiol, 64*, 189-222. doi:10.1146/annurev.physiol.64.082701.102219

Syrovatkina, V., Alegre, K. O., Dey, R., & Huang, X. Y. (2016). Regulation, Signaling, and Physiological Functions of G-Proteins. *J Mol Biol, 428*(19), 3850-3868. doi:10.1016/j.jmb.2016.08.002

Tebar, F., Enrich, C., Rentero, C., & Grewal, T. (2018). GTPases Rac1 and Ras Signaling from Endosomes. *Prog Mol Subcell Biol, 57*, 65-105. doi:10.1007/978-3-319-96704-2_3

Toya, M., & Takeichi, M. (2016). Organization of Non-centrosomal Microtubules in Epithelial Cells. *Cell Struct Funct, 41*(2), 127-135. doi:10.1247/csf.16015

Upadhyay, G., Goessling, W., North, T. E., Xavier, R., Zon, L. I., & Yajnik, V. (2008). Molecular association between beta-catenin degradation complex and Rac guanine exchange factor DOCK4 is essential for Wnt/beta-catenin signaling. *Oncogene, 27*(44), 5845-5855. doi:10.1038/onc.2008.202

van Haren, J., Boudeau, J., Schmidt, S., Basu, S., Liu, Z., Lammers, D., . . . Galjart, N. (2014). Dynamic microtubules catalyze formation of navigator-TRIO complexes to regulate neurite extension. *Curr Biol, 24*(15), 1778-1785. doi:10.1016/j.cub.2014.06.037

Weiner, A. T., Lanz, M. C., Goetschius, D. J., Hancock, W. O., & Rolls, M. M. (2016). Kinesin-2 and Apc function at dendrite branch points to resolve microtubule collisions. *Cytoskeleton (Hoboken), 73*(1), 35-44. doi:10.1002/cm.21270

Weiner, A. T., Seebold, D. Y., Torres-Gutierrez, P., Folker, C., Swope, R. D., Kothe, G. O., . . . Rolls, M. M. (2020). Endosomal Wnt signaling proteins control microtubule nucleation in dendrites. *PLoS Biol, 18*(3), e3000647. doi:10.1371/journal.pbio.3000647

Wu, J., & Mlodzik, M. (2008). The frizzled extracellular domain is a ligand for Van Gogh/Stbm during nonautonomous planar cell polarity signaling. *Dev Cell, 15*(3), 462-469. doi:10.1016/j.devcel.2008.08.004

Yalgin, C., Ebrahimi, S., Delandre, C., Yoong, L. F., Akimoto, S., Tran, H., . . . Moore, A. W. (2015). Centrosomin represses dendrite branching by orienting microtubule nucleation. *Nat Neurosci, 18*(10), 1437-1445. doi:10.1038/nn.4099

Zhang, Y., Neo, S. Y., Wang, X., Han, J., & Lin, S. C. (1999). Axin forms a complex with MEKK1 and activates c-Jun NH(2)-terminal kinase/stress-activated protein kinase through domains distinct from Wnt signaling. *J Biol Chem, 274*(49), 35247-35254. doi:10.1074/jbc.274.49.35247

Appendix

Supplemental to Chapter 2

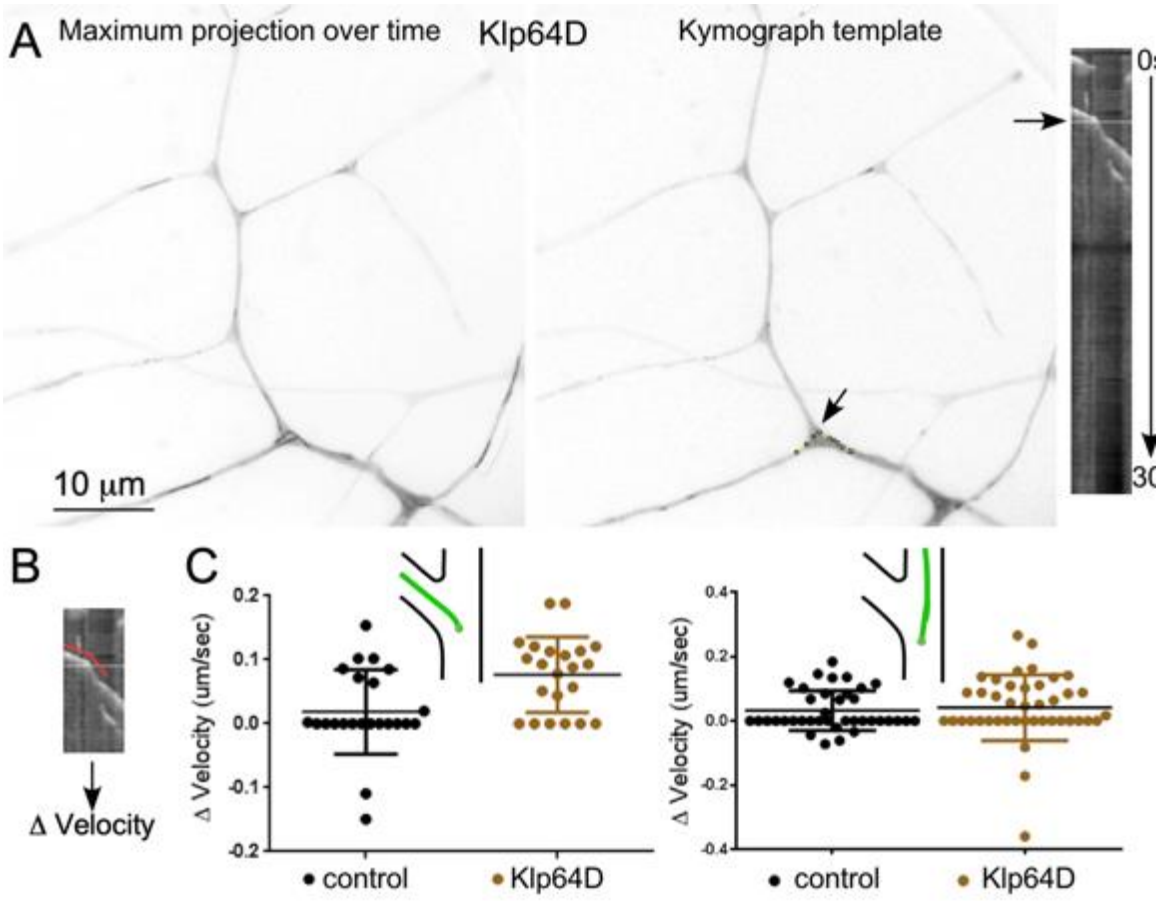

Figure A-S1. Speed measurements of comets in branch points.

A. The steps to generate kymographs of microtubules growing through branch points are shown. The image at the left is a maximum projection through time of EB1-GFP. The middle image shows the time projection with kymograph template drawn on it, and the right panel shows the resulting kymograph. In B, the kymograph is annotated at the left to show how lines to measure angle changes are drawn. In C, the resulting speed changes within the branch are plotted in control and Klp64D RNAi genotypes. Comets entering the branch from the periphery are shown at the left, and within the main trunk at the right. Each spot represents the measurement from a single microtubule. The average is represented by a horizontal line and error bars indicate the standard deviation.

VITA

Alexis Thomas Weiner

Ph.D Candidate in Molecular Cellular and Integrative Biosciences – The Huck Institutes of the Life Sciences
125 Huck Life Sciences Building University Park PA 16802 ATW5062@psu.edu

Education

Pennsylvania State University, University Park, PA BS Biology 08/2008-05/2013

Research Experience

Huck Institute of the Life Sciences
Advisor: Dr. Melissa Rolls
Undergraduate Researcher 2011-2013
Research Technician 2014-2015
PhD Graduate Student 2015 -2020

Publications

Complete List of Published Work in My Bibliography:
https://www.ncbi.nlm.nih.gov/pubmed/?term=alexis+weiner

Positions and Employment

2014- 2015	Research Technologist 1
2015 -	PhD Graduate Candidate, Penn State University

Other Experience and Professional Memberships

2013 -	Member, Pittsburgh Local Traffic Meeting
2016 -	Member, American Society for Cell Biology

Talk/Poster Invitations

2013 -2015	Pittsburgh Local Traffic Meeting poster presentation
2016	Pittsburgh Local Traffic Meeting student talk and poster
2016	American Society for Cell Biology poster presentation
2017	Pittsburgh Local Traffic Meeting poster presentation
2017	American Society for Cell Biology minisymposium talk and poster
2018	2018 EMBO Mechanisms of Neuronal Remodeling poster presentation

Honors and Awards

The Huck Life Sciences Travel Award (2018)
The EMBO Journal poster prize – EMBO Mechanisms of Neuronal Remodeling (2018)
Graduate Student Excellence in Mentoring Award – Penn State University (2018)

Science Outreach

Pennsylvania Junior Academy of Science (PJAS) 2009-present
Research Experience for Teachers (RET) 2016-present
Higher Achievement 2015-2017